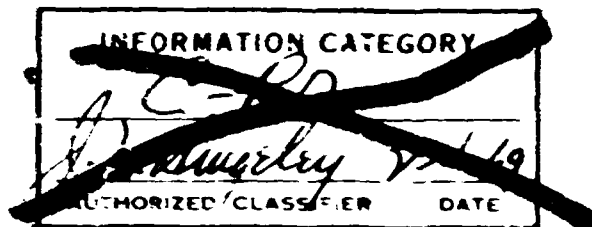
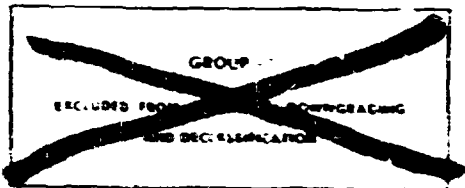


~~CONFIDENTIAL~~
~~RESTRICTED DATA~~

NOTICE
The report was prepared as an account of work performed by the United States Government for the United States and the United States Atomic Energy Commission. It is the property of the United States Government and is loaned to your agency. It and its contents are not to be distributed outside your agency without the express approval of the agency to which it was loaned. It is to be destroyed when it is no longer needed for the purpose for which it was prepared.

MASTER

Westinghouse Astronuclear Laboratory



J. DeStefano
Technical Editor

Prepared By:
Test Engineering

Approved By:

C. R. Dippel
C. R. Dippel, Manager
Technology Engineering

A. C. Sanderson
A. C. Sanderson, Manager
Technology Department

Classification cancelled by authority of *DAAG* *SEP 10 1973*

WANL-TNR-224

NRX-A6 FINAL REPORT

(Title Unclassified)

Subcontract NP.1

~~CONFIDENTIAL~~
~~RESTRICTED DATA~~
Atomic Energy Act - 1954

BLANK PAGE

ACKNOWLEDGMENT

The material presented in this report represents contributions from members of several organizations--the Space Nuclear Propulsion Office (SNPO), Aerojet-General Corporation (AGC), NERVA Test Operations (NTO) as well as the Westinghouse Astronuclear Laboratory (WANL). At WANL, specific sections of this report were prepared by various departments--Reactor Design, Control Systems Engineering, Thermal and Nuclear Design, Electronics and Instrumentation, Systems Analysis, Fuel Development, and Test Engineering. Full credit is extended to these groups for their participation. The references enumerated in the bibliography of this report will provide more comprehensive information in specific areas of interest.

BLANK PAGE

TABLE OF CONTENTS

<u>Section</u>	<u>Page</u>
1. INTRODUCTION	1-1
Summary of NERVA Program	1-1
Summary of Previous Reactor Tests	1-1
NRX-A1	1-1
NRX-A2	1-2
NRX-A3	1-2
NRX/EST	1-2
NRX-A5	1-2
2. SUMMARY AND CONCLUSIONS	2-1
Summary	2-1
Conclusions	2-3
3. TEST ASSEMBLY AND FACILITIES DESCRIPTION	3-1
Reactor	3-1
Test Facilities	3-12
Control Systems and Safety Systems	3-18
Functional Description of Test System	3-29
Reactor Assembly, Checkout, Transfer, and Testing	3-35
4. TEST DESCRIPTIONS	4-1
Facility Checkout Tests	4-1
EP-I, Initial Criticality, Flow Tests, Neutronic Calibration, Low Power Dosimetry, and Control	4-5
Drum and Shield Worth Measurements	4-6
EP-II, Scram Checks and System Interaction Checkout Tests	4-7
EP-III, Full Power Run	4-8
EP-III A, Full Power Duration Test	5-1
5. TEST RESULTS	5-1
Transient and Steady-State Performance Analysis	5-31
Control Systems Performance	5-32
Nuclear Analysis	5-36
Reactor Safety	5-37
Instrumentation Performance	

TABLE OF CONTENTS (CONTINUED)

<u>Section</u>	<u>Page</u>
Reactor and Feedsystem Dynamic Analysis	5-47
Component Evaluation	5-48
Disassembly and Post-Operational Examination	5-60
Fuel Element Performance	5-74
Chemical and Radiochemical Measurements Results	5-98
Environmental Radiation	5-101
Pneumatic Actuator Side-By-Side Experiment	5-102
 6. BIBLIOGRAPHY	 6-1

CONFIDENTIAL



(THIS PAGE IS UNCLASSIFIED)
LIST OF ILLUSTRATIONS

<u>Figure</u>		<u>Page</u>
3-1	(CRD) NRX-A6 Reactor Configuration (U)	3-2
3-2	(CRD) NRX-A6 Reactor Flow Path (U)	3-3
3-3	(CRD) Trimetric View of Filler Strip Periphery (U)	3-5
3-4	(CRD) NRX-A6 Particle Catcher (U)	3-7
3-5	(CRD) NRX-A6 Reflector/Lateral Support Arrangement (U)	3-10
3-6	(CRD) NRX-A6 Aft End Support System (U)	3-11
3-7	(U) Test Cell "C" Control Room Flow Schematic	3-13
3-8	(U) Test Cell "C" 360° Shield	3-19
3-9	(U) NRX-A6 Control System	3-21
3-10	(U) NRX-A6 Operating Map	3-31
4-1	(U) NRX-A6 Full Power Test, EP-IIIA, Performance Profiles	4-9
4-2	(U) NRX-A6 Full Power Test, EP-IIIA, Operating Map	4-10
5-1	(U) NRX-A6 Full Power Test, EP-IIIA, Performance Profiles	5-3
5-2	(CRD) Comparison of Power, Nozzle Torus Flow, Average Fuel Exit and Chamber Temperature Predictions with Measurements During EP-IIIA Startup (U)	5-8
5-3	(CRD) Comparison of Component Pressure Drop Predictions with Measurements During EP-IIIA Startup (U)	5-9
5-4	(CRD) Comparison of Tie Rod Exit Material and Reactor Plenum Temperature Predictions with Measurements During EP-IIIA Startup (U)	5-10
5-5	(CRD) Comparison of Core Station Temperature Predictions with Measurements During EP-IIIA Startup (U)	5-11
5-6	(CRD) Comparison of Power, Nozzle Torus Flow, Chamber Temperature Predictions with Measurements During EP-IIIA Shutdown (U)	5-12

(THIS PAGE IS UNCLASSIFIED)

CONFIDENTIAL

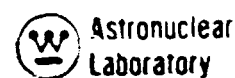
~~CONFIDENTIAL~~

LIST OF ILLUSTRATIONS (CONTINUED)

<u>Figure</u>		<u>Page</u>
5-7	(CRD) Comparison of Tie Rod Exit Material and Reactor Plenum Temperature Predictions with Measurements During EP-IIIA Shutdown (U)	5-13
5-8	(CRD) Comparison of Core Station, Temperatures and Control Drum Motion Predictions with Measurements During EP-IIIA Shutdown (U)	5-14
5-9	(CRD) NRX-A6 Thermal Capsule Data Versus Core Radius (U)	5-16
5-10	(CRD) Axial Temperature Distribution for Central Region at Control Room Time of 14300-EP-III-A (U)	5-17
5-11	(CRD) Axial Temperature Distribution for Peripheral Region at Control Room Time of 17800-EP-IIIA (U)	5-18
5-12	(CRD) EP-IIIA Temperatures Versus Radius at Control Room Time 14400 and Drum Position 105° (CRD)	5-19
5-13	(CRD) EP-IIIA, Radial Temperature Distribution Obtained From Multiple Regression Analysis at Control Room Time 14400 (U)	5-20
5-14	(CRD) EP-IIIA Radial Temperature Distribution Obtained From Multiple Regression Analysis at Control Room Time 17800 (U)	5-21
5-15	(CRD) Normalized Lateral Support Seal System Pressure Distribution at Start of Full Power Hold (14400 Control Room Time) (U)	5-24
5-16	(CRD) Radial Distribution of Overall Weight Losses in NRX/EST, NRX-A5, and NRX-A6 (U)	5-28
5-17	(CRD) Radial Distribution of Overall and Bore Weight Losses	5-29
5-18	(CRD) Axial Bore Weight Loss Distribution for Non-OD Coated Elements (CRD)	5-30
5-19	(U) Measured Versus Ideal (Synchronized) Program Outputs for EP-IIIA NRX-A6 Full Power Run	5-33
5-20	(CRD) Variation of Cumulative Reactivity Loss with Time for the NRX/EST, NRX-A5, and NRX-A6 Reactors (U)	5-35

~~CONFIDENTIAL~~

~~CONFIDENTIAL~~



LIST OF ILLUSTRATIONS (CONTINUED)

<u>Figure</u>		<u>Page</u>
5-21	(U) Comparison of Pressures During EP-IIIA Full Power Run with Analog Simulation	5-49
5-22	(CRD) Comparison of Temperatures During EP-IIIA Full Power Run with Analog Simulation (U)	5-50
5-23	(CRD) Comparison of Shutdown Data During EP-IIIA Full Power Run with Analog Simulation (U)	5-51
5-24	(U) Comparison of Shutdown Data During EP-IIIA Full Power Run with Analog Simulation	5-52
5-25	(U) NRX-A6 FEP-II Open Loop LF-10 Flow to Turbine Valve Demand Response	5-53
5-26	(U) Simulation of NRX-A6 FEP-III Emergency Shutdown From Design Flow	5-54
5-27	(U) Simulation of NRX-A6 FEP-III Emergency Shutdown From Design Flow	5-55
5-28	(U) Simulation of NRX-A6 FEP-III Emergency Shutdown From Design Flow	5-56
5-29	(U) NRX-A6 Feedsystem and Reactor Schematic of Modeled Components	5-57
5-30	(U) Overall View of Test Assembly After Return to R-MAD	5-61
5-31	(CRD) Appearance of Beryllium Piece Found in a Control Drum Cavity After Removal of Upper Half of Reflector (CRD)	5-63
5-32	(CRD) Appearance of Insulating Tiles, Grafoil Wrapper, and Displaced Seal Segments (CRD)	5-68
5-33	(CRD) Appearance of a Grafoil Wrapper Layer Showing Corrosion Patterns Corresponding to Filler Strip Gaps (CRD)	5-69
5-34	(CRD) Radial Distribution of Gross Weight Loss for Matrix-Coating Types (U)	5-78
5-35	(CRD) Comparison of Radial Distribution of Gross Weight Loss in NRX-A6 with NRX-A5 (U)	5-80

~~CONFIDENTIAL~~

CONFIDENTIAL

LIST OF ILLUSTRATIONS (CONTINUED)

<u>Figure</u>		<u>Page</u>
5-36	(CRD) Comparison of Radial Distribution of Pinhole Frequency and Density in NRX-A5 with NRX-A5 (U)	5-81
5-37	(CRD) Radial Variations of Incremental Weight Loss in the Axial Region 0-30 Inches for NRX-A5 and NRX-A6 Fuel Elements (CRD)	5-82
5-38	(CRD) Radial Variations of Incremental Weight Loss in the Axial Region 30-52 Inches for NRX-A5 and NRX-A6 Fuel Elements (CRD)	5-83
5-39	(CRD) NRX-A6 Fuel Element "Notch" Corrosion (U)	5-85
5-40	(CPD) Radial Distribution of NRX-A6 Fuel Element Pull-Out (U)	5-90
5-41	(CRD) Radial Distribution of Matrix-Additive $\overline{\Delta W}$ (U)	5-91
5-42	(CRD) Weight Loss Index of Performance Estimate for NRX-A6 Experimental Fuel Elements (U)	5-93
5-43	(CRD) Core Average Axial Variation in Flexure Strength for 79 NRX-A6 and 63 NRX-A5 Fuel Elements (U)	5-95
5-44	(CRD) Comparison of Gross Gamma and Two Point Gamma Radial Fission Distribution (U)	5-100
5-45	(U) Measured Gamma Dose Rate on the Privy Roof as a Function of Hydrogen Coolant Flow for the NRX-A6 Reactor	5-102
5-46	(U) Block Diagram of NRX-A6 Side-By-Side Actuator Test Set-Up	5-104
5-47	(U) NRX-A6 Side-By-Side Actuator Test Position Diagram	5-106
5-48	(U) NRX-A6 Side-By-Side Actuator, Pedestal, and Simulated Drum Load	5-107
5-49	(U) NRX-A6 Side-By-Side Actuator Test Assembly	5-108
5-50	(U) Completely Assembled NRX-A6 Side-By-Side Actuator Test Assembly	5-109
5-51	(U) NRX-A6 Side-By-Side Actuator Test Assembly Mounted on Test Car	5-110

CONFIDENTIAL

LIST OF ILLUSTRATIONS (CONTINUED)

<u>Figure</u>			<u>Page</u>
5-52	(U)	NRX-A6 Side-By-Side Actuator Test Closed Loop Frequency Response (U)	5-113
5-53	(U)	NRX-A6 Side-By-Side Actuator Temperatures and Coolant Gas Pressures During Full Power Run (U)	5-114
5-54	(U)	NRX-A6 Side-By-Side Actuator Gamma Dose (U)	5-116
5-55	(U)	NRX-A6 Side-By-Side Actuator Fast Neutron Flux (U)	5-117
5-56	(U)	NRX-A6 Side-By-Side Slow Neutron Flux (U)	5-118
5-57	(U)	NRX-A6 Side-By-Side Actuator Post-Test Condition (Torque Motor, Solder Points, Lead Wire, and Miscellaneous Servo Valve Components) (U)	5-119
5-58	(U)	NRX-A6 Side-By-Side Actuator Post-Test Condition (Lock Indication Switches, Solder Connections, Wires, Lock, and Lock Shutoff Valve) (U)	5-120
5-59	(U)	NRX-A6 Side-By-Side Actuator Post-Test Condition (Three Deck Potentiometer, Solder Points, Wire, and Insulating Sleeves) (U)	5-121
5-60	(U)	NRX-A6 Side-By-Side Actuator Post-Test Condition (P ₁ Piston and Rack Assembly, P ₂ Piston and All Piston Rings) (U)	5-122

CONFIDENTIAL

BLANK PAGE

~~CONFIDENTIAL~~



LIST OF TABLES

<u>Table</u>			<u>Page</u>
4-1	(U)	Test Objectives	4-2
4-2	(U)	Summary of Tests Performed During NRX-A6 Test Series	4-3
4-3	(U)	NRX-A6 Power Integral Summary	4-4
5-1	(U)	NRX-A2 Through NRX-A6 Major Reactor Performance Summary	5-2
5-2	(U)	Major NRX-A6 Operating Conditions	5-4
5-3	(CRD)	NRX-A6 EP-IIIA Best Estimated Flow Rate, Chamber Temperature and Thermal Power (U)	5-6
5-4	(CRD)	Steady-State Comparison of EP-IIIA Best Estimate Study with TNT Pre-Test Predictions (U)	5-7
5-5	(CRD)	Comparison of Measured with Calculated Core Pressure Drops for NRX/EST, NRX-A5, and NRX-A6 (U)	5-23
5-6	(CRD)	Comparison of Predicted and Post-Test Calculated Beryllium Reflector Temperatures with Measured Data-EP-IIIA (CRD)	5-26
5-7	(CRD)	NRX-A6 Fuel Element Weight Loss and Visual Data Summary (U)	5-75
5-8	(CRD)	Key to Table 5-7 (U)	5-76
5-9	(CRD)	NRX-A6 Matrix-Coating Performance (U)	5-79
5-10	(CRD)	NRX-A6 Fuel Element Notch Corrosion Summary (U)	5-86
5-11	(CRD)	Peripheral NRX-A6 Fuel Element Performance Summary (U)	5-89
5-12	(CRD)	Overall Bore Weight Loss Performance of NRX-A6 Experimental Elements Based on Preliminary Estimates of Performance Index (U)	5-94
5-13	(CRD)	NRX/EST, NRX-A5, and NRX-A6 Reactor Comparison (U)	5-96
5-14	(CRD)	NRX-A5 and NRX-A6 Manufacturer's Comparisons (U)	5-97

~~CONFIDENTIAL~~

SECTION 1

(U) INTRODUCTION

(U) SUMMARY OF NERVA PROGRAM

(U) The overall objective of the NERVA (Nuclear Engine for Rocket Vehicle Application) program is the development of a solid-core nuclear reactor-powered flight engine for space vehicles. The specific impulse advantages of such a system over chemical-powered rockets, especially in the upper stages of an interplanetary mission vehicle, have been well documented and require no discussion here. The NRX technology phase of the NERVA program, which is now in progress, is a continuation and extension of the KIWI series of tests performed by Los Alamos Scientific Laboratory. Both the KIWI and NRX tests have utilized the test facilities at the Nuclear Rocket Development Station (NRDS) at Jackass Flats, Nevada.

(U) The objectives of the NRX technology phase of the NERVA program were as follows:

- 1) To develop a nuclear reactor capable of operating at full NRX power and temperature (1120 MW and 4090°K) for 60 minutes.
- 2) To evaluate the performance capabilities and to demonstrate the stable operation of the hot-bleed cycle.
- 3) To provide the necessary information for the design of future reactor and engine systems.
- 4) To develop a simple, reliable reactor control system.
- 5) To experimentally determine the extremes of the steady-state operating map of the NRX reactor.
- 6) To demonstrate the multiple full power restart capability of the NRX reactor.

(U) SUMMARY OF PREVIOUS REACTOR TESTS

(U) The reactor tests performed prior to the NRX-A6 endurance test series in the NRX technology program are the NRX-A1 cold flow test series, unfueled graphite core, the NRX-A2 power test series, the NRX-A3 power test series, the NRX/EST engine system test series, and the NRX-A5 power test series (References 1, 2, 3, 4, and 5, respectively). The results of these previous tests are briefly summarized in this section.

(U) Significant accomplishments of these tests were as follows:

(U) NRX-A1

- 1) Verified reactor structural integrity under rated pressure loading.
- 2) Obtained reactor performance data under ambient and cold flow conditions.



(U) NRX-A2

- 1) Provided significant information for verifying the steady-state design analysis for power operation.
- 2) Provided information confirming the suitability of the reactor for operation at the steady-state power levels and temperatures required of the reactor as a component of a nuclear rocket-engine system.

(U) NRX-A3

- 1) Proved the capability of the reactor for continuous nominal operation at, or near, rated power for more than 15 minutes with margin for restart.
- 2) Proved the capability to start up from a low-power, low-flow, steady-state operating condition and to shutdown from a medium power level on liquid-hydrogen flow control only.
- 3) Provided direct performance data on the nozzle and pressure vessel.
- 4) Conclusively demonstrated that the reactor is inherently stable on liquid hydrogen flow control only.

(U) NRX/EST

- 1) Demonstrated the feasibility of the hot-bleed cycle for transient and steady-state operation.
- 2) Demonstrated the capability of the NRX-A reactor to operate at, or near, rated conditions for a cumulative period of approximately 30 minutes. (In addition, the total equivalent run time at rated power was 54.4 minutes.)
- 3) Demonstrated the suitability of control-system concepts and stability for transient and steady-state conditions over a broad area of the operating map.
- 4) Demonstrated the multiple-restart capability with various control modes by starting eight times to an intermediate power level and three times to rated power.
- 5) Demonstrated the capability of the NRX reactor to accomplish bootstrap startup at a chamber-temperature ramp at or above 100°R/sec.

(U) NRX-A5

- 1) The Test Assembly was operated for 29.4 minutes at, or above, chamber temperatures of 3800°R and for 22.4 minutes at, or above, chamber temperatures of 4000°R.
- 2) Operation of a new eight decade neutronic system was demonstrated. The neutronic detectors were located on the test car under the Test Article and used as the neutronic system feedback.
- 3) The reactor was checked out and operated at rated conditions using a temperature control system without the neutronics power control as an inner loop.
- 4) The acceptability of a startup from low power to near rated conditions using programmed LH₂ flow with drums in a fixed position was demonstrated.
- 5) For the first time all poison wires were removed at the Reactor Maintenance, Assembly and Disassembly (R-MAD) Building.

(U) During the NRX-A1 tests, there was no evidence of large, low frequency vibrations (such as had occurred in the KMW reactor series), either forced or self-excited, which would imply possible dynamic instability in the reactor assembly. The absence of these vibrations verified the adequacy of the design of the core support structure. Post-operative examination revealed few signs of the effects of the testing on the reactor components.

(U) The NRX-A2 reactor was operated at, or above, 800 MW for 5 minutes. The liquid hydrogen flow rate averaged 75.6 ± 1.5 lb/sec. During the five (5) minutes power reached 1096 ± 50 MW for 30 seconds, which verified the ability of the reactor and nozzle to withstand the environment at full power. During the test series, reactor stability was demonstrated with constant control drum position for propellant flow rates between 5.2 and 13.5 lb/sec in the power range of 2.0 to 4.7 percent of full power (1120 MW). The fixed control drum test demonstrated the feasibility of controlling the reactor on propellant flow only. Another test was performed with flow rates between 8.3 and 13.5 lb/sec on dewar pressure alone (no pump operating) at a constant 3.4 percent of full power.

(U) Power testing on NRX-A3 consisted of three (3) tests to intermediate or rated conditions. The first test (Experimental Plan IV) was terminated after 3.5 minutes at nominal rated conditions due to a spurious trip of the automatic shutdown system. During Experimental Plan V the reactor was operated at nominal rated conditions for 13.1 minutes. Experimental Plan VI was a medium power mapping and controls test. During this test, the reactor was operated over the operating map up to 500 MW power and 3700°R chamber temperature. Fixed control drums mode (power being controlled with propellant flow rate only) was utilized during startup and during part of the subsequent mapping experiments. This test conclusively demonstrated that the reactor is inherently stable on liquid hydrogen flow control only, which was a major step in the continuing effort to obtain a simple, reliable control system for future NERVA engines.

(U) The NRX/EST test series coupled an NRX reactor with a "breadboard" arrangement of engine components in which the components were connected in a flight functional configuration. During this test series, the hot-bleed, bootstrap principle of nuclear rocket engine operation was utilized for the first time. In accomplishing the endurance objective, the engine was operated for a total of 143.8 minutes, of which 105.6 minutes were at thrust chamber temperatures above 1700°R. 23.7 minutes were at power levels at, or above, 1000 megawatts and 16.7 minutes were at thrust chamber temperatures at, or above 4000°R.

(U) The prime objective of the NRX-A5 test program was to operate at design conditions for a total accumulated time of forty (40) minutes. Two tests to rated conditions were performed, Experimental Plan III (EP-III) was the first full power test. Shortly after reaching the top of the startup ramp of EP-III, power oscillations of ± 300 MW resulted from a noise signal from one of the control thermocouples. This thermocouple was automatically rejected as an input to the control system and the test continued. After 7.9 minutes at, or above 4000°R nozzle chamber temperature the test was terminated when the level in the Li_2 storage dewars reached the low level limit cut point.



(5) Significant operations of EP-IV were (1) fixed drum startup from 20 kW and 10 lb/sec flow to near rated conditions and (2) 14.6 minutes operation at, or above, 4000°R nozzle chamber temperature and 1000 MW. EP-IV was terminated by pre-test established limit of 145 degrees control drum angle position. Although several minutes of operating time remained on the core, the test series was terminated to preserve the core for post-operative examination.

CONFIDENTIAL



SECTION 2

(CRD) SUMMARY AND CONCLUSIONS (U)

(CRD) SUMMARY (U)

(U) The NRX-A6 test series was successfully conducted at the Test Cell "C" facility of the Nuclear Rocket Development Station, Jackass Flats, Nevada, between 27 November 1967 and 15 December 1967.

(CRD) The NRX-A6 test was extremely successful and exceeded its primary objective which was to operate at rated conditions for 60 minutes or to a predetermined loss of reactivity. The total run time of 62 minutes above a nozzle chamber temperature of 4100°R more than doubled the full power and temperature endurance of previous reactors with a reduction of 75 to 80 percent in the fuel element time rate of corrosion compared with that observed in the NRX/EST and NRX-A5 reactors.

(U) All secondary test objectives, as defined in Table 4-1 were also achieved. Pre-test steady-state and transient predictions were, with a few exceptions, in good agreement with test results. A gonu analog systems model for Test Cell "C" in the NRX-A6 Test Configuration was developed and verified.

(CRD) Total reactor reactivity, loss due to carbon, uranium, and niobium was 0.85\$ which was significantly lower than previous reactors, i.e., 3.2\$ for NRX/EST and 2.1\$ for NRX-A5. Change in control drum cold critical angle was from 97.0 degrees at initial criticality to 100.5 degrees following the power run as compared with 99.1 degrees to 147.6 degrees for NRX/EST and 99.3 degrees to 137.3 degrees for NRX-A5.

(U) All reactor control systems performed well. All reactor control systems performed almost exactly as predicted except that the temperature controller was a little more sluggish than predicted. The temperature controller held the measured temperature to within 50°R of the demand except during transient conditions. During the ramp from 2000°R hold of Experimental Plan (EP)-IIIA to design conditions, the measured temperature lagged demanded temperature by approximately 3 seconds or 100°R. Temperature trim operations appeared to be smooth and responsive. One false scram occurred on the first attempted full power run. This inadvertent shutdown was due to the noise sensitivity of the hardware used to implement the minimum drum position scram. The difficulty was isolated and corrected prior to EP-IIIA.

(U) The performance of the NRX-A6 internally mounted reactor instrumentation was excellent. The zero shifts noted for several differential-pressure transducers during the full power runs were expected and were caused by purposely exceeding the range of the transducers. The performance of externally mounted instrumentation was also very good, and described the environment that existed in the test assembly. One anomaly which is being investigated is the low reading chamber

CONFIDENTIAL

CONFIDENTIAL

temperature thermocouples which occurred during the one hour full power hold of EP-111A. The four thermocouples indicated an average chamber temperature of approximately 3650°R, whereas the best estimate of chamber temperature was in the range of 4000 to 4400°R. This difference is larger than the 100°R difference that could result from the measurement and data system uncertainties. Investigation revealed no hardware and/or system anomalies that would invalidate the measured temperature. Analysis is presently being performed to determine the upper and lower limits of flow and temperature distribution which could result from a lack of complete mixing within the chamber.

(CRD) Disassembly and post-operative examination of the reactor was started on 20 December 1967. Disassembly of all subassemblies was completed on 3 March 1968. The results of the disassembly and post-operational examinations confirmed that the NRX-A6 reactor can operate at or above rated conditions for 60 minutes without deleterious effects on reactor system components. One significant anomaly that did occur, however, were the axial and circumferential cracks which were found in the beryllium reflector. These cracks which occurred near the end of the full power hold had no significant effect on any parameter measured during testing. Considerable analysis of the reflector has since been performed from the standpoint of materials properties, design requirements and reactor operating parameters. As a result of this analysis, it was concluded that the cracks occurred about two minutes before the end of the full power run and resulted from thermal stresses in the reflector rings.

(CRD) The performance of the core was the most optimistic result obtained from the NRX-A6 test. The interior fuel element and the central elements survived the full hour run with no structural damage and a smaller than expected corrosion weight loss.

(CRD) The tight core experiment (close element envelope and average size tolerance and selective assembly of central elements) was very successful, eliminating the problem of fuel element surface corrosion.

(CRD) Performance of the NRX-A6 fuel elements typically was characterized by inter-element bonding, mild surface corrosion, low pinhole densities, lower mid-band weight losses and higher hot end weight losses relative to NRX-A5 and excellent corrosion resistance and integrity of the aft unfueled tip. The inter-element bonding was caused by pyrolytic graphite deposition at the core mid-plane. Except for heating disassembly problems, this effect was not harmful to the NRX-A6 operation.

(CRD) Midband weight losses of typical NRX-A6 fuel elements appeared to be approximately one-tenth that of the NRX-A5 fuel elements. The hot end weight losses for both the NRX-A6 and NRX-A5 fuel elements were of the same order of magnitude. NRX-A6 demonstrated excellent corrosion resistance and integrity in the aft non-fuel tip joints. Some variation in corrosion performance was noted between the various matrix-coating batch types and with respect to core radius. These variations were not nearly as pronounced, however, as had been observed in previous NRX reactor tests.

CONFIDENTIAL

~~CONFIDENTIAL~~



(CRD) Notch-type corrosion patterns similar to those observed on peripheral NRX-A5 elements were again observed on the peripheral faces of some NRX-A6 peripheral elements, although the fraction of peripheral NRX-A6 elements affected was lower. The post test analysis on the peripheral fuel elements show that this notching was due to high thermal stresses at the peripheral corners of certain fuel elements. This high thermal stress occurred during startup and was due to the combined effects of the heat flow from the core to the hot buffer filler strips and unfueled partial elements, and the cooling effect of a high leakage flow between the filler strips at locations where shifting of the element filler strips created large flow gaps.

(CRD) The weight losses observed in the NbC matrix-additive and Nb resinate impregnated experimental elements was somewhat higher than that of comparable core fuel elements. Flexure strength changes corresponded to the axial variations in fuel element incremental weight loss.

(CRD) Chemical and radiochemical measurements performed on fuel elements indicated that there were no significant anomalies or asymmetries in radial or axial fission distributions throughout the core. The total integrated energy generated in the reactor was $1.57 \pm 0.07 \times 10^{23}$ fissions or 4.85×10^{12} watt-seconds. This is equivalent to 66.8 minutes at rated power as compared with 54.2 minutes for NRX/EST and 32.4 minutes for NRX-A5.

(CRD) During the NRX-A6 test, a pneumatic control drum actuator, similar in design with actuators to be used in the advanced NERVA reactor, was mounted side-by-side with the NRX-A6 reactor to obtain data on the effects of a radiation environment on component performance and operation. Very little change in performance occurred after radiation exposure. The results indicate that the pneumatic control drum actuator will perform as designed in a radiation field well in excess of the predicted XE engine field, and approximately equivalent to that expected on the advanced NERVA reactor.

(U) Several other significant accomplishments achieved during the test series were (1) demonstration of the adequacy of the Test Cell "C" emergency LH₂ cool-down system, (2) demonstration of the capability of the reactor outlet gas filtering device (FROG) to reduce reactor effluent contamination in the immediate Test Cell "C" area during LN₂ pulse cooling, and (3) determination of the reactivity worth of the Test Cell "C" facility shield and its effectiveness in reducing radiation exposure demonstrated.

(CRD) CONCLUSIONS (U)

(CRD) The successful completion of the NRX-A6 test resulted in the following significant conclusions:

(CRD) 1) The results of the NRX-A6 test demonstrated the endurance capability of the NRX-A6 reactor at rated conditions.

(U) 2) A good analog systems model for the reactor and Test Cell "C" in the NRX-A6 test configuration was developed and verified.

~~CONFIDENTIAL~~

CONFIDENTIAL

(U) 3) Test Monitor Room operation was developed to give the capability of allowing continued operation with a major discrepancy in the indicated primary control variable.

(CRD) 4) Demonstration of the capability of a grafoil wrapper to provide radial flow impedance at the core periphery was accomplished; verification of the applicability of an out-of-pile core periphery test device was also accomplished.

(CRD) 5) Observed damage confirmed the decision to avoid periphery designs in the future which utilize "hot" filler strips and irregular peripheral cluster support devices capable of being influenced thermally by cooler peripheral flows.

(CRD) 6) The combination of improved fuel element coating techniques, across flats dimensional control, attention to coefficient of thermal expansion, flattened core power distribution, and changes in core interstitial pressure distribution resulted in marked improvements in core corrosion performance.

(CRD) 7) Fuel bore corrosion improvement efforts, primarily in the mid-band region have resulted in elements capable of 60 minute one-cycle operation at exit gas temperatures up to 4440°R with weight losses of approximately 13 grams.

(CRD) 8) Comparison of NRX-A6 Quality Control corrosion test data and subsequent parametric corrosion tests of NRX-A6 elements indicated reasonably successful correlation of corrosion test results with reactor results. Further, the corrosion test results indicated that at NRX conditions, two and perhaps more cycles could be tolerated for 60 minutes operating time.

CONFIDENTIAL

~~CONFIDENTIAL~~



SECTION 3

(CRD) TEST ASSEMBLY AND FACILITIES DESCRIPTION (U)

(U) The NRX-A6 test assembly consisted of a nuclear subsystem, pressure vessel, and nozzle mounted on a test car. The test assembly, with its associated piping, shielding, controls, and instrumentation was installed into the Test Cell 'C' facility at NRDS. The Test Cell 'C' complex includes fluid storage (gaseous and liquid hydrogen and nitrogen, helium, and process water), piping, and control systems necessary to complete a test series on an upward firing reactor system.

(CRD) REACTOR (U)

(CRD) The NRX-A6 reactor, which had the same general configuration as the NRX-A2 through NRX-A5 reactors, was an epithermal nuclear reactor consisting of a fueled graphite core, surrounded by a beryllium reflector assembly, and enclosed in an aluminum pressure vessel. The principal differences in the NRX-A6 design from previous reactors was the elimination of the graphite inner reflector and consequent modifications in core periphery and core lateral support system, and that the reactor was supported from the aft (nozzle) end. These design differences resulted from two of the NRX-A6 design objectives: (1) that the reactor have a basic structure applicable to reactors of greater power density and size, and (2) that the core periphery and lateral support system design lead to the reduction of core corrosion.

(CRD) Figures 3-1 and 3-2 show some details of the mechanical configuration and flow paths of the NRX-A6 reactor. Coolant enters the test assembly at the nozzle torus and passes through the 186 nozzle tubes into the reflector inlet plenum. The coolant is then divided among channels through the reflector, control drums, and reflector/pressure vessel annulus, is discharged into the reflector outlet plenum, and proceeds through the first pass (peripheral section) of the simulated shield into the dome end plenum. The direction of flow is then reversed, with the coolant flowing through the second pass (central section) of the shield and through the flow screens which assure removal of any particles sufficiently large to cause blockage of a fuel element orifice. The flow continues through the core support plate and into the core inlet plenum. There it is divided into parallel flow paths through fuel element, tie rod, and unfueled partial element channels, and lateral support system. Flow distribution is approximately 92.2 percent through the fuel elements, 6 percent through the tie rod channels, 0.3 percent through the unfueled partial elements, and 1.5 percent bypass flow through the lateral support system. The effluent of these flow systems exhausts into the nozzle chamber, providing the required mixed mean temperature and flow rate. From the nozzle chamber the propellant is expanded through the nozzle throat and exhausted to the atmosphere.

(U) The following subsections present a brief description of the principal NRX-A6 reactor components and identify the major design changes from the NRX-A5 reactor. A more detailed description of the reactor may be found in References 6 and 7.

~~CONFIDENTIAL~~

CONFIDENTIAL

NRX-A6 REACTOR CONFIGURATION

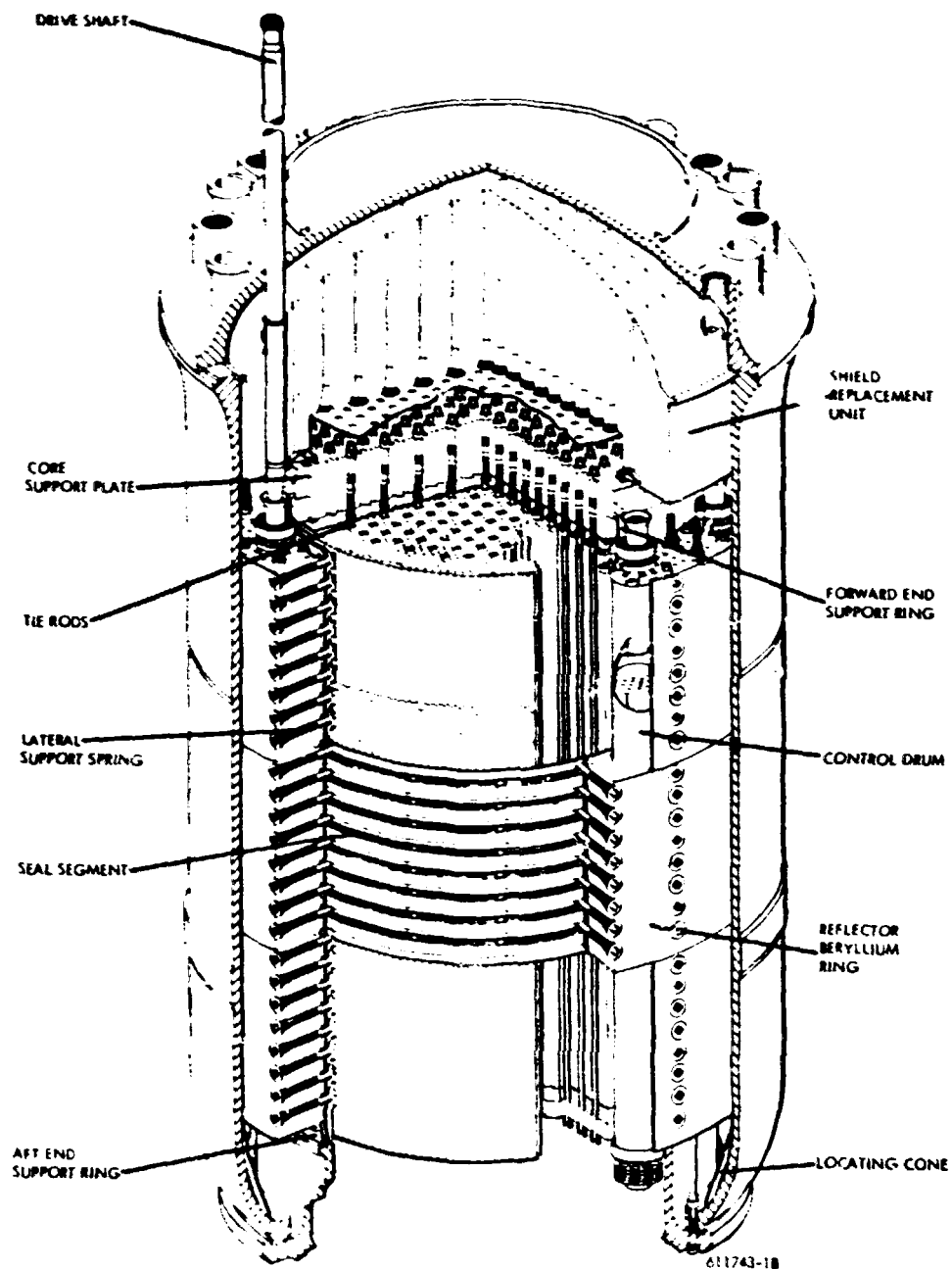


Figure 3-1. (CRL) NRX-A6 Reactor Configuration (U)

CONFIDENTIAL

~~CONFIDENTIAL~~

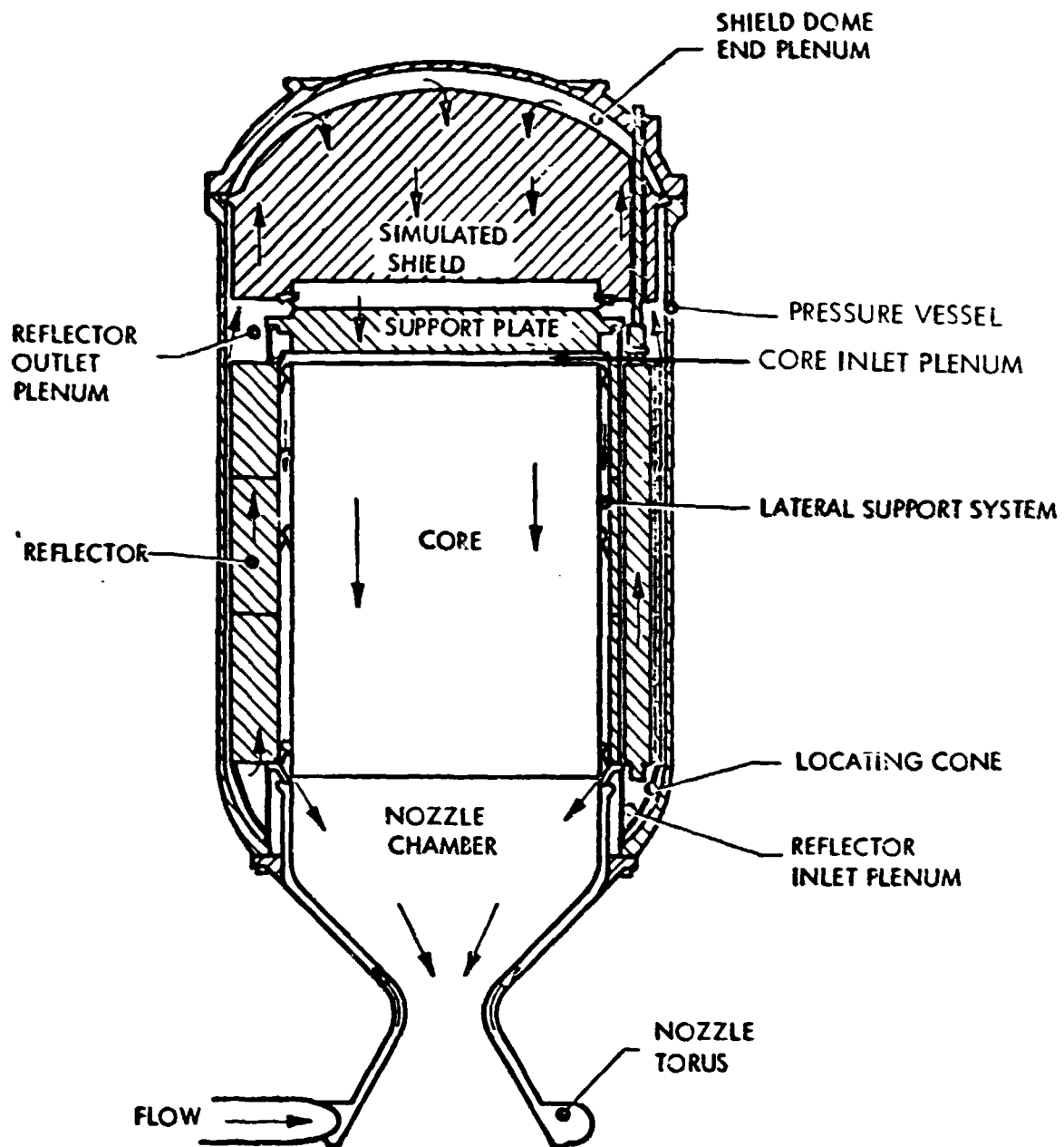


Figure 3-2. (CRD) NRX-A6 Reactor Flow Path (U)

~~CONFIDENTIAL~~

~~CONFIDENTIAL~~

(CRD) Core and Core Periphery (U)

(CRD) The NRX-A6 core was nominally made up of clusters of six fuel elements and a central, unfueled element. Each cluster was supported axially by means of a tie rod attached to the support plate. The tie rod passed through the central element and was connected to a support block at the aft end of the cluster. Irregular cluster assemblies were used at the core periphery. Partial unfueled elements and filler strips completed the cylindrical shape of the core at its periphery.

(CRD) To minimize fuel element corrosion and to avoid the hot buffer filler strip breakage that occurred in the NRX-A5 reactor, several design modifications were incorporated into the NRX-A6 core periphery. Hot buffer filler strips were used without coolant holes and with niobium carbide (NbC) coating on the radial outward facing surface. A graphite pyrofoil wrapper covered the outside surface of the filler strips. Forty inch long pyrographite insulating tiles were placed outboard of the wrapper and held in place by the lateral support seal forces (Figure 3-3). The wrapper extended from Station 12 to 52 and consisted of six staggered layers of 5-1/2 mil thick pyrofoil with 24 sheets in each layer. The pyrofoil was designed to eliminate radial inflow from the periphery and the core interelement gap thereby reducing filler strip corrosion and eliminating thermal stress cracking of the peripheral fuel elements. The wrapper permitted seal chamber pressure to be increased, thereby increasing bundling pressure on the core, reducing interelement gaps and thus reducing severity of pinhole corrosion. A total average bundling of about 40 psi was produced using controlled flow through the periphery seals, in comparison to the NRX-A5 filler strip bundling of about 15 psi. Testing also showed that the pyrofoil wrapper on the external surface of the filler strips was effective in impeding radial inflow and could bridge gaps without tearing due to the pressure drop across the wrapper. A 3 to 5-mil slip plane of pyrofoil was placed between the coated fuel periphery and the filler strips to provide a reduced coefficient of friction for relative motion between the fuel and fillers.

(U) Radial constraint of these components was achieved by the lateral support system as shown in Figure 3-1.

(U) By comparison, NRX-A5 did not have a pyrofoil slip plane or wrapper, and only 120 degrees of the periphery were covered with pyrofoils external to the filler strips. The remainder of the periphery had pyrofoils internal to the filler strips as in prior NRX reactors.

(CRD) To insure that the filler strips could survive the expected startup and shutdown transient conditions, the average steady-state gap between filler strips (Station 12 to 48) was increased from 0.0005 inches (NRX-A5) to approximately 0.0030 inches. This was expected to minimize circumferential bridging between filler strips even during emergency shutdown. Also the minimum gap between the filler strip key-ways and forward ledge of the keys on the elements was made equal to the maximum possible gap between the aft end of the filler strips and the support ledges. This was designed to prevent the filler strips from axially loading the forward edge of the keys by providing adequate axial clearance.

~~CONFIDENTIAL~~

~~CONFIDENTIAL~~

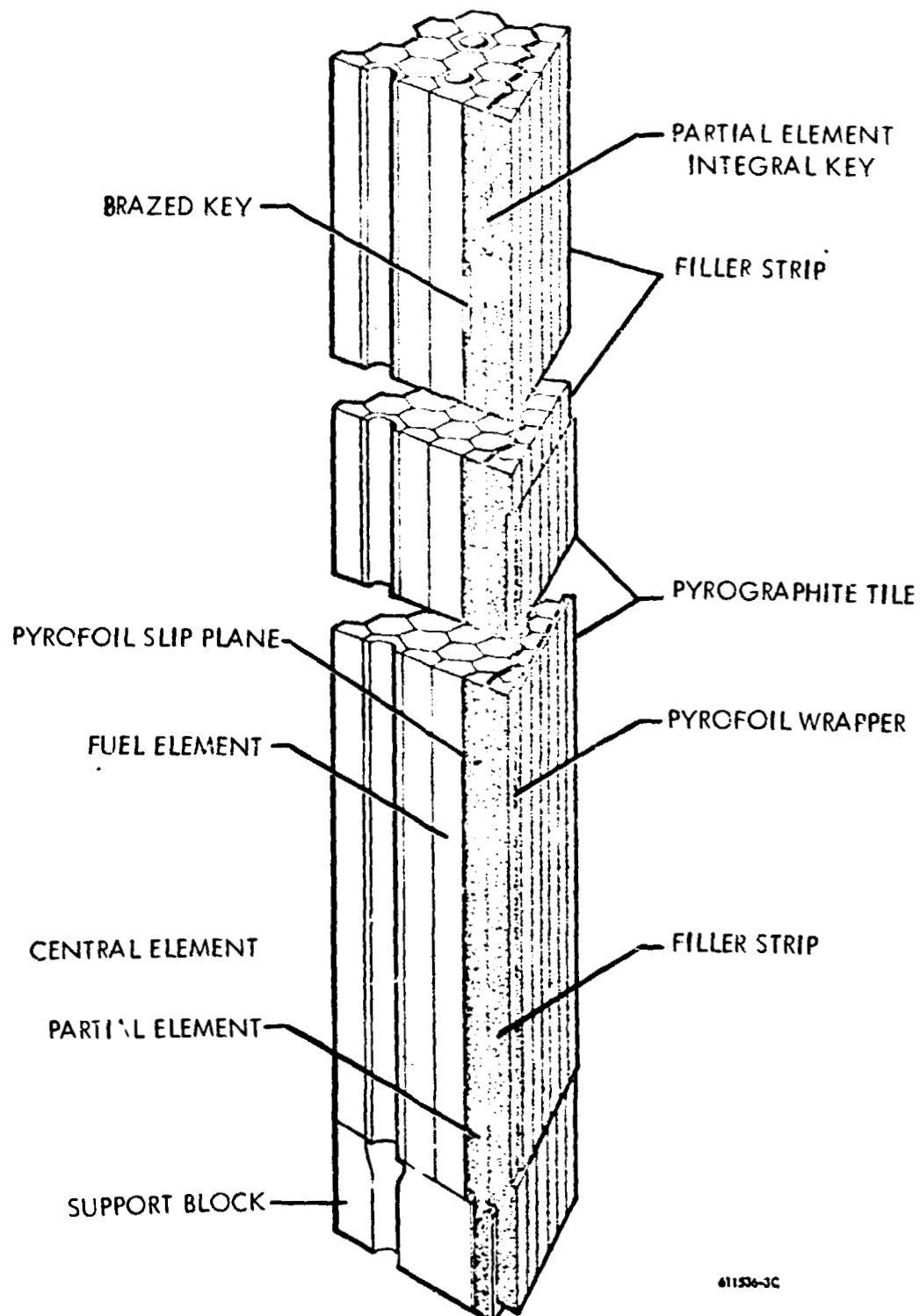


Figure 3-3. (CRD) Trimetric View of Filler Strip Periphery (U)

~~CONFIDENTIAL~~

CONFIDENTIAL

(CRD) In the NRX-A5 reactor test, particles of graphite from broken forward ends of the filler strips had entered the core inlet plenum between the core support plate and forward ends of the filler strips. These particles became lodged between the core support plate and cluster plate, ultimately resulting in severe local overheating and accelerated corrosion of a fuel element and support block. In the NRX-A6 reactor, a particle catcher was incorporated at the inlet end of the core periphery to eliminate this potential problem. The design of the particle catcher is shown in Figure 3-4 and consists of numerous metal finger springs trapped against the aft side of the core support plate by a bolted metal ring. Stress analysis of the particle catcher indicated that the clearance between segments of the particle catcher was sufficient to prevent interference during reactor operation.

(CRD) Fuel Cluster Support Blocks (U)

(U) In previous reactors, the support block extended aft of the tie rod. This extension or "skirt" was lined with a pyrographite cup, and the combination of skirt and cup provided the necessary thermal protection of the tie rod and support blocks.

(CRD) The support blocks used in NRX-A6 were "skirtless" and protection cups made of graphite-niobium carbide composite and a pyrographite cup were used to protect the tie rod ends which would otherwise be exposed to the core exit temperature and flow environment. Tungsten protection cups and pyrographite cups were used for the irregular clusters at the core periphery and for the exit gas thermocouples. The tungsten and composite cups were used for the first time in the NRX-A6 reactor.

(CRD) Fuel Element (U)

(CRD) Changes from NRX-A5 in the design of the regular fuel elements, consisted of: (1) changes in fuel loading, (2) fuel element coatings, and (3) fuel raw materials and processing. The core had fourteen loading zones which required eleven separate fuel loadings ranging from 132.4 grams/element (enriched to 93.15 percent U-235) to 23.9 grams/element. The increased number of loading zones was designed to provide minimum variation in power density across the core, thereby reducing pressure differences between bores to decrease pinholing. Niobium carbide (NbC) channel coating thickness was decreased to improve NbC adherence and crack distribution, and molybdenum overcoating was applied on fuel element channel bores to reduce midband corrosion. New improved requirements were added to the fuel element specifications to make the elements more uniform. These requirements consisted of: (1) a tolerance on the transverse coefficient of thermal expansion limiting the range to $2.54 \pm 0.24 \times 10^{-6}$ in./in.-°R (NRX-A5 nominal ranged from 2.5 to 2.8×10^{-6} in./in.-°R), and thus minimizing thermally induced stresses and the opening of hot end gaps due to differential growth; (2) tighter dimensional tolerances of both the fueled and unfueled elements by reducing the across flats tolerance for all fueled elements, except two coated peripheral rows, from ± 0.001 to ± 0.007 inches, and controlling across flats size for fueled and unfueled elements, with and without coating, to an average of 0.7530 ± 0.0001 inches, and thereby improving core bundling by reducing individual element size

CONFIDENTIAL

~~CONFIDENTIAL~~

As nuclear
lab tory

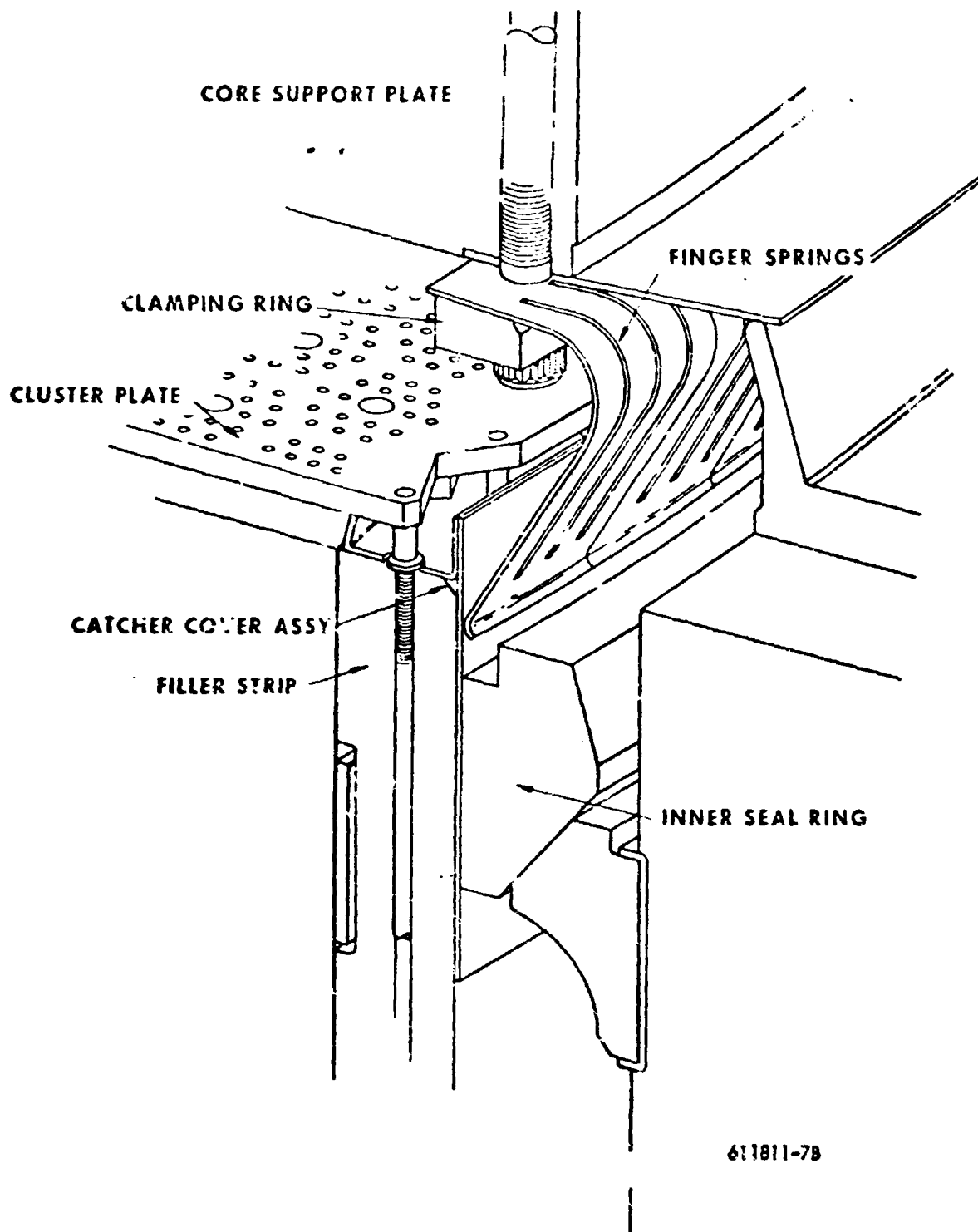


Figure 3-4. (CRD) NRX-A6 Particle Catcher (U)

~~CONFIDENTIAL~~

~~CONFIDENTIAL~~

variation; (3) changing the graphitization cycle from 2200°C for 1 hour to 2200°C for 3 hours to assure more uniform element sizing and improved dimensional stability; (4) modification of the fuel element aft end from the undercut to tapered configuration; (5) utilization of a less permeable matrix (170 cc/min maximum for full body leakage using 10 psig air) to reduce porous flow through the matrix; (6) improved graphite flour blend based on electric furnace tests for improved corrosion performance; (7) use of uniform fuel beads from single supplier for improved corrosion performance; and (8) increased flexure strength from 4440 ± 500 psi for NRX-A5 to 5100 ± 500 for NRX-A6 for increased design structural margin. To provide a performance evaluation of the variations in fuel processing between Westinghouse (WNCO) processed fuel elements and Oak Ridge (Y-12) fuel elements, a statistically designed fuel element performance experiment was incorporated into the core. The elements used were extruded and coated at both WNCO and Y-12 utilizing four extrusion-coating combinations. In addition, elements made with various new coatings and new fuel matrix compositions were included in the core. The specific placement of elements within the core is given in Reference 6.

(CRD) Reflector (U)

(CRD) Previous NRX-A reactors used two reflectors: an inner, graphite cylinder, and an outer cylinder made up of twelve full-length, beryllium sectors. The functions of these two reflectors were combined in the single NRX-A6 reflector. In addition to its nuclear function, the reflector was a major structural component in that it contained the control drums, housed the lateral support system springs and plungers and transmitted the axial core load from the support plate to the nozzle flange as shown in Figure 3-1.

(CRD) The reflector assembly consisted of three identical annular beryllium rings stacked to form a continuous cylinder 52 inches high with an ID of 37.662 and OD of 49.460 inches. A titanium core support ring extended from the inner edge at the forward end of the reflector to support the core via the core support plate. The aft end support ring extended from the inner edge at the aft end of the reflector to the nozzle, providing the support for the reflector and the core in the pressure vessel. Eighteen titanium tie bolts axially clamped together the three beryllium stacked rings, as well as attaching the core support ring and the aft end support ring.

(U) There were several axial penetrations in the reflector including the 4.300 inch diameter holes for the control drums and coolant holes spread throughout the cross section, with a greater number of coolant holes at the inner periphery. The control drums used in the NRX-A6 reactor were essentially the same as those used in the NRX-A5.

(U) The reflector assembly was cooled by hydrogen after the propellant left the nozzle tubes. Part of this flow was diverted to the pressure vessel annulus where it cooled the pressure vessel and the outside of the reflector. The balance of the coolant flowed through holes in the reflector control drums.

~~CONFIDENTIAL~~

~~CONFIDENTIAL~~



(CRD) Lateral Support and Seal System (U)

(CRD) The inside diameter of the beryllium cylinder has 24 circumferential grooves which locate and support the outer seal segments (seal rings) of the 24 rows of the core periphery seals. The lateral support seal segments are shown in Figure 3-5. Each core periphery seal ring is made up of twelve overlapping segments and consists of both an inner ring sealing against the core periphery, and an outer ring sealing against the reflector. The outer seal segments are fastened to the reflector with latches. Radial penetrations in the reflector provide housing for the lateral support plunger assemblies shown in Figure 3-5. Two plungers bear against each segment of the inner seal rings. Due to the design of the seal rings, a wedging action takes place which forces the inner seal segments against the core periphery and the outer seal segments against the reflector. Thus contact (and therefore the seal) was maintained as the core underwent thermal expansion. Lateral support was accomplished by coil springs which exerted force on the core outer diameter. Force was transmitted from the springs to the inner seal segments by plunger pins. Sleeves and seals were placed around the plunger pins where they intersected axial coolant holes near the inner surface of the reflector. These sleeves and seals prevented reflector coolant from leaking into the core periphery.

(U) Holes, drilled in the seal segments, provided controlled coolant flow through the lateral support system and maintained the desired axial pressure profile to insure adequate core bundling. Three rows of heavier springs at the forward end were used to replace the bundling band. Lateral support in previous NRX-A reactors used a titanium bundling band at the top of the reactor as well as seal rings of rectangular cross section and leaf springs housed in the inner reflector.

(CRD) Core Support Plate and Axial Support System (U)

(CRD) The NRX-A6 core was supported axially by means of a core support plate at the forward end, and tie rods, as shown in Figure 3-1. The 289 fuel cluster tie rods extended through and attached to the support plate. The support plate was attached to the beryllium reflector assembly by means of the forward end support ring. The reactor was attached to the pressure vessel by six reflector tie bolt standoffs and the reflector axially loaded by the nozzle through the aft end support ring, as shown in Figure 3-6. In the NRX-A5 reactor, a dome end support ring, connected to the forward vessel flange, supported the reactor.

(U) Shield and Screen Assembly

(U) A domed aluminum replacement shield was used in the NRX-A6 reactor to simulate the flow characteristics of a radiation shield in the NRX reactors as was done in prior reactors. The replacement shield was cooled by the propellant as it left the reflector and pressure vessel annulus.

(U) Annular passages around the drum drive shafts along the periphery of the shield, and holes drilled in the shield, directed the coolant leaving the reflector and pressure vessel annulus to the dome end of the pressure vessel. The

~~CONFIDENTIAL~~

CONFIDENTIAL

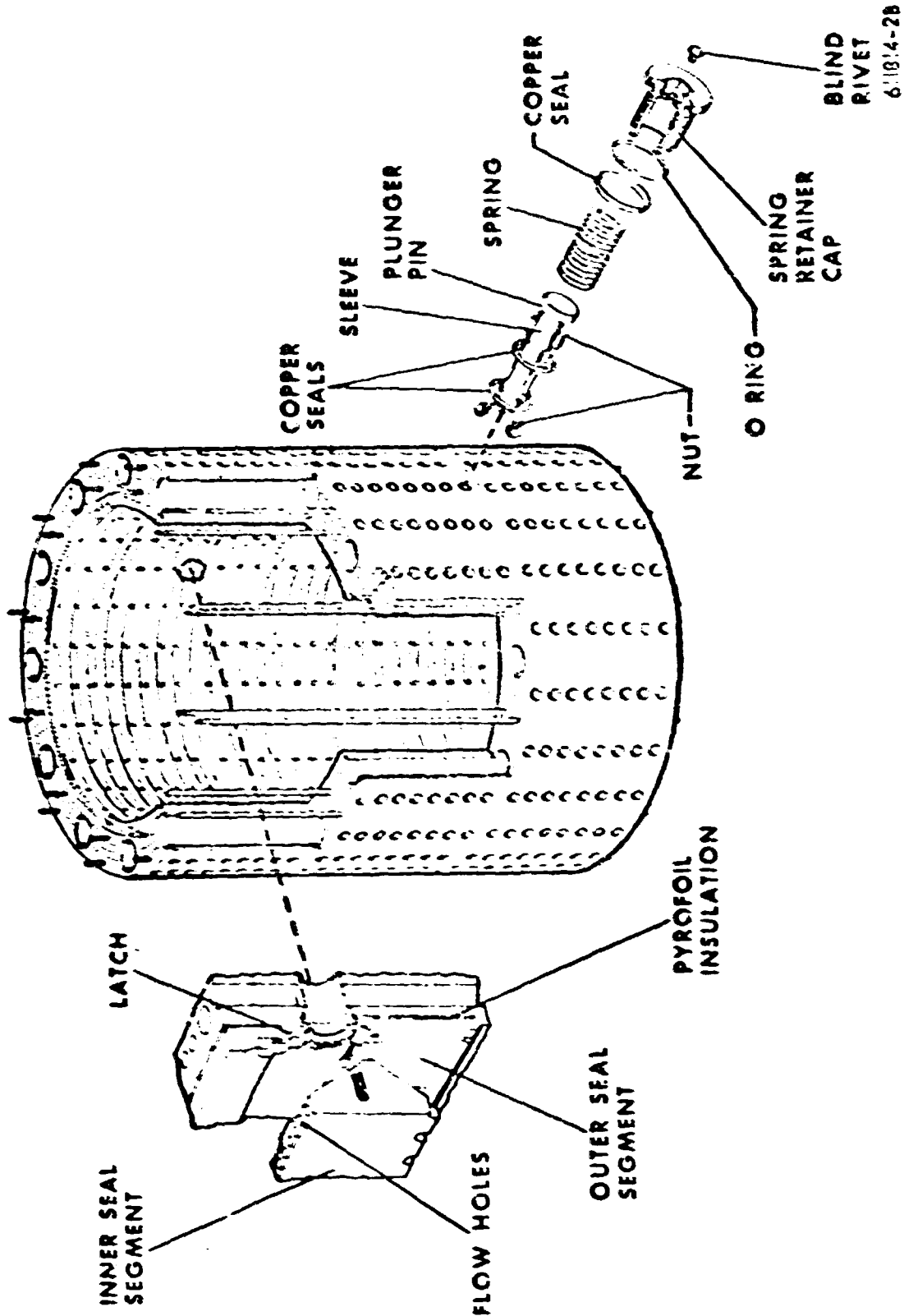
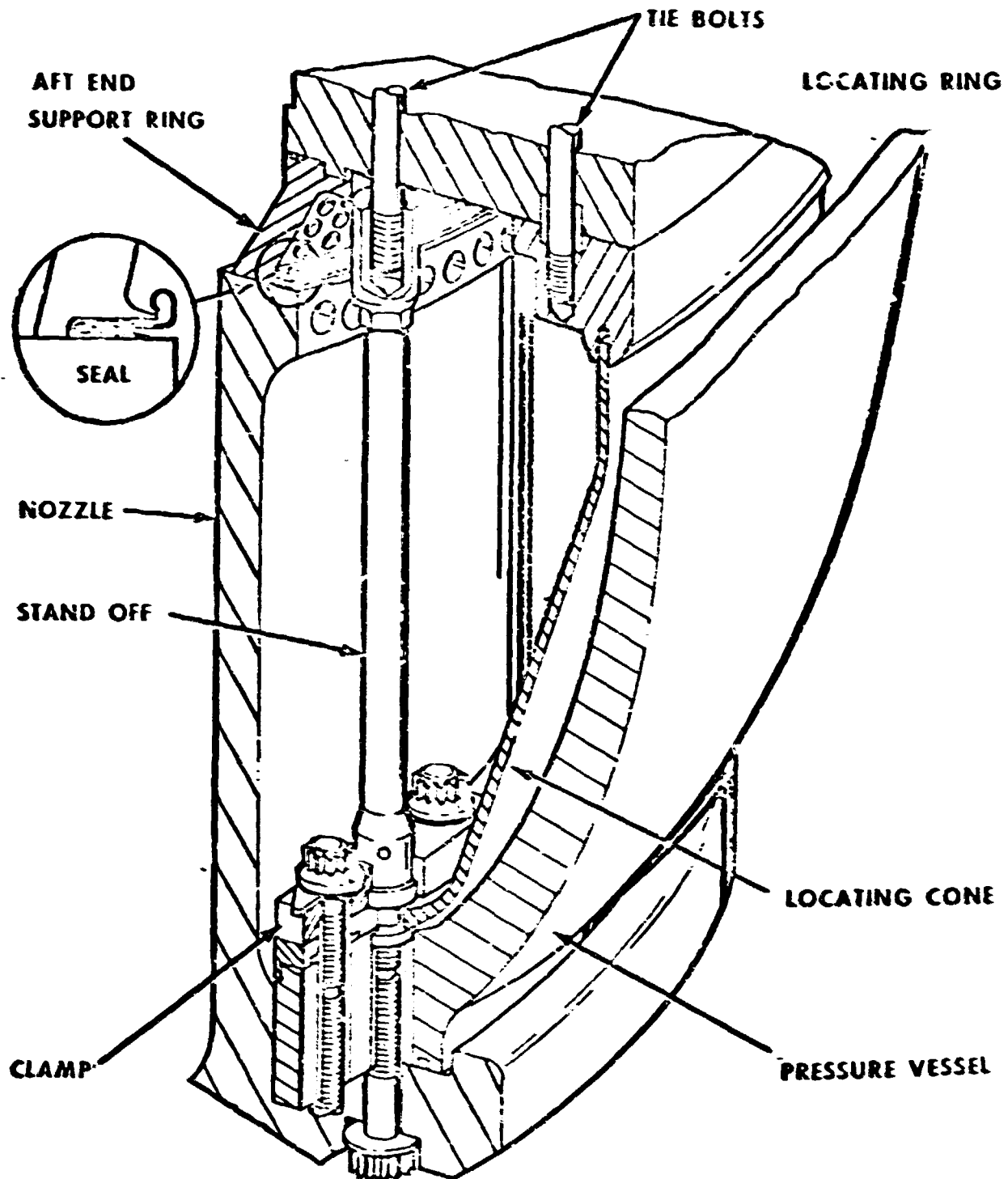
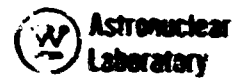


Figure 3-5. (CW) HBY-AF Reflector/Lateral Support Arrangement (U)

CONFIDENTIAL

CONFIDENTIAL



611812-23

Figure 3-6. (CRD) Aft End Support System (U)

CONFIDENTIAL

CONFIDENTIAL

(THIS PAGE IS UNCLASSIFIED)

coolant then flowed through holes in the central part of the shield in the direction of the support plate and core. Individual screens were placed at the aft end of each of the second pass holes in the shield; where they served to remove particles from the propellant. Figure 3-1 shows the shield and individual screens. The NRX-A5 reactor differed from NRX-A6 in that it contained one large particle screen between the shield and support plate.

(U) TEST FACILITIES

(U) The test facility used at NRDS to conduct the NRX-A6 test series was the Test Cell "C" complex. Cryogenic, gaseous, hydraulic, pneumatic and electrical systems are provided at Test Cell "C" to support either NRX or Phoebus type reactor testing at this facility. A brief description of these systems and their primary function is given below. A more complete description of all Test Cell "C" systems can be found in Reference 8. A schematic of the basic Test Cell "C" flow system is shown in Figure 3-7.

(U) Propellant Feed System (L System in Figure 3-7)

(U) The LH₂ propellant feed system consisted of, (1) Dewars 1 and 2, (2) the vacuum jacketed piping from the Dewars to the turbopump, (3) the turbopump assembly, and (4) the vacuum jacketed piping from the turbopump to the test cell interface.

(U) The primary function of the system was to deliver LH₂ to the reactor at the required flow rates and pressures and to provide LH₂ to the Turbine Energy Source (TES) exchanger for turbine drive usage.

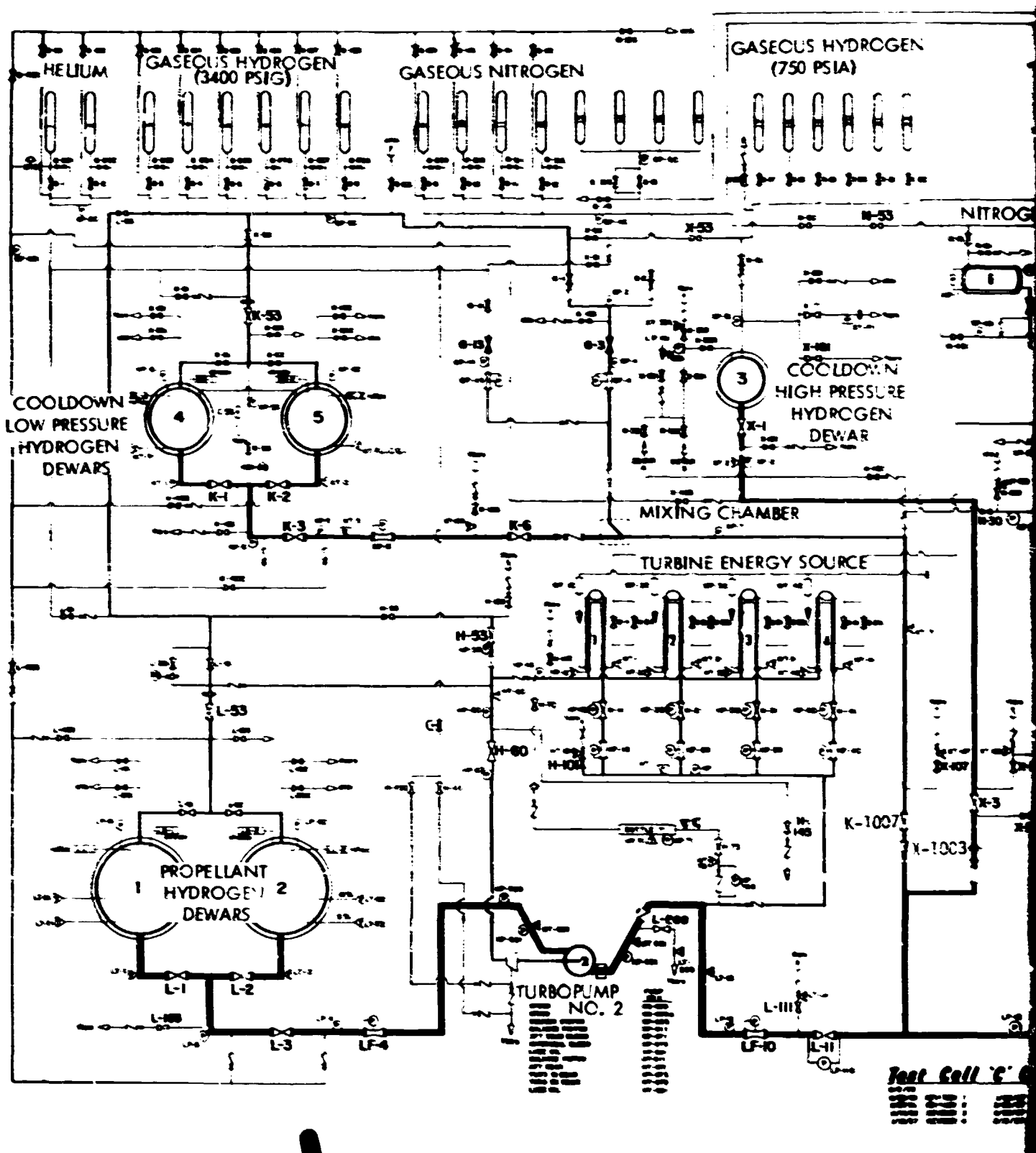
(U) The liquid hydrogen supply for the propellant feed system was stored in Dewars 1 and 2. The total deliverable capacity from both of these vacuum jacketed Dewars was approximately 1,012,000 gallons or 600,000 lb of LH₂ when pressurized up to a maximum of 75 psig. This capacity is substantially in excess of the requirements for a one hour run of an NRX-A type system.

(U) The Dewars were pressurized to approximately 75 psig by the G₂ storage bottles or the TES in order to maintain the required net positive suction head at the turbopump assembly inlet.

(U) Two Mark XXV turbopumps, mounted in parallel, were available for increasing this pressure to the required levels. Each turbopump consisted of a pump capable of delivering 165 lb/sec with a pump discharge pressure of 1800 psi at 34,000 rpm, well above the maximum NRX-A6 requirements. Hence, only one pump (No. 2) was used for NRX-A6, with the line to the other pump blocked. The turbine was a five stage gaseous hydrogen turbine capable of operating at 22,000 HP. At the outlet of the turbopump some LH₂ was bled off and fed through an LH₂/hot water counterflow heat exchanger or Turbine Energy Source (TES) to produce sufficient ambient temperature G₂ to drive the turbopump assembly. At NRX-A6 rated conditions, approximately 9.4 lb/sec of LH₂ was bled from the main propellant feed system to supply the TES, while 72 lb/sec was being delivered to the reactor.

(THIS PAGE IS UNCLASSIFIED)

CONFIDENTIAL



BLANK PAGE

The gaseous hydrogen required as the energy source for the turbopump was initially supplied from the gaseous hydrogen storage bottles. However, once a stable bootstrap operation was completed, the turbopump was driven by GH_2 from the TES. During the NRX-A6 full power test, the turbopump operated at approximately 23,500 RPM, while delivering a total flow rate of 112 lb/sec at a pump discharge pressure of 940 psig and a specific speed of 1200.

(U) The main propellant line from the turbopump to the reactor contained two venturis for flow determination, LF-10 and BF-13. Downstream of LF-10 was the main propellant line control valve L-11 and a bypass line containing valve L-111.

(U) To insure that the turbopump operated away from the pump stall region, a specific speed loop was provided. The function of the control system was to bypass pump flow through the pump bypass valve L-209 to maintain a constant ratio of pump flow rate to speed; thus providing sufficient stall margin for the turbopump during normal operation. The turbopump Specific Speed Control Valve (L-209) was located in a 6-inch line which branched off from the pump discharge line immediately downstream of the turbine flow meter (HF-691). This valve was used in conjunction with the specific speed control loop to operate the pump at a preselected specific speed by venting the required quantity of liquid hydrogen to the main flare stack. During the NRX-A6 full power test approximately 30 lb/sec of LH_2 was vented to the flare stack to maintain a specific speed of 1200.

(U) Turbine Drive System (H System in Figure 3-7)

(U) The turbine drive system consisted of, (1) the TES heat exchangers and associated piping and components, (2) the vacuum jacketed piping from the pump discharge piping to the TES inlet manifold, (3) the discharge piping from the TES outlet manifold to the turbine inlet control valve (H-60), and (4) the initial turbine drive system which included the piping from the Dewar pressurization header to the TES discharge piping.

(U) The primary function of the system was to provide sufficient ambient temperature gaseous hydrogen to drive the turbopump assembly. The GH_2 could be used interchangeably with the GH_2 from the tank farm, except that the tank farm had a fixed capacity limit whereas the TES was limited only by the availability of hot water.

(U) A secondary function was to provide GH_2 for the pressurization of Dewars 1 and 2 during bootstrap operations. The primary component of the turbine drive system was the turbine energy source (TES) which was an LH_2 /hot water counter flow heat exchanger. Its function was to vaporize the LH_2 being bled from the pump discharge line and supply the ambient GH_2 to drive the turbine.

(U) The TES unit consisted of four heat exchanger sections connected in parallel. Each section was designed to vaporize 12.5 lb/sec of LH_2 and produce gaseous hydrogen at approximately 520°R. The temperature of the water leaving the heat exchangers was approximately 80°F. The pressure of the GH_2 being supplied to the turbine control valve H-60, from the heat exchangers, was approximately 100 psi less than the pump discharge pressure.



(U) During NRX-A6 testing, the TES was to supply approximately 6.9 lb/sec of GH_2 for turbine drive and approximately 0.7 lb/sec of GH_2 for Dewar pressurization. Only two heat exchanger sections of the TES were required to deliver this total GH_2 flow rate of 7.6 lb/sec. The water flow rate to each of these two sections was approximately 1000 gpm while the other two sections were set up for bypassing 100 gpm of water each. Therefore, the total TES water usage rate for NRX-A6 testing was to be approximately 2200 gpm.

(U) High Pressure LH_2 Cooledown System (X System in Figure 3-7)

(U) The high pressure LH_2 cooledown system consisted of, (1) an 8,000 gallon high pressure Dewar 3, (2) six GH_2 ullage bottles, (3) the gas line from the ullage bottles to Dewar 3, (4) the gas line from valve X-50 to the ullage bottles, (5) the main 8-inch vacuum jacketed LH_2 propellant line from Dewar 3 to the main LH_2 propellant feed line, and (6) the Dewar 3 fill line from Dewars 4 and 5.

(U) The primary function of the high pressure LH_2 cooledown system was to provide LH_2 cooling to the reactor in the event that an emergency shutdown occurred at any time after the startup of the run profile until the initial cooledown period was over. This system was also used during NRX-A6 testing to provide the initial cooling to the reactor following a normal programmed shutdown.

(U) The pressure in the ullage bottles and Dewar 3 was programmed as a function of run time and pump discharge pressure. The pressure was automatically increased by pressure control valve X-53 during the ramp up to full power and manually increased during the full power operation. During a normal shutdown, the pressure in the ullage bottles and dewar was vented to atmosphere.

(U) The high pressure LH_2 Cooledown System utilized an open valve (X-3) concept with Dewar 3 riding on-line. Since the Dewar 3 pressure was always maintained lower than the pump discharge pressure, the pressure in the main propellant feedline held the check valve (X-1003) closed. Had the pump discharge pressure suddenly decreased to a value less than the pressure in the high pressure Dewar at any time during a run, the check valve (X-1003) would have opened and LH_2 coolant flow would have been provided to the reactor from Dewar 3. This type of malfunction would have scrambled the reactor as a result of a loss of flow shutdown (FSD).

(U) Accumulator System

(U) A 10 cubic foot gas accumulator branched into the main propellant feed line immediately downstream of the turbopump discharge check valve for the specific purpose of reducing the pressure oscillations or "water hammer" effects that could occur as a result of several types of accidents or flow shutdown. This modification was made based on CAM studies of flow shutdown. Without the accumulator, these pressure oscillations could violate the minimum nozzle flow requirements and consequently cause nozzle burn-out. Flow from the X system is initiated through check valve X-1003 as soon as the main propellant line pressure falls

below the demand level required to prevent nozzle tube burnout. Flow from Dewar 3 continues until its discharge pressure falls below the 100 psig level of Dewars 4 and 5. Since the programmed Dewar 3 pressure for the 2000°R hold of Experimental Plan III (EP-III) was less than 100 psig, the high pressure Dewar was not used for this shutdown. It was used, however, during the EP-IIIA shutdown for a period of 22 seconds following reactor scram at 2500°R chamber temperature.

(U) Low Pressure LH₂ Cooldown System (K System in Figure 3-7)

(U) The low pressure LH₂ cooldown system consisted of, (1) Dewars 4 and 5, (2) the vacuum jacketed piping from the Dewars to valve K-6, (3) the mixing chamber, and (4) the foam insulated piping from check valve KC-1006 to the main LH₂ propellant feedline.

(U) The primary function of this system was to provide LH₂ for reactor cooldown for a substantial period of time immediately following the initial coolant flow from the high pressure Dewar system. This system provided approximately 37 minutes of LH₂ coolant to the reactor during the NRX-A6 cooldown.

(U) Dewars 4 and 5 are vacuum jacketed, perlite insulated, spherical Dewars with a combined total deliverable capacity of approximately 58,000 pounds of LH₂ when pressurized to 160 psig. Flow from these Dewars was measured at venturi KF-5 and controlled with analog control valve K-6. The LH₂ could be mixed with ambient GH₂ in the mixing chamber to provide "cold" gaseous hydrogen to the reactor.

(U) The low pressure LH₂ Cooldown System also utilized an open valve (K-7) concept with Dewar 4 and 5 riding on-line. The higher pump discharge pressure held the check valve (KC-1007) closed. Following an emergency or normal flow shutdown, LH₂ coolant flow would be continued from these Dewars after the pressure in Dewar 3 dropped below the pressure in Dewars 4 and 5.

(U) LH₂ Cooldown System (N System in Figure 3-7)

(U) The LN₂ Cooldown System included three LN₂ Dewars, two reactor cooldown vaporizers and all piping, valves instrumentation and controls necessary to provide either cold gaseous or liquid nitrogen to the reactor during decay heat removal operations.

(U) For NRX-A6, LH₂ pulse cooling was to be used during final reactor cooldown after the 90°R GH₂ was no longer required. During the NRX-A6 cooldown sequence, LN₂ cooling of the reactor was initiated at 58.3 minutes after shutdown and continuous flow was maintained for approximately 17 minutes. LH₂ pulse cooling was then provided to the reactor until 75 hours after shutdown.

(U) The total LN₂ storage in Dewars 6, 7, and 8 was approximately 580,000 pounds at minus 320°F. Design pressure of the internal vessel was 160 psig, with the external jacket designed to full vacuum.



Astronuclear
Laboratory

(U) The Reactor Cooldown Vaporizer (RCV) vent used for converting LN_2 to GN_2 , was an integral part of the LN_2 cooldown system and was located on the Flow Control Room roof. The RCV was an LN_2 /hot water counter flow heat exchanger. LN_2 was supplied to the RCV from the LN_2 Dewars at 140°R with hot water from the Process Water Storage tank supplied at 660°R .

(U) Gas Systems (GH_2 , GN_2 , GHe-G and Q Systems in Figure 3-7)

(U) The gas systems included ambient hydrogen, nitrogen, and helium. The GH_2 system was available for prepurging, cooldown, LH_2 Dewar pressurization, and for initial turbine drive. The GN_2 system was used for post-test reactor cooldown and purging, test cell area purging and inerting, pressurization of the process water tank and LN_2 Dewars, activation of remote control valves, and cooling of various instrumentation. The gaseous helium system was used for pre-test reactor purge, post-test reactor cooldown and purge, purging of various lines and Dewars, and cooling of reactor instrumentation.

(U) Borated Water/Shield System

(U) The borated water (BH_2O)/shield system consisted of, (1) the mixing tank and agitator, (2) the BH_2O storage tank (BWT), (3) four heat exchangers, (4) two hot water heaters, (5) two heater pumps, (6) one circulating pump, (7) one privy pump, (8) two shield pumps, (9) the 360 degree shield, and (10) all associated piping and instrumentation.

(U) The primary function of the 360 degree shield was to reduce activation of the Test Cell, and the primary function of the flow system was to provide an adequate flow of BH_2O to the privy roof and the reactor shield halves for neutron protection and cooling purposes. A mixture of borax and boric acid was used to give a solution of sodium pentaborate having a pH of 6.8 which would act as a neutron absorber and therefore provide protection for the test cell wall and the equipment inside the privy. This system could be operated during startup, power runs and cooldown (normal and emergency). Figure 3-8 illustrates the shield and support system in place. Each half of the shield consisted of four (4) interlocking aluminum tanks with five internal passages which accommodated the total shield flow of approximately 4500 gpm of the borated water solution. The flow rate used was sufficient to maintain shield material temperature well within reasonable limits.

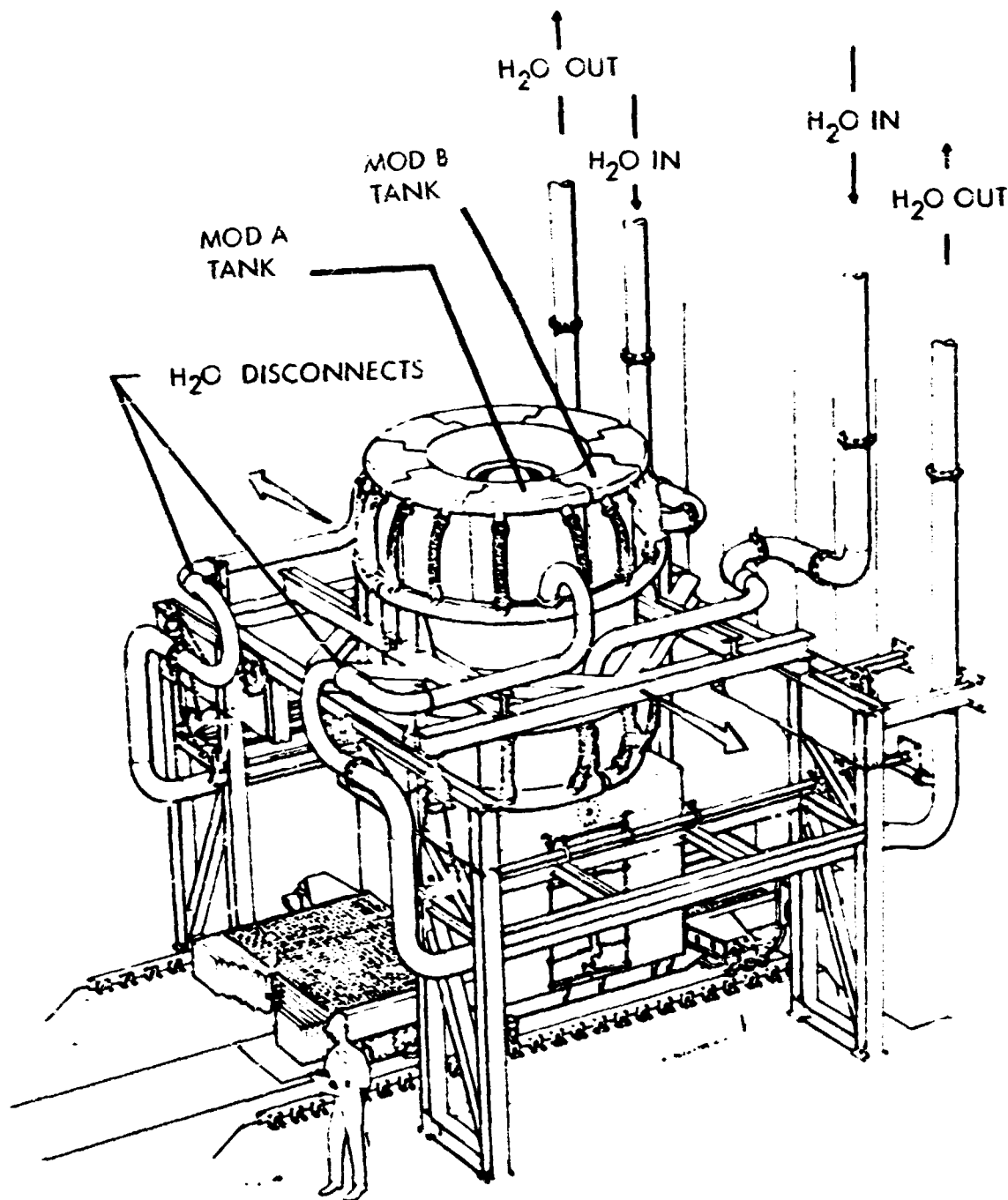
(U) The BH_2O system had the capability of providing a gravity flow to the shield halves and privy roof in the event of loss of the privy and/or shield pumps due to a power failure. The flow, which decayed exponentially, was provided by the static head in the borated water tank and flowed to drain via the pumps, shield halves and privy roof.

(CRD) CONTROL SYSTEMS AND SAFETY SYSTEM (U)

(U) A description of the reactor control systems, safety systems, and facility control systems is given in this section. These systems were designed to meet the requirements of flexibility, safety, reliability, and performance.

~~CONFIDENTIAL~~

(THIS PAGE IS UNCLASSIFIED)



Figures 3-8. (U) Test Cell "C" 360 Degree Shield
(THIS PAGE IS UNCLASSIFIED)

~~CONFIDENTIAL~~

~~CONFIDENTIAL~~

(CRD) Reactor Control System and Safety System (U)

(U) The reactor control system consisted of two basic loops, a power or temperature loop which controlled the position of the control drums and a flow loop which controlled the position of the turbine power control valve (H-60). A block diagram of the control system is shown in Figure 3-9; a more detailed description and schematics of the control system may be found in Reference 9.

(CRD) Temperature Control (U)

(U) The NRX-A6 temperature controller was similar to the "no-flux" loop temperature controller used during NRX-A5.

(U) The temperature controller changes drum position in response to error between demanded temperature and the average of 4 nozzle chamber thermocouple readings.

(U) The temperature demand, temperature measured, and temperature trim were summed to produce a compensated temperature error. This error signal was then converted to a control drum velocity demand. This latter signal was fed to the output amplifier which converted the velocity demand to a drum position demand. The temperature trim was a manual adjustment of the programmed demand with an adjustment range of $\pm 500^{\circ}\text{K}$. A 45 degree/sec limit on maximum drum velocity at the output of the temperature controller was utilized.

(U) The temperature controller design was a compromise between conflicting requirements of good transient response and small static errors at the high end (4090°R) and adequate stability margins at the low end (200°R) of its operating range.

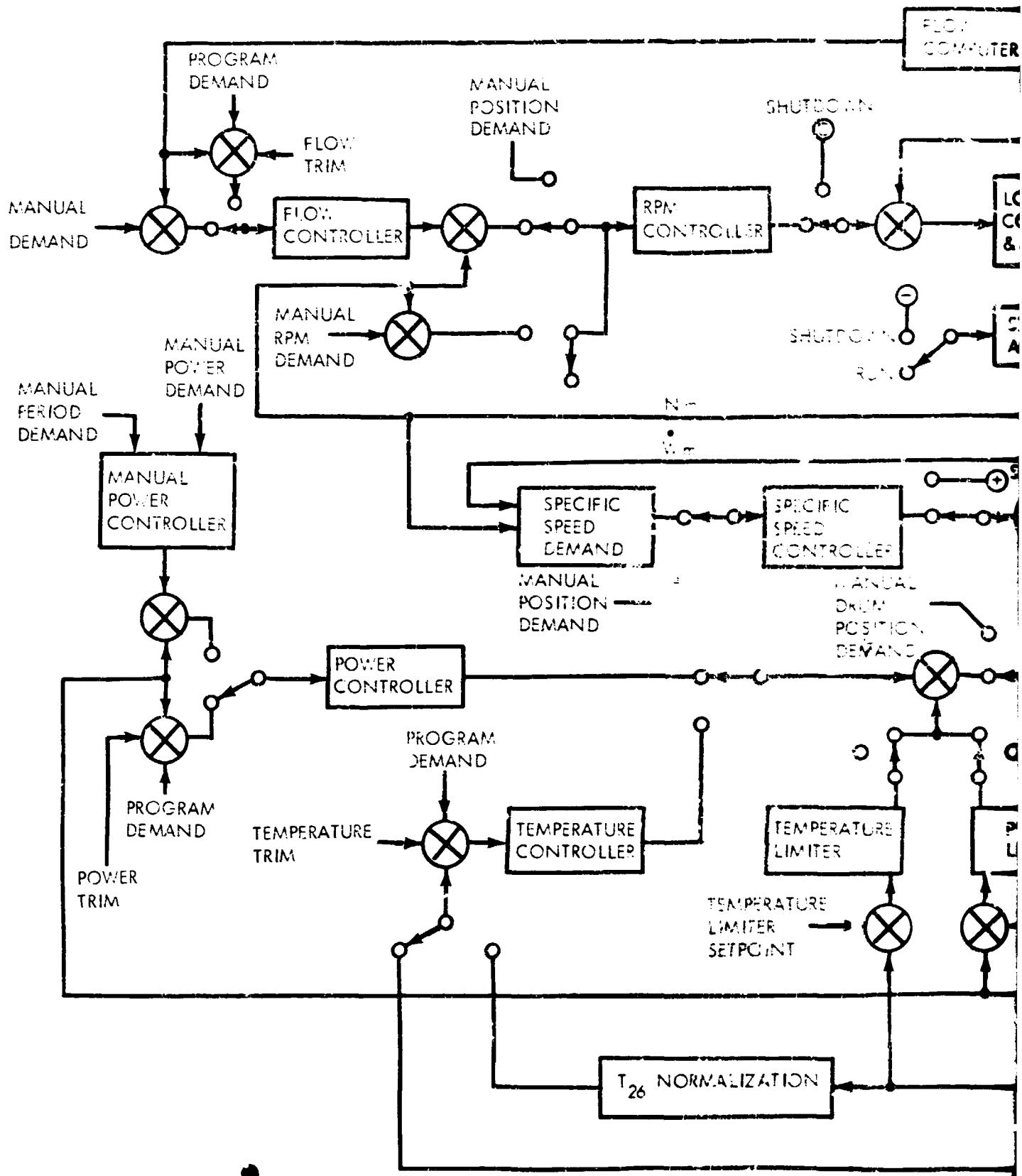
(CRD) Provision was made for the controller to operate with an alternate feedback signal, the average of ten thermocouples located in unfueled elements of the core at Station 26. This, among several other options, could have been selected by the Chief Test Operator. The other options were direct control of drum position or power control.

(U) Power Control

(U) The NRX-A6 power controller was similar to that used during NRX-A5 except that the temperature trim was eliminated. This control mode was to be used at powers below the operating range of the temperature controller (preliminary testing and during startup to full power), and as a backup control mode for high power operation if the temperature controller failed.

(U) Log power demand, log power measured, and power trim were summed to produce a compensated log power error. This error signal was then integrated to become a control drum velocity demand. The velocity demand was fed to the output amplifier which converted the velocity demand to a drum position demand. The log power demand could be either manual or programmed. The power trim was a manual adjustment of the programmed power with an adjustment range of a factor of 2 of the demanded power ($1/2$ to 2).

~~CONFIDENTIAL~~



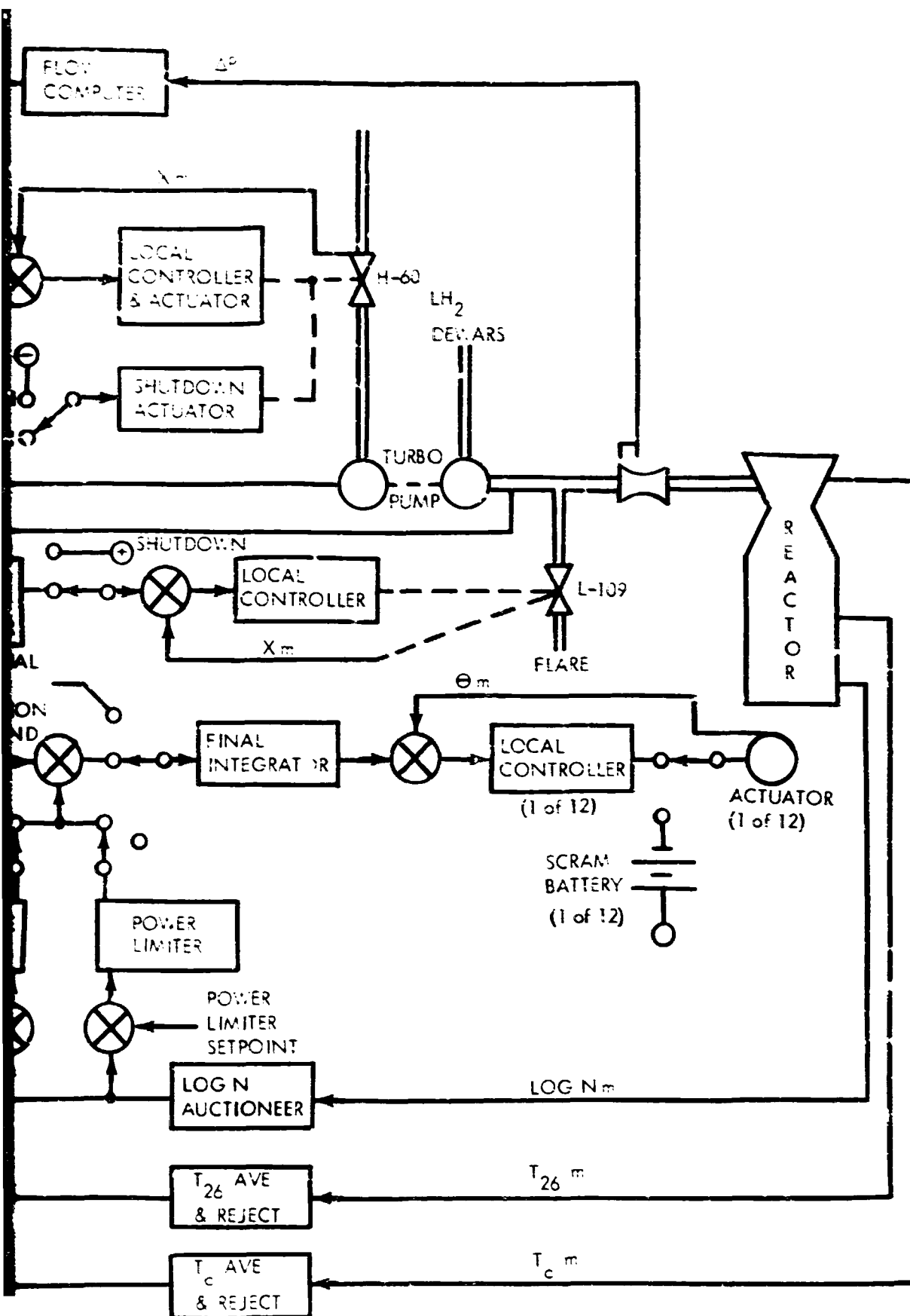
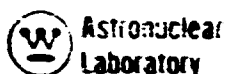


Figure 3-9. (U) NRX-A5 Control System

BLANK PAGE



(U) Follow-up amplifiers were incorporated in the power controller so the manual log power demand would follow the measured log power when this demand mode was not being used. Error meters allowed switching between modes with minimum transient effects.

(U) The controlled channel was automatically selected from a group of four detectors. The selection criteria were such that the control signal was neither the highest or the lowest of the four, thus protecting the system from a failure of a single channel.

(U) The log power control system was an eight-decade system which covered the range from about 100 Watts to 10,000 MW. The eight decades were taken from about the middle of the nine decade log amplifier (i.e., about 1/2 decade on each end of the eight decades).

(U) The measured log power signals from the individual channels were used for the power scram circuits (fixed power, floating power, programmed power, and period).

(U) An automatic startup control mode similar to NRX-A5 was provided to initiate reactor operation. In this mode, the control drums are programmed slowly through the critical drum position and when a preselected power level is attained the power control mode is automatically selected.

(U) Drum Position Control

(U) The drum position control for NRX-A6 was gang control. The one exception to gang control was that two drums could be "bumped" (not controlled) to 180 or 0 degrees with the other drums in gang position control.

(U) The output amplifier of the power or temperature controller (same amplifier) became a unity gain amplifier when the position control mode was selected. The drum position demand (either manual or programmed) was summed with measured drum position, manual trim, and "zero offset" signals to produce an error signal. This error signal was sent to the actuator servo amplifier.

(U) The control drums were scrambled by an actuator scram relay between the amplifier and actuator servo of each control drum actuator. This relay was normally energized. A scram de-energized the relay, thus connecting the actuator servo to the scram battery which caused the servo to drive the drum in. Each actuator had a separate battery.

(U) Limiters

(U) Power and temperature limiters were provided for NRX-A6 which could be used in temperature and power control, but not in position control. The limiters enter the control system upstream of the output amplifier of the power or temperature controller. The limiters were similar to those used in NRX-A5. Station 26 temperature was the measured temperature input to the temperature limiter.

(U) Flow Control

(U) The flow control at Test Cell "C" was similar to that used at Test Cell "A". The flow control loop consisted of inner loops of RPM and turbine valve (H-60) position. A specific speed loop protected the pump from operation in the stall region of the pump operating map.

(U) The flow rate demand (programmed or manual) was summed with measured flow rate, and the error converted to an RPM demand. Either this RPM demand or a manual RPM demand was compared with measured RPM and the error converted to a change in turbine control valve (H-60) position. Either this demand or a manual H-60 position demand was compared to measured position with the result being the demanded change in H-60. The flow rate used for control was measured at a flow venturi which was downstream of the pump and the bypass line for the TES. A flow bias was incorporated to allow stable pump operation until a flow rate suitable for control was obtained.

(U) To prevent operation of the turbopump in the stall region an automatic control system opened a bypass valve (L-109) downstream of the pump if the ratio of pump flow rate to pump speed became too small.

(U) Follow-up amplifiers were incorporated so when the manual demand modes of flow, RPM, and H-60 position were not being used the manual demand followed the measured parameter. Error meters were incorporated to allow switching between modes with minimum transient effects.

(U) Reactor Simulation

(U) A reactor simulator was provided to assist in checkout of the control system prior to a reactor run, checkout of the run procedures, and to supplement operator training in simulated normal and malfunction conditions. The reactor simulation was composed of two parts:

- 1) A kinetics simulator,
- 2) Flow and temperature simulation.

(U) A reactor kinetics simulator was a three group log model which included temperature and flow reactivity feedback. The simulator could be used with or without the neutronics system. The neutronics system could be bypassed and a log power signal generated internally in the simulator or a simulator detector current could be fed into the log amplifiers and the remainder of the actual neutronics circuit used.

(U) Flow and temperature simulation was divided into the following sections: Dewar, turbine and pump, propellant line, turbine energy source, reactor thermodynamics, high pressure Dewar, cooldown lines, and mixing chamber. The GH_2 pressure upstream of the turbine control valve (H-60) was controlled by H-53. Chamber and Station 26 temperatures were generated for control and readout. There were other temperatures calculated but not brought out for external use.

(U) Emergency Shutdown

(U) An emergency shutdown was used to protect both the test article and the facility in the event of a malfunction. Inputs to the emergency shutdown system for NRX-A6 included fixed power, floating power, programmed power, period, flow trip, minimum drum position, loss of critical power supplies, turbine speed, turbine inlet pressure, and low control drum hydraulic pressure. These inputs protect the reactor, assure that it can be shutdown in a safe manner, and protect the turbopump by scrambling the reactor and terminating normal propellant flow.

(U) The period circuit was similar to that used for NRX-A5 except that silicon diodes were used upstream of the period circuit to reduce the chances of a scram due to noise.

(U) The flow trip monitored the rate of change of pressure in the main propellant line to initiate an emergency shutdown if the rate was too great. The pressure was measured downstream of the point that the high pressure Dewar entered the propellant line. Either a rise or decline in pressure greater than 50 psi/sec could trip the shutdown chain depending on the length of time the transient continued. A lag (capacitor) was included in the circuit to eliminate trips from noise. Any pressure ramp would have had to continue long enough to overcome the lag.

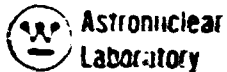
(U) Typical Reactor Startup Sequence

(U) The following is a typical sequence of reactor control modes required for a high power test of the NRX-A6 reactor.

- 1) Initially the reactor power is at "source" level of a few milliwatts, and the drums are at zero degrees, the position corresponding to maximum poison. Upon autostart command, the drums are programmed through critical.
- 2) At around one megawatt, power control is automatically selected and power demand is programmed.
- 3) When nozzle chamber temperature reaches 2000°R, temperature control is selected and temperature is programmed to the full power hold.
- 4) Following full power operation, temperature demand is programmed down to 2500°R at which point reactor control is terminated and the drums are rotated to zero degrees.

(U) Facility Control System

(U) A brief description of the facility coolant and hydraulic control systems are given below. A description of the facilities was given previously in this section of the report and only a discussion of the controls is described herein. A more detailed description may be found in References 8 and 10.



(U) Turbine Energy Source

(U) The turbine energy source (TES) vaporized and heated liquid hydrogen (LH_2) bled from the propellant line. The GH_2 produced by the TES was used to drive the turbine and pressurize LH_2 Dewars 1 and 2. TES control consisted of LH_2 flow control and hot water (used to heat the hydrogen) flow control. The control system for the TES could be operated in either the manual or automatic control mode from the control point.

(U) Dewar Pressurization

(U) The high pressure LH_2 cooldown Dewar 3, the two LH_2 run Dewars 1 and 2, the two low pressure LH_2 cooldown Dewars 4 and 5, and the three LH_2 Dewars all had automatic pressurization control, with follow-up amplifiers incorporated so manual demands could follow measured parameters when this mode was not being used. Error meters allowed switching between modes with minimum transient effects. In all cases, measured Dewar pressure was compared with demanded Dewar pressure (manual or programmed) and the error converted to a valve position demand.

(U) Mixing Chamber Control

(U) The mixing chamber was a device to mix controlled quantities of LH_2 , from the low pressure cooldown Dewars, and GH_2 to obtain hydrogen at a specified temperature at the nozzle torus inlet. The valves involved in the control system were K-6, the valve controlling LH_2 flow from the low pressure cooldown Dewars, and G-3, the valve controlling GH_2 flow from the tank farm.

(U) The desired flow and temperature was obtained by demanding a total flow rate from the mixing chamber and a flow rate ratio, which was gas flow rate over total flow rate. By monitoring the resulting mixture temperature the ratio could be manually changed to obtain the desired temperature. The gas flow rate demand was compared with a flow rate obtained from a pressure measured upstream of valve G-3 (see Figure 3-7). The error then converted to a G-3 position demand. The remaining flow rate, the LH_2 flow rate demand, was compared with a flow rate obtained from a pressure measured upstream of valve K-6 (see Figure 3-7). This error was then converted to a K-6 position demand.

(U) Logic Sequence Control

(U) Logic sequence control was added to the Test Cell "C" control system in order to simplify the checklists during control room operations. This sequence control reduced the number of operator actions required for operation. Operational use of any or all of the logic sequences available was left to the discretion of the Test Director.

(U) The sequence could have included the operation of valves (opening or closing) and waiting until a certain parameter, such as temperature or pressure, reached a predetermined level. The number of sequential operations was limited by the number of relays (30) in the logic chassis. Different operations required different numbers of relays, at least one being required for each operation.

(U) Any individual logic unit could be manually bypassed in the sequence. The entire sequence could be stopped at any point. If the HOLD button was pushed the operation in progress would be completed then the sequence would hold. By again pushing the HOLD button the sequence would continue. The OFF button could also be pushed at any point in the sequence. The operation in progress would not be completed and the sequence halted. To restart the sequence the ON and START buttons would be pushed. The sequence would restart from the beginning but since the valve operations would have already been completed (unless another operation on the same valve appeared later in the sequence) the time to repeat the completed portion of the sequence would be much less than the first time.

(U) Logic sequences available at Test Cell "C" were:

- 1) LN₂ chill down
- 2) Mixing chamber initial chill
- 3) High pressure Dewar final chill
- 4) Dewar pressurization

(U) Servo Hydraulic Valve System

(U) The system provided fluid power to the actuators of all servo actuated hydraulic valves as required for valve positioning.

(U) The system included two identical hydraulic power units which operated in parallel. Each unit consisted of an electric motor driven axial piston pump and an oil reservoir, both mounted on a common frame. The pump discharge of both units connected to a common header from which a transfer line connected to the individual valve headers. Each valve header had connected to it one to five hydraulic valves, and each valve header was provided with two or more accumulators. Upstream of the accumulators in each header was a check valve which allowed hydraulic fluid flow only in the direction of the hydraulic valves. The accumulators provided several functions:

- 1) They provided assurance of continued valve operability for a finite time period should a fluid failure occur upstream of the header check valves.
- 2) They maintained the system hydraulic pressure at the instant of hydraulic valve operation without the possible effect of momentary decrease of pumped system pressure.

The valve header concept design provided continued valve operability in the other header should a fluid failure occur in one header. The hydraulic valves were assigned to individual headers so that a loss of one header would not prevent an alternate header from supplying reactor coolant flow.

(U) Each accumulator was of the bladder type, its capacity was 10 gallons and it was rated at 3,000 psig. The accumulators were pre-pressurized prior to test operations with GN₂.



(U) Oil to water coolers were installed in the return line to each reservoir to maintain oil operating temperature. A bypass line with a solenoid valve installed allowed the oil to bypass the cooler and return directly to the reservoir. The two reservoirs were connected by a 3-inch line to equalize their levels. The capacity of each reservoir was 200 gallons.

(U) The discharge pressure on each pump was maintained at 2800 psig by means of a pressure control valve located in a bypass line which discharged oil into the oil return line to the reservoir. During test operation, both pump units would be operating, in case of failure of one unit. Each unit was rated for 20 gpm, which was sufficient to fulfill normal fluid requirements to the valve actuators.

(U) OBV (ON-OFF Block Valve) Hydraulic Valve System

(U) This system functions were to, (1) provide fluid power to the OBV hydraulic valve actuators as required for valve positioning, and (2) provide fluid power to the hydraulic screws which provide an automatic disconnect of the test car from the test cell. Fluid power could also be applied to the hydraulic pins which locked the test car to the test cell.

(U) The system included an electric motor driven axial piston pump mounted on an oil reservoir. This unit was similar to the units which supplied fluid power to the servo actuated valve. The pump discharge line connected to the OEV (ON-OFF electric valve)solenoid valves, groups of which were mounted in racks at appropriate locations in the various areas of the test cell. Each OBV valve had associated with it an OEV solenoid valve which directed the flow of hydraulic fluid to either the "open" or "close" cylinder of the OBV actuator. The pump discharge pressure was maintained at 2800 psig by means of a pressure control located in a bypass line which discharged oil into the return line to the reservoir. The pump was rated at 35 gpm. The hydraulic pressure in this branch line was reduced to 1000 psig and then to 600 psig for final service by two pressure control valves. A relief valve set at 1100 psig was installed in this line downstream of the first pressure control valve. An oil to water cooler was installed in the return line from the OBV valve actuators to maintain oil operating temperature. The capacity of the reservoir was 260 gallons.

(U) An accumulator was installed on the common header upstream of the OEV's which served the hydraulic actuated valves in the flow control room. The high pressure room and tank farm hydraulic valves had a separate accumulator. Another accumulator was installed on the separate header which served the Dewar area hydraulic valves. These accumulators provided a surge volume of fluid to maintain hydraulic pressure during the instant of hydraulic valve operation. They were not required to provide for a finite time of valve operation should a fluid failure occur in the system, since it was not necessary to operate these valves during a reactor cooldown operation.

(U) Control Drum Hydraulic System

(U) The function of this system was to provide power to the control drum actuators as required for control drum positioning.

(U) The system included an electric motor driven vane type hydraulic pump which obtained suction from an oil reservoir. The pump was rated at 10 gpm at 1,000 psig. The pump discharge supplied fluid to two manifolds located on the test car. Each manifold serviced six drums. Each manifold had an oil supply and oil return chamber. A supply and a return line from each manifold connected to a Moog electro-hydraulic servo valve which serviced one control drum actuator. There were 12 Moog servo-valve systems to control fluid to each of the 12 control drum actuators. The Moog servo-valve directed flow to either the "0" or "180" side of the actuator vane as required to move the drum; concurrently, oil flowed back from the appropriate side of the actuator vane through the appropriate ports of the Moog valve to the return chamber of the manifold and the oil reservoir. A flow limiting orifice and check valve arrangement was installed in the transfer line to the 0 degree side (drive drums from 0 towards 180 degrees) of the actuator vane. This arrangement,

- 1) Controlled the rate of supply flow to the 0 degree side of the actuator vane to limit control drum movement toward 180 degrees to a nominal 50 degree/second.

- 2) Permitted a maximum return flow rate through the parallel check valve path from the 0 degree side of the actuator vane during movement of the drum toward 0 degrees; thus allowing the drums to travel at a maximum rate to 0 degrees during a scram.

(U) An accumulator was connected to the supply line to each of the manifolds. A check valve installed in the supply line upstream of each accumulator allowed flow only in the direction of the control drum actuators. Immediately downstream of each accumulator a pressure transducer was connected to the supply line. It provided a signal which would cause a scram at 400 psig. Each accumulator contained sufficient fluid and pressure to scram its respective bank of six drums.

(U) Pump discharge pressure was regulated at 700 psig by a pressure regulating valve which dumped excess fluid back to the reservoir. This regulating valve also served as a relief valve to prevent system overpressure which had a maximum working pressure of 1,000 psig.

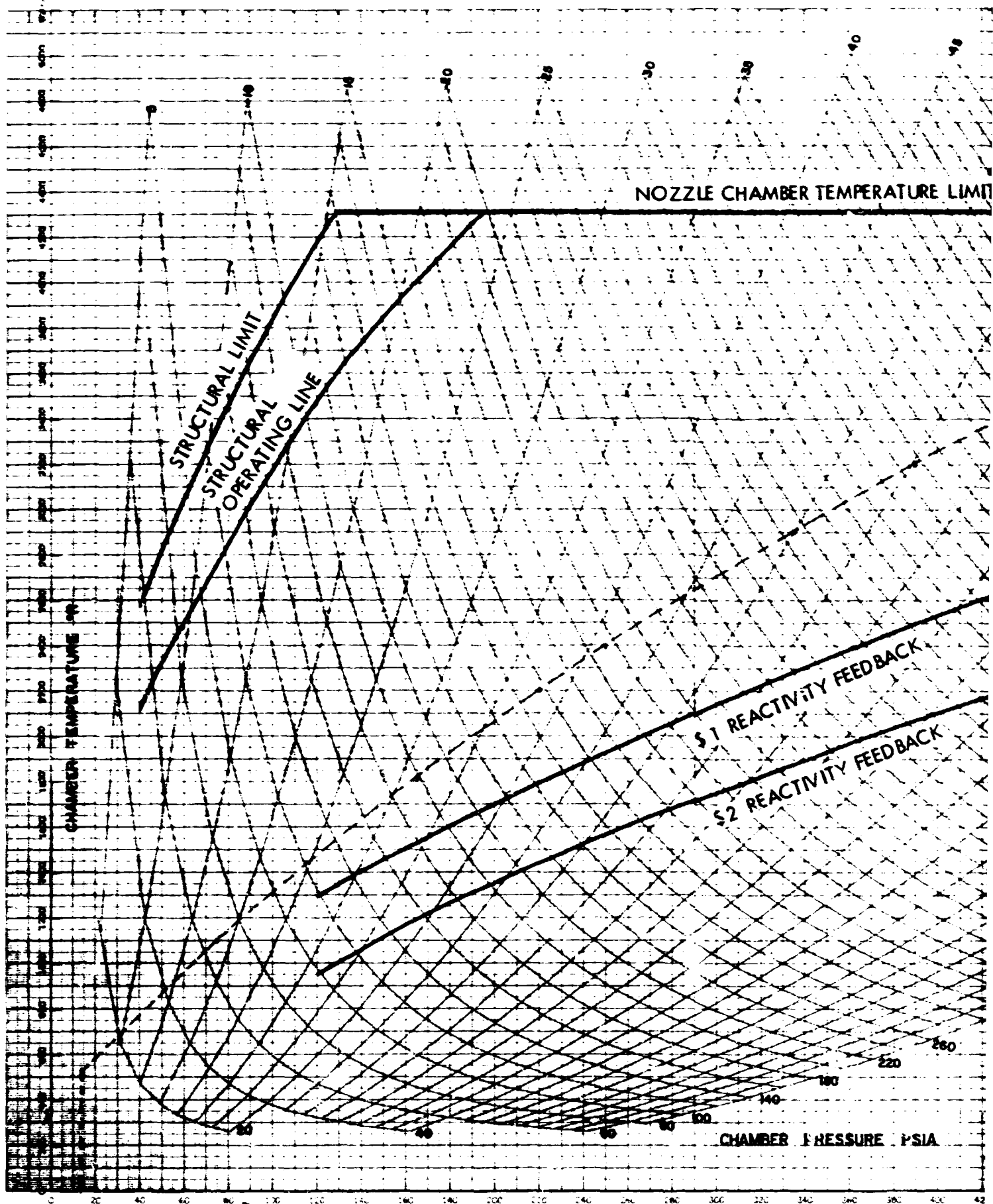
(U) The return line to the reservoir contained an oil to water cooler for maintaining oil operating temperature.

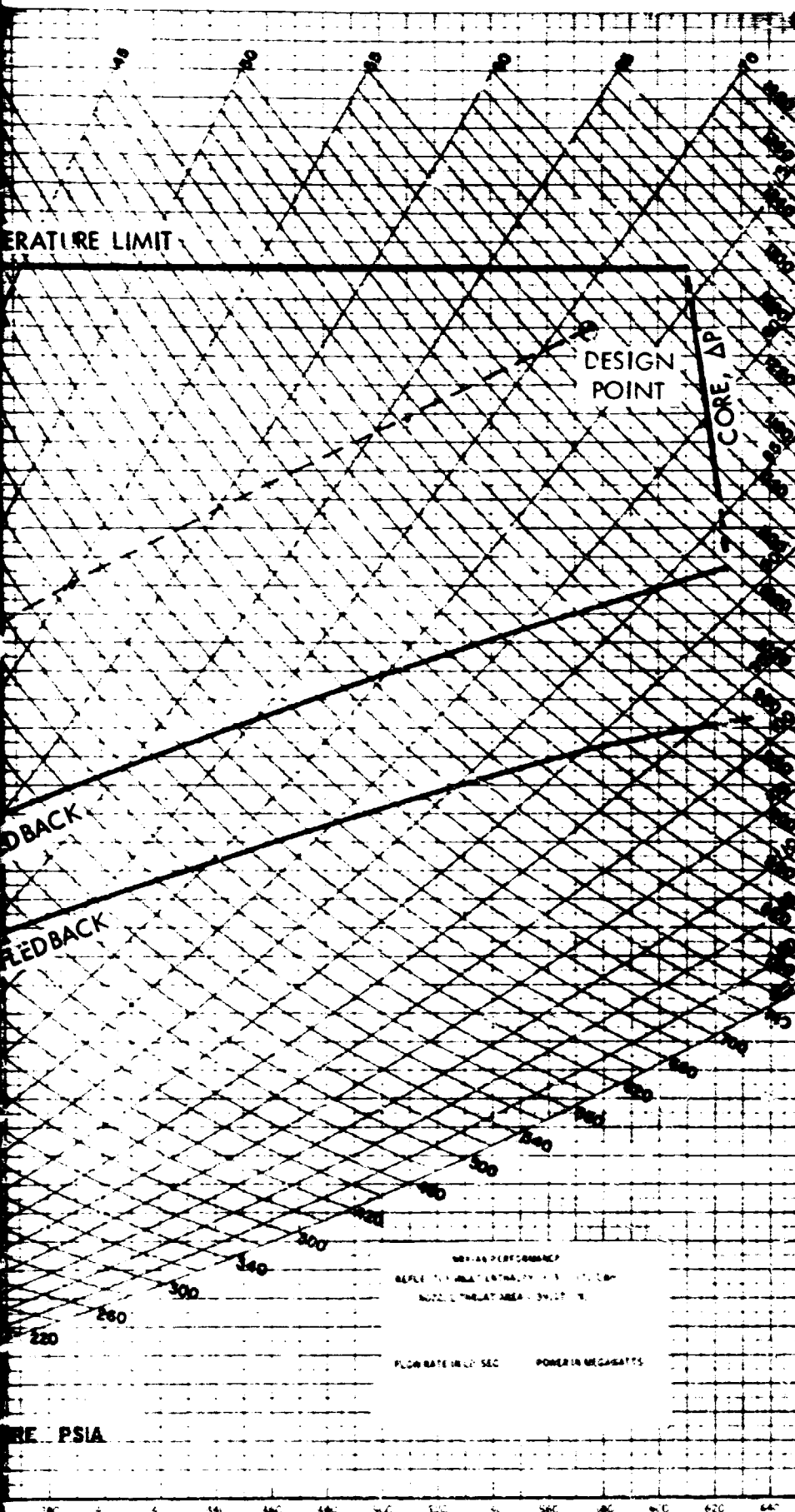
(U) FUNCTIONAL DESCRIPTION OF TEST SYSTEM

(U) The basic operations of the reactor included pre-operational, startup, power operation, decay heat removal or cooldown, and a post-run criticality test. This section presents a brief description of these operations for the NRX-A6 full power test. A more complete description is given in References 11, 12, and 13. A schematic of the basic Test Cell "C" flow system is shown in Figure 3-7.

(U) The operating envelope and normal NRX-A6 operating line of the reactor is shown in Figure 3-10. This envelope consisted of chamber pressure as the abscissa and chamber temperature as the ordinate and includes flow rate and reactor power

BLANK PAGE





2

Figure 3-10. (U) NRX-AE Operating Map

BLANK PAGE

level as intersecting curvilinear axes and was based on reflector inlet enthalpy and nozzle throat area of 300 Btu/lbm and 59.175 square in., respectively.

(U) The reactor constraints are also shown in Figure 3-10. The tie rod exit gas temperature limit (structural limit) was determined from stress considerations for the tie-rod material; the maximum allowable chamber temperature limit was determined from the nozzle tube cooling characteristics; the core pressure drop limit was based on fuel cluster support block stress considerations and a safety limit associated with hydrogen density in the core equivalent to increasing the reactivity of the core by 1.00\$ was chosen to complete the constraints.

(U) Pre-Operational Phase

(U) The pre-operational phase was initiated with the transfer of systems and valves to Control Point (remote) control. The 360 degree shield cooling water was established and the valves in the Flow Control Room (FCR), and other areas to be inerted were exercised. After the correction operation of the Emergency Shutdown Chain was verified, the initial inerting of the test cell commenced and the remaining valves were exercised. The control drums were unlocked and switched to Control Point (remote) control, and the area was cleared of all personnel.

(U) Following a routine gas and cryogenic fluids pressurization phase and scram check phase, Dewars 1 and 2 (see Figure 3-7) were pressurized to start the system chill-down phase in preparation for the full power run. During chill-down, liquid flow was from Dewars 1 and 2 through Turbopump No. 2 and out, (1) valve L-209 to chill the turbopump, (2) valve L-111 to chill the main propellant line to valve L-11, and (3) valve H-10 to chill the TES inlet. A 15-minute cryogenic soak was then initiated. During the cryogenic soak, the LH₂ system was chilled. Following the cryogenic soak, a turbopump overspeed trip check was performed and the hot water system for the TES was set up.

(U) Startup Phase

(U) The startup phase was initiated with an automatic nuclear startup to a power level of 10 kW at which point the power control loop was closed. Upon completion of line chilldown and Dewar 3 topping fill operations a 2 pounds per second GH₂ flow to the reactor was established, the helium purge terminated, and the high pressure LH₂ cooldown Dewar 3 system valves switched to pressure control. A reactor power level of 1 MW was then established in power control. Reactor control was then switched to power program, and main propellant line control valve L-11 and LH₂ flow rate control switched to program control. A turbopump rpm bias was then used to establish 250 psig pump discharge pressure and to obtain TES bootstrap.

(U) Run Phase (Power Operation)

(U) On Test Director (TD) command, the Chief Test Operator (CTO) switched the programmers to run. The programs utilized were, (1) LH₂ flow, (2) valves L-111 and L-11 position, (3) Dewar 3 pressure, (4) reactor power, and (5) nozzle



chamber temperature. During the initial part of the run phase, program operations accomplished the following:

- 1) Valve L-11 ramped open at 1.1 lb/sec^2 ,
- 2) Valve L-111 closed,
- 3) Dewar 3 pressure ramped up at 2.6 psi/sec ,
- 4) Reactor flow ramped up from 15 lb/sec at 1.1 lb/sec^2 , and
- 5) Reactor power increased to yield chamber temperature ramp of 50°R/sec .

(U) At the 40 lb/sec reactor flow program hold the programmers were automatically switched to hold, and the CTO trimmed LH_2 flow rate to 40 lb/sec at BF-13, and chamber temperature to an indicated 2000°R .

(U) The CTO then switched from Program Power Control to Power Control and then to Temperature Control with measured chamber temperature feedback. When the gas accumulator was placed on line, valve H-75 was opened and valve H-70 was closed. A negative step response measurement was then performed on the Temperature Loop. The operation of the power limiter was then verified by reducing the power limiter setting until limiting had occurred. The power limiter was set up for full power operation and bypassed in preparation for the ramp to full power. After approximately 6.2 minutes at the 40 lb/sec hold, the CTO switched the programmer to run.

(U) At the 65.5 lb/sec reactor flow program hold the programmers were automatically switched to hold, and chamber temperature immediately trimmed down 100°R ; approximately one minute later chamber temperature was trimmed down another 100°R ; seventeen seconds later chamber temperature was trimmed down an additional 200°R . After approximately two minutes at the 65.5 lb/sec hold, the CTO switched the programmer to run.

(U) At the 71.3 lb/sec reactor flow program hold the programmers were automatically switched to hold and the 3600 second timer started. At the start of the full power hold, chamber temperature was trimmed down 200°R to design conditions. During the 60 minute full power hold, chamber temperature of flow was trimmed at the following times after start of the hold (2.7 minutes, $\Delta\dot{w} = +0.5 \text{ lb/sec}$; 7.8 minutes, $\Delta T_c = +40^\circ\text{R}$; 35 minutes, $\Delta T_c = +20^\circ\text{R}$; 50 minutes, $\Delta T_c = +10^\circ\text{R}$; and 53 minutes, $\Delta T_c = +60^\circ\text{R}$). At the completion of the full power hold, the CTO switched the programmer to run. At 43 lb/sec on the ramp down from full power, a shutdown was initiated from the CTO console.

(U) Cooldown

(U) At the initiation of reactor shutdown the liquid hydrogen high pressure Dewar 3 came on line and flowed for approximately 77 seconds with a maximum flow rate of 21 lb/sec . Dewars 4 and 5 came on-line and valve K-6, in Flow Control, was used to control LH_2 flow rate to maintain chamber temperature below $1,000^\circ\text{R}$.

(U) Approximately 32 minutes after shutdown, the tank farm "maneuver" was initiated: GH_2 Bottles 3 through 7 were secured, the GH_2 header was depressurized

to a pressure equal to that in Bottle 8, and Bottle 8 was opened to the GH₂ header. Valve K-6 was closed 36.9 minutes after shutdown with valve G-3 in Flow Control, low pressure GH₂ was used to purge LH₂ from the K-system line through the reactor. The GH₂ header pressure was then increased by adding Bottles 3 through 7 to Bottle 8. GH₂ cooling of the reactor was continued, maintaining chamber temperature at less than 1,000°R and reactor tie rods below 1,200°R.

(U) GH₂ was stopped and LN₂ cooling of the reactor (Maximum flow rate = 24 lb/sec) was initiated at 58.9 minutes after shutdown. When tie-rod temperatures were 450°R (65.5 minutes after shutdown), LN₂ flow was terminated. The first LN₂ pulse was initiated 71.5 minutes after shutdown with the reactor shed in-place and the Filter Reactor Outlet Gas (FROG) fission product removal device engaged.

(U) Approximately three hours after shutdown, a minimum secure of the test cell was completed. With the exception of LN₂ pulse cooling, control room operations were terminated. After 75.3 hours the last LN₂ pulse was completed, as tie rod temperature had stabilized at approximately 450°R.

(U) Post-Run Criticality Test

(U) A post-run reactor criticality test was performed. LN₂ and GH₂ were used to cool the reactor until reflector material and core inlet temperatures were near ambient. The CTO Manual, Fixed Power, Floating Power, and Period Scrams were checked. With the reactor shed in-place and the FROG engaged, a reactor power level of 10 kW was established in Position Control. Reactor control was then switched to power control and after 100 seconds in Power Control, drum positions were recorded. A shutdown was then initiated from the CTO console. The FROG was then retracted and the reactor shed withdrawn. A reactor power of 10 kW was established and drum positions recorded. A shutdown was initiated from the CTO console.

(U) REACTOR ASSEMBLY, CHECKOUT, TRANSFER, AND TESTING

(U) The Reactor/Pressure Vessel Assembly (PVARA) was shipped by train from Pittsburgh, Pennsylvania to Las Vegas, Nevada, and by trailer truck from Las Vegas to NRDS. During shipment, the reactor core contained 6990 boron carbide (B₄C) poison wires to protect against inadvertent criticality.

(U) The NRX-A6 PVARA was received at the Engine Maintenance, Assembly, Disassembly (E-MAD) building on 14 October 1967. Mating of the test cell and test car, and final pre-test preparations were completed by 13 November 1967. In general, the assembly operations at the E-MAD Building and the mating and pre-test preparations at Test Cell "C" were accomplished as planned and without major difficulty.

(U) Assembly operations at E-MAD included receipt, inspection, checkout, and installation or assembly of all test assembly components, coolant systems, and instrumentation. The assembly operation also included flame spraying of all instrumentation and leads on the exterior surface of the pressure vessel. Peripheral and central poison wires were removed during the assembly operations at E-MAD.

(U) The test car buildup had previously been completed in E-MAD, and the installation of the test article on the test car, instrumentation hookup, and checkout proceeded as planned. The NRX-A6 utilized the T-7 test car. This test car, reworked after use on NRX-A3, was structurally unchanged but did incorporate some modifications to adapt it to the facility. A center electrical coupler was used for the first time to connect reactor instrumentation and control wiring to test cell recorders and amplifiers through a remote disconnect plug in the test cell pad. A shield annulus purge system provided gaseous nitrogen purge flows of 5 and 10 lb/sec to the area between the test article and the Phoebus IB 360 degree shield. The GN_2 purge gas flowing between the test article and the shield insured an inert atmosphere and was kept at a slight positive pressure through the use of a thin stainless steel impedance collar attached to the shield near the nozzle torus level. The 360 degree shield, constructed in two remotely separable halves to provide radiation protection for the test cell has been previously described in this section of the report.

(U) A continuous purge of the NRX-A6 reactor was maintained during reactor shipment and throughout the assembly operations, and prior to testing in Test Cell "C" to preclude possible fuel element hydrolysis. The purge gas utilized was dry, chlorine free air during shipment and assembly operations and dry, chlorine free helium in Test Cell "C". The detailed purge requirements are given in Reference 14.

(U) Pre-test operations are discussed in detail in Reference 15. The NRX-A6 test series was conducted between 21 November 1967 and 15 December 1967, inclusive, and consisted of three (3) experimental plans (EP's). The individual tests were designed to meet the requirements of the NRX-A6 Test Specification (Reference 11). Each experimental plan is described in Section 4 of this report, and detailed results of the tests are described in Section 5.

(U) The test assembly was retrieved from Test Cell "C" following the full power endurance test and transported to the Reactor Maintenance, Assembly, Disassembly (R-MAD) Building for disassembly. Disassembly was accomplished in the R-MAD hot disassembly bay and the non-nuclear hardware transferred to E-MAD for post-operative examination. The core was disassembled in the R-MAD core disassembly balcony and the fuel processed through the R-MAD fuel element processing system.

(U) The fuel post-operative examination was accomplished in both R-MAD and E-MAD hot cells. All instrumentation post run calibration, metallography, and non-nuclear hardware examination was performed at E-MAD. All radiochemistry, gamma scanning, and whole element weighing was performed at R-MAD. Detailed results are discussed in Section 5.

SECTION 4

(U) TEST DESCRIPTIONS

(U) The NRX-A6 Test Series was, operationally, the least complicated of any of the NRX tests performed to date. The entire test series was aimed at one primary objective: to operate the NRX-A6 reactor at or above rated chamber temperature and pressure for 60 consecutive minutes. To achieve this objective, all other phases of the series were limited to those tests necessary to check out and/or calibrate instrument control and safety systems and to confirm operating procedures. The secondary, or experimental objectives of the NRX-A6 test series are listed in Table 4-1.

(U) The test series, as originally planned, consisted of 3 Experimental Plans (EP's); EP-I to achieve initial criticality, check control drum worth, calibrate the neutronic instrumentation, etc.; EP-II to check the performance of all systems; and EP-III, the power test. Except for an inadvertent shutdown which occurred on the startup of EP-III, the entire series would have been completed in two test days, 21 November and 6 December 1967. Due to the shutdown, however, EP-III was rescheduled as EP-IIIA and run on 15 December 1967.

(U) The reactor operated at a chamber temperature of 4100°R or greater and thermal power of 1100 MW or greater for 60 minutes. A summary of the tests performed during NRX-A6 is shown in Table 4-2, and the power integral summary of the individual EP's is shown in Table 4-3. The following sections describe each experimental plan, and the facility checkout tests performed prior to the experimental plans. For a more detailed description of each experimental plan and the facility checkout tests see References 12, 16, 17, 18, 19, 20, and 21.

(U) FACILITY CHECKOUT TESTS

(U) A series of Facility Checkout Tests (FEP's) were conducted at Test Cell "C" during September and October 1967. The purpose of these tests was to insure that the test facility was in the proper condition for conducting the upcoming reactor test program.

(U) Some of the specific objectives of the Facility Checkout test series were as follows:

- 1) To determine the adequacy of the Emergency Cooldown System (including the newly installed gas accumulator) to protect the reactor from malfunctions in the propellant feed system.
- 2) To establish proper operating techniques for the Emergency Cooldown System to insure satisfactory operation.
- 3) To experimentally determine proper control valve demand profiles for smooth and reproducible propellant feed system startup.
- 4) To check out the feed system controllers.

TABLE 4-1
(U) TEST OBJECTIVES

Primary (Operational) Objective

Endurance was the prime operational objective for NRX-A6. The reactor was to be operated at rated conditions to a predetermined loss of reactivity, or for a time of 60 minutes.

Secondary (Experimental) Objectives

- 1) Evaluation of the effects, of rated conditions duration testing, in fulfillment of the prime objective, on the structural integrity of the test assembly.
- 2) Evaluation of the capability of experimental fuel elements to withstand the effects of rated conditions duration testing.
- 3) Evaluation of the performance of NRX-A6 design changes and hardware modifications.
- 4) Experimental evaluation of the effects of an aft-supported reactor on the pressure vessel and nozzle.
- 5) Evaluation of the nuclear performance of the test article.
- 6) Evaluation of the thermal and fluid flow performance of the test article.
- 7) Further evaluation of the performance of the control instrumentation.
- 8) Evaluation of the performance of improved resistance temperature transducers, accelerometers and a control pressure transducer for use on future test programs.
- 9) Further evaluation of the performance of the NRX control systems.
- 10) To obtain accurate evaluation of the decay heat after extended operation at rated conditions.

TABLE 4-2

(U) SUMMARY OF TESTS PERFORMED DURING MRX-A6 TEST SERIES

<u>EP</u>	<u>Date</u>	<u>Title and Accomplishments</u>
I	21 November 1967	<ol style="list-style-type: none"> 1) Initial Criticality 2) Irradiated neutronic calibration devices and performed frequency response measurements on power control loop during this hold. 3) Performed LN₂ and GN₂ flow tests 4) Control drum worth measurements 5) Low power dosimetry irradiation 6) 360 degree facility shield worth measurements
II	6 December 1967	<ol style="list-style-type: none"> 1) Performed reactor scram checks 2) Exercised all valves and systems to check for any system interaction
III	7 December 1967	<ol style="list-style-type: none"> 1) Planned full power test initiated, but unplanned shutdown occurred after approximately 80 seconds at the 40 pounds per second hold. 2) Verified satisfactory reactor operation at 40 pounds per second and 2150°R chamber temperature.
III	8 December 1967	<ol style="list-style-type: none"> 1) Corrected anomaly which caused unplanned shutdown on previous day. 2) Planned to perform full power test but did not run due to unfavorable meteorological conditions.
IIIA	14 December 1967	<ol style="list-style-type: none"> 1) Planned to perform full power test, but did not run due to problems in setup of hot water system and unfavorable meteorological conditions.
IIIA	15 December 1967	<ol style="list-style-type: none"> 1) Performed planned full power duration test. Operated at a chamber temperature of 4100°R or greater for 62 minutes and thermal power of 1120 MW or greater for 60.4 minutes.

TABLE 4-3

(U) NRX-A6 POWER INTEGRAL SUMMARY

<u>EP</u>	<u>Date</u>	<u>Watt-sec</u> ⁽¹⁾
I	21 November 1967	2.75×10^8 (2)
II	6 December 1967	2.65×10^7 (2)
III	7 December 1967	2.81×10^{10} (2)
III	8 December 1967	5.67×10^7 (2)
IIIA	14 December 1967	4.68×10^8 (2)
IIIA	15 December 1967	4.46×10^{12} (2), (3)
Post Test Critical	19 December 1967	3.94×10^6 (2)
Total, NRX-A6		4.49×10^{12} (2)
Total, NRX-A5		2.2×10^{12} (4)
Total, NRX/EST		3.68×10^{12} (4)
Total, NRX-A3		1.8×10^{12} (4)
Total, NRX-A2		0.38×10^{12} (4)

(1) All power integrals for low power operation after EP-I were corrected to account for the anticipated 15 percent shift in sensitivity due to the cold-to-hot swing for full power operation.

(2) Power integrals based on neutronic wire (gold) calibration of EP-I.

(3) Calculated thermal power integral: 4.47×10^{12} Watt-sec.

(4) Calculated thermal power integral.

(U) As a result of the Facility Checkout Tests, several changes were made to the facility.

- 1) Backflow into the gas accumulator caused unacceptably low temperatures. An unused vent line was blanked off to minimize leakage from the accumulator.
- 2) The turbopump specific speed setting was increased from 950 to 1200 to improve the stall margin during emergency shutdown.
- 3) Position demand profiles for propellant valves L-II and L-III were modified. The result was a flow profile during the power test startup which was very smooth and close to the predictions which were based upon FEP results.
- 4) The turbopump specific speed controller was modified slightly to eliminate a sustained flow oscillation noted at low flow rates.

(U) A more detailed discussion of the Facility Checkout tests may be found in References 19, 20, and 21.

(U) EP-1 - INITIAL CRITICALITY, FLOW TESTS, NEUTRONIC CALIBRATION, LOW POWER DOSIMETRY, AND CONTROL DRUM AND SHIELD WORTH MEASUREMENTS

(U) Experimental Plan I of the NRX-A6 Test Series was conducted on 21 November 1967, at Test Cell "C". The specific objectives of this experimental plan were as follows:

- 1) To determine the cold critical drum position of the reactor with the vertical shield in place and with borated water flow.
- 2) To verify the operation of the control drums scan system.
- 3) To operate the reactor at low power for irradiating the in-core gold wire and sulphur samples for calibrating the neutronics power system.
- 4) To measure the frequency response of the reactor power control and drums position control systems.
- 5) To perform control drum integral and control bank differential reactivity worth tests.
- 6) To perform automatic reactor startups.
- 7) To evaluate the structural integrity of the propellant line final mateup connections and of the reactor reflector system.
- 8) To checkout and evaluate the flow performance of the reactor and to verify the pressure and temperature instrumentation with gaseous and liquid nitrogen flow.
- 9) To determine the reactivity worth of the reactor vertical shield system.
- 10) To complete final checkout of the FRGG, "Elephant" Gun, JATO, and side-by-side pneumatic control drum actuator and experimental transducer systems.
- 11) To irradiate dosimetry with the reactor at low power.

(U) All of the above objectives were successfully achieved during Experimental Plan I.



(U) Initial criticality of NRX-A6 was attained with an average control drum position at delayed critical (θ_{dc}) of approximately 97.3 degrees. This θ_{dc} is applicable when the vertical shield is in place and with borated water flow. The scram check phase following initial criticality was performed with no anomalies.

(U) Frequency response measurements were performed on the Power Control Loop and the Drums Position Control system. Evaluation of the measurements indicated that the operation of both systems was satisfactory.

(U) The calibration run was performed at a nominal 10 kW to irradiate in-core gold wires and nozzle mounted sulphur samples. The results of this run were used to establish the power calibration factor which was applied to the appropriate neutronics channels.

(U) Temperature stimulus of NRX-A6 temperature instrumentation was provided during the LN₂ flow test, and the low power dosimetry irradiation of approximately 150 kW-hr.

(U) The following reactivity worth measurements were performed: (1) Integral worth of Control Drums 2 and 8; (2) Differential worth of the control drum bank; (3) Worth of the reactor vertical shield system without borated water in its open and closed position.

(U) During the LN₂ flow test, the FROG was mated to the NRX-A6 nozzle. No anomalies were noted in the FROG performances; the operation of mating the FROG to NRX-A6 was performed successfully in CP control.

(U) A more detailed discussion of this EP may be found in Reference 16.

(U) EP-II SCRAM CHECKS AND SYSTEM INTERACTION CHECKOUT TESTS

(U) Experimental Plan II of the NRX-A6 Test Series was conducted on 6 December 1967 at Test Cell "C". The specific objectives of this experimental plan were as follows:

1) To operate all systems and subsystems to verify their performance and to check for system interaction.

2) To provide a coordination run for all Control Room Operators and associated personnel in preparation for the Full Power Run.

(U) All of the above objectives were successfully achieved during Experimental Plan II.

(U) With the reactor power level at 10 kW, all valves and systems to be operated during the Full Power Hold were exercised to determine possible system interactions. One interaction, which was not unexpected, was verified; when the fans and louvers were operated in the "penthouse" (where neutronics instrumentation is located) a reactor scram occurred. No other system interactions were observed.

(U) During this EP the following scram checks were successfully performed at the indicated power levels:

- 1) CTO Manual Scram, all drums withdrawn approximately 20 degrees
- 2) Fixed Power Scram at 1 kW
- 3) Power Scram Trim at 500 Watts
- 4) Floating Power Scram at 500 Watts
- 5) Period Scram at 500 Watts
- 6) Program Power Scram at 2 mW
- 7) Minimum Drum Position Scram at $\theta = 30$ degrees

(U) A more detailed discussion of the conduct of this EP may be found in Reference 17.

(U) EP-III - FULL POWER RUN

(U) The specific objectives of this experimental plan were as follows:

- 1) To evaluate the effects of Full Power Testing for 60 minutes on the structural integrity of the test assembly.
- 2) To evaluate the performance of experimental fuel elements under the effects of Full Power Duration Testing.
- 3) To evaluate the performance of the NRX-A6 test assembly design changes.
- 4) To evaluate the nuclear and mechanical performance of the entire test assembly.
- 5) To obtain data to be used in evaluating the performance of several side-by-side experiments.

(U) Efforts to achieve the objectives of Experimental Plan III were made on three occasions: (1) Following Experimental Plan II on 6 December; (2) 7 December; and (3) 8 December 1967. On 5 December, operational problems combined with a time-of-day limitation on operation at full power were responsible for postponement of operation until the next day. On 7 December, the programmed Full Power Run was initiated; however, after approximately 75 seconds at the 40 lb/sec hold, a shutdown occurred. Control Room Operations were suspended for the day to investigate further the cause of the shutdown and to effect necessary repairs. On 8 December, the preliminary phases of Control Room Operations were primarily associated with verification of the "fix" of the cause of the shutdown of the previous day. Following a lengthy weather hold, operations for the Full Power Run were suspended at midday due to predictions of continuing unfavorable meteorological conditions.

(U) Although none of the primary objectives of Experimental Plan III were achieved, the 75-second hold at 40 lb/sec on 7 December 1967, provided a useful bench-mark to evaluate the operation of the reactor and the facility. An extensive data analysis effort showed that reactor temperatures, pressures and differential pressures were, in general, quite satisfactory at the 40 lb/sec hold with the reactor at a power level of 301 MW. One major problem in facility



operation was that the Specific Speed at the 40 lb/sec hold was 1300 instead of the desired 1200. This problem was analyzed and corrected prior to the initiation of EP-IIIA.

(U) A more detailed discussion of this EP may be found in Reference 17.

(U) EP-IIIA - FULL POWER DURATION TEST

(U) Experimental Plan III of the NRX-A6 Test Series was redefined as EP-IIIA and conducted on 15 December 1967, at Test Cell "C". The specific objectives of this experimental plan were the same as EP-III and were as follows:

- 1) To evaluate the effects of full Power Testing for 60 minutes on the structural integrity of the test assembly.
- 2) To evaluate experimental fuel elements under the effects of Full Power Duration Testing.
- 3) To evaluate the performance of the NRX-A6 test assembly design changes.
- 4) To evaluate the nuclear and mechanical performance of the entire test assembly.
- 5) To obtain data to be used in evaluating the performance of several side-by-side experiments.

(U) All of the above objectives were successfully achieved on 15 December following postponements due to adverse weather conditions on 13 December, and a combination of facility operational problems and adverse weather conditions on 14 December 1967.

(U) The duration of the Full Power Hold was over 60 minutes; the power integral was approximately 4.5×10^{12} Watt-seconds. Nominal operating conditions during the Full Power Hold were as follows:

Thermal Power	1,130 MW
Neutronic Power	1,250 MW
Nozzle Chamber Pressure	593 psia
Nozzle Chamber Temperature	4,140°R
Flow Rate (BF-13, Figure 4-1)	72.0 lb/sec

(U) Reactor performance parameters during the test run and the performance operating map are shown in Figures 4-1 and 4-2, respectively.

(U) Control drum position near the start of the Full Power Hold was 104.5 degrees; at the conclusion of the hold, the indicated drum position was 115.4 degrees. Control drum position near ambient temperature, as determined on the post-run criticality test, was 100.9 degrees; control drum position prior to the Full Power Run was 95.5 degrees.

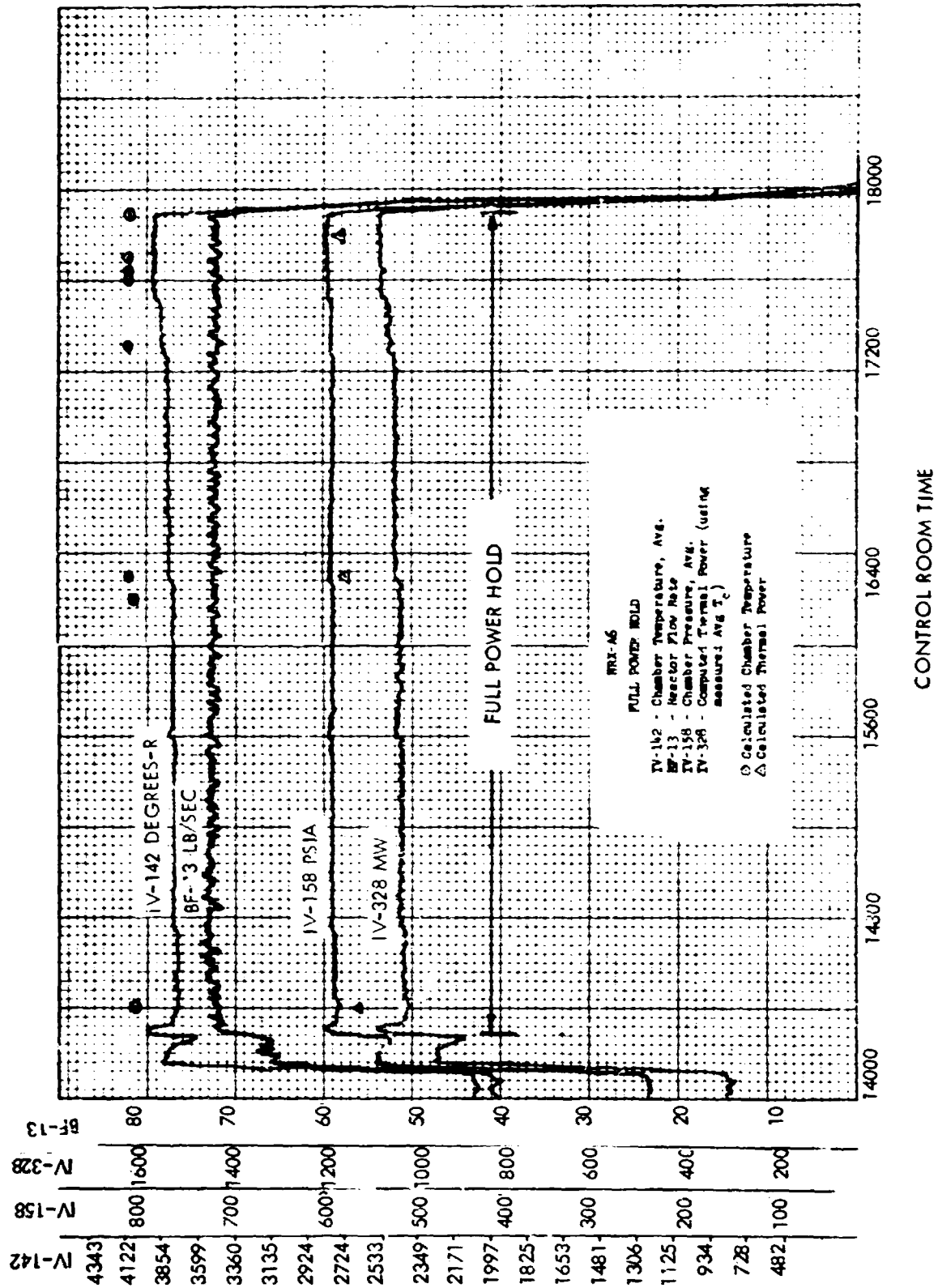
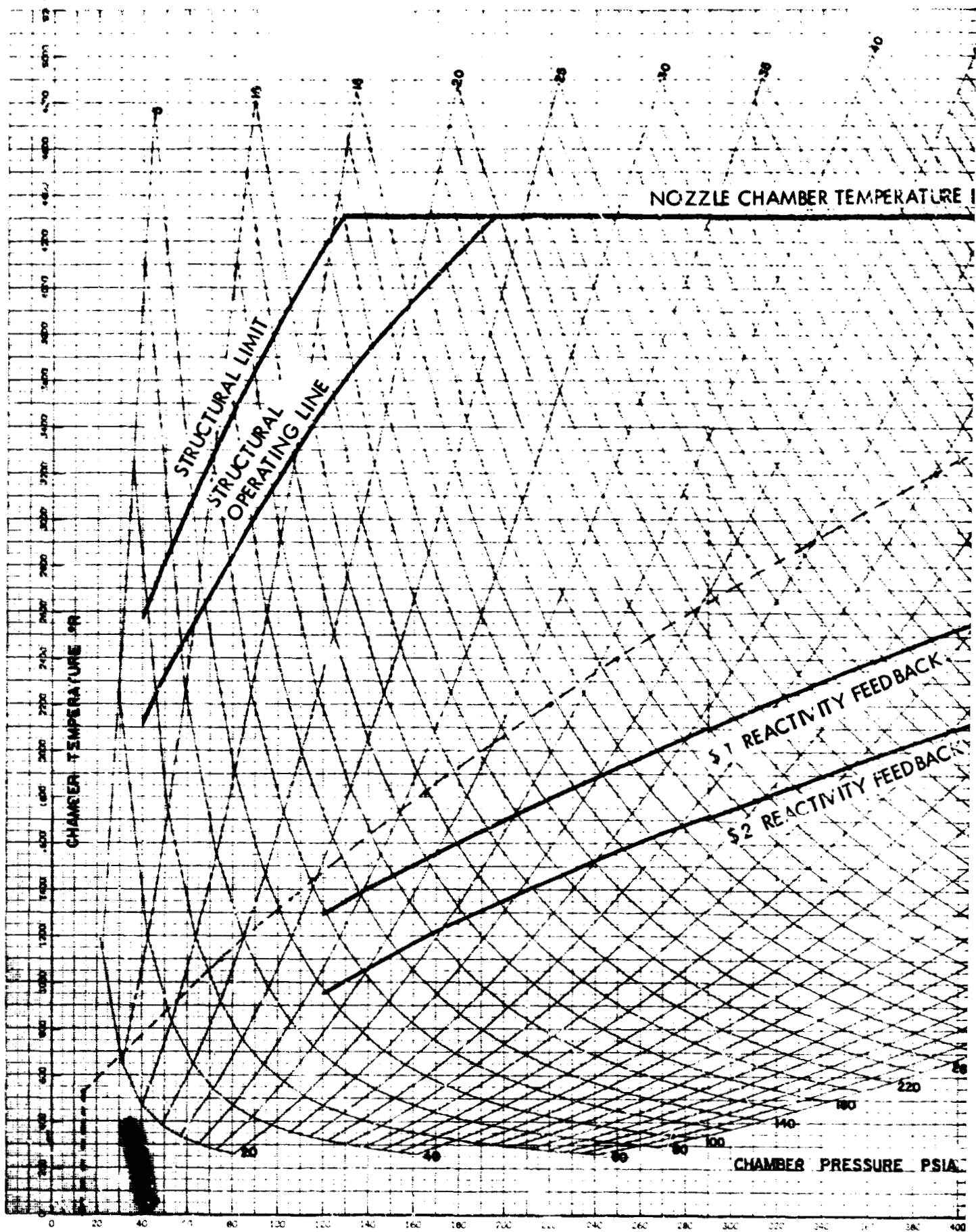


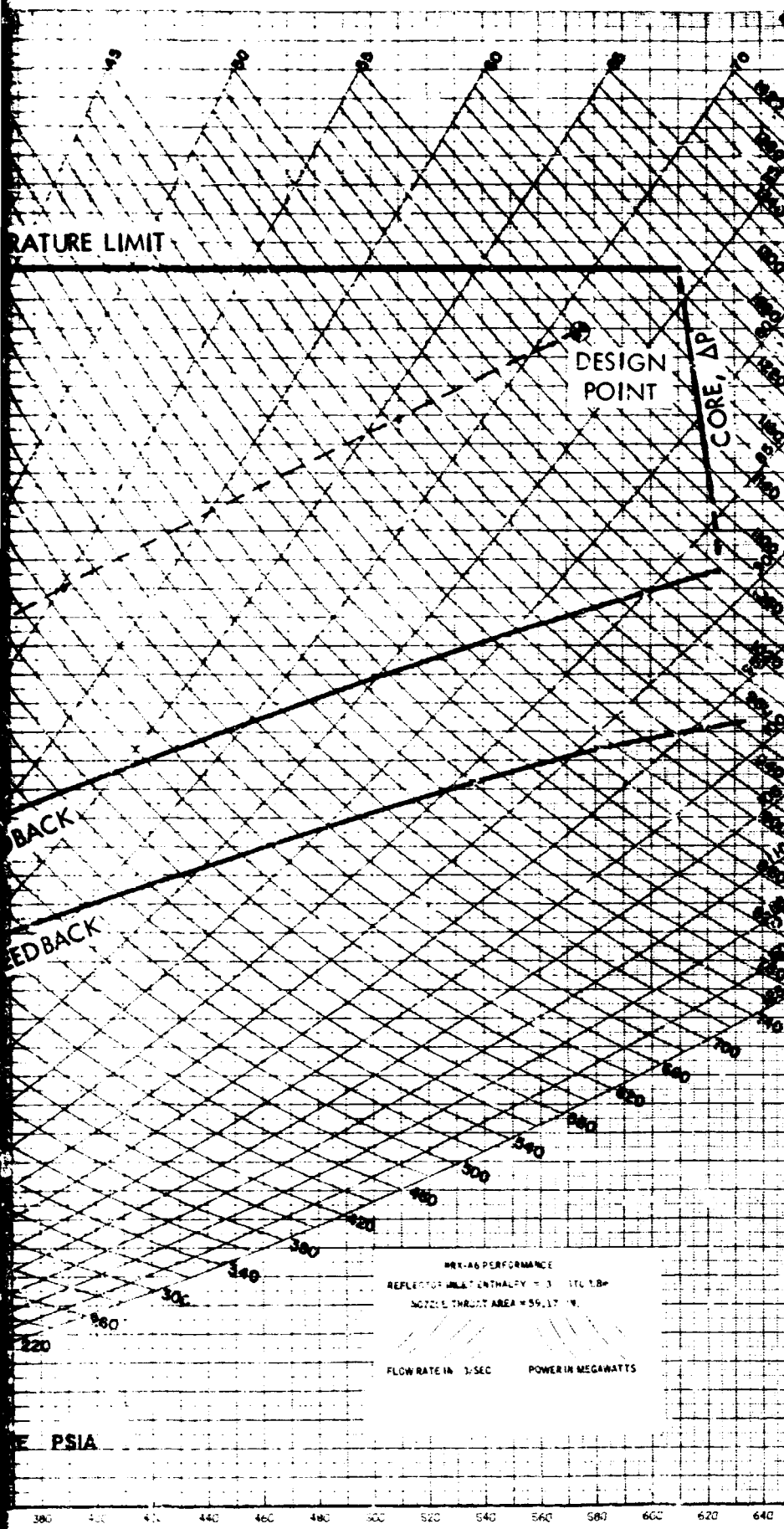
Figure 4-1. (U) NRX-A6 Full Power Test, EP-III A, Parameter Run Time Profile



(U) The operation of all cooldown systems following the planned shutdown at 43 lb/sec was satisfactory. LN₂ pulse cooling was terminated on 18 December. For the post-run criticality test on 19 December, GN₂ was used to cool the reactor to near ambient temperature. The NRX Test Assembly was disconnected on 20 December and transferred to the R-MAD Building.

(U) A more detailed discussion of this EP may be found in Reference 18.





2

Figure 4-2.
(U) NRX-A6 Full Power Test,
EP-III A, Operating Map

~~CONFIDENTIAL~~



SECTION 5

(CRD) TEST RESULTS (U)

(CRD) TRANSIENT AND STEADY-STATE PERFORMANCE ANALYSIS (U)

(CRD) Reactor System Performance (U)

(CRD) This section summarizes the detailed thermal and corrosion analysis of the NRX-A6 power test. A more complete discussion is presented in Reference 22. The NRX-A6 test was extremely successful and exceeded its test objectives. The total run time of 62 minutes above a chamber temperature of 4100°R * more than doubled the full power and temperature endurance of previous reactors with significantly less corrosion. A 4100°R chamber temperature corresponds to an average fuel exit gas temperature of 4335°R .

(U) A summary of major reactor performance conditions of the NRX-A2 through A6 tests is given in Table 5-1. Included are, (a) total run times within different chamber temperature intervals, (b) equivalent full power radiation, (c) maximum flow rate and power, (d) number of startup and shutdown cycles, (e) maximum ramp rates, and (f) total reactivity loss.

(U) The NRX-A6 test was of particular significance since it demonstrated the endurance capability of the NRX-A6 reactor.

(CRD) Operating Conditions (U)

(U) EP-III A time profiles of nozzle chamber temperature, flow rate, nozzle chamber pressure, and control drum position are shown on Figure 5-1. All parameters with the exception of control drum bank position are nearly constant throughout the full power hold. The total control drum roll out of 11 degrees during the full power hold was significantly less than predicted. Points A through D indicate times at which best estimated calculations and state point comparisons with predictions are presented in the following two sections.

(CRD) A summary of major NRX-A6 operating conditions is given in Table 5-2. NRX-A6 operated for 62 minutes above a chamber temperature of 4100°R (design temperature was 4090°R) which is more than twice the endurance of any previous NRX reactor. Peak chamber temperature conditions of 4330°R which correspond to 4600°R average fuel exit temperature and 1199 MW thermal power existed for approximately 30 seconds at the start of the full power hold.

* Note: In this section, chamber temperature is defined as the mixed mean temperature immediately downstream of the core exit.

~~CONFIDENTIAL~~

(THIS PAGE IS UNCLASSIFIED)

TABLE 5-1
(U) NRX-A2 THROUGH NRX-A6 MAJOR REACTOR PERFORMANCE SUMMARY

Reactor	NRX-A2	NRX-A3	NRX/EST	NRX-A5	NRX-A6
Chamber Temperature ("R)	Time within chamber temperature interval (minutes)				
3700-3800	0.8	0.2	3.6	0.7	0.1
3800-3900	--	13.4	6.1	3.0	0.1
3900-4000	--	3.0	5.3	11.3	0.1
4000-4100	--	--	7.3	12.8	0.6
4100-4200	--	--	7.8	2.3	54.6
4200-4300	--	--	--	--	6.8
4300-4400	--	--	--	--	0.6
Equivalent Full Power Radiation (Minutes,					
a. Entire Test Series	5.7	26.8	54.4	32.2	66.9
b. Single Run	5.1	14.3	14.5	16.4	66.6
Maximum Flow Rate (lb/sec)	75.6	73.5	87.9	71.9	72.0
Maximum Power (MW)	1096	1100	1155	1120	1200
Number of Startup and Shutdown Cycles Above 2500 R	1	3	6	2	1
Maximum Startup Ramp ("R/sec)	125	80	140	70	88
Maximum Shutdown Ramp ("R/sec)	-350	-300	-141	-80	-63
Observed Total Reactivity Loss (\$)	0.1	0.9	3.2	2.1	0.7

(THIS PAGE IS UNCLASSIFIED)

~~CONFIDENTIAL~~

(THIS PAGE IS UNCLASSIFIED)



Astronautics
Laboratory

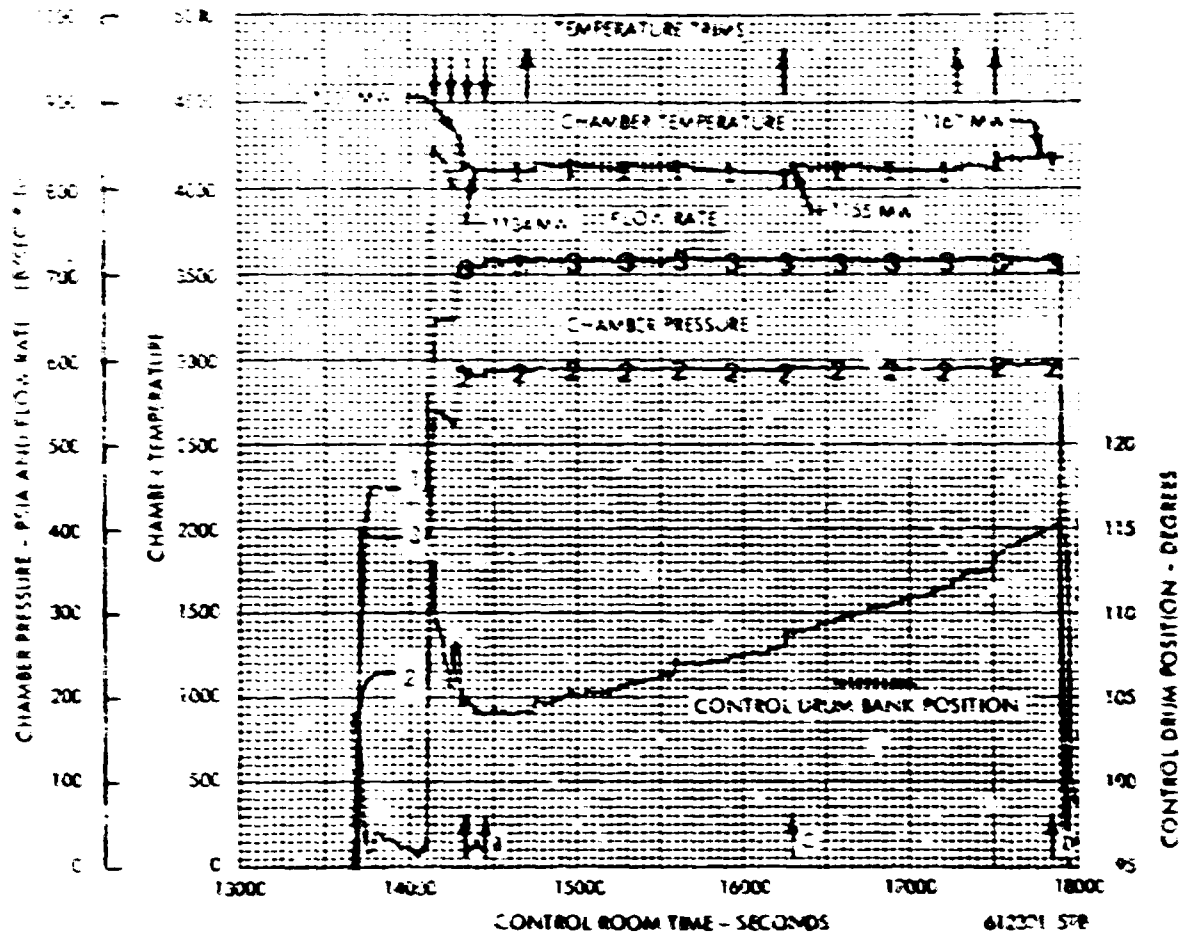


Figure 5-i. (U) NRX-A6 Full Power Test, EP-III A, Performance Profiles

(THIS PAGE IS UNCLASSIFIED)

~~CONFIDENTIAL~~

~~CONFIDENTIAL~~

TABLE 5-2
(CRD) MAJOR NKA-A6 OPERATING CONDITIONS (C)

Temperature Range (°R)	Time Within Temperature Interval (Minutes)	
	Chamber Temperature	Average Fuel Exit Temperature
4000-4100	0.6	0.1
4100-4200	54.6	0.1
4200-4300	6.8	0.7
4300-4400	0.6	41.3
4400-4500	0	20.0
4500-4600	0	0.7

Thermal Power Range (Mw)	Time Within Power Range Interval (Minutes)
1000-1100	2.3
1100-1200	60.4

	Design	Maximum Attained During Test
Chamber Temperature (°R)	4090	4330
Fuel Exit Temperature (°R)	4325	4600
Thermal Power (Mw)	1120	1199
Time at Design Temperature (min)	60	62
Integrated Thermal Power (Watt-sec)		4.5×10^{12}

~~CONFIDENTIAL~~

~~CONFIDENTIAL~~
(THIS PAGE IS UNCLASSIFIED)



(U) Best Estimates of Flow Rate, Chamber Temperature, and Power

(U) Best estimates of reactor flow rate, chamber temperature, and thermal power were computed at 24 steady state times during EP-IIIA. These calculations were performed with the most accurate procedures and the best available data. Normalized digital data at 40 samples per second averaged over 5 second time intervals (200 points) with pressure and pressure drop measurements corrected for offsets determined at zero flow were used for the calculations. The results of these calculations were used to define the operating conditions of NRX-A6 and for input to the detailed thermal calculations presented in Reference 22.

(U) Table 5-3 summarizes the results with three sigma uncertainties for four steady state times during EP-IIIA. Nozzle chamber temperature was calculated three ways: (1) based on the flow weighted average fuel exit gas temperature measurements, (2) based on the station 26 core temperature and (3) based on the nozzle equation using flow rate and average measured chamber pressure. The best estimated chamber temperature is the weighted average of these three chamber temperatures with each calculated temperature weighted according to its uncertainty. The calculation procedure is described in detail in Reference 22, Appendix B.

(CRD) Steady State and Transient Comparisons with Predictions (U)

(U) Steady state and transient comparisons between test data and TNT pre-test calculation results are presented in this section. One of the major uses of the TNT (Thermal and Nuclear Transient) program is for pre-test predictions. Therefore, comparisons with test data are essential to verify the accuracy of the TNT program and to indicate possible areas of improvement.

(U) Steady state comparisons for the four times indicated by letters A through D on Figure 5-1 are given in Table 5-4. The TNT pre-test prediction for the planned flow rate, power and chamber temperature profiles are compared with the data. The planned profiles were closely duplicated during the first 60 seconds of startup and shutdown prior to scram. The second part of the startup was conducted at higher than planned chamber temperatures because the chamber temperature measurements which were used for control did not read the true chamber temperature. At the planned 3700°R hold the actual chamber temperature was 4250°R. The differences between the planned and actual profiles are shown on Figures 5-2 through 5-8. The lower than predicted reflector pressure drop was the result of greater than expected flow through the reflector/pressure vessel annulus, lower than predicted reflector inlet plenum temperature, and lower reflector heating. Also, following scram the flow rate was higher than predicted.

(U) The comparisons between TNT pre-test calculation results and test measurements are excellent when the differences between the planned and actual test profiles are considered. Detailed parameter comparisons for all phases of EP-IIIA are presented in Reference 22.

(THIS PAGE IS UNCLASSIFIED)

~~CONFIDENTIAL~~

CONFIDENTIAL

TABLE 5-3
(CRD) NRX-A6 EP-IIIA BEST ESTIMATED FLOW RATE, CHAMBER TEMPERATURE,
AND THERMAL POWER (U)

Steady State Point (See Figure 5-1)	A	B	C	D
Control Room Time (sec)	14295	14400	16200	17800
Average Flow Rate (lb/sec)	71.4 \pm 1.6	71.3 \pm 1.6	72.0 \pm 1.6	72.0 \pm 1.6
Chamber Temperatures ($^{\circ}$ R)				
(1) Based on Weighted Average Fuel Exit Gas Temperature	4343 \pm 111	4340 \pm 105	4162 \pm 105	4200 \pm 107
(2) Based on Station 26 Core Temperature	4233 \pm 192	4053 \pm 183	4145 \pm 188	4199 \pm 190
(3) Based on Nozzle Equation	4507 \pm 339	4289 \pm 321	4355 \pm 320	4393 \pm 330
Best Estimated Chamber Temperature ($^{\circ}$ R)	4330 \pm 93	4131 \pm 88	4173 \pm 89	4215 \pm 90
Thermal Power (MW)	1199 \pm 41	1133 \pm 39	1157 \pm 39	1170 \pm 39

NOTE: The three sigma uncertainties are given.

TABLE 5-4

(CRD) STEADY-STATE COMPARISON OF EP-III A BEST ESTIMATE STUDY WITH TNT PRE-TEST PREDICTIONS (U)

Point (See Figure 5-1)	Units	TNT Pre-Test Predictions*			
		A	B	C	D
Control Room Time	sec	14295	14400	16300	17800
Thermal Power	MW	1199	1134	1155	1167
Reactor Flow Rate	lb/sec	71.4	71.3	72.0	72.0
Control Drum Position	degrees	108.2	104.7	109.1	115.3
		97 (SOL)**			
Reflector Inlet Pressure	psia	760	739	751	753
Temperature	°R	150	143	150	152
Core Inlet Pressure	psia	728	706	712	719
Temperature	°R	213	223	228	230
Core Exit Pressure	psia	602	585	596	599
Temperature	°R				
Tie Rod		694	656	660	685
Average Fuel Chamber		4604	4385	4408	4450
		4330	4131	4173	4215
Component Pressure Drops	psi				
Reflector Core		16.9	16.2	17.2	17.1
		127.5	120.5	122	120.5
Unfueled Temperature	°R				
Station 20		3389	3221	3332	3391
Station 26		3937	3769	3855	3905

* See Reference 23

** Start of Reactor Life

CONFIDENTIAL



CONFIDENTIAL

~~CONFIDENTIAL~~

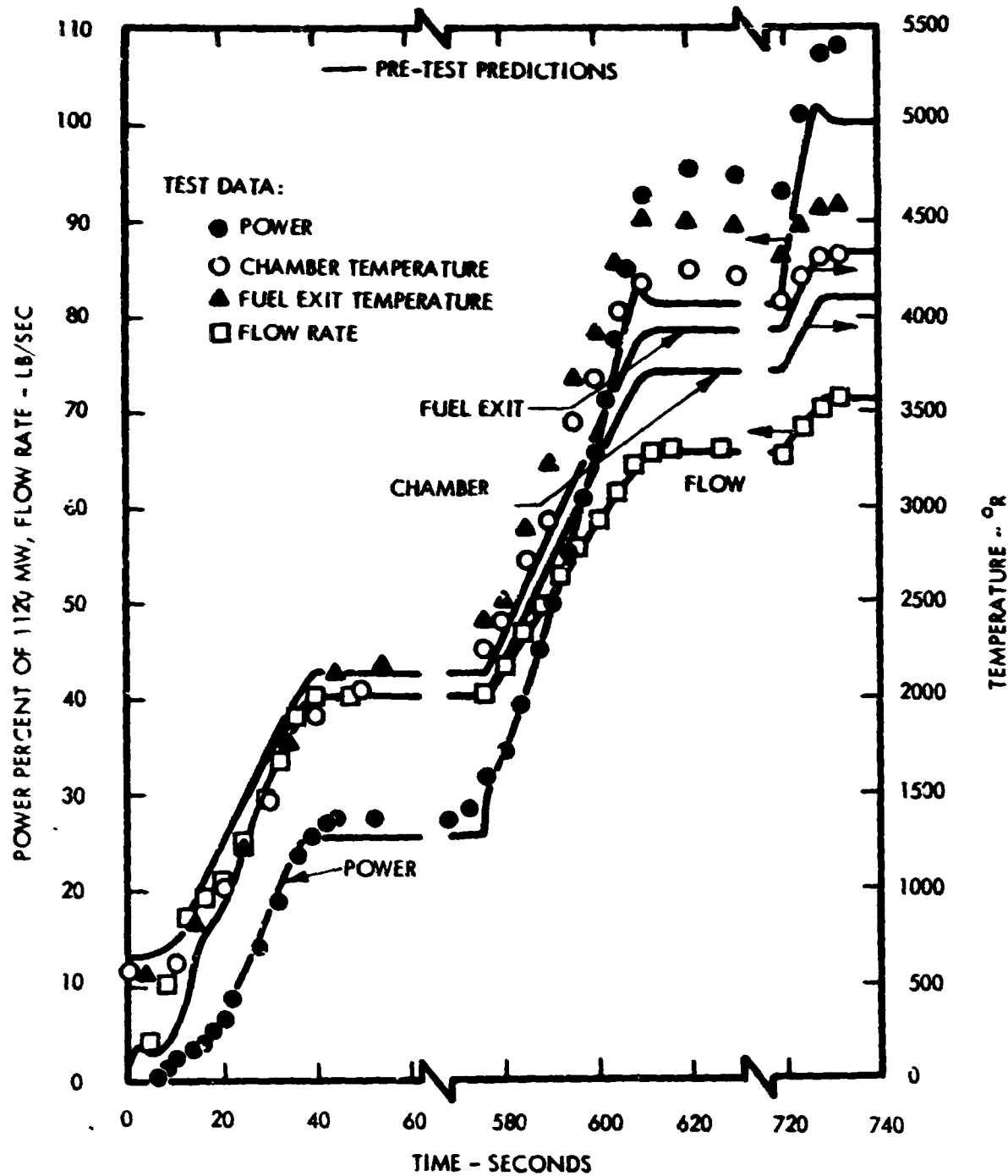


Figure 5-2. (CRD) Comparison of Power, Nozzle Torus Flow, Average Fuel Exit and Chamber Temperature Predictions with Measurements During EP-III A Startup (U)

~~CONFIDENTIAL~~

~~CONFIDENTIAL~~
(THIS PAGE IS UNCLASSIFIED)

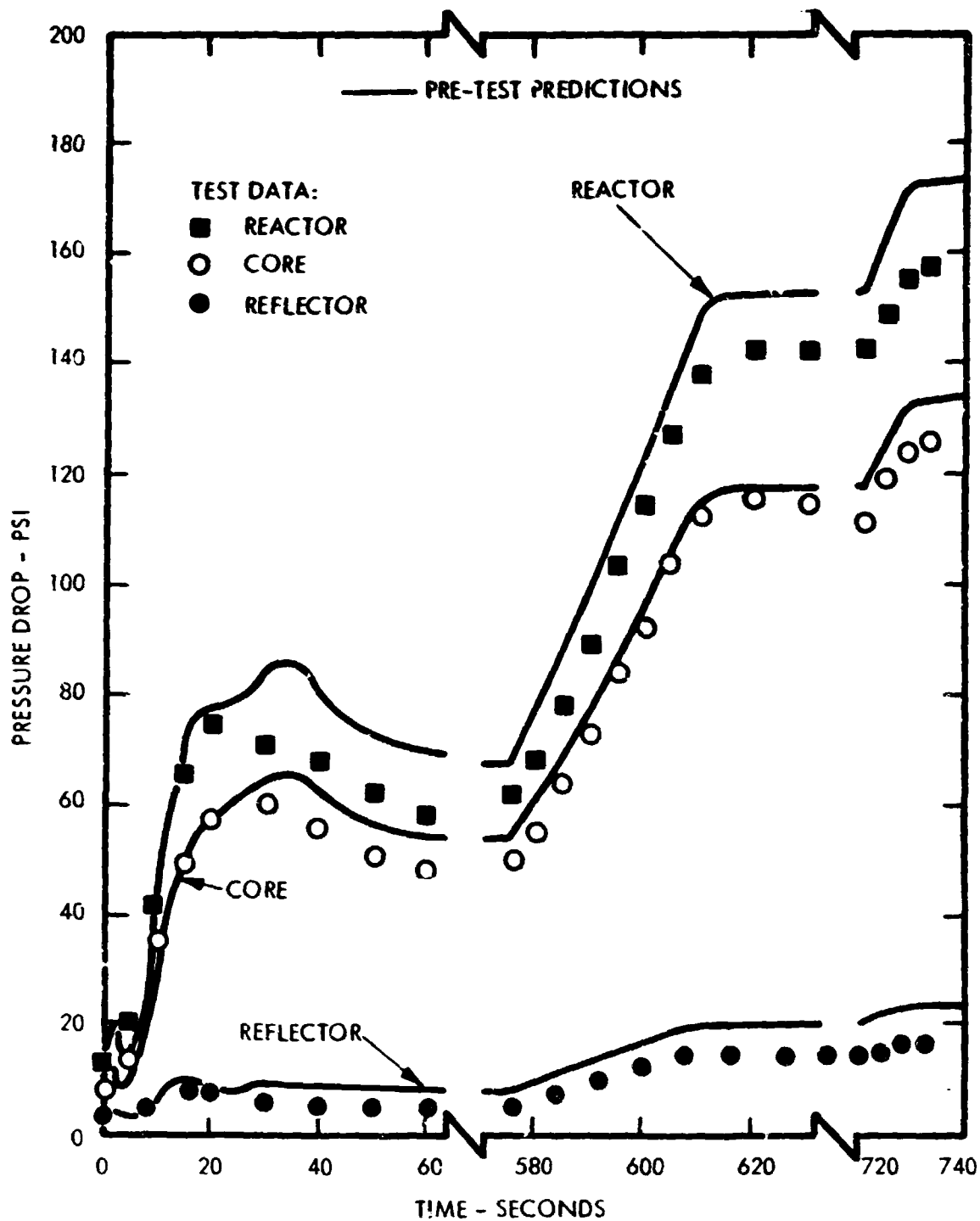


Figure 5-j. (U) Comparison of Component Pressure Drop Predictions with Measurements During EP IIIA Startup

(THIS PAGE IS UNCLASSIFIED)
~~CONFIDENTIAL~~

CONFIDENTIAL

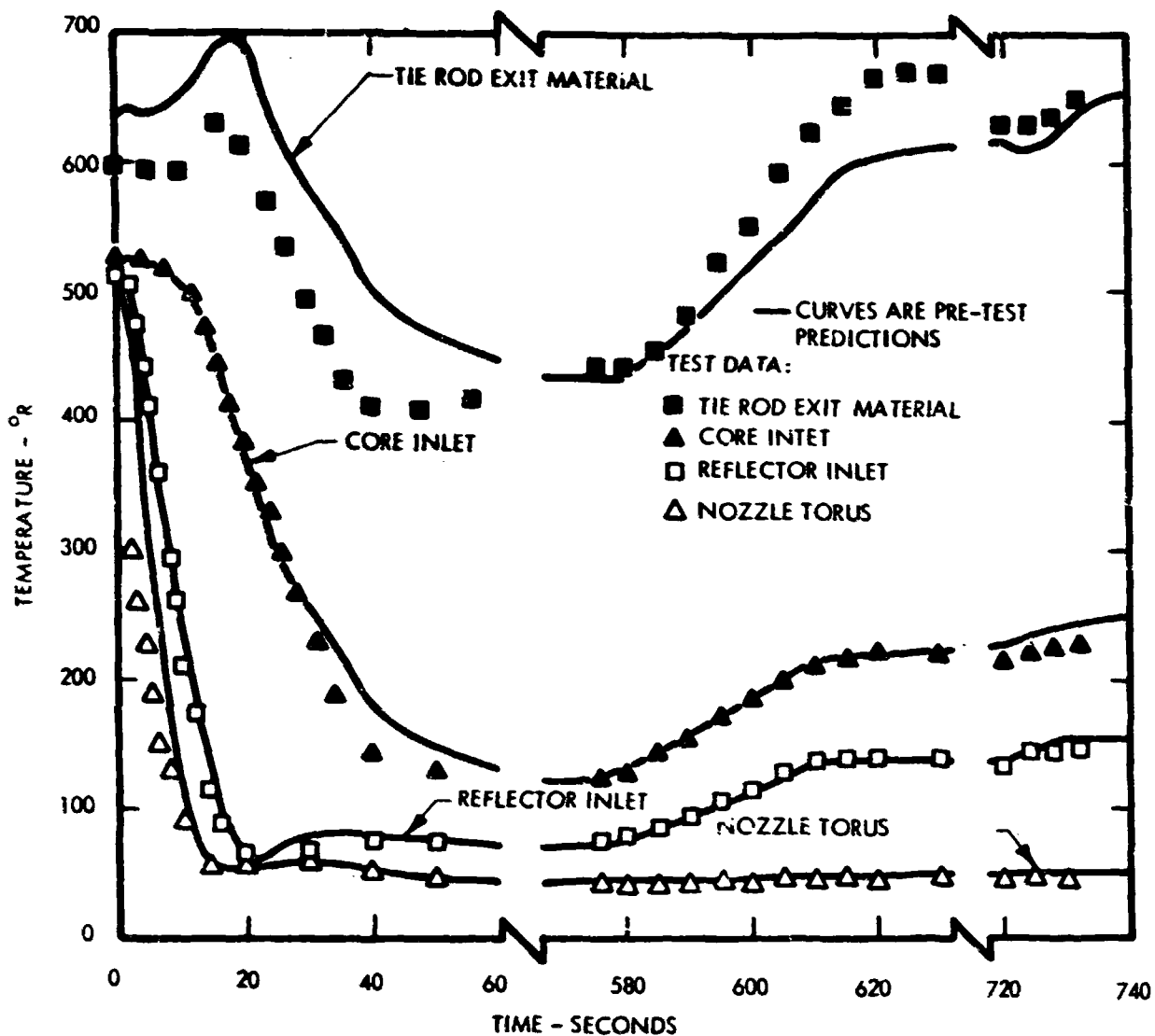


Figure 5-4. (CRD) Comparison of Tie Rod Exit Material and Reactor Plenum Temperature Predictions with Measurements During EP-IIIA Startup (U)

CONFIDENTIAL

~~CONFIDENTIAL~~

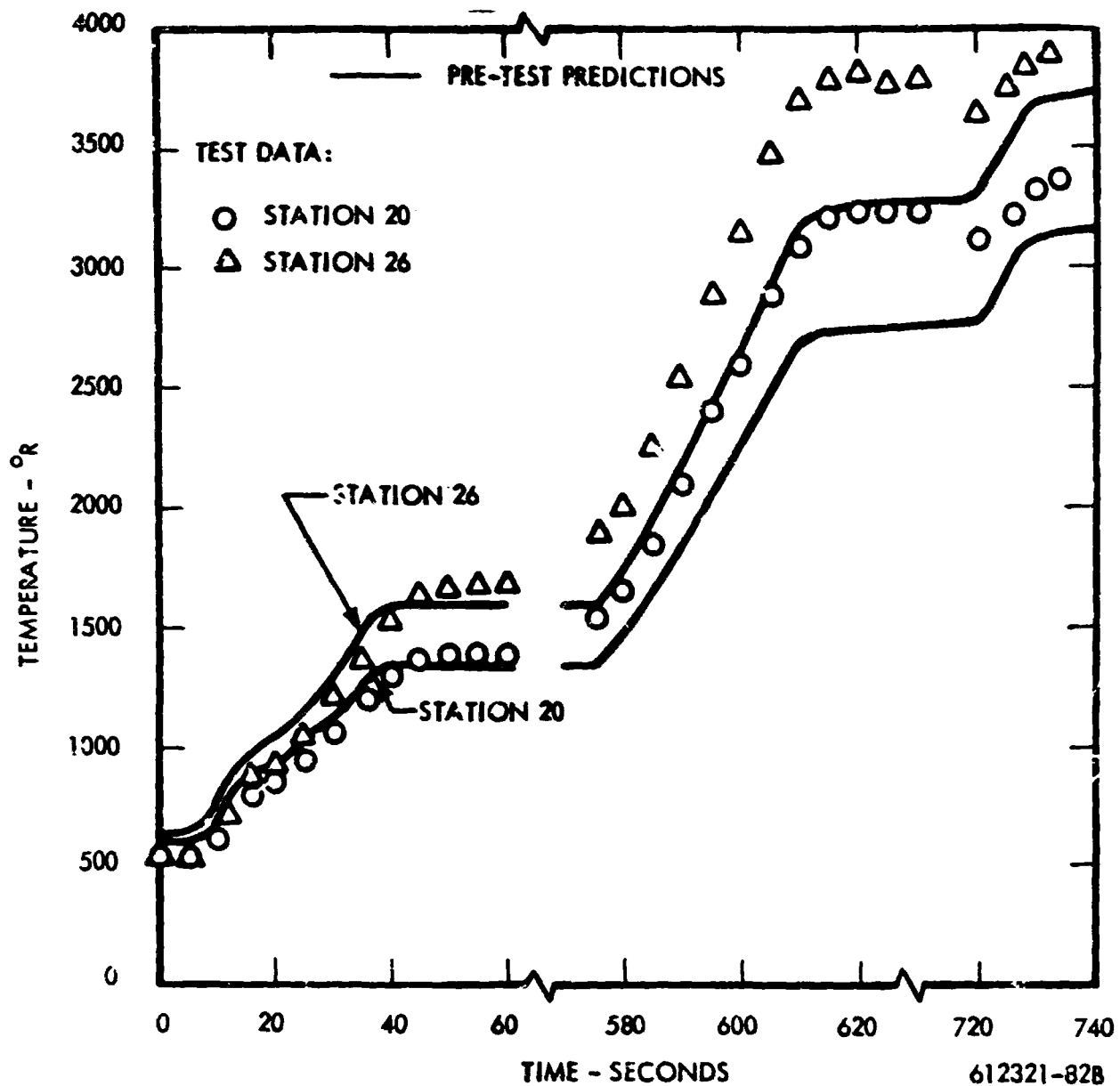


Figure 5-5. (CRD) Comparison of Core Station Temperature Predictions with Measurements During EP-IIIA Startup (U)

~~CONFIDENTIAL~~

~~CONFIDENTIAL~~

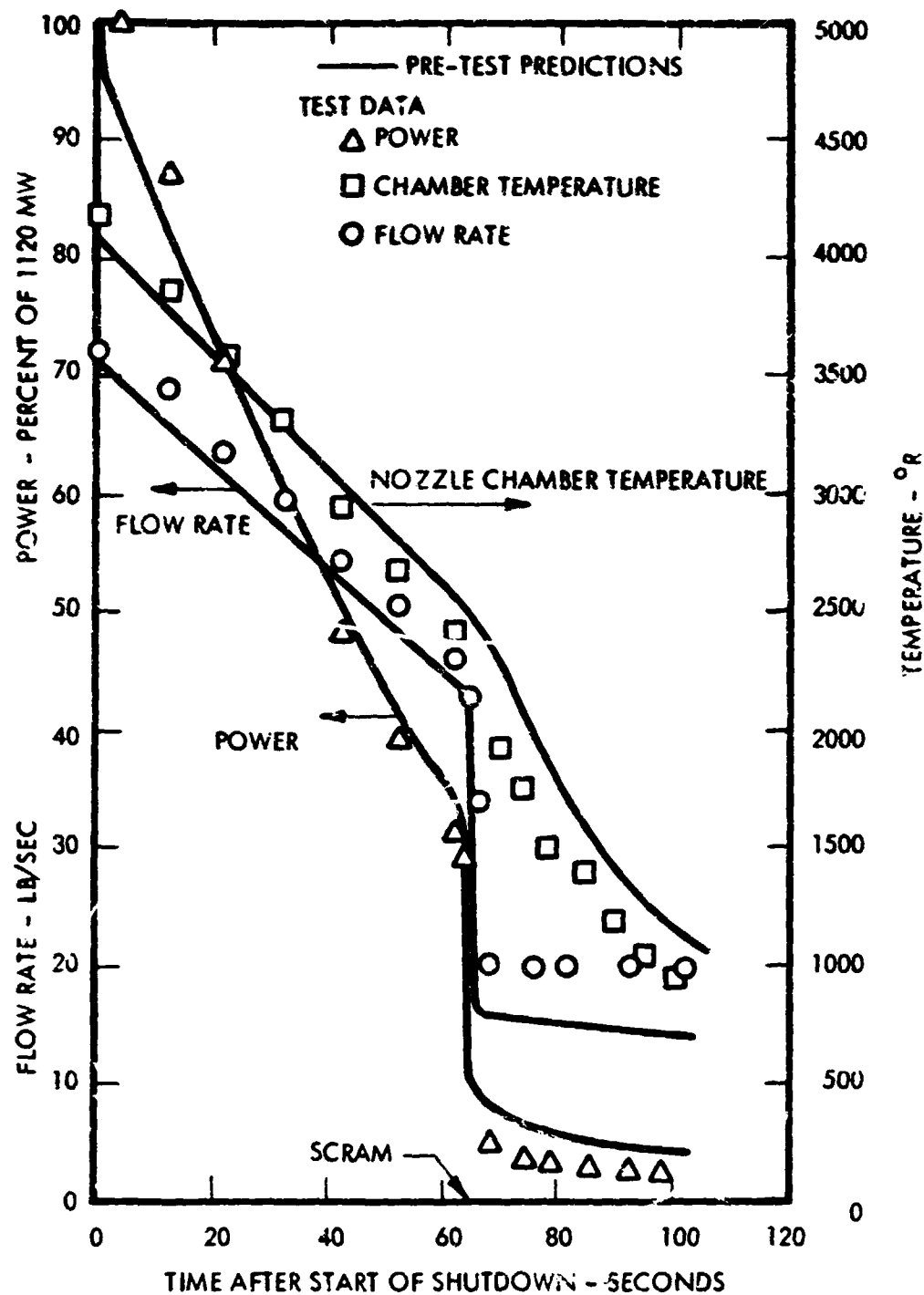


Figure 5-6. (CRD) Comparison of Power, Nozzle Torus Flow, and Chamber Temperature Predictions with Measurements During EP-IIIA Shutdown (U)

~~CONFIDENTIAL~~

~~CONFIDENTIAL~~

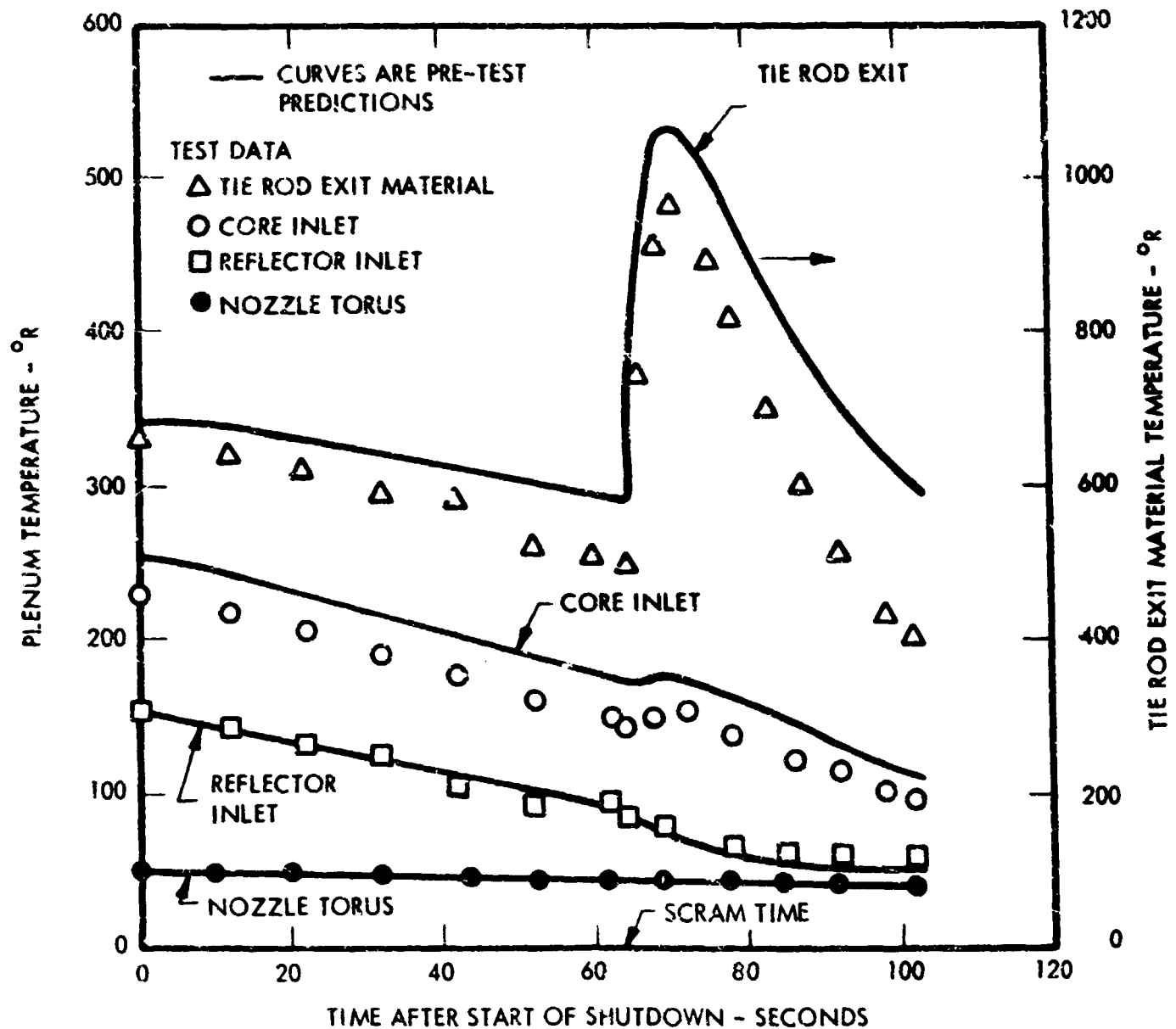


Figure 5-7. (CRD) Comparison of Tie Rod Exit Material and Reactor Plenum Temperature Predictions with Measurements During EP-IIIA Shutdown (U)

~~CONFIDENTIAL~~

CONFIDENTIAL

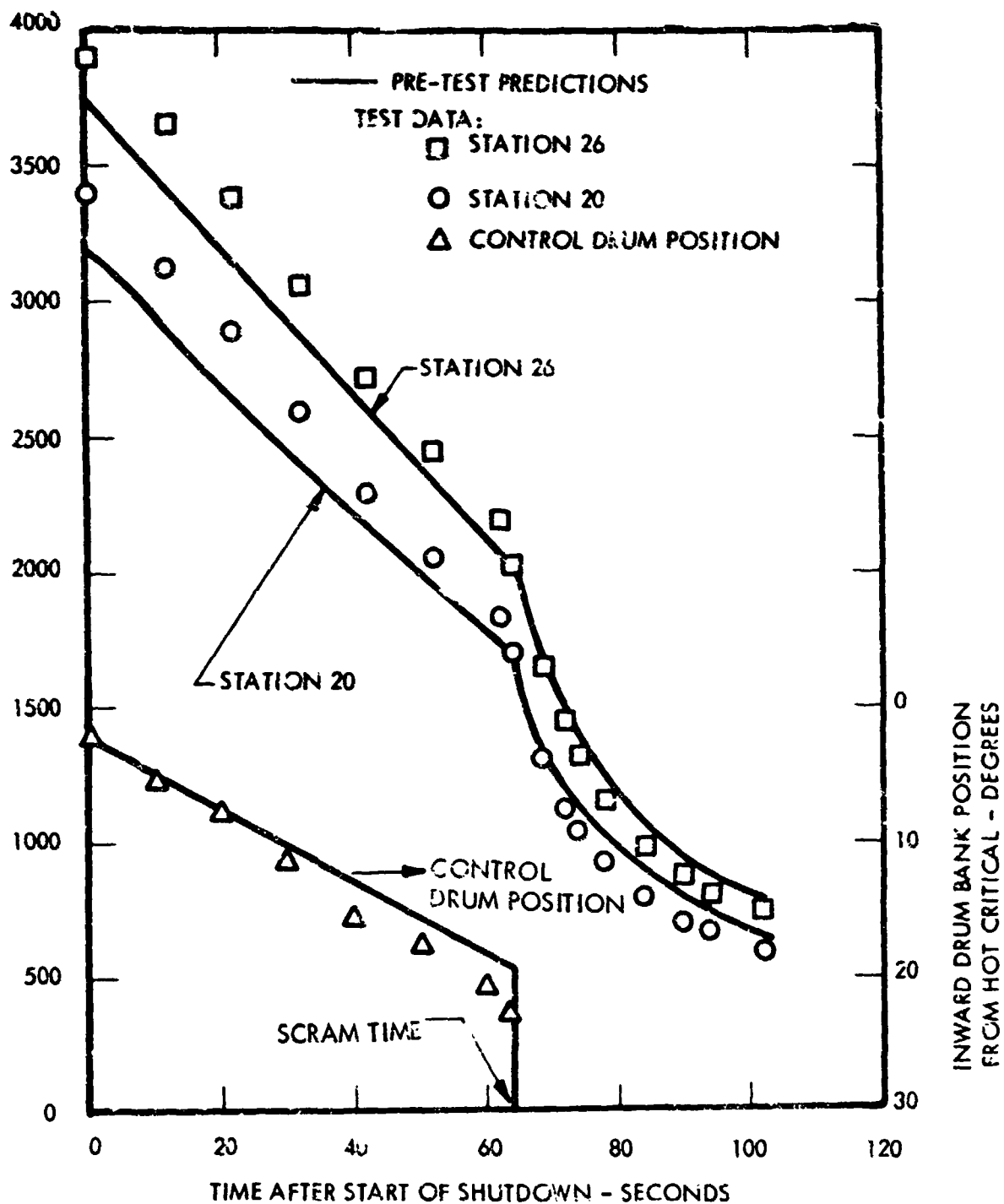
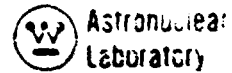


Figure 5-8. (CRD) Comparison of Core Station Temperatures and Control Drum Motion Predictions with Measurements During EP-III A Shutdown (U)

CONFIDENTIAL

CONFIDENTIAL



(CRD) Core Thermal Performance (U)

(U) The core operated at or above design temperatures for 62 minutes and met the endurance objective of 60 minutes with only an 11 degree drum rollout. Post-test calculated data compared with test data showed good agreement. The following is a brief summary of the detailed core thermal analysis. A more detailed discussion may be found in Reference 22.

(CRD) Figure 5-9 shows a radial profile of the maximum measured temperatures during EP-IIIA based on the station 44 thermal capsules. The thermal capsule measurements indicate the highest temperature reached during power operation. The peak central region temperatures of 5000°R occurred during the power peak at the start of the run (approximately 14300 seconds control room time). Post-test calculations indicated that the peak peripheral temperatures of 4700°R probably occurred both at this power peak and also at the end of the full power hold. The calculated central and fueled element axial temperature profiles for the core central region at the power peak and for the peripheral region at the end of the full power hold are shown on Figures 5-10 and 5-11 respectively. Central element temperature measurements with thermocouples and thermal capsules and fueled exit gas temperature measurements are also shown. The comparison between calculations and measurements is very good.

(U) Fuel exit gas thermocouples which were used for the first time, correctly measured fuel exit gas temperatures. Measured temperatures agreed well with calculations and were generally consistent with measurements at other core stations. Measured fuel exit temperatures were therefore used in the best estimate of the nozzle chamber temperature.

(U) Comparisons between calculated and measured fuel exit and station 26 unfueled element radial temperature profiles near the start of the full power hold are shown on Figure 5-12. The measured core inlet conditions and corrected post-test power factors, average in 1 inch radial increments, were used for the calculation. Again, the comparison is very good. Probably most of the scatter is caused by uncertainties in predicting the power generation, core inlet temperature and tolerance in each individual fuel element. The calculated maximum station 26 fuel temperature is also shown in the figure.

(CRD) Radial temperature profiles of fuel exit, station 26, station 20 and the rod material at the start and end of the full power hold are shown on Figures 5-13 and 5-14. The multiple regression curve fits with three sigma uncertainty bands are shown for each parameter. At the start of the full power hold the fuel exit gas temperature was 200°R cooler at radius 12-16 inches than at the center of the core. The multiple regression analysis indicated a flat radial temperature profile at the end of the full power hold.

CONFIDENTIAL

CONFIDENTIAL

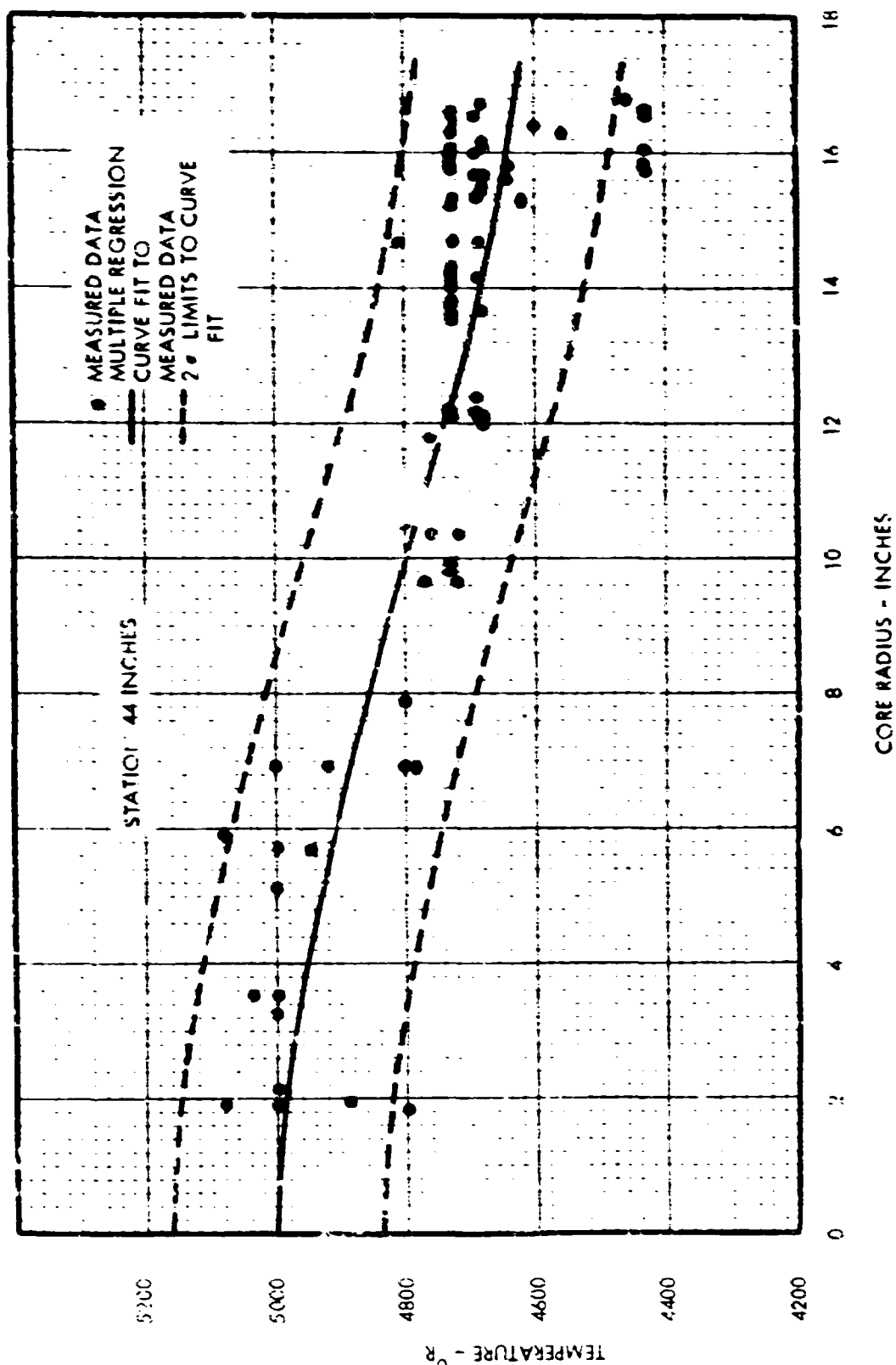


Figure 5-9. (CRD) NRX/A6 Thermal Capsule Temperatures vs Core Radius (U)

CONFIDENTIAL

CONFIDENTIAL

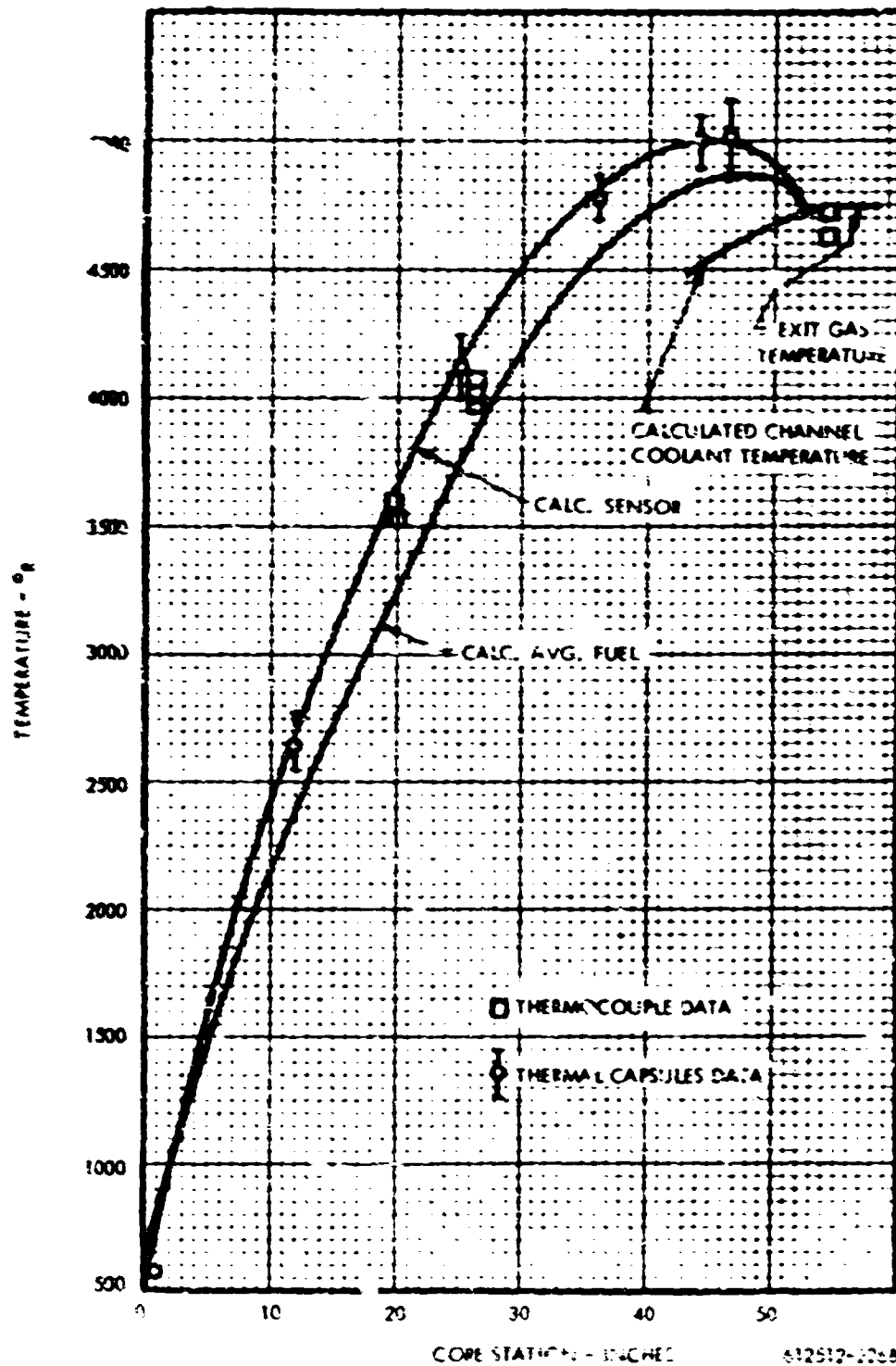
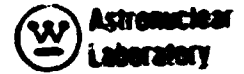


Figure 5-10. (CRD) Central Region, Total Temperature Distribution EP-111A at CRT 14300 (0)

CONFIDENTIAL

CONFIDENTIAL

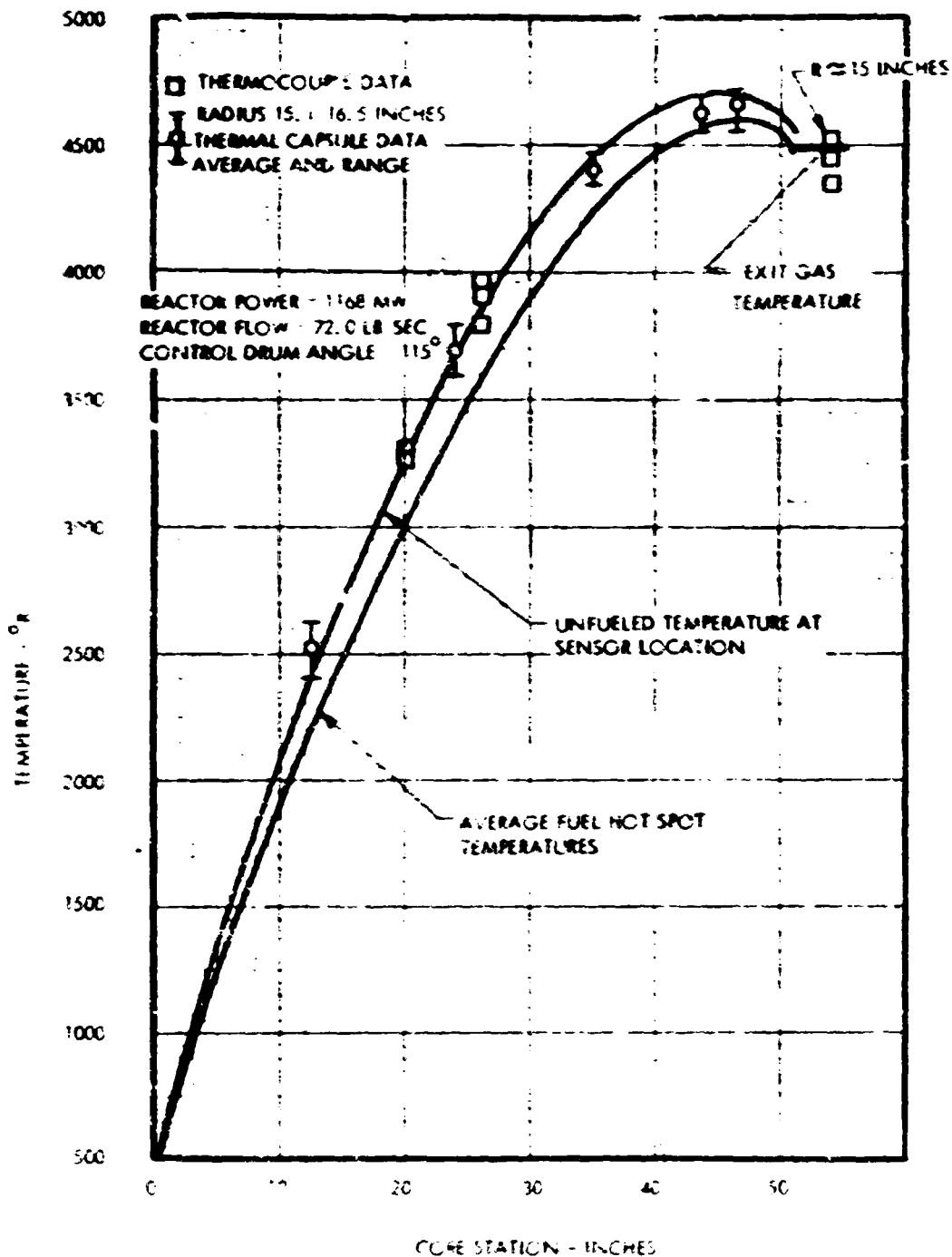


Figure 5-11. (CRD) Peripheral Region Axial Temperature Distribution for EP-III A at CRT 17600 (U)

CONFIDENTIAL

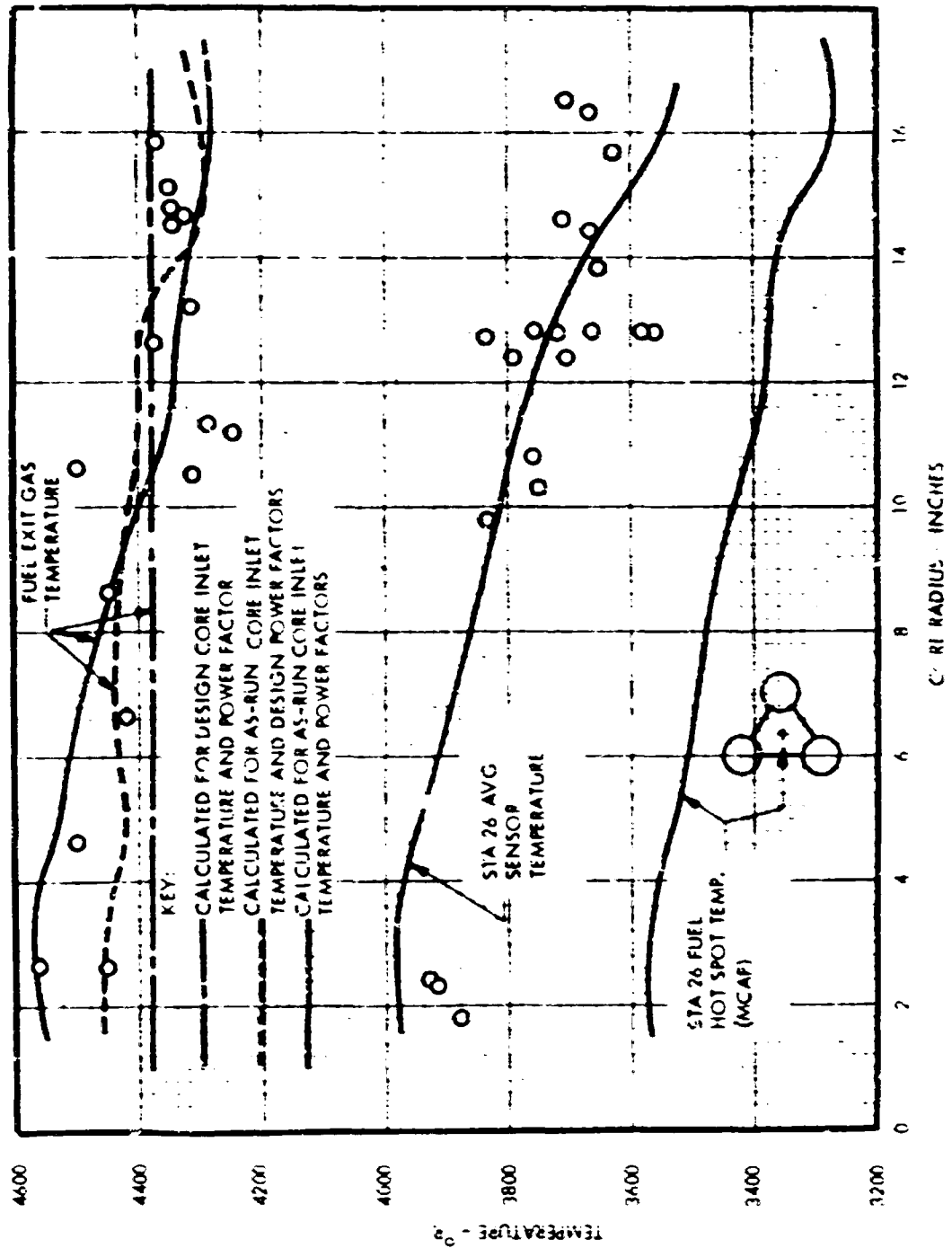


Figure 5-12. (CRD) Core Temperatures Versus Radius During EP-111A at CRT 14400 and Drum Position 105" (U)

~~CONFIDENTIAL~~

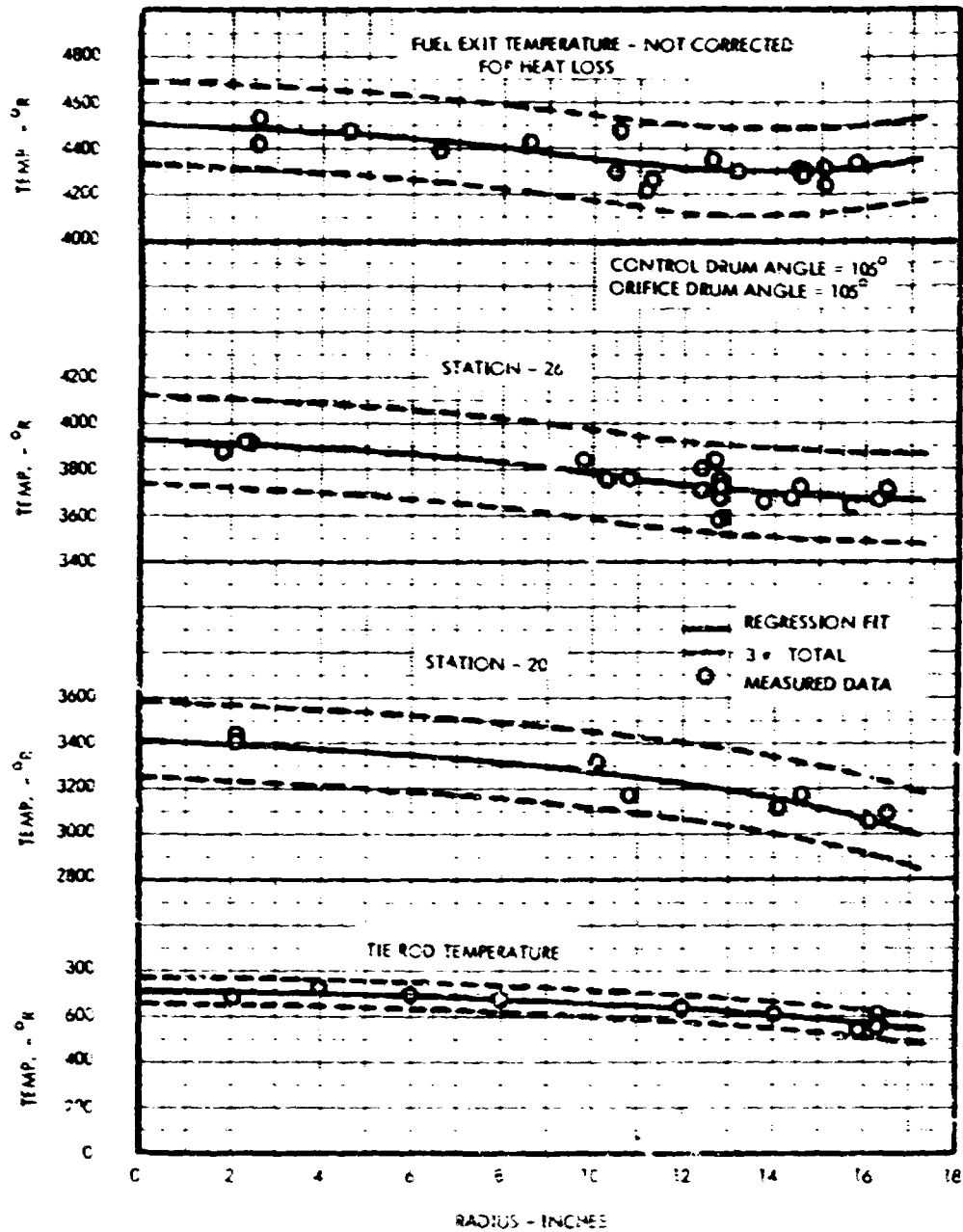


Figure 5-13. (CRD) Radial Core Temperature Distributions Obtained From Multiple Regression Analysis, EP-IIIA at CRT 14400 (U)

~~CONFIDENTIAL~~

~~CONFIDENTIAL~~

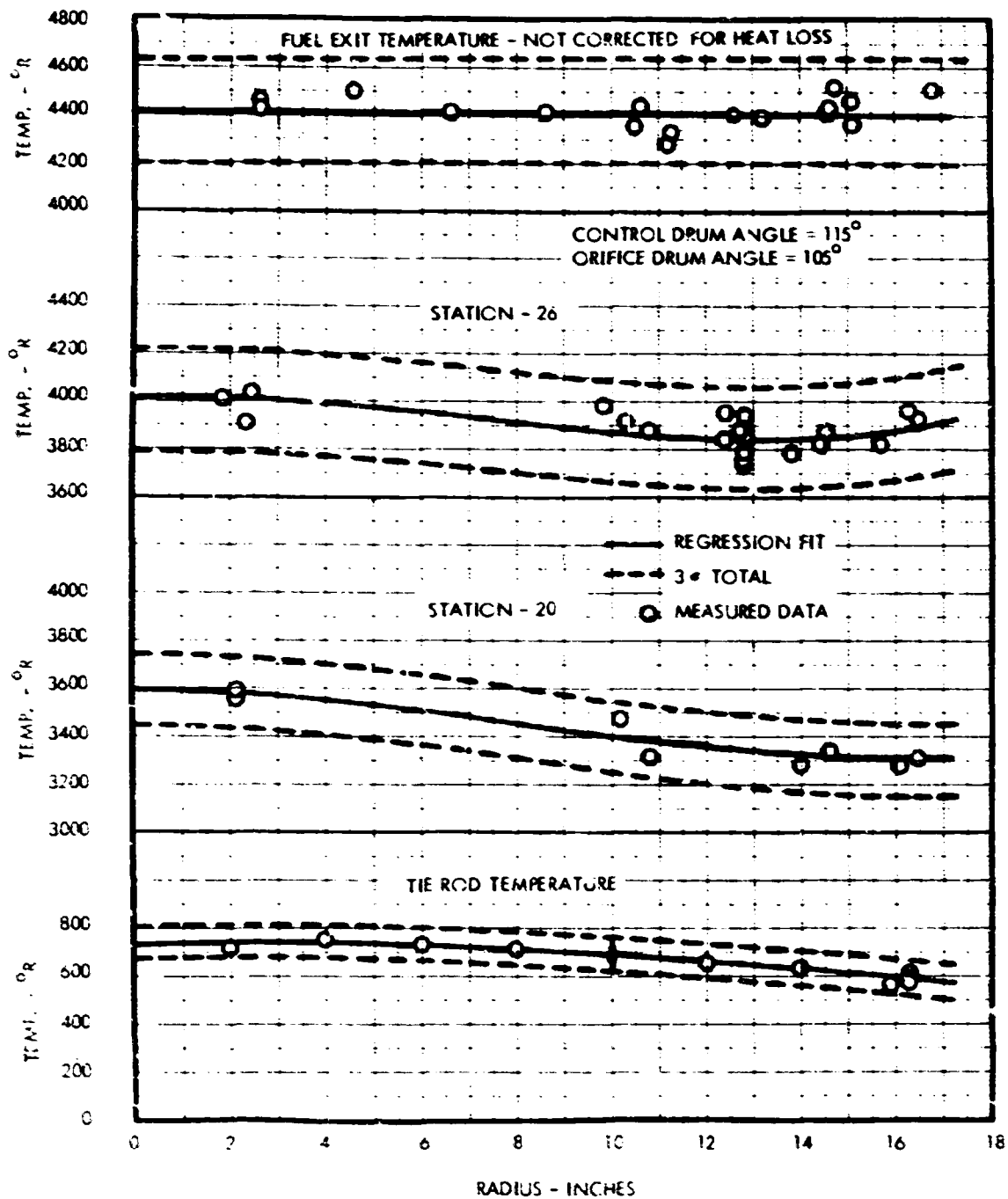


Figure 5-14. (CRD) Radial Temperature Distributions Obtained From Multiple Regression Analysis, EP-IIIA at CRT 17800 (U)

~~CONFIDENTIAL~~

~~CONFIDENTIAL~~

(CRD) The measured core pressure drop was from 0.5 to 5.5 percent lower than post test calculations using the pre-test models at full power. Table 5-5 compares the measured and calculated core pressure drops at full power for NRX/EST, NRX-A5, and NRX-A6. The deviation between calculated and measured pressure drops was smaller for NRX-A6 than for the previous reactors. This is attributed to an improvement in the friction factor correlation used in the calculation for the NRX-A6 core. The increasing difference with run time is probably due to an increase in the average effective air impedance diameter caused by loss of excess molybdenum overcoating and by corrosion.

(CRD) Lateral Support, Reflector, and Support Plate Thermal and Fluid Flow Performance (U)

(U) This section summarizes the thermal and fluid flow performance of the lateral support system, reflector system, and core support plate during the EP-IIIA power test, including comparison with analysis. A more detailed analysis may be found in Reference 22. All components performed satisfactorily during the test series and met all functional objectives. Test data were generally in very good agreement with predictions. However, two deviations from prediction were found, (1) a reflector pressure drop noticeably lower than pre-test predictions, and (2) at disassembly the beryllium reflector was observed to be cracked. The lower than predicted reflector pressure drop was accounted for in the post-test calculations by inclusion of experimental conditions including the reduced effective flow impedance of the locating cone. The locating cone provides the principal impedance to coolant flow in the reflector-pressure vessel annulus. The cracks which were observed in the beryllium reflector at disassembly did not impair the NRX-A6 reactor operation.

(CRD) Lateral Support System (U)

(CRD) The performance of the lateral support system was excellent. At the start of the EP-IIIA full power hold the seal chamber coolant axial pressure and temperature distribution was in excellent agreement with predictions. A comparison of the pre-test predicted and measured normalized lateral support seal system pressure distributions at this time is shown on Figure 5-15. At the end of the full power hold the axial pressure profile was only slightly lower in the core mid-plane region than at the start. This was attributed to slight edge corrosion of the pyrographite insulating tiles and local wrapper corrosion which increased the seal bypass flow approximately 5 percent by the end of the full power hold. The degradation of the lateral support system performance was significantly less after 60 minutes of full power operation than had been observed on prior NRX reactors operating for 30 minutes or less. No corrosion was noted in the seal segments.

(U) Reflector Pressure Drop

The measured reflector pressure drop at the start of EP-IIIA full power was 5.2 psi. This was lower than the pre-test prediction. In-

~~CONFIDENTIAL~~

(;CRD) COMPARISON OF MEASURED WITH CALCULATED CORE PRESSURE DROPS
FOR NRX/EST, NRX-A5 AND NRX-A6 (U)

~~CONFIDENTIAL~~

All data are for a 5 second interval starting at the indicated control room time.

~~CONFIDENTIAL~~

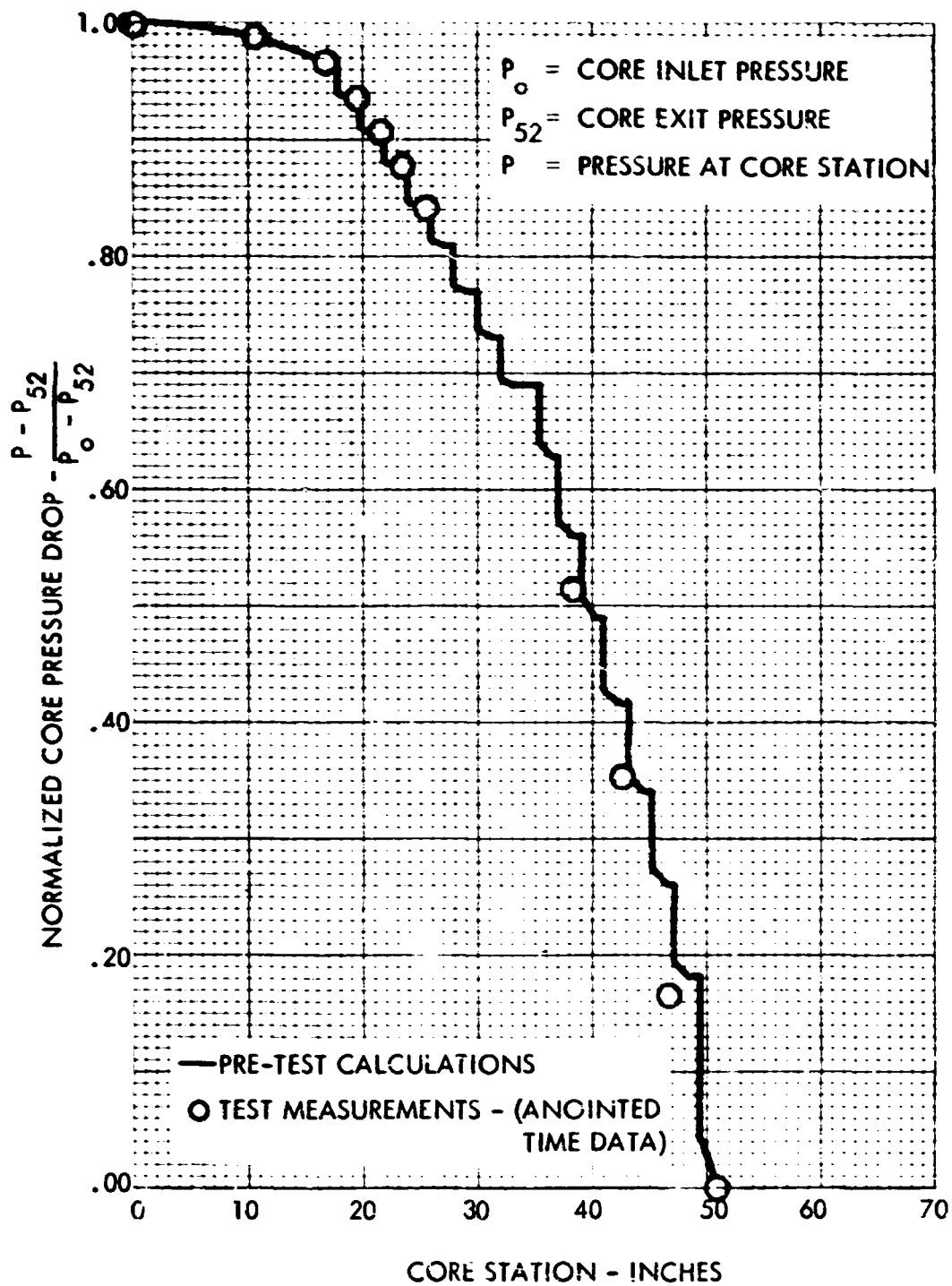


Figure 5-15. (CRD) Normalized Lateral Support Seal System Pressure Distribution During EP-IIIA Full Power Hold (U)

~~CONFIDENTIAL~~

clusion of the approximately 10°R lower than predicted reflector inlet temperature, approximately 18 percent lower than predicted start of life heating and correction for the flow distribution to the pressure vessel/reflector annulus from measured pressures yielded a calculated pressure drop of 18 psi. This agreement between analytical model and measured data is considered good since the NRX-A6 reflector represented a major change from all previous NRX reactors.

(U) Component Temperatures

(U) The measured temperatures in the beryllium reflector at full power conditions shown in Table 5-6 were generally within the pre-test prediction uncertainties. However, the measured inner web temperatures were higher than predicted. Post-test calculations of the reflector material temperatures are in good agreement with the measured test data.

(U) A detailed analysis of the reflector cracks which were observed during disassembly may be found in Reference 22. The data gives evidence that many of the cracks were formed approximately two minutes before the end of the full power hold and affected the seal flow very slightly. This did not affect the functional performance of the reflector or the reactor. These cracks are attributed to excessive thermal stress at the end of the full power hold relative to the strength of irradiated beryllium.

(U) The measured control drum axial temperature distribution at full power conditions is in good agreement with pre-test predictions. Temperatures in the core support plate were in very good agreement with analysis. There was a slight increase in the core support plate material temperature as the full power test progressed. This effect was expected and is due to the increased component heating and the increase in temperature of the coolant coming from the reflector and simulated shield with run time.

(CRD) Corrosion (U)

(CRD) The corrosion performance of the fuel elements represented a dramatic improvement over the NRX/EST and NRX-A5 elements even though NRX-A6 operated twice as long at full power conditions. This is best illustrated by the following comparison of key parameters:

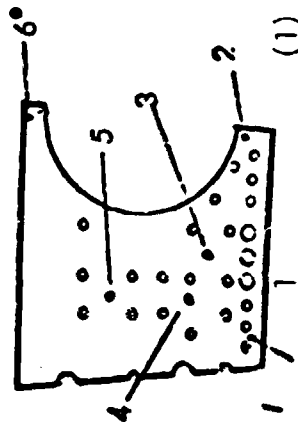
	<u>NRX-A6</u>	<u>NRX-A5</u>	<u>NRX/EST</u>
Average overall element weight loss (gm/element)	11*	27	32
Average pinholing (pinholes/element)	5	10	21
Average channel exposure (inches/element)	9.3	19	22
Net reactivity loss (dollars)	0.7	2.1	3.2

* Corrected for average molybdenum overcoat loss of two grams/element.

CONFIDENTIAL

TABLE 5-6

(CRD) COMPARISON OF PREDICTED AND POST TEST CALCULATED BERYLLIUM
REFLECTOR TEMPERATURES WITH MEASURED DATA - EP-III A (U)



*
AT 322, 323 are at Core Station 17-
All others are at Core Station 21

Location	Data Channel	(1) A 14400 CRT		(2) B Predicted		C Post Calculations		A-B		A-C	
1	AT 303	362		352		364		+ 10		- 2	
1	AT 308	348		352		364		- 4		- 16	
2	AT 304	378		338		344		+ 40		+ 34	
2	AT 307	348		338		344		+ 10		+ 4	
3	AT 305	348		362		352		- 14		- 4	
3	AT 309	375		362		352		+ 13		+ 23	
4	AT 302	331		355		350		- 24		- 19	
4	AT 311	350		355		350		- 5		0	
5	AT 301	298		319		322		- 21		- 24	
5	AT 312	315		319		322		- 4		- 7	
6*	AT 322	221		251		220		- 30		+ 1	
6	AT 323	221		251		220		- 30		+ 1	

(1) Measured Value Corrected Except for Installation Error - Start-of-Life
(2) From Reference 7 (15 Minute into Full Power Hold)

CONFIDENTIAL

~~CONFIDENTIAL~~



The radial distribution of overall weight loss is compared with NRX/EST and NRX-A5 results on Figure 5-16. This figure illustrates the much lower weight loss and more consistent corrosion behavior than was the case for the earlier NRX reactors.

(CRD) Radial distributions of overall and bore weight losses are shown in Figure 5-17. The overall weight loss represents the difference between the pre and post test weights. Two different procedures were used to estimate surface weight loss for the fuel elements. By the VESL visual examination procedure this loss was estimated to be 0.8 grams per element. By the SLEDS mechanical measurement system, the estimate was 1 to 4 grams per element depending on data interpretation. The actual average surface corrosion was estimated to be near 1 gram per element. The typical fuel element external corrosion occurred in a pattern of shallow corrosion in a band between 17 and 25 inches followed by a carbon deposition and a second band of element corrosion and/or shrinkage aft of 35 inches. For comparison, the average estimated surface weight loss was between 4.5 and 9 grams per element for NRX/EST and NRX A5. The average bore weight loss on Figure 5-17 was obtained by subtracting the estimated surface weight loss and molybdenum overcoat loss (approximately two grams/element) from the overall weight loss. The axial profile of average bore weight loss for 5 inch increments is shown in Figure 5-18. The weight loss per element is very small from 0 to 30 inches, and therefore increases approximately linearly to a value of 2.2 grams per 5 inches at the aft end.

(CRD) Corrosion "notching" occurred on 22 J row peripheral elements. This local external corrosion occurred on the outermost edge of these elements, sometimes deep enough to reach the corner bore, beginning at about station 20 and occurring every inch or so. The corrosion could be due to local coating cracks, the high bore to external pressure difference near the core periphery, or corrosion in thermal stress induced element matrix cracks.

(CRD) The non-fueled peripheral components, pyrographite tiles, pyrofoil wrapper, and filler strips, performed adequately. However, the inner surface of the pyrofoil wrapper and some of the radial filler strip surfaces corroded more than expected, probably because the filler strips did not arrange themselves with uniform gaps but unevenly with occasional wide gaps. Furthermore, the notch corrosion of the peripheral elements provided an unexpected source of fresh hydrogen in this local peripheral region.

(CRD) The plan to study the effects of fuel element matrix, bore coating, and bore overcoat source in the production reactor elements yielded two significant results. Elements with a WNCU niobium carbide coating clearly showed less pinholing (average of 2 pinholes per element) than elements with Y-12 NbC bore coating (7.5 to 9 pinholes per element). However, these results implying a difference in bore corrosion performance for elements from the two coating sources, are clouded by the fact that post test gross ionization measurements indicate WNCU coated elements operated at a one percent lower power generation rate. This is equivalent to a 40°F lower temperature.

~~CONFIDENTIAL~~

CONFIDENTIAL

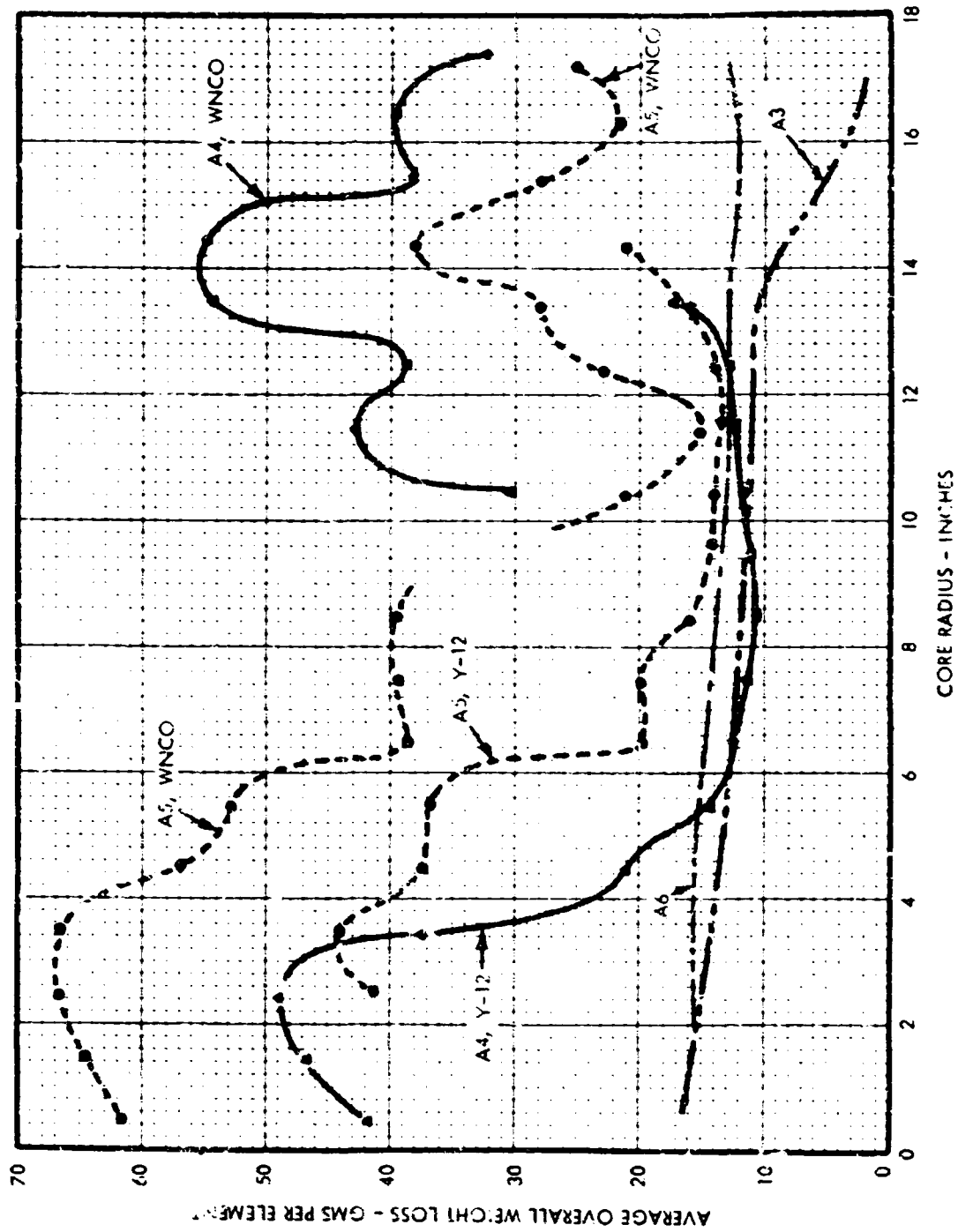


Figure 5-16. (CRD) Radial Distribution of Overall Weight Losses in the
NRX-A3, NRX/EST, NRX-A5, and NRX-A6 (U)

CONFIDENTIAL

CONFIDENTIAL

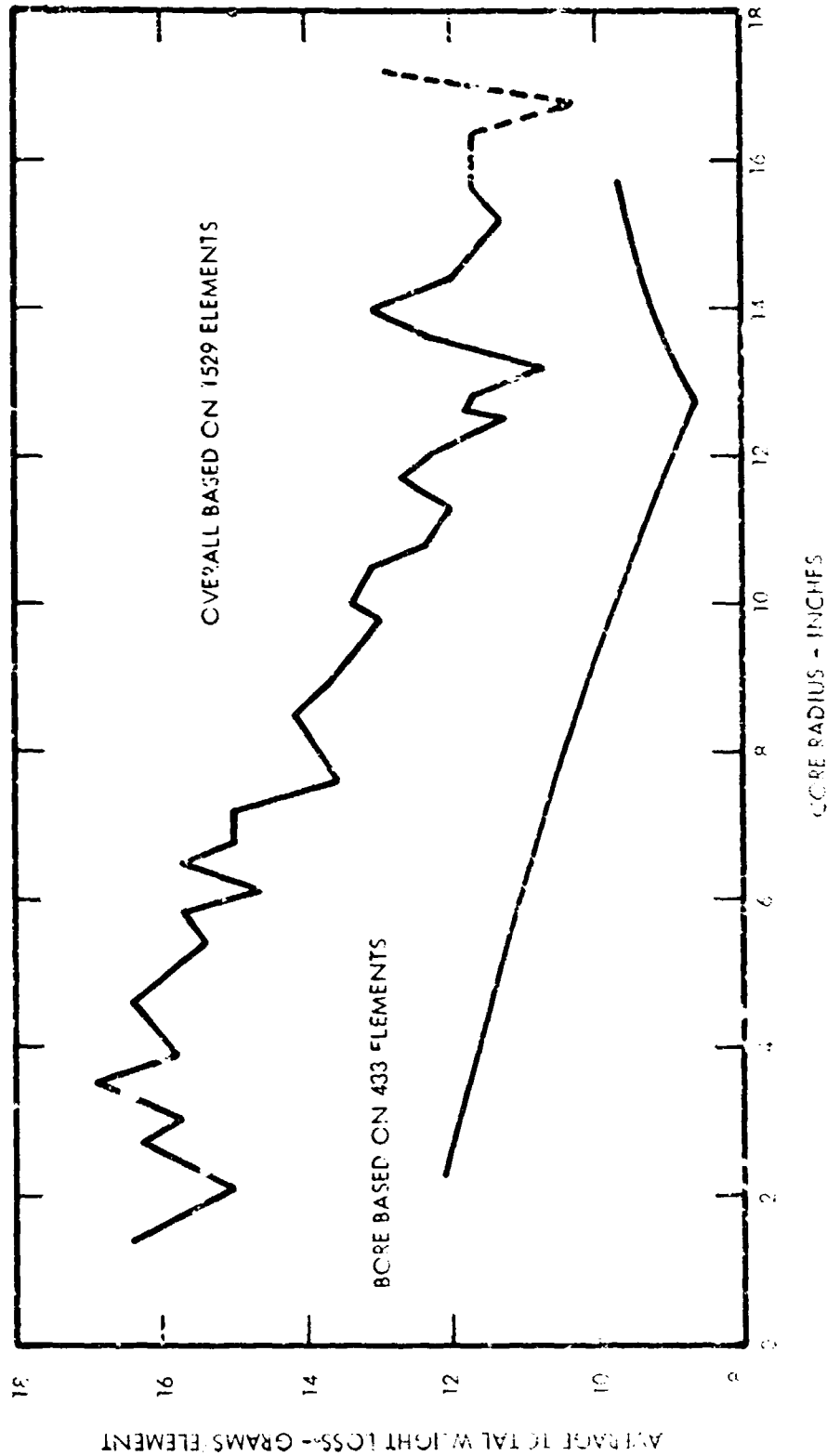


Figure 5-17. (CRB) Radial Distribution of Overall and Bore Weight Losses (U)

CONFIDENTIAL

CONFIDENTIAL

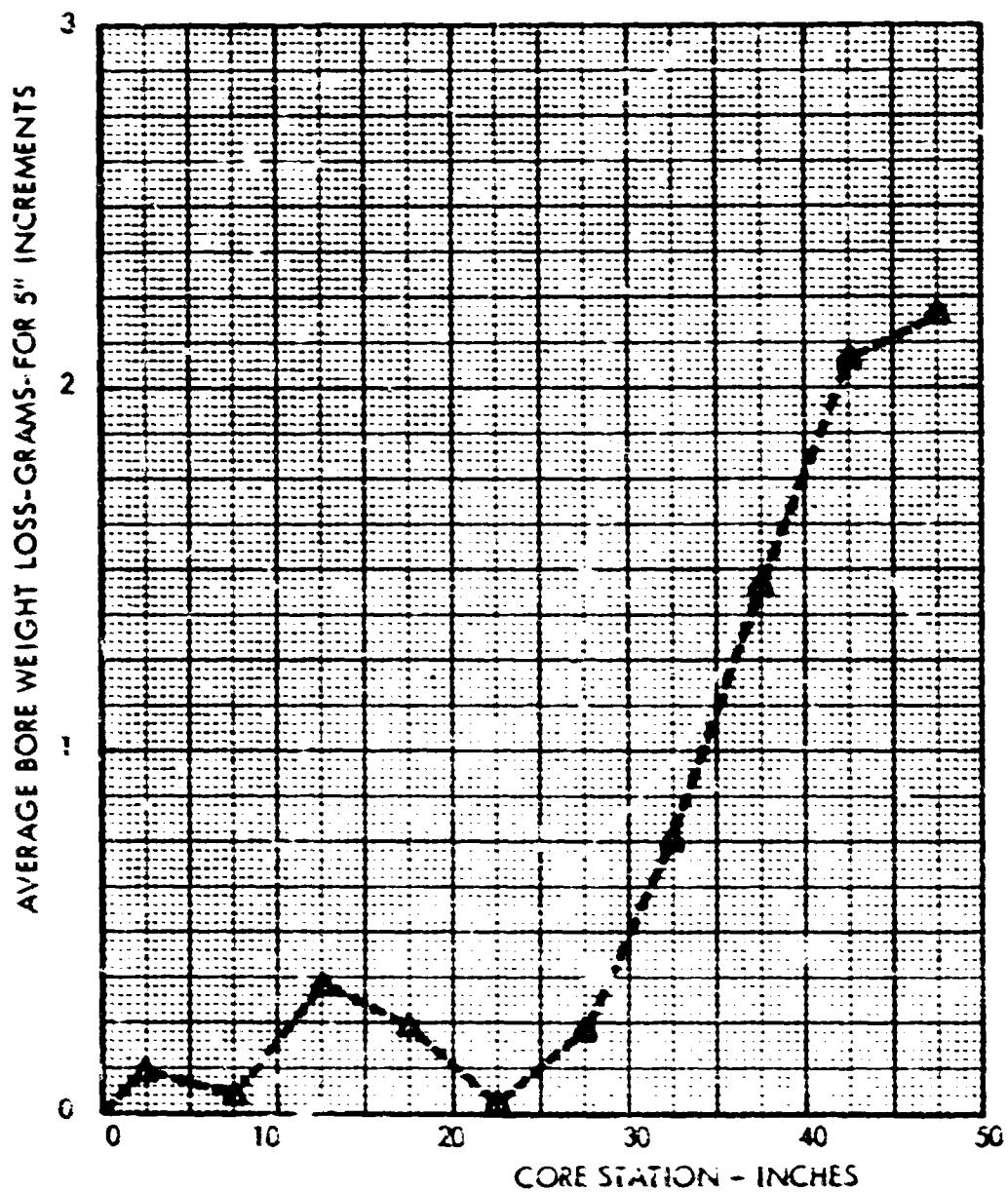
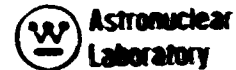


Figure 5-18. (CRD) Axial Distribution of Bore Weight Loss (G)

CONFIDENTIAL

~~CONFIDENTIAL~~



(CRD) The NRX-A6 quality control (QC) furnace testing was successful in screening element batches which would not perform adequately in the power test. Moreover, the ranking of element types as deduced from the furnace testing agrees well, though not exactly, with the ranking based on the reactor test data. The furnace testing, however, failed to detect hot end pinholing tendencies, probably due to the furnace condition of external helium pressure being higher than bore pressure over the aft portion of the elements.

(CRD) The predictions of overall element weight loss were about 50 percent higher than the measurements. The hot end weight loss was approximately as predicted. The surface loss estimate was high, principally due to a gross overestimate of the number and location of pinholes and thereby the pinhole corrosion. The midband corrosion correlations were partially based on NRX-A5 experience and partially based on NRX-A6 two cycle QC test results.

(U) A more detailed discussion of the NRX-A6 corrosion performance may be found in References 22 and 38.

(U) CONTROL SYSTEMS PERFORMANCE

(U) All reactor control systems performed well. All reactor control systems performed almost exactly as predicted except that the temperature controller was a little more sluggish than predicted by the Common Analog Model (CAM). The temperature controller held the measured temperature to within 50°R of the demand except during transient conditions. During the ramp from the 2100°R hold of EP-IIIA to design conditions, the measured temperature lagged demanded temperature by approximately 3 seconds or 100°R. Temperature trim operations appeared to be smooth and responsive.

(U) NRX-A6 power testing was performed with 6 programmed parameters: (1) propellant feed line LH₂ control valve L-11 stem position, (2) propellant feed line LH₂ vent valve L-111 stem position, (3) LH₂ flow rate, (4) Dewar 3 pressure, (5) reactor power, and (6) chamber temperature.

(U) Prior to the successful full power test, all six programs were checked out by cross-plotting one program with another. During the startup of the full power run, the programs controlled these six parameters to within 3 percent (full scale) of the desired values for the crucial portions of each program. The only exception to this was that the stem position of valve L-111 was 5 percent (of full scale) more than the specified position. With the exception of the LH₂ flow rate program, on the basis of time, all the programs were within 1 second of each other; LH₂ flow rate was purposely delayed 2 seconds with respect to the L-11 program. This timing offset for LH₂ flow rate was also present during FEP-III and the EP-III Abort. The performance of the main propellant line, reactor power, and Dewar 3 pressure during the startup to the intermediate power hold was excellent, exhibiting good reproducibility with data measured during the aborted EP-III startup on 7 December 1967.

~~CONFIDENTIAL~~

~~CONFIDENTIAL~~
(THIS PAGE IS UNCLASSIFIED)

The investigation of the operation and performance of the six programmed parameters consisted of evaluating first the recorded data of the program output, and second, the recorded response of the controlled parameter. Figure 5-19 presents the variation between reduced data from the program output and the ideal, specified program output, assuming zero timing error for all six program drums. A detailed discussion of the programmed parameter performance is given in Reference 12.

One false scram occurred on the first attempted full power run. This inadvertent shutdown was due to the noise sensitivity of the hardware used to implement the minimum drum position scram. The difficulty was isolated and corrected prior to EP-III A. A detailed discussion on the investigation of the cause of this shutdown is given in Reference 24.

(ORD) NUCLEAR ANALYSIS (U)

(U) The NRX-A6 test series provided an abundance of nuclear data applicable to future NERVA nuclear design. In this section the principal results of the test analysis are presented in the test sequence. A detailed discussion of the nuclear analysis is given in Reference 22.

(U) Subcritical Operations

During the removal of the shipping poison wires in the E-MAD Building, subcritical multiplication data were taken to insure that the reactivity shutdown was adequate. As in the NRX-A5 test, rotation of a single control drum provided a continuing calibration of the apparent multiplication against reactivity, permitting a final shutdown estimate which was within 15c of the shutdown estimate based on drum worth measurements.

(U) Neutronic Tests

The reactor was brought to criticality at the 97 degree drum position, 9 degrees above the predicted 88 degrees angle, but within the + 10 degrees assigned uncertainty (see Reference 6). The associated reactivity error was -59c, an accuracy comparable to previous reactor predictions. In view of the major nuclear changes in NRX-A6, the reactivity shimming was considered to be very good.

(U) The reactivity worth of the dry Test Cell "C" shield was found to be +41c, in good agreement with the predicted +46c (see Reference 23). The reactivity effect of adding boric acid water to the shield was also measured to be -23c, as compared to the predicted -25c.

(U) A very detailed post-test analysis of the EP-I drum calibration data was made. A best value of the integral drum worth of 7.6\$ has been derived by correcting each measurement for the effects of small deviations from delayed criticality.

(THIS PAGE IS UNCLASSIFIED)

~~CONFIDENTIAL~~

CONFIDENTIAL
(THIS PAGE IS UNCLASSIFIED)

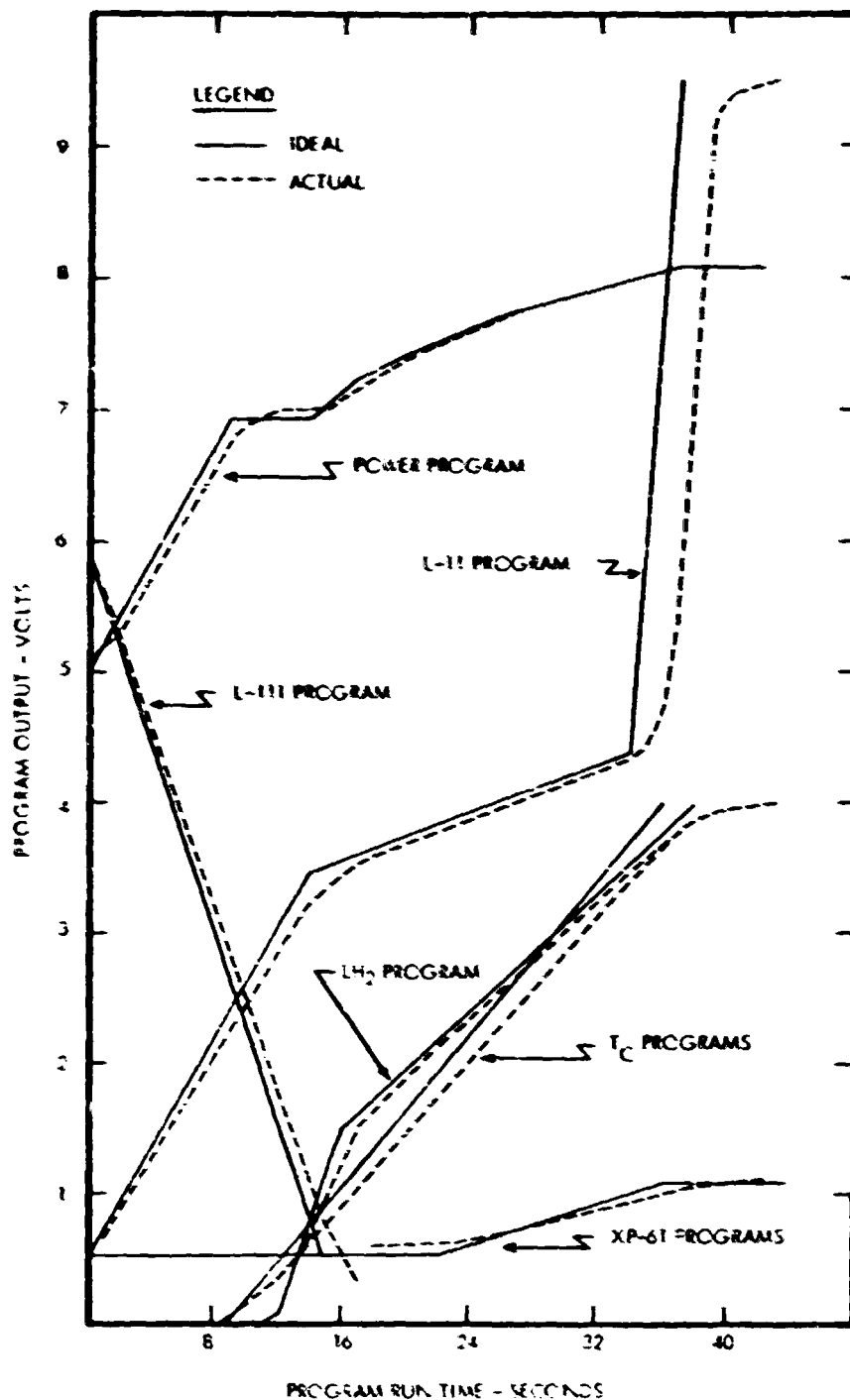


Figure 5-19. (U) Measured Versus Ideal (Synchronized) Program Outputs for EP-III A NRX-A6 Full Power Run, (Calcomp Data) (U)

(THIS PAGE IS UNCLASSIFIED)

CONFIDENTIAL

~~CONFIDENTIAL~~

The three different kinds of worth measurements yielded very similar estimates. Most of the 5 percent difference from the 8.0 - 8.35 prediction, which was based on PAX measurements (Reference 25) can be attributed to small differences between the mock-up and the test article.

(U) The two drums whose worth was individually measured appeared to differ in worth by 2.8c. The difference was shown to be a result of detector geometry similar to that observed in NRX/EST testing.

(U) The small reactivity loss of 6.5c observed in the NRX-A6 GN_2 test was in disagreement with the predicted 9.3c gain. Post-test analysis has explained this in terms of differences in propellant distribution and worth from those in the NRX-A3 GN_2 test on which the prediction was based (Reference 23).

(CRD) Design Power Test (U)

(U) A detailed post-test analysis established that the difference in feedback reactivity between ambient and operating conditions was -72c for NRX-A6. This change was in fact observed in the EP-111A startup and shutdown, since post-test analysis has shown that no material losses, such as molybdenum loss, occurred during these events. Although the expected feedback change was exactly -72c, the predicted net reactivity change during startup was only -12c, since a 60c reactivity gain was expected to occur because of molybdenum loss.

(U) The time variation of the critical drum position during the high power hold, shown in Figure 5-20, implies a marked improvement in fuel performance over prior NRX reactors.

(CRD) The 65c reactivity loss associated with the total drum movement during the hold is the sum of the reactivity effects of graphite moderator loss due to corrosion, molybdenum blowoff, and fission product poisoning; the post-test analysis therefore emphasized the separation of these effects.

(U) The reactivity effect of Xe^{135} buildup during the high power hold was calculated to be -17c at the time of shutdown. (Later when the post-run critical was performed it was only -1c).

(CRD) The total molybdenum coating loss during the test series, as established by post-test chemistry, implied a 61c reactivity gain, in good agreement with the predicted 60c. The time behavior of the molybdenum loss was, however, not well predicted. In the absence of reactor test data, it has been assumed that all of the loss would occur in the first power hold. A detailed analysis of the operating and ambient criticality data established that about two-thirds of the total molybdenum loss actually occurred during the 60-minute hold at design power.

~~CONFIDENTIAL~~

CONFIDENTIAL

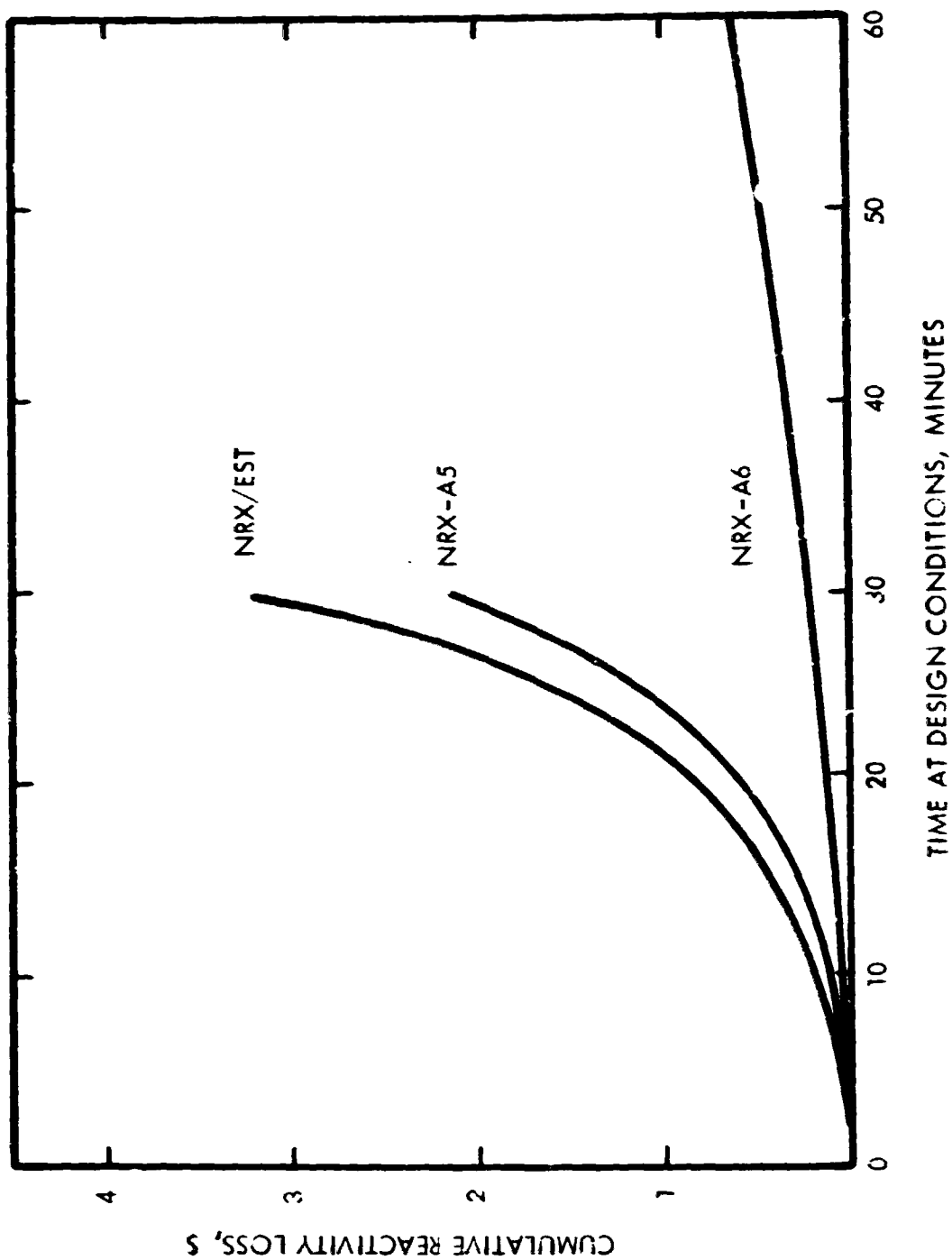


Figure 5-20. (CRD) Variation of Cumulative Reactivity Loss with Time for the NRX/EST, NRX-A5, and NRX-A6 Reactors (U)

CONFIDENTIAL

~~CONFIDENTIAL~~

(CRD) If the observed 65c reactivity loss during the high power hold is corrected for the 37c reactivity gain due to molybdenum loss, and the 17c reactivity loss due to Xe-135 buildup, the part of the reactivity change due to corrosion of the fuel materials, carbon, uranium, and niobium, is calculated to be $(65c + 37c - 17c =) 85c$. This quantity is of special interest since it is an indication of the extent of the corrosion of the fuel matrix, comparable to the reactivity loss in NRX reactors in which neither molybdenum coating or Xe-135 buildup contributed significant reactor effects. The total reactivity loss due to carbon, uranium, and niobium in the entire test series may also be calculated directly from the change in the cold critical angle from 97.0 degrees at initial criticality to 100.5 degrees following the power run. If the associated 22c reactivity loss is increased by 61c, to account for the effect of molybdenum blowoff, a value of 83c is obtained. Essentially all of the corrosion represented by this reactivity change occurred in the design power hold, so that this number is comparable to the 85c derived above. The close agreement indicates that the separate reactivity changes are understood. A further check was obtained by utilizing the measured fuel element weight losses to estimate the reactivity loss due to corrosion. The result of this calculation was that a 77c reactivity loss occurred as a consequence of the graphite moderator loss. Uranium and niobium losses had negligible effect, while molybdenum blowoff produced a 61c reactivity gain, as noted above. Again, the agreement between the 77c number and the earlier 83c and 85c numbers confirms the separation of the various reactivity components.

(U) REACTOR SAFETY

(U) Reactor safety for NRX-A6 was similar to that provided for previous reactor tests, and a complete safety analysis is presented in Reference 26.

(U) Analyses were performed to determine credible conditions that could lead to unsafe operation and release of fission products above the level expected for normal operations. The safety evaluation of NRX-A6 operations was based on descriptions and operations presented in Reference 11. These analyses showed that the predicted radiological hazards from normal operations or from test failure of NRX-A6, while greater than those predicted for NRX-A5, were acceptable and it was therefore concluded that NRX-A6 operations could be conducted without exposure of personnel, either on or off the site, to excessive radiation levels. This conclusion was based on conduct of the tests during favorable weather conditions.

(U) To prevent damage to the test article or excursions of the reactor during operations, operating and shutdown limits were established on various test parameters. A complete list and discussion of these limits is given in Reference 27. To prevent exceeding these limits during reactor operation, limiters (see Section 3), operator action, and emergency (scram) shutdown settings were utilized. The settings and actions are given in Reference 11.

(U) An accident analysis that covers excursion magnitudes and other consequences of various credible accidents may be found in Reference 26. A fission-product-release analysis that covers the radiological consequences is also presented in Reference 26.

~~CONFIDENTIAL~~

(CRD) INSTRUMENTATION PERFORMANCE (U)

(U) The instrumentation used for NRX-A6 served two basic functions. First, it provided reactor state feedback signals to the control system, and, second, it provided diagnostic data necessary to monitor reactor operation and provide the data for post-test analyses. Critical parameters for which operating limits had been established were monitored by the diagnostic instrumentation, as noted in Reference 11. Additional sensors provided signals to maintain reactor operation within critical control limits, or to effect automatic emergency action if these limits were exceeded.

(U) NRX-A6 used a total of 409 reactor channels to monitor reactor system performance. The type and location of transducers, the operating range, and other functional information are listed in Reference 11. Redundant measurements were taken for those parameters used for reactor control and those considered essential for reactor performance analysis.

(U) Overall performance of the instrumentation system was considered excellent. All control parameters performed reliably throughout the test series, and anomalies that occurred are discussed in References 28 and 29.

(U) Nuclear Subsystem Instrumentation

(U) The performance of the transducers during the test series was excellent. The zero shifts noted for several differential-pressure transducers during the full power runs were expected and were caused by purposely exceeding the range of the transducers.

(U) There were a total of 265 WANL-supplied nuclear subsystem diagnostic and control sensors for the NRX-A6 test series. A total of 177 sensors were installed inside the PVARA and 88 sensors were mounted external to the reactor. (See Reference 11 for specific sensor locations and parameters for the internally mounted sensors). The externally mounted sensors consisted of the following:

<u>Quantity</u>	<u>Sensor Type</u>	<u>Location</u>
1	Potentiometer	Actuator side-by-side test
33	Pressure transducers	WANL pressure-transducer box
2	Pressure transducers	Actuator side-by-side test
12	Thermocouples (low temp)	Calorimeters
4	Resistor	LN ₂ reference junction



6	Resistance thermometers	Calorimeters
3	Accelerometers	Actuator side-by-side test
22	Thermocouple (low temp)	Actuator side-by-side test
2	RTT	LN ₂ reference junction
3	Rate sensors (1, 2)	Privy roof

(U) The table below indicates the total number of sensors required for installation as stated by the Measurement Requirement List (MRL) Reference 11 and the number of sensor channels operating after each phase of assembly and test. The chart also shows the number of channels deleted after each phase and the number of channels questionable. The table further breaks down the questionable channels as being associated with either sensor or data system or as being unresolved.

Phase	Channels Operational	Channels Deleted	Channels Non- Operational	Channels Questionable		
				Sensor	Data System	Not Resolved
Req'd Installation (MRL)	265	---	---	---	---	---
After WANL assy.	262	3	---	---	---	---
Prior to tests	259	4	2	---	---	---
After EP-I	259	5	1	---	2	3
After EP-II	260	5	---	---	1	3
After EP-III (abort)	260	5	---	---	1	4
After EP-IIIA	259	5	1	5	---	3

The total number of channels operating at the conclusion of all testing represented 97.7 percent of the required instrumentation.

(U) Assembly and Installation

(U) A total of 177 sensors were installed in the reactor. New transducers used in this reactor include four VR type and one S/G type pressure transducers (evaluation units) and the core radial displacement transducers, which are half-bridge strain gage type sensors and 21 exit gas thermocouples. All drawings were reviewed and approved for correctness of sensor type, applicable process specification, installation design, and compatibility with the Measurement Requirement

List. Sensor history sheets were initiated for each sensor delivered to the Reactor Assembly Laboratory for internally-mounted sensors or to NRDS for the externally mounted sensors. A continuous sensor history including electrical data, installation information, and any pertinent facts relative to the sensor was maintained from initial sensor acceptance testing through WANL assembly, NRDS electrical and visual receiving inspection, NRDS assembly, and the end-to-end checkout of instrumentation from the sensor to the test cell. During the complete instrumentation assembly and installation, only three measurements were lost.

Reference 30 gives a complete history of sensor installation.

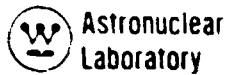
(U) Performance

(U) The performance of sensor instrumentation associated with the testing of the NRX-A6 was considered to be very good. The types of sensors used in this test series and their performance during tests are summarized in the following table. A complete and detailed sensor evaluation is given in Reference 31.

<u>Type</u>	<u>Total Required</u>	<u>Sensors Operational</u>	<u>Sensors Deleted</u>	<u>Sensors Questionable</u>
Thermocouple (high temp)	52	52	0	1
Thermocouple (low temp)	122	121	1	0
Resistance thermometer	14	14	0	1
Strain gage	14	12	2	7*
Pressure, absolute	18	18	0	0
Pressure, differential	22	22	0	0
Displacement (LVDT)	3	3	0	3
Displacement (S/G)	6	6	0	0
Accelerometer	6	5	1	2
Resistor	4	4	0	0
Potentiometer	1	1	0	0
Rate sensor	<u>3</u>	<u>1</u>	<u>2</u>	<u>0</u>
TOTAL	265	259	6	12

*

All of the strain gages were in high radiation fields during the full power run, and exhibited varying degrees of output drift. The condition of the sensors however, as observed during post-operative examination was excellent.



(U) Displacement Sensors - All three LVDT's were questionable due to difficulty with signal conditioning and they exhibited some drift in output. The data was qualitatively usable however, when the drift due to radiation was discounted.

(U) All six strain gauge transducers were consistent in performance and considered to be excellent.

(U) Pressure Transducers - The four variable-reluctance internally mounted pressure transducers (Wianko) were operating at the conclusion of the reactor test. These transducers indicated lower pressures than their externally mounted counterpart. Three of these transducers were evaluation units. They indicated an improvement in performance over the variable-reluctance transducers of the older design.

(U) The one S/G internally mounted pressure transducer operated satisfactorily throughout tests, although it indicated very slightly lower pressure than its externally mounted counterpart.

(U) Externally mounted transducers of the strain gage type (CEC) performed very well. All 35 transducers were operating and none were considered questionable.

(U) Accelerometers - The three strain gage type accelerometers (Statham) mounted on the actuator side-by-side test fixture performed well.

(U) Of the three internally mounted VR type accelerometers (Wianko), one became inoperative prior to tests and was cancelled. The remaining two showed degradation of signal above 80 percent reactor power.

(U) Thermocouples - All but one of the 110 externally and internally mounted low temperature thermocouples were operating at the end of testing. One was deleted following damage during reactor build.

(U) All of the 52 reactor high temperature thermocouples were operating at the end of testing. Only one sensor, at Station 26, was considered questionable. This was resolved to be real data when disassembly revealed that the plug in the thermocouple hole had blown out permitting gas flow around the thermocouple.

(U) RTT - All eight RTT's performed satisfactorily throughout tests. One RTT was under-ranged in EP-1.

(U) Potentiometer - The actuator position indicating potentiometer performed well during all tests.

(U) Resistor - The four LN₂ reference junction liquid level indicators were completely operational.

(U) Calorimeters - The one resistance thermometer and two chrome!-alumel thermocouples installed in each of the six calorimeters performed satisfactorily during the test series.

(U) Strain Gages - Fourteen weldable-type strain gages were installed: four were mounted on the reflector standoff bolts to measure reactor axial loading mounted on each of five different tie rods and were mounted opposite each other to eliminate the bending component of the measured stresses. One tie rod strain gage became shorted during assembly of the reactor and was deleted; also one reflector standoff strain gage became open during NRDS setup operation and was deleted. All strain gages exhibited varying degrees of drift during the full power run due to the high radiation field.

(U) Rate Sensors - An attempt was made to utilize three evaluation rate sensor channels, one for gamma rate and two for fast neutron rate, for privacy roof measurements on the test article. The gamma channel was set up and performed well throughout the test series. The two neutron channels were unable to be satisfactorily set up prior to the test series.

(U) Post Test Electrical Checks

(U) The post-test electrical checks were made following the test series to establish the electrical condition of the sensors and their connections into the test cell. Results of this check were then compared with those for the identical check made prior to the start of the test series. All sensors noted as questionable during the test series were found to have no electrical deviations from the pre-test condition.

(U) Disassembly

(U) Visual observations were made during the disassembly operation to verify installation position and outward physical appearance of the sensors at the earliest possible time after the reactor tests, as well as to ensure the integrity of the sensors that required closer observation during the post-operative examination. In general, these visual observations showed all instrumentation to be in excellent condition.

Reference 28 presents a detailed history of sensor disassembly.

(U) Post-Operative Examination

(U) After testing was completed, the core instrumentation, data channel post calibration, and test cell wiring were checked. Only the examination of core instrumentation has been completed. This examination consisted of a visual inspection. Radiography of core thermocouples showed no confirmation of discrepancy in the questionable or deleted channels. Transducer performance was evaluated and validity of the output data was confirmed.



(U) Non-Nuclear Mounted Instrumentation

(U) Non-nuclear mounted instrumentation performance was very good and described the environment that existed in the test assembly. A total of 90 measurements were provided for the NRX-A5 test series to monitor parameters of temperature, pressure, strain, and vibration. Fifty-one of these measurements were diagnostic to evaluate test article performance, and 39 were for evaluation of new transducer designs and new installation techniques, or were used to monitor environments in the vicinity of new transducer designs.

(U) Sixteen anomalies were noted in the diagnostic measurements and twelve were noted in the evaluation measurements.

(U) The performance of the instruments during the NRX-A6 test series, the information obtained regarding environmental suitability, and the corrective action taken for future tests are summarized in the following sections. A more detailed discussion of sensor performance is given in Reference 29.

(U) Control Pressure Transducers

(U) Three test car wall-mounted pressure transducers were used to measure nozzle chamber pressures. Data analysis of the three pressure channels showed excellent correlation; the maximum channel-to-channel deviation observed throughout the full power run was 5 psi.

(U) Diagnostic Pressure Transducers

(U) Three test car mounted pressure transducers were used to measure diagnostic pressures. Data of the two absolute pressure channels showed excellent correlation; the maximum channel-to-channel deviation observed throughout the full power run was 6 psi. Analysis of the differential pressure transducer showed no data anomalies.

(U) Resistance Type Temperature Transducers (RTT's)

(U) One Rosemount Model 134EB platinum temperature transducer was used to monitor the LH_2 temperature at the nozzle manifold inlet. This transducer, PN 248635, was identical to the transducers used successfully in all previous NRX tests. The transducer operated satisfactorily throughout the test with no anomalies. The transducer data revealed no changes from radiation induced neutron damage to the transducer sensing element.

(U) Surface Mounted Thermocouples

(U) Nozzle, pressure vessel, and pressure vessel forward end closure surface temperature measurements were made with 39 surface mounted thermocouples. Twenty-one

were used for diagnostic measurements and 18 were used to support evaluation of surface mounted development instrumentation. Anomalies were noted in 4 of the 39 measurements. One measurement channel was excessively noisy throughout all test phases; one channel was noisy and temperature exceeded the channel range; the temperature of the other two channels exceeded the channel range.

(U) Thrust Chamber Thermocouples

(U) Four thrust-chamber thermocouples, mounted in pass-through bosses on the convergent section of the nozzle wall and extending at least 1.6 in. into the hot gas stream, were used for the test series. The thermocouples were made of tungsten with 5 percent rhenium and tungsten with 26 percent rhenium (W-5%Re/W-26%Re), insulated with beryllium oxide (BeO), sheathed by a W-26%Re tube, and grounded at the sensory junction formed in the probe tip. These thermocouples were identical to the thermocouples used successfully on NRX-A5.

(U) During the one-hour full power hold, the four thermocouples indicated an average temperature of approximately 3650°R, whereas the best estimate of chamber temperature was in the range of 4040 to 4150°R (see Table 5-3). The difference between the thermocouple values and the estimated values is considerably larger than the 100°R difference that could result from the measurement and data system uncertainties.

(U) The temperature spread between the highest and lowest reading thermocouples was approximately 350°R, as compared with the expected spread of approximately 100°R.

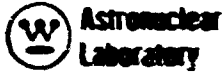
(U) In an effort to explain these deviations, the following instrumentation items were checked: (1) Pre- and post-electrical calibrations of the data system, (2) reference temperatures during the power run, (3) probe serial numbers vs probe location, (4) depth of probe penetration, (5) types of wire used that might form secondary junctions, and (6) post-test recalibration of two of the four probes in an NTO hot cell. No anomalies were found that would invalidate the measured temperatures.

(U) Analysis is presently being performed to determine the upper and lower limits of flow and temperature distribution which could result in a lack of complete mixing within the chamber.

(U) Accelerometer

(U) Six strain gage type (Statham) accelerometers were used for diagnostic vibration measurements to experimentally determine structural vibration characteristics during the NRX-A6 tests.

(U) Overheating probably caused the failure of three of six strain gage accelerometers, as well as the observed off-scale drift of the fourth accelerometer. As a result of the overheating, the data from the remaining two strain gage transducers are questionable with respect to magnitude, but not frequency.



(U) Strain Gages

(U) Eight weldable full bridge strain gages were installed on the NRX-A6 pressure vessel external surface to measure hoop and longitudinal strains during the steady state portion of the full power test. The data obtained were required for pressure vessel design verification. One strain gage opened during installation and was subsequently deleted from the test data. The remaining strain gages operated throughout the test.

(U) Five of the remaining strain gages failed to provide valid data during the test due to installation difficulties with the resistance spotweld process, not due to engine environment. Two transducers provided valid data throughout the test. The data agreed well with the predicted strain magnitude and were comparable to data obtained from similar engine locations in previous NRX tests.

(U) Environmental Testing of New Instrumentation Designs

(U) 1) Evaluation Accelerometers

(U) Six evaluation accelerometers (Electra Scientific) were installed in various locations on the nozzle torus and the aft flange of the pressure vessel for qualitative evaluation in the higher flux rates during the NRX-A6 full power test.

(U) No conclusions could be drawn about the performance of the evaluation transducers in the NRX-A6 radiation environment. The data from all channels contained extraneous noise, apparently introduced in the data acquisition system, that invalidated the data during various time intervals throughout the test. Although each of the data channels contained time intervals in which the data appeared valid, an extensive survey of all channels was not performed to define the various time intervals. This anomaly is believed to have originated in the data acquisition system.

(U) 2) Sheathed Cable Flame Spray Test

(U) One effect of gamma fields on instrumentation systems is to change transmission cable characteristics by increasing the temperature of the cable.

(U) Eight thermocouples were used in the flame-spray test; six were standard surface-mounted thermocouples and two were special ungrounded thermocouples. The primary objective was to determine the effectiveness of a flame-sprayed aluminum coating in providing a thermal path between the gamma-heated sheathed cables and the reactor pressure vessel. The secondary objective was to determine the effectiveness of flame spraying in connection with various methods of bonding the surface-mounted thermocouples (totally bonded, bonded junction and unbonded cable, unbonded junction and bonded cable, and totally unbonded). These bonding methods were selected to aid in determining:

- a) The thermal gradient between cable sheaths, conductors, and mounting surfaces for cooled and uncooled cables.
- b) The effect on surface-temperature measurements of using various thermocouple bonding methods.
- c) The effect on the response characteristics of surface-mounted thermocouples.
- d) The effect of gamma radiation on cable insulation resistance.
- e) The design verification of the predicted temperatures for cooled and uncooled cables.
- f) The ability of the flame-sprayed material to withstand thermal shocks and temperature gradients without separating, cracking, or spalling.

(U) Primary interest was in the effects obtained during the steady-state period of the full power test when the heating rates were maximum.

(U) All test objectives were met, except for one totally bonded thermocouple, which showed a temperature differential of approximately 350°R above the surface temperature. Post-test examination revealed that this thermocouple had partially lifted from the pressure vessel surface. The resulting data were indicative of extremely poor thermal contact and were not representative of the temperature for an unbonded surface thermocouple. No conclusions were drawn from this data.

(U) The flame-sprayed aluminum effectively reduced cable and conductor temperatures to the temperature of the pressure vessel surface. No significant differences could be detected between conductor temperature, cable sheath temperature, and pressure vessel surface temperature. Totally bonded surface thermocouples provided the lowest surface temperature measurements. All other bonding methods tested indicated higher temperatures than those indicated by the totally bonded surface thermocouples:

(U) 3) Pressure Transducers

(U) Five redesigned Statham pressure transducers were tested for nuclear evaluation as control transducers for use on NERVA engines. These transducers were similar to transducers tested previously on NRX-A5, except that the electrical connector had been removed and replaced with integral cable and the height of the transducer had been reduced 60 percent.

(U) The test results showed that side-by-side testing of transducers in simulated mounting bosses on the engine nozzle is difficult because of the problems in adequately defining the nozzle heat-sink temperatures. A redesign of the



mounting bosses is required to improve the thermal paths so they will be similar to those for the active mounting bosses.

4) RTT's

(U) Six redesigned Rosemount Model 134JA-1 resistance temperature transducers (RTT's) were installed in various locations in the propellant feed system of the engine for a nuclear evaluation test. These transducers were similar to Model 134EB used previously in all NRX tests, except that the electrical connector had been removed and replaced with integral cable.

(U) A radiation induced temperature error of 1.7°R was observed with an average neutron fluence of 4×10^{16} nvt, which correlated with the results of irradiation testing. No failures or other anomalies were noted.

(U) NRX-A6 Data System Performance

(U) Data system performance is defined as the performance of the instrumentation, data acquisition, and data reduction systems. A description of the NRX-A6 data acquisition and data reduction systems and their operation may be found in Reference 32.

(U) Instrumentation End-to-End Checkout

(U) The end-to-end instrumentation checkout was performed for NRX-A6 as described in Reference 32. The following were verified and documented: (1) continuity of each channel from the transducer, or closest point of termination to it, to the final recording or display device in the control point; (2) correct polarity of each channel; and (3) gain or setup range (or both) of each channel.

(U) A stimulus was applied to all accessible transducers over their full range by the methods prescribed in Reference 32. Those that were inaccessible were checked out to the control point by applying a voltage or making a similar substitution at the closest termination point to the transducer.

(U) Data Evaluation and Channel Performance

(U) Instrumentation for the NRX-A6 full power run included a total of 409 reactor channels and 464 facility channels. There were 328 reactor channels and 437 facility channels multiplexed and recorded on tape (narrow band). Channels needed for data analysis were processed, and Cal-Comp plots were made for 4,600 seconds of the reactor operation and 4,000 seconds of cooldown. Additional plots were produced for special time intervals as required for data analysis.

(U) There were numerous channel changes incorporated into the data and instrumentation system prior to the NRX-A6 full power test. The changes, over the entire period of time that NRX-A6 was at the test cell, were as follows: 590 new channels, 153 cancelled channels, and 706 channel revisions.

(U) Wide-band measurements were made on 110 channels with bandwidths up to 10,000 Hz. The wide-band system was used to measure acceleration, displacements, strains, and selected pressures. Channels assigned to the wide-band system were recorded on magnetic tape and could also be displayed on a CEC oscillograph recorder in real time. For NRX-A6, 27 wide-band (real time) oscillograph recordings were made.

(U) The Sanborn strip charts were used to record selected high level channels (0-10 volts) during the NRX-A6 test series. The Sanborn charts were used during a test to provide quick-look data and trend information. The capability for this form of recording included 128 channels at the CP and an additional 16 channels in the Local Control Room at the test cell. This does not include the 32-channel capability of the Control Room Sanborns, nor the 15 channels of basement Sanborns for the side-by-side experiments.

(U) The Vidar System was used to record Dewar levels and perform digital data logging. This system should have provided a digital printout of 99 channels during NRX-A6. However, a failure of the constant current power supply in the Vidar System before the start of the full power run prevented the acquisition of any data. An investigation of the failure of the power supply is now in progress.

(U) One "brown-plated" channel (cart venturi differential pressure) was recorded with a response of 42,000-52,000 Hz for increased channel response.

(U) Two events recorders were used to record the binary indications of 116 channels. These included selected Open-Close limit indications of valves and an On-Off condition of alarms, scrams, and commands.

(U) Quick-look data for NRX-A6 was reduced at 0.125 samples per second in order to present the history of the startup ramp, full power hold, and shutdown ramp on one 10-inch Cal-Comp plot. This extremely low sampling rate resulted in considerable noise on the data. Only frequencies up to 0.0625 Hz are represented with fidelity.

(U) A pictorial history of the NRX-A6 Reactor Test Series was made on film with movie cameras, kinescopes, and video tape. This included views of the PPR and FCR, as well as the reactor during reactor operation.

(U) REACTOR AND FEEDSYSTEM DYNAMIC ANALYSIS

(U) Reactor

(U) Since the primary objective of the NRX-A6 test was reactor endurance, no system transfer functions were measured. However, the transients between hold points and especially shutdown transients are valuable for model evaluations. A comparison of analog predicted system pressures and data for the EP-IIIA full-power

run is given in Figure 5-21 and shows generally good agreement. The three holds were arbitrarily compressed into 20 seconds to reduce analog computer run time. The reflector inlet temperature and tie rod temperature are shown in Figure 5-22. Special note should be made of the good agreement of the peak tie rod temperature during a shutdown.

(U) Feedsystem

(U) The simulation of the facility components during the shutdown from the EP-III A full-power run is in general agreement with test data as seen in Figures 5-23 and 5-24. The difference between predicted flow and the on-line calculated flow during the first one-half second after the shutdown, indicates that the dynamic impedance of the model should be refined in this region.

(U) During the facility checkout tests, both open and closed loop frequency response measurements were performed to determine the dynamics of the feedsystm and to evaluate the analog model of the feedsystm. Based on the comparison of the analytical model with the experimental data from FEP-II and FEP-III, some revisions were made in the previously formulated Test Cell "C" model (See Reference 33). These revisions include: (a) new Mark 25 pump head and torque characteristics, (b) new bypass valve (L-209) in Figure 3-7 characteristics, and (c) a new turbine torque equation. The improvement in frequency response due to these revisions can be seen in Figure 5-25. The data indicate that segmentation of the heat exchanger model into more nodes may better simulate the rapid increase in phase shift at frequencies greater than 2 Hz.

(U) The predicted emergency shutdown (ESD) from design flow conditions shows good agreement with data from FEP-III as can be seen in Figures 5-26 and 5-27. Figure 5-28 shows the agreement of the analog simulation with the ESD data from a low flow condition.

(U) It is believed that the updated analytical model is sufficient to accurately predict the Test Cell "C" system response while feeding a load orifice. The system components included in the model are shown schematically in Figure 5-29.

(U) Further results of reactor and subsystem dynamic analysis comparisons for NRX-A6 may be found in Reference 34.

(U) COMPONENT EVALUATION

(U) Information for the evaluation of the component performance of the NRX-A6 originated from two sources: (1) data obtained during the tests from reactor instrumentation and (2) data from post-operative examinations made during and after reactor disassembly. In this section the results of information obtained from reactor data is discussed. The observations and analyses made as a result of post

~~CONFIDENTIAL~~
(THIS PAGE IS UNCLASSIFIED)

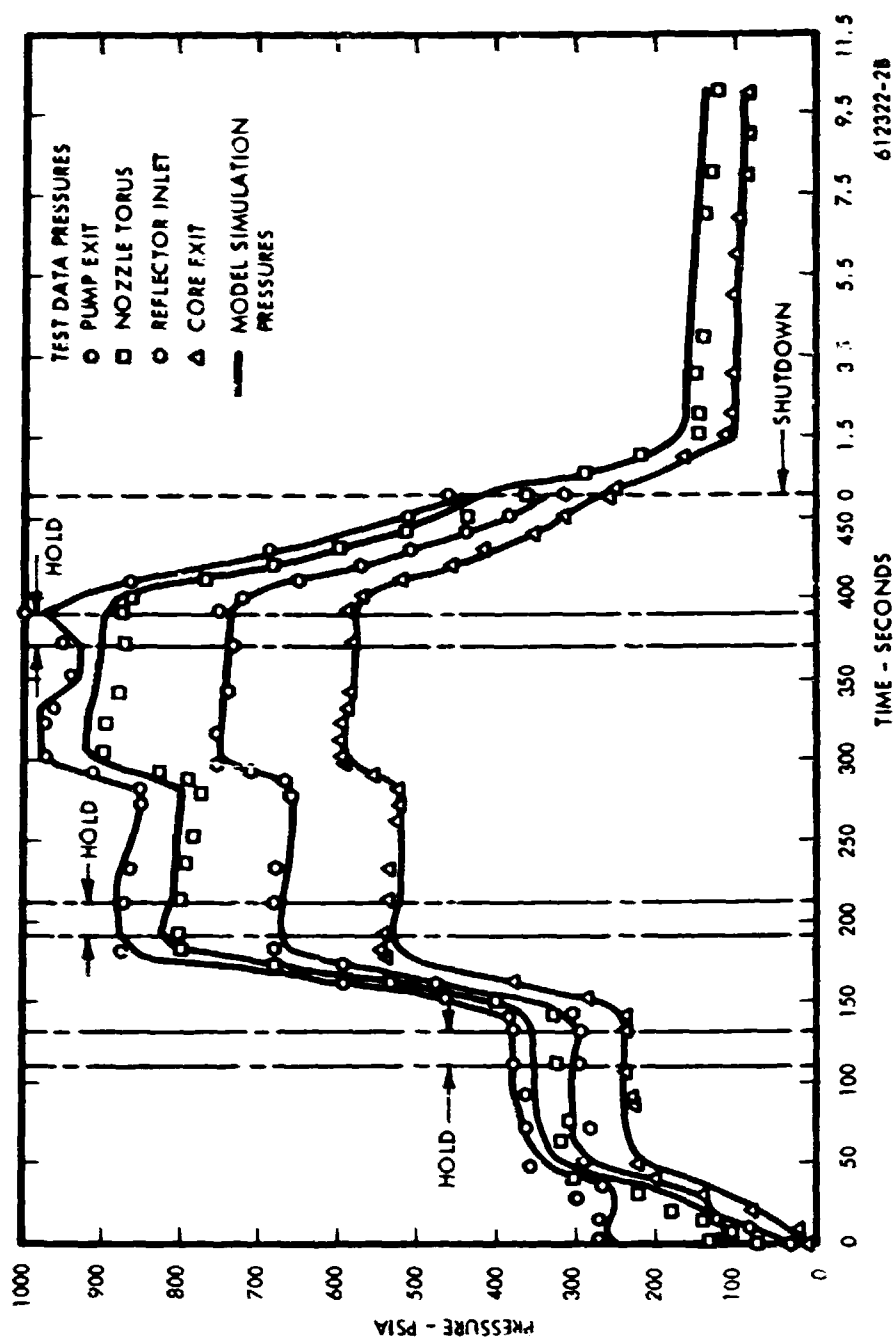


Figure 5-21. (U) Comparison of Pressures During EP-111A Full Power Run with Analog Simulation

(THIS PAGE IS UNCLASSIFIED)

~~CONFIDENTIAL~~

CONFIDENTIAL

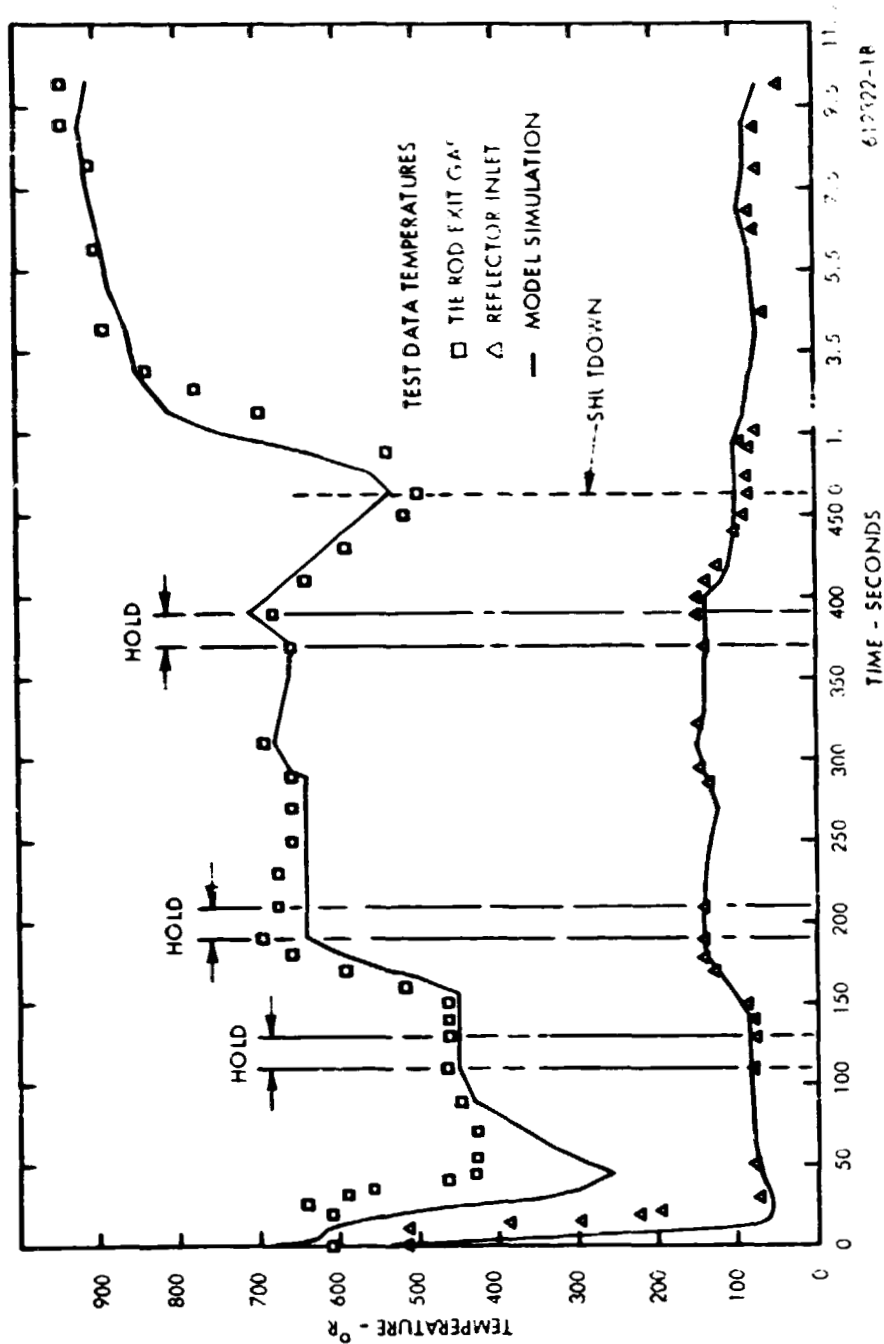


Figure 5-22. (CRD) Comparison of Temperatures During EP-III A Full Power Run with Analog Simulation (U)

CONFIDENTIAL

~~CONFIDENTIAL~~

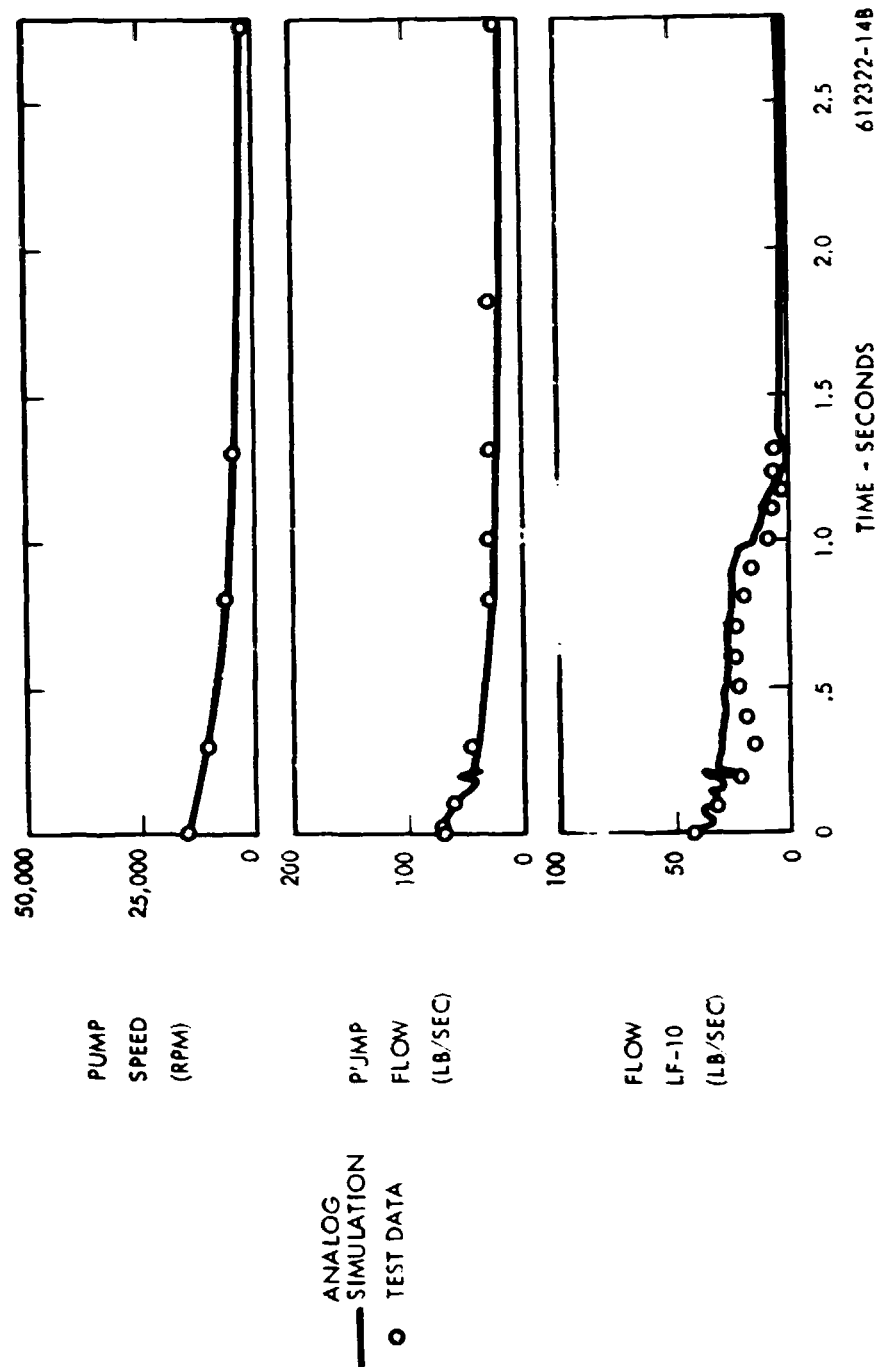


Figure 5-23. (CRD) Comparison of Shutdown Data During EP-III A Full Power Run with Analog Simulation (U)

~~CONFIDENTIAL~~

~~CONFIDENTIAL~~
(THIS PAGE IS UNCLASSIFIED)

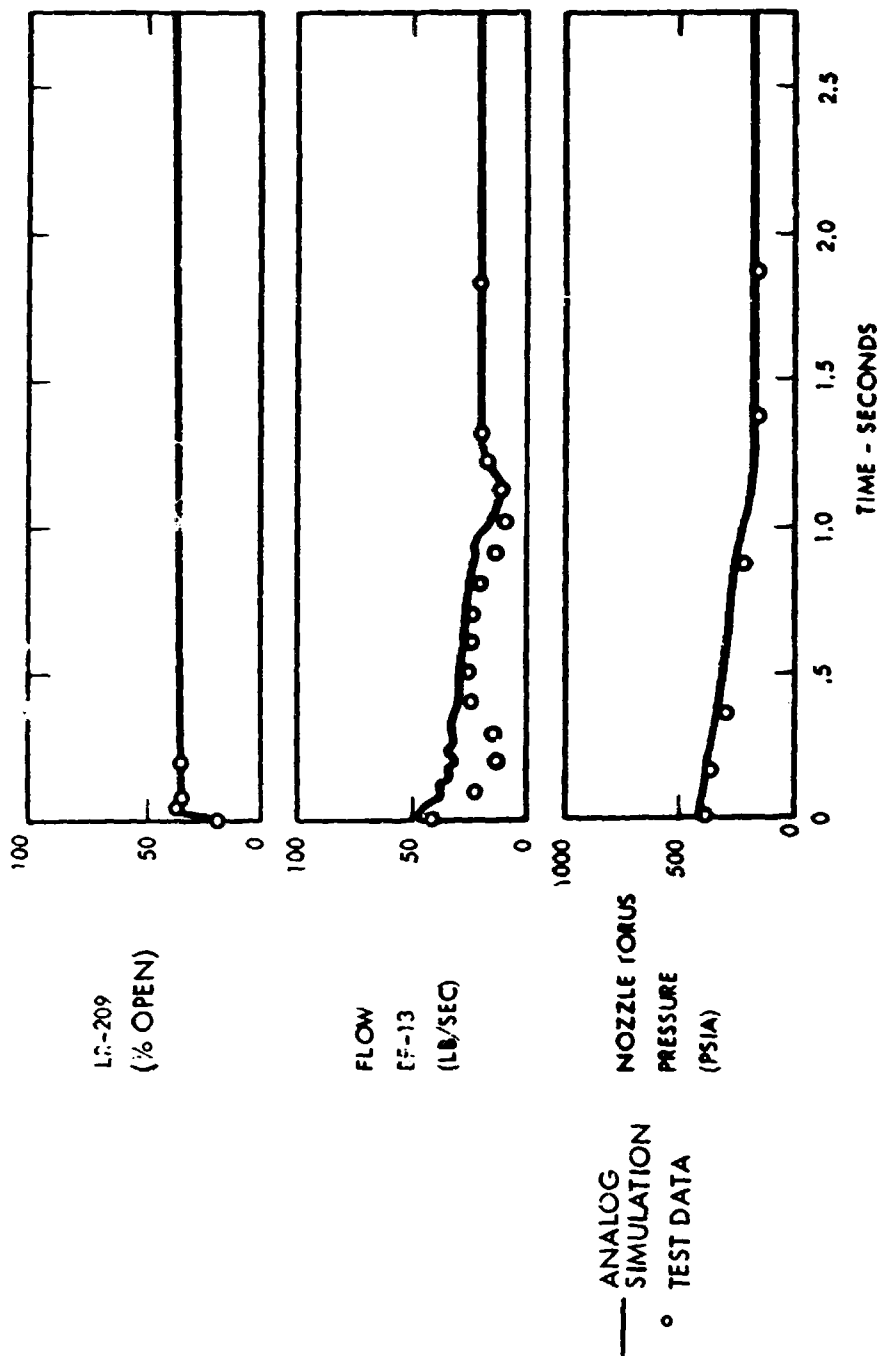


Figure 3-24. (U) Comparison of Shutdown Data During EP-111A Full Power Run with Analog Simulation (U)

(THIS PAGE IS UNCLASSIFIED)

~~CONFIDENTIAL~~

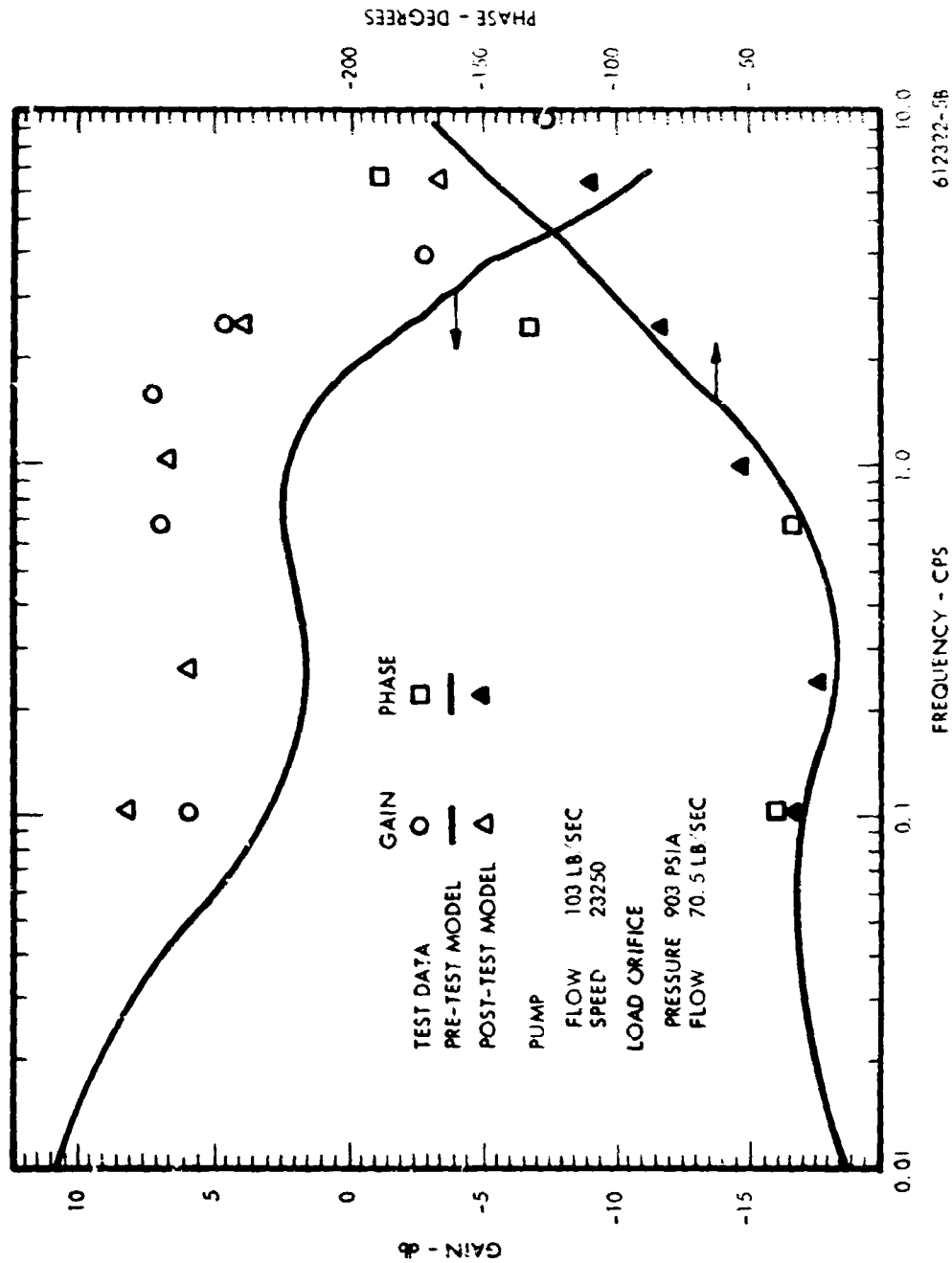


Figure 5-25. (U) NRX-A6 FEP-II Open Loop LF-10
Flow to Turbine Valve Demand Response

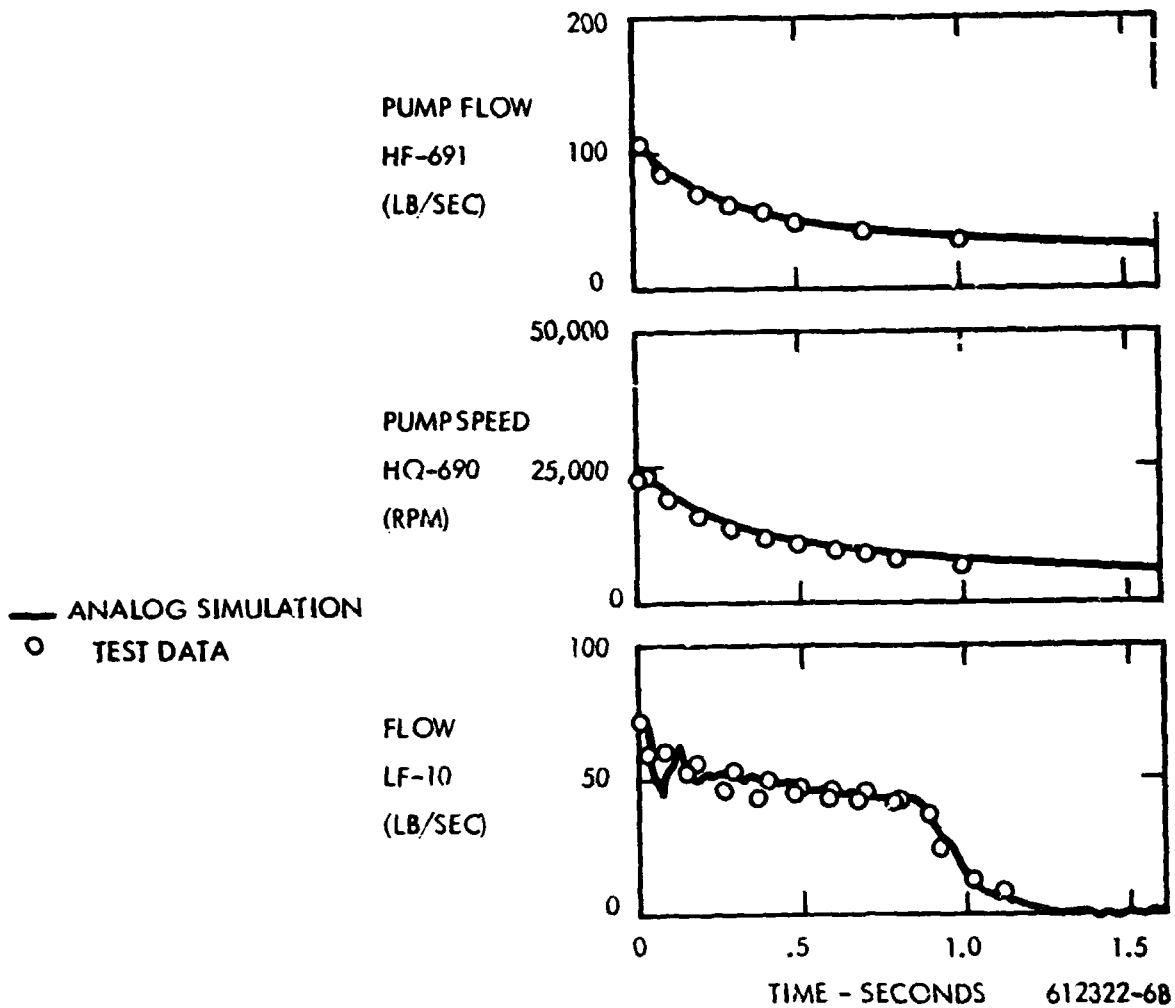


Figure 5-26. (U) Simulation of NRX-A6 FEP-III
Emergency Shutdown from Design Flow

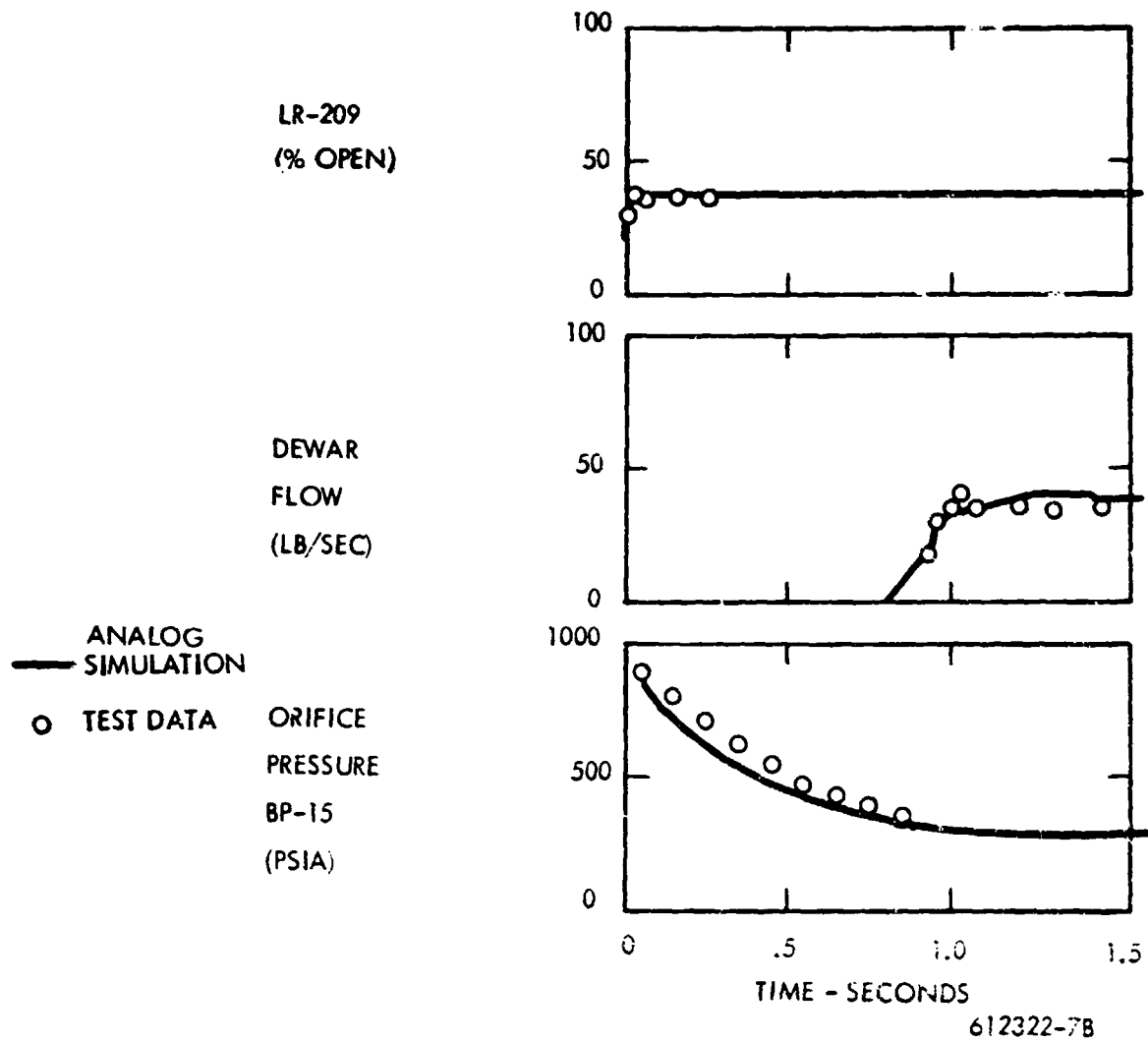


Figure 5-27. (U) Simulation of NRX-A6 FEP-III Emergency Shutdown from Design Flow

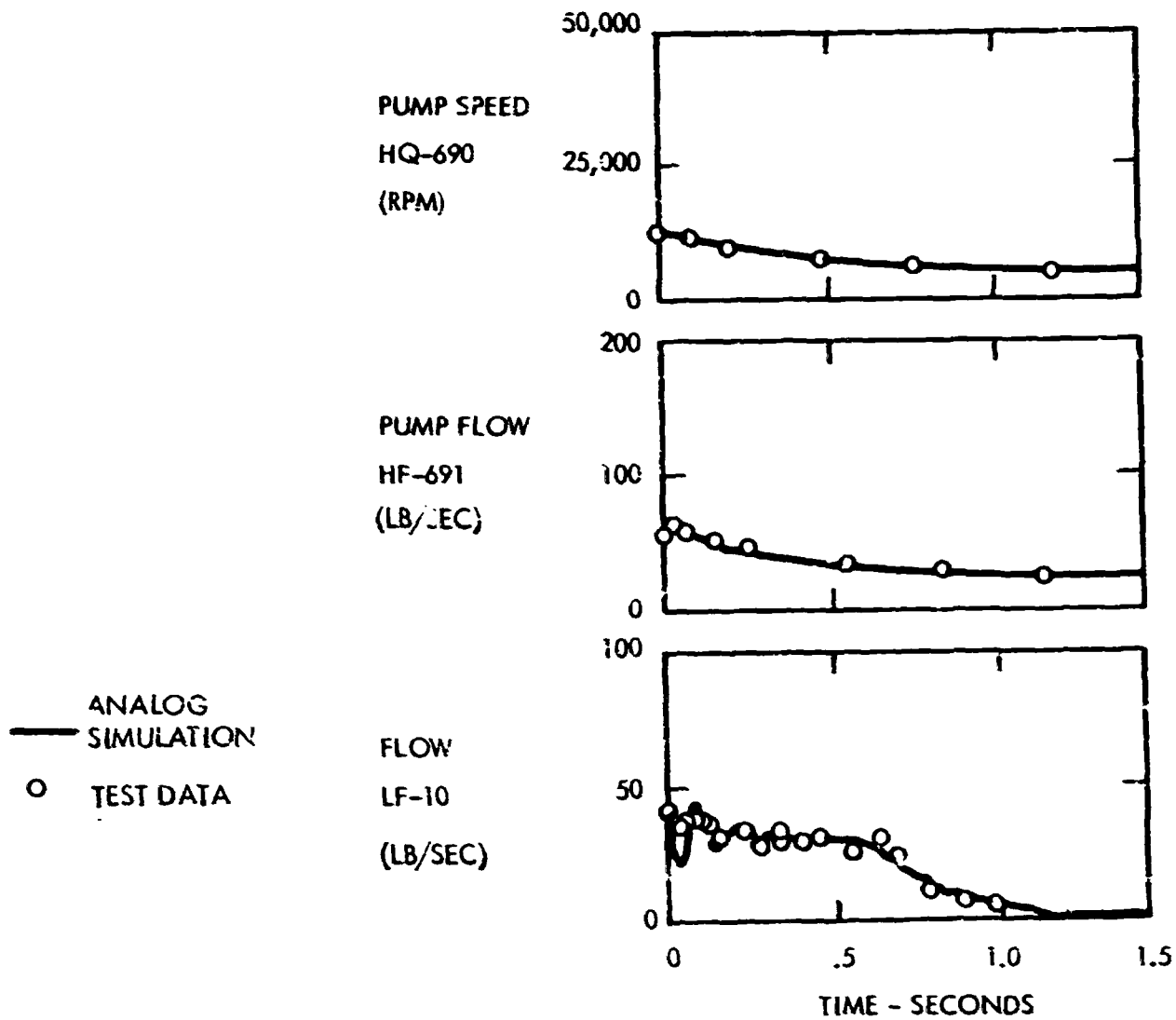
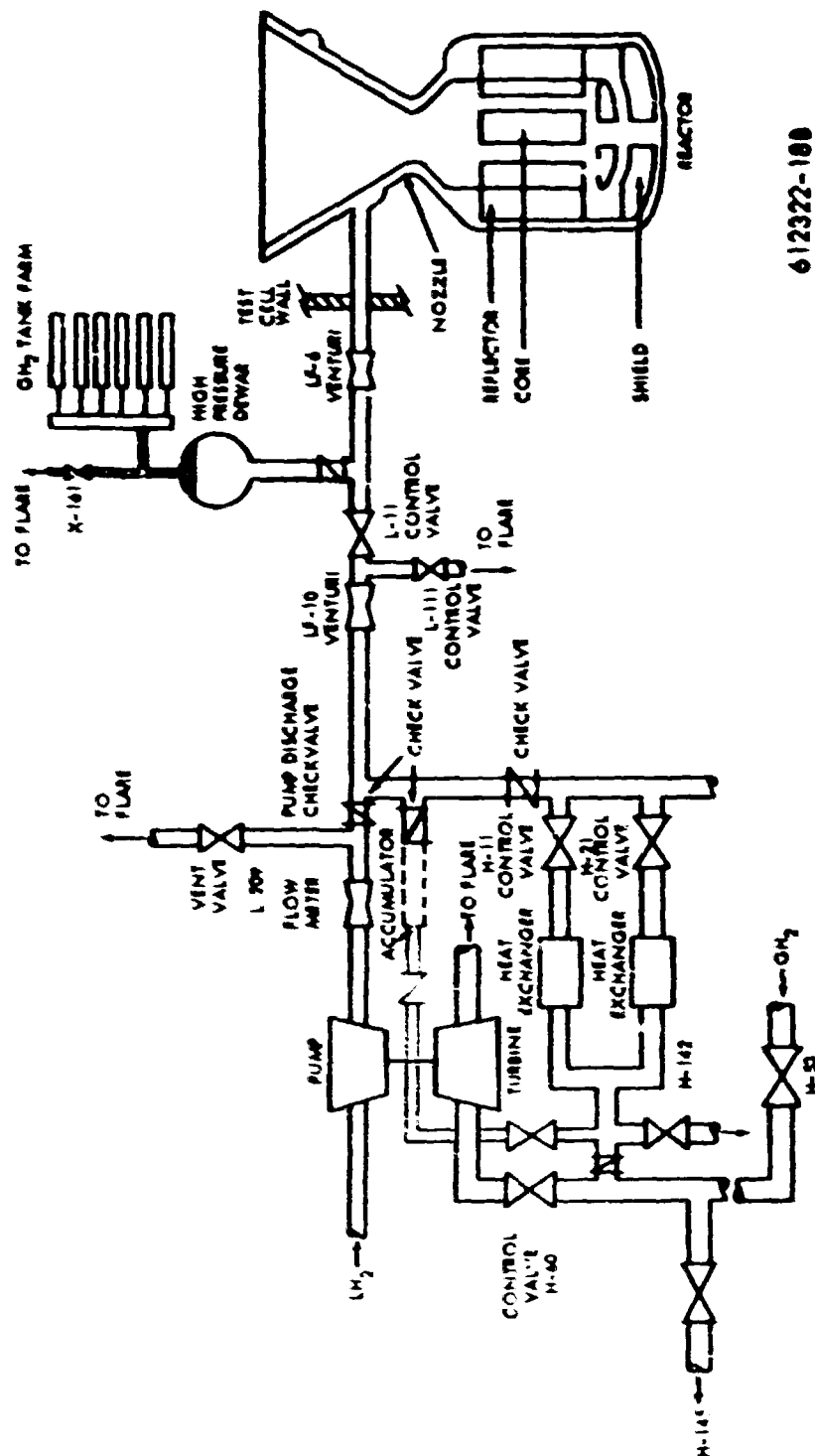
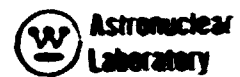


Figure 5-28. (U) simulation of MAX-A6 FEP-III Emergency Shutdown from Low Flow

CONFIDENTIAL
PAGE 10 (CLASSIFIED)



612322-188

Figure 5-29. (U) NRX-A6 Feedsystem and Reactor Schematic of Modeled Components (U)

CONFIDENTIAL

CONFIDENTIAL

operative examinations are discussed later in Section 5 under the headings Disassembly and Post-Operative Examinations and Fuel Element Performance.

(U) Component performance is based on two major areas, data analysis and the discussion of component performance. Considered in the data analysis are both quasi-static responses (less than 1 Hz; i.e., the slow responses of the reactor to such factors as power ramps, shutdowns, and very-low-frequency pressure oscillations) and dynamic responses (shock and vibration).

(U) The quasi-static data analysis included the data from the tie rod strain gages, the tie bolt standoff strain gages, the core radial displacement transducers, and the core axial displacement transducers. The responses of these transducers were compared with the responses predicted by the Reactor Analytical Transient Stress computer program (RATS). The dynamic data was also reduced and a summary of the conclusions from this data is included.

(U) A more detailed discussion of the results of the data analysis is presented in Reference 35.

(CRD) Data Analysis (U)

(U) Data Reduction System and Reactor Model

(U) The coupling of the NUMAD program (Mechanical Analysis of Data) to the RATS program provided a powerful tool for the reactor post test data analysis. The RATS program calculated the displacements of the major reactor components, system forces, certain critical stresses, and other parameters of structural interest. The output from RATS was stored on magnetic tape and available for further analysis, tabulations, or plotting. These plotted results produced the calculated quasi-static structural responses of the NRX-A6 reactor for the measured thermal and pressure test conditions.

(U) The dynamic analysis started with a visual review of the oscillographic replays of the analog wide band type channels. Time slices of interest were then subjected to wave analysis to obtain power spectral density data (PSD) and to determine the frequency control of the dynamic signals.

(CRD) Core/Reflector Relative Radial Displacements (U)

(CRD) The measured average gap change was always higher than the calculated gap change, the maximum error being about 20 percent. This difference was apparently due to the inversed transverse thermal expansion coefficient of the NRX-A6 fuel relative to earlier NRX fuel. The increase was due to a lower temperature bore coating on the NRX-A6 fuel element. The higher expansion of the bore coating caused an increased expansion of the graphite matrix.

CONFIDENTIAL

(U) Tie Rod Strains

(U) The one operable tie rod strain gage provided good data which compared well with calculations during startup and at the core start-of-life. However, all gages drifted excessively during full power, probably due to radiation exposure. This drift was so great that the tie rod strain data was of little value after the start of the power run.

(U) Core Axial Displacements

(U) The LVDT's (displacement transducers) between the core and the support plate gave readings during the startup and start-of-life that were in very good agreement with predictions. These transducers also exhibited a significant amount of drifting due to radiation damage or internal heating.

(U) Standoff Bolt Strains

(U) The standoff bolt strain gages gave data which appeared valid during the test. The drifting was much less than with the tie rods and displacement transducers, probably due to the lower radiation exposure.

(U) The agreement between the calculated and predicted values from these gages was not as good as for the other instruments. The cause of the differences has not yet been determined.

(U) Control Drum Torques

(U) Examination of the control drum torque data found no evidence of control drum rubbing or sticking. The torques were all less than 50 in-lb throughout the run. Because of the large channel setup to detect drum rubbing, it was not possible to distinguish the actual torque level below 50 in-lbs.

(U) Dynamic Data

(U) The NRX-A6 dynamic data indicated that the vibrational environment during the startup to the full power run was very severe, at least on the pressure vessel. The severe pressure vessel vibrations were attenuated before they reached the reactor, and no dynamic breakaway of the core was indicated during the test.

(U) It appeared that the large engine vibrations during the startup were caused by the coupling between the nozzle mechanical vibrations and the nozzle chamber acoustic vibrations during the 2000°R hold. As the frequency of the acoustic vibrations depends on the chamber temperature, which was relatively constant during the 2000°R hold, the vibrations can largely be detuned for any future reactor test by changing the nominal chamber temperature hold (to 1800°R, for example).

(U) The quality of the dynamic data was poor. The variable reluctance accelerometers on the core support plate should be replaced or modified to perform at operational temperature limits. The frequency range of the dynamic displacement



gages was insufficient to provide adequate information during reactor vibrations.

(U) DISASSEMBLY AND POST-OPERATIONAL EXAMINATIONS

(U) The NRX-A6 Test Assembly was returned to the Disassembly Bay of the R-MAD Building on 20 December 1967. Disassembly was initiated at the time and continued until approximately 3 March 1968, at which time all subassemblies had been dismantled. Post-operational examinations took place in the disassembly bay and R-MAD hot cells, and in the disassembly bay and hot cells associated with the E-MAD Building.

(U) The general appearance of the NRX-A6 test article was excellent, as shown in Figure 5-30, which is a photograph of the test article taken immediately after return to the R-MAD disassembly bay.

(U) The results of the disassembly and post-operational examinations confirmed that the NRX-A6 reactor can operate at or above rated conditions for 60 minutes without deleterious effects on the reactor system components.

(U) This section contains a summary of the results of the NRX-A6 disassembly and post-operative examinations on all major reactor components, except fuel element performance which is discussed later in this section of the report. Evaluation and analysis of the dynamic test data has been previously described in this section. A more detailed discussion of the disassembly and post-operational examinations is given in References 35, 36, 37, and 38.

(U) Non-Nuclear (Structural) Reactor Component Examination

(U) Simulated Shield

(U) The simulated shield was in excellent condition following the test with no test induced damage observed. A small amount of debris was observed on the forward face in the seal block areas. Analysis of this debris indicated it resulted from grinding of the seal blocks and instrumentation leads during disassembly.

(U) Flow Screens

(U) All flow screens (located on the underside of the simulated shield) were in excellent condition and were free of reactor operation debris. There was, however, slight evidence of staining on some of the screens.

(U) Core Support Plate

(U) The core support plate was in excellent condition with no evidence of



Figure 5-30. (U) Overall View of Test Assembly After Return to R-MAD (U)

debris or wear marks on either forward or aft surfaces. Metallographic samples of the support plate showed no unexpected anomalies.

(U) Control Drum Drive Shafts

(U) All were in generally excellent condition. A small amount of dark granular contaminant was present at the forward ends of some of the shafts. Slight wear, or burnish marks were observed on the face of the tooth nearest the double tooth of shafts 9 and 10.

(U) Drive Shaft Guide Tube

(U) A small amount of dark granular material, subsequently analyzed as cutting debris, was observed on the ends of the tubes. The tubes were otherwise in excellent condition.

(U) Reflector Assembly

(U) The NRX-A6 was the first reactor to employ the three annular beryllium rings assembled (stacked) into a single reflector. Previous reactors had utilized a two-reflector system, an inner graphite cylinder, and an outer beryllium cylinder made up of 12 full-length segments. This new system required a considerably different disassembly technique and both disassembly and post-operational examinations were modified to take into account the somewhat different requirements. The NRX-A6 reflector was functionally adequate for the NRX-A6 test. The reflector performance did not limit the reactor performance.

(U) During an early stage of disassembly, the presence of cracks was noted in the central and forward end reflector rings. The cracks, which had not been detected in the reflector sectors of any previous reactors, except NRX-A1, which was a cold-flow test only were quite extensive and occurred on both internal and external reflector surfaces, particularly in areas adjacent to control drum positions 3, 4, 6, 9, 10, and 12. During separation of the upper and lower reflector ring halves, (which was accomplished after scoring and wedging apart the upper ring halves at the no. 4 and no. 10 control drum cavity areas), triangular shaped pieces of beryllium fell from the parted surface into the control drum cavities. The appearance of these pieces, as well as the appearance of the parted reflector surface in some locations possessed a brittle, glassy fracture indicative of an irradiated type failure, See Figure 5-31.

(U) An extensive dye penetrant examination and crack mapping program was carried out to evaluate the total reflector crack pattern. As a result, axial cracks were determined to be present in two of the three rings of the reflector. The axial cracks were generally limited to the vicinity of control drum cavities, although some axial cracking was also observed in axial coolant hole locations. The most severe axial cracks were those associated with control drum webs.

~~CONFIDENTIAL~~


 Astronuclear
Laboratory



Figure 5-31. (CRD) Appearance of a Beryllium Piece Found in a Control Drum Cavity After Removal of Upper Half of Reflector. The Brittle, Glossy Nature of the Fracture is Indicative of an Irradiated Type Failure. (CRD)

~~CONFIDENTIAL~~

~~CONFIDENTIAL~~
(THIS PAGE IS UNCLASSIFIED)

(U) The most severe circumferential cracks occurred in the center ring at the outermost spigot surface on the aft end, and the innermost surface of the groove on the forward end. The aft end ring did not contain axial cracks, although small circumferential cracks were observed on its forward face near the no. 3, 6, and 11 control drum locations.

(U) Although numerous axial and circumferential cracks occurred in the NRX-A6 reflector near the end of the full power hold, the presence of these cracks had no significant effect on any parameter measured during testing. Considerable analysis of the reflector has since been performed from the standpoint of materials properties, design requirements and reactor operating parameters. As a result of this analysis the following conclusions have been reached:

- 1) The cracks resulted from thermal stresses in the reflector ring.
- 2) The cracks occurred about two minutes before the end of the full power run. At this time the increased thermal stress exceeded the strength of the beryllium reflector material. The thermal stress increase and the fracture toughness decrease were both due to irradiation effects on the beryllium material.
- 3) The sequence of cracking appears to have been as follows:
 - a) The outer web cracks developed
 - b) The inner web and tongue and groove cracks developed
- 4) As a result of the post test analysis and testing, improved thermal and structural techniques have been developed for the analysis of the stresses in the ring design beryllium reflector.
- 5) Future reflector designs will have to be subjected to a very detailed thermal and structural analysis, including the effects of variations, to assure reliable operation for the NERVA reactors.

The instrumentation on the reflector tie bolts indicated that the tie bolts operated at a higher stress than predicted, but still below the yield strength. However, the reflector reached a temperature of 525°F while in the R-MAD building. Calculations indicate that yielding of the tie bolts would occur at this temperature.

The aft support ring adequately supported the core and reflector loads. It exhibited discoloration and chipping at the aft end which requires further metallographical tests.

(U) Seal Rings Between Core Support Plate and Shield

(U) Wear marks or slight burnishing marks were observed in locations corresponding to seal ring interfaces. These markings were considered normal.

(THIS PAGE IS UNCLASSIFIED)

~~CONFIDENTIAL~~

~~CONFIDENTIAL~~



(U) Cluster Plates, Cold End Cluster Hardware

(U) Although the overall view of the cluster plates showed a discoloration pattern, a close visual examination showed the discoloration to be superficial. (This condition has been noted on cluster plates from nearly all previous reactors). The orifices in the center bushings were observed to be unobstructed. All cold end hardware; i.e. tie rod nuts, holders, split bushings and washers, preload springs, were observed to be in good condition.

(CRD) Aft End Support Ring (U)

(CRD) The inside surface of the aft end support ring showed discoloration flow lines and several chipped or deposited areas were observed. The area around the chipped or deposit locations appeared yellow in color and was found to be very brittle. Metallographic examination showed the base material to be contaminated. Initial testing has not shown what the contaminant is and further testing will be required. All the chips or deposits were on the aft end inside diameter of the rings.

(U) Tie Bolt Standoffs

(U) Two of six tie bolt standoffs were examined in detail, and were in excellent condition.

(U) Lateral Support System

(U) The NRX-A6 reactor had a completely redesigned lateral support system. This system was built into the beryllium reflector and utilized angled seals to provide bundling to the core and axial sealing in the space between the core and the reflector.

(U) This redesigned lateral support system functioned perfectly in the NRX-A6 test. The test demonstrated that an angled seal lateral support system can perform properly in a reactor environment and indicates that it is a suitable choice for the NERVA reactor.

1) Inner Seal Segments - The general condition of all seal segments was good. All segments had clear flow holes with minor coating present on some of the aft end segments. Some slight polishing of the segments was observed where plunger contact was made. No cracks or corrosion of segments was noted.

2) Aft Outer Segments - No evidence of corrosion was noted on these segments, although the coating on these segments contained peeled flaked areas.

~~CONFIDENTIAL~~

CONFIDENTIAL

3) Insulating Segments - The insulating segments, located behind the outer seal segments, were in excellent condition with no indication of flow or corrosion.

4) Outer Seal Segments - All appeared in excellent condition, with no evidence of wear, damage, or corrosion. All flow channels were open, and there was no indication of segment displacement during operation.

5) Plunger Pins, Plunger Pin Sleeves, and Plunger Pin Caps - All plunger pins were in good condition. Polished or burnished marks were typically observed on pins as follows: On the surface where the spring made contact, on the surface where contact with the seal segments was made and on the surface where the pin rides against the inside diameter of the reflector.

The plunger pin sleeves were also in excellent condition, although some showed a brownish contaminant on the OD surface.

Plunger pin caps were in excellent condition, with no observable evidence of leakage.

5) Lateral Support Springs - All lateral support springs were in excellent condition when examined post-operationally. Post-test spring constant determinations were performed on a number of springs to determine the effects of the full power run on stress relaxation. No permanent set could be detected within the accuracy of the measurements (approximately 5 percent).

(U) Reactor Core Component Examination

(U) The performance of the core was the most optimistic result obtained from the NRX-A6 test. The interior fuel element and the central elements survived the full hour run with no structural damage and a smaller than expected corrosion weight loss.

(U) The tight core experiment (close element envelope and average size tolerance and selective assembly of central elements) was very successful, eliminating the problem of fuel element surface corrosion.

(U) Pyrolytic graphite deposition again occurred at the mid-plane of the core, bonding the elements together. Except for creating disassembly problems, this effect was not harmful.

(CRD) Insulating Pyrolytic Tiles (U)

(CRD) Tiles were bowed no more than the bow of the tiles in the unrestrained conditions prior to assembly. Light sooting was present at locations between the rows of seal segments. Some light corrosion was observed on the ID side (fuel side) occurring along tile edges from approximately Station 16 to 50. None of the tiles were broken as a result of the test run.

CONFIDENTIAL

(U) The general appearance of pyrolytic tiles as observed during disassembly operations is shown in Figure 5-32.

(CRD) Grafoil Wrapper (U)

(CRD) The grafoil wrapper was removed a layer at a time, and was photographed to show the corrosion patterns which were present. In general, the wrapper layers contained corrosion voids of varying size and number which occurred in greater degree on the aft ends of the wrapper. Detailed examination showed that two main patterns of axial corrosion were present. One pattern progressed from the outside in (i.e.: the heaviest corrosion occurred on the outer layers of the wrapper at locations corresponding to the gaps between overlying insulating tiles), and the second pattern progressed from the inside out (the heaviest corrosion occurred on inner wrapper layers at locations corresponding to gaps between underlying filler strips). In general, the corrosion patterns were less severe near the middle layers of wrapper than those on either inner or outer surface layers. When viewed externally, wrapper indentations were observed from the outboard side of the foil layers, beginning three or four inches from the forward edge of the wrapper and continuing the length of the wrapper. These indentations were due to pressure deformation of the wrapper into corroded gaps between filler strips. When viewed internally, it was observed that corrosion was most extensive in areas adjacent to thinner filler strips and to periphery elements that possessed notch-type bore corrosion.

(CRD) A few locations were observed where corrosion paths existed through all nine layers of foil. Where this condition occurred, the layers still retained sufficient integrity to permit them to be removed individually. Even though all nine layers had been penetrated locally by corrosion patterns, the wrapper was sufficiently intact to retain its function of sealing against core radial inflow. The appearance of a single thickness of grafoil is shown in Figure 5-33 after removal from the core periphery. Corrosion channels, depicting the filler strip gaps over which they lie, are shown.

(U) The wrapper experiment on NRX-A6 was successful in spite of the severe test. The wrapper gave a radial flow seal over most of the core for the entire test in spite of corrosion from the wide filler strip gaps on the inside and the insulating tile gaps on the outside. The good appearance of many of the peripheral fuel elements showed the benefit to be obtained from sealing the core from the cold lateral support coolant flow.

(U) There was no evidence of tearing of the wrapper due to the thermally imposed strain in this single cycle test.

(CRD) Filler Strips (U)

(CRD) The filler strips in the NRX-A6 were of the hot buffer type. These types of filler strips are placed immediately adjacent to the core, with the thermal insulation outside the filler strips. As a result of the hot buffer experiment and post test analysis of NRX-A5, it was realized that hot buffer filler strips were marginal. An attempt to improve the performance of the NRX-A6 hot buffer



~~CONFIDENTIAL~~

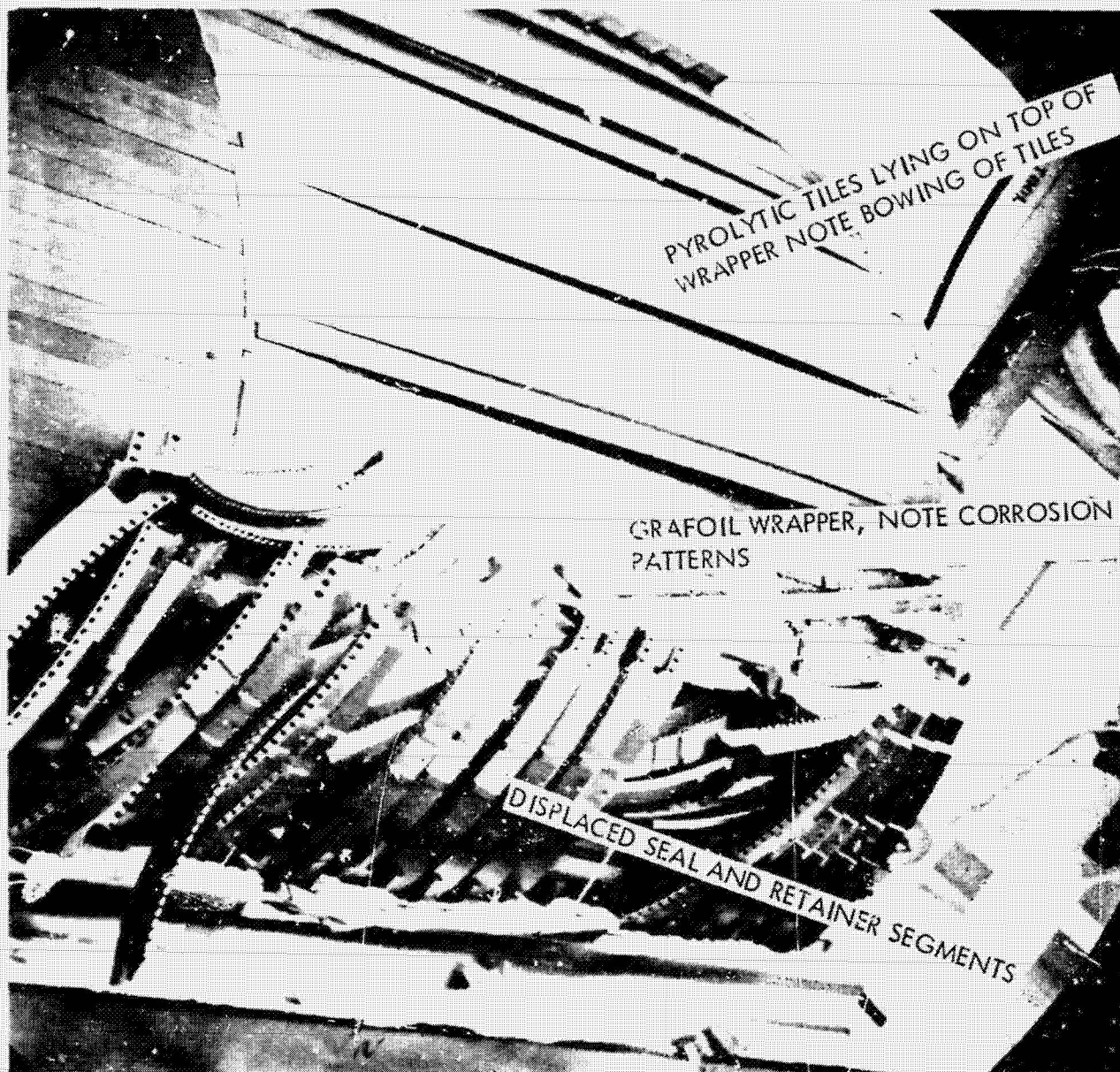


Figure 5-32. (CRD) Appearance of Insulating Tiles, Underlying
of Foil Wrapper, and Displaced Seal Segments. (CRD)

~~CONFIDENTIAL~~

CONFIDENTIAL


 Astro-nuclear
Laboratory



Figure 5-33. (CRD) Appearance of a Grafoil Wrapper Layer, Showing Corrosion Patterns Corresponding to Filler Strip Gaps. (CRD)

CONFIDENTIAL

~~CONFIDENTIAL~~

strips was made by the insertion of a pyrofoil slip plane between the filler strips and the core to reduce friction forces during the startup transient.

(U) This improvement was successful in that the filler strips did not degrade the reactor performance. However, they were not sufficient to prevent filler strip damage and local peripheral element damage under the actual run conditions.

(U) Some cracking of the small filler strips probably occurred during the start-up transient to rated conditions. Full breaks formed in these and other strips during shutdown under the combined effects of corrosion, gradient stresses and filler strip bridging.

(CRD) During disassembly, a total of 71 filler strips were observed to be broken, with the breaks occurring most frequently in the region between Station 25 and Station 35. A summary of the filler strip breaks is shown below.

Summary of the Filler Strip Breaks

<u>Sector Number</u>	<u>Number of Broken Fillers</u>
1	12
2	11
3	10
4	12
5	17
6	9
Total	71

(CRD) Typically, filler strips had the following general appearance:

Adhering grafoil friction foil on the first 3-8 inches of faces adjacent to fuel elements.

(CRD) Light to moderate sooting from Station 16 to 26 inches on faces adjacent to fuel elements, with heavier corrosion near the aft end.

Discoloration and/or blemishing of the coated surface from mid-band to aft end.

Little or no corrosion of the coated aft ends of the filler strips.

(U) Although approximately 45.5 percent of the filler strips sustained one or more breaks, when examined post-operationally, only four small pieces of filler strips became displaced from the core, and these did not become displaced until after termination of the test run. These pieces were the aft two inch sections of fillers 3-11, 4-11, 4-13, and 5-13, which fell from the nozzle during trunnioning in the disassembly bay. Examination of the fracture surfaces of the four

~~CONFIDENTIAL~~

~~CONFIDENTIAL~~



pieces indicated they were mechanical breaks rather than corrosion separations. The overall performance of the filler strips was not noticeably affected by the breakage sustained.

(U) Filler Strip Keys

All filler strip keys were detached from the fuel elements when examined during disassembly operations. Examination of the keys indicated that they did not break, peel, or shear off, as no evidence of mechanical damage to edges or surface of the keys was noted. Some information is available which indicates the keys may have become detached from the elements during the post-test cooldown period. There was no indication that loss of the keys produced any adverse effect upon reactor operation.

(U) Anti Friction Foil

(U) The anti-friction foil was added to the core periphery region to permit relative movement of peripheral elements and filler strips during startup transients with minimal friction force. The foil generally remained in place throughout the test run, although some corrosion was present, particularly at the aft ends, the general condition was excellent. Significant corrosion of the foil was present at the element corners where notch type cracking of the elements occurred. Generally, the foil became bonded during the test run to the coated lower ends of the fuel elements; but remained attached to the forward end of the filler strips. There was no indication of circumferential displacement.

(CRD) Liner Tubes

(CRD) All liner tubes examined appeared in good condition. Generally, the exterior surface was clean except for ring deposits or discoloration which occurred at nearly all insulating sleeve joints between Station 10 and 40. The forward portion of the liner tube contained more discoloration than the aft end.

(CRD) Pyro Insulating Sleeves

(CRD) The pyrofoil and pyrolytic graphite sleeves forward of Station 20 (approximately) were relatively unaffected by corrosion. Joint corrosion and streaking occurred on sleeves beginning at about the midplane and continuing to the aft end, with some pinholing and/or undercutting observed at the spigoted joints. The aft end sleeve sustained corrosion on the OD approximately 8 mils deep on the last 1 1/2 inches. There was no indication of gross liner tube damage as a result of pyro-graphite sleeve corrosion, and the components successfully fulfilled their intended objective of protecting the tie rods from overheating.

~~CONFIDENTIAL~~

~~CONFIDENTIAL~~

~~(THIS PAGE IS UNCLASSIFIED)~~

(U) Jet Orifices

(U) All orifices were in place prior to removal of the cluster plates. However, examination of the forward end of the core showed that the orifice cement was loosened and embrittled by exposure in the high radiation field during and following the test run. During the lengthy disassembly sequence, the orifice cement continued to deteriorate from subjection to the high gamma levels present, and as a result of the pounding given to the core during attempts to unbond fuel elements. This resulted in many orifices becoming detached from the fuel during subsequent handling.

(U) Support Blocks

(U) The support blocks in NRX-A6 also functioned satisfactorily. The regular blocks finished the test in near-new condition, the irregular peripheral blocks suffered external surface cracking, probably during the faster than planned startup. The 3700°R hold planned to limit the block stresses was not utilized and calculated stresses for the actual transient exceed the support block strength in the peripheral blocks. The subsequent corrosion during the hour run did not destroy the load carrying capability of the blocks.

The sooting which has been encountered on blocks from previous reactors was noticeably absent on NRX-A6. Instead, there were present bluish deposits, indicative of foreign material probably oxides of molybdenum. Some peripheral blocks showed sidewall cracking and subsequent minor undermining corrosion where the cracks occurred. Some also contained cracks on the forward faces, but little or no corrosion was associated with the forward cracks. All regular support blocks retained excellent adhesion of the NbC coating which was deposited at lower temperatures than used previously.

(U) Composite Cups

(U) The condition of composite protection cups was generally good. Typically, the cups showed little or no coating loss; they possessed some bluish or brownish discoloration, and a few contained minor surface cracks on the aft rim. A few cups sustained more severe damage. These seven contained longitudinal sidewall cracks and radial cracks on the flanges. These cracks are apparently caused by the combination of the transient thermal stress during startup and the chilling effect of leakage flow which appeared at the cluster aft end hardware.

(U) The axial crack in the peripheral composite cups resulted from the high non-symmetric transverse temperature gradient across the diameter of these cups. The post test analysis indicates that a gradient of twice the allowable existed in these cups. These cracks did not degrade the reactor performance.

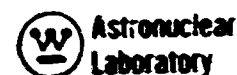
(U) Tungsten Cups

(U) The condition of these cups was generally excellent. However, one cup contained a small crack in the shortcup and seven other cups contained small side-

~~(THIS PAGE IS UNCLASSIFIED)~~

~~CONFIDENTIAL~~

~~CONFIDENTIAL~~



~~(THIS PAGE IS UNCLASSIFIED)~~

wall blisters. Performance of both types of tungsten cups did not appear impaired by their post test condition.

(U) Insulating Cups, Pyrofoil Washers

(U) Typical insulating cups contained intact inside diameter coating, missing OD coating, light corrosion on the forward face (associated with insulating sleeve corrosion) and light corrosion on the OD of the cups.

(U) The pyrofoil washers were substantially corroded in most cases, a condition which is believed to have contributed to the aft insulating sleeve corrosion mentioned previously.

(CRD) Central Unfueled Elements

(CRD) The central unfueled elements were in excellent condition with little or no surface corrosion and intact bore coating. This was the first reactor in which all the central elements were coated.

(U) The faster than planned startup on the EP-IIIA test increased the stress in the central element, but not to an unacceptable level.

(U) Tie Rods

(U) All tie rods appeared in excellent condition, with no observable damage other than slight discoloration. Room temperature and elevated temperature tensile tests of irradiated NRX-A6 tie rods are being performed.

(U) Locating Cone, Particle Catchers, Particle Catcher Screens

(U) These components were found to be in generally excellent condition. Wear or deformation indicative of run damage was not detected.

(U) Test Article Radiation

(U) Radiation readings taken one-quarter inch from the surface of the pressure vessel mid-point indicated a radiation of 330,000 R/hour, approximately 72 hours after the final EP.

Radiation readings taken of the test car after removal of the PVARA/nozzle assembly averaged 200 mr/hour, at twelve inches from the test car surface, although one area of the car gave a reading of 2 R/hour. Considering the 1 hour duration of full power testing, this value is extremely low, and attests to the effectiveness of the external shield employed during the experimental test runs.

~~(THIS PAGE IS UNCLASSIFIED)~~

~~CONFIDENTIAL~~

~~CONFIDENTIAL~~

(CRD) FUEL ELEMENT PERFORMANCE (U)

NRX-A6, the fifth NERVA reactor, was successfully tested for 60 minutes under single cycle, full power conditions on 15 December 1967 at Test Cell C. The reactor was returned to R-MAD on 21 December for disassembly. Unstacking of the core was completed in April 1968. A total of 1571 fuel elements were weighed, 1493 were photographed on 70 mm film and were examined visually by a film viewer. Approximately 1300 elements were sectioned for incremental weight loss evaluation. A discussion of the results of the fuel element examination is given in this section. A more detailed discussion of the NRX-A6 fuel element examinations is given in Reference 39. Some hot cell examinations of fuel elements, such as metallography, are still in progress and will not be discussed in this report.

(CRD) General Observations (U)

(CRD) The performance of the NRX-A6 fuel elements typically was characterized by inter-element bonding, mild surface corrosion, low pinhole densities, lower mid-band weight losses, and higher hot end weight losses relative to NRX-A5, and excellent corrosion resistance and integrity of the aft unfueled tip. Some variation in corrosion performance was noted between the various matrix-coating batch types and with respect to core radius. These variations were not nearly as pronounced, however, as had been observed in previous NRX reactor tests (see References 40, 41 and 42). Notch-type corrosion patterns similar to those observed on peripheral NRX-A5 elements (see Reference 41) were again observed on the peripheral faces of some NRX-A6 peripheral elements, although the fraction of peripheral NRX-A6 elements affected was lower. The weight losses observed in the NbC matrix-additive and Nb resinate impregnated experimental elements were somewhat higher than that of comparable standard core fuel elements. Flexure strength changes corresponded to the axial variations in fuel element incremental weight loss.

(CRD) Overall Core Average Performance (U)

(CRD) An overall core summary of gross weight loss, gross mid-band and hot end weight losses and visual data results is presented in Tables 5-7 and 5-8. Where possible, corresponding data obtained during the NRX-A5 post-mortem has been included. The core average values for gross weight loss and pinhole frequency (pinholes per element) in NRX-A6 elements were approximately 50 percent lower than the corresponding NRX-A5 values. Pinholes in the NRX-A6 fuel elements typically occurred in the 40 to 50 inch axial region while those in NRX-A5 were in the 22 to 25 inch and 38 to 41 inch axial regions.

(CRD) The gross incremental weight loss data in Table 5-7 is based on a preliminary sampling of the NRX-A6 results. The mid-band weight losses of typical NRX-A6 fuel elements appears to be approximately one-tenth that of the NRX-A5 fuel elements. The hot end weight losses for both NRX-A6 and NRX-A5 fuel elements are of the same order of magnitude. NRX-A6 demonstrated excellent corrosion resistance and integrity in the aft non-fuel tip region. Only 30 fuel elements exhibited corrosion in the region of the tip joints.

~~CONFIDENTIAL~~

CONFIDENTIAL

TABLE 5-7
(CRD) NRX-A6 FUEL ELEMENT WEIGHT LOSS AND VISUAL DATA SUMMARY (U)

(See Key, Table 5-7A)

<u>Parameters</u>	<u>Core Average Per Element</u>	<u>Range</u>
Gross Weight Loss*, $\overline{\Delta W}_G$	13.1 grams (NRX-A5 = 27.0 grams - see Reference 42)	3.4 to 42.6 grams
Gross Mid-band Weight* Loss, 0 to 30"	2.3 grams (NRX-A5 = 25.8 grams - see Reference 42)	0.2 to 5.4 grams
Gross Hot End Weight* Loss, 30 to 52"	10.9 grams (NRX-A5 = 8.5 grams - see Reference 42)	5.6 to 35.4 grams
Algebraic MESL**, \overline{M}	-0.2 gram	-9.9 to +7.1 grams
VESL***, \overline{V}	0.7 gram	0 to 7.4 grams
pinholes (PH) ⁺	4.9 grams (NRX-A5 = 10.0 grams - see Reference 42)	0 to 59 grams
BAR ⁺⁺	95% (NRX-A5 = 98% - see Reference 42)	50 to 100%
CAR (Side Flats) ⁺⁺⁺	95% (NRX-A5 = 94% - see Reference 42)	70 to 100%
Molybdenum Loss, \overline{X}^{++++}	1.7 grams	0.8 to 2.5 grams

CONFIDENTIAL

~~CONFIDENTIAL~~

TABLE 5-8

(CRD) KEY TO TABLE 5-7 (U)

- * Gross weight loss core average is based on a total of 1566 NRX-A6 fuel elements (1549 NRX-A5 fuel elements) weighed and includes data from 1350 intact and 216 broken fuel elements. Gross values are not corrected for mechanical effects of inter-element bonding or foil adherence (MESL), surface corrosion losses (VESL) or molybdenum overcoat reactor blowdown. The gross incremental weight loss values are based on 156 NRX-A6 fuel elements (126 NRX-A5 fuel elements) representing all non-experimental manufacturing origins and a typical radial distribution. The 156 NRX-A6 elements were picked to correspond radially with the incremental data from NRX-A5.

- ** Net algebraic correction to the core average gross weight loss per element (MESL). Correction necessary due to the mechanical effect of inter-element bonding pull-out (negative), inter-element bonding pull-in (positive) and anti-friction foil adherence (positive). Net effect calculated from visual estimates performed on 1493 fuel elements.

- *** Visual estimate of surface corrosion loss (VESL), based on the visual examination of 1493 fuel elements.

- + Average based on 1493 fuel elements examined. There were 1138 NRX-A6 fuel elements with pinholes. There were 1082 NRX-A5 fuel elements with pinholes; however, only 1372 fuel elements received visual examination in this reactor.

- ++ Percent of bearing area remaining (BAR) on the exit face. Based on visual examinations of the exit face on 1324 fuel elements.

- +++ Percent of back or OD coating area remaining (CAR) based on visual examination of 1493 fuel elements.

- ++++ Core average loss per element of molybdenum overcoat from the bores due to reactor test blowdown. The pre-reactor test average molybdenum weights per element were:

<u>Mo Coating Origin</u>	<u>Avg. Mo</u>
WNCO	3.6
Y-12	3.1
Overall Core	3.4

Molybdenum analyses were performed post-operationally on 20 fuel elements at six axial locations per element. The comparison of these results with pre-reactor distribution indicates that the amount of molybdenum remaining in the coolant channels of the NRX-A6 elements was 50 ± 10 percent of the pre-reactor level.

~~CONFIDENTIAL~~

~~CONFIDENTIAL~~



(CRD) A core average bore weight loss per element, $\overline{\Delta W_B}$, can be calculated using the following expression:

$$\overline{\Delta W_B} = \overline{\Delta W_G} + \overline{M} - \overline{V} - \overline{X}$$

where

$\overline{\Delta W_G}$ = Core Average Gross Weight Loss

\overline{M} = Average Algebraic MESL (Mechanical Estimate of Surface Loss) Correction

\overline{V} = Average Surface Corrosion Loss

\overline{X} = Average Molybdenum Loss Due to Reactor Blowdown

(CRD) Using this expression and the data in Table 5-7, an estimate of the overall average bore weight loss of a typical NRX-A6 fuel element is approximately 10.5 grams.

(CRD) Matrix-Coating Batch Type Performance (U)

(CRD) Table 5-9 is a summary of average gross weight loss, pinholes (PH), visual estimate of surface loss (VESL) and channel exposure (CEX) for the various matrix-NbC bore coat - Mo overcoat types present in NRX-A6. The YWW elements had both the lowest average gross weight loss and the lowest pinhole frequency data of all matrix-coat combinations in the core. Excluding experimental elements, the worst performing matrix-coating batch type in the NRX-A6 core, based on average gross weight loss, was the WYW combination, 4.1 grams higher than the YWW average. The Y-12 NbC bore coated elements had pinhole frequencies approximately four times as great as the WNCO bore coated elements.

The average gross weight loss for the various matrix-coating types by 2cm radial increments is presented in Figure 5-34. There is essentially no change in the order of weight loss performance in this data compared to that in Table 5-9.

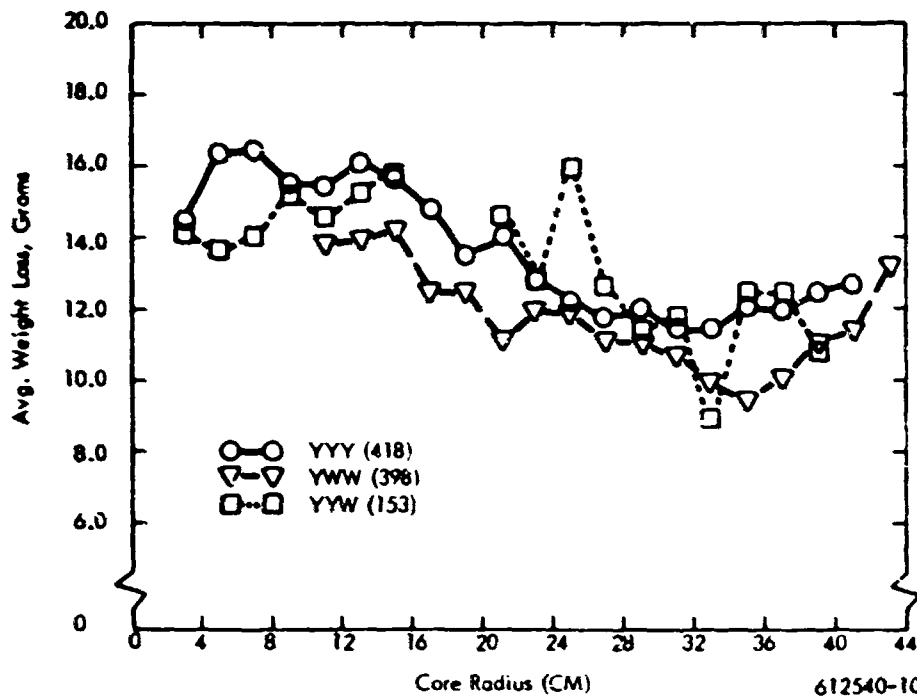
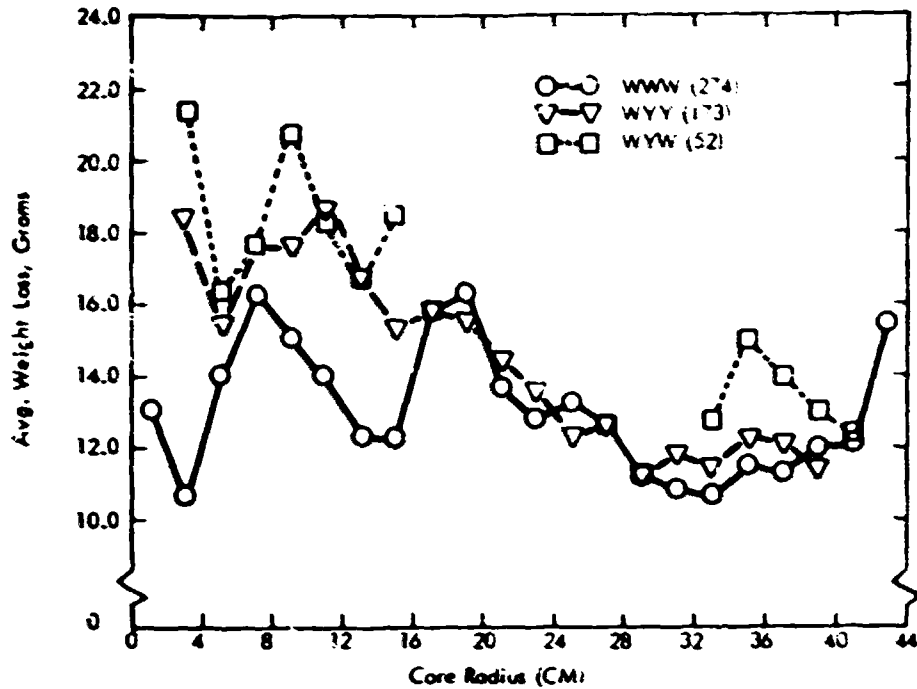
(CRD) Radial Variations (U)

(CRD) A radial distribution of gross weight loss averages is presented in Figure 5-35 for NRX-A6 and NRX-A5 fuel elements. Radial variations in PH densities of NRX-A6 and NRX-A5 fuel elements are presented in Figure 5-36. Both plots illustrate the higher corrosion rate at or near the center of the core in both reactors, but clearly indicate the superior performance of NRX-A6.

Figures 5-37 and 5-38 illustrate the radial variations in the 0 to 30 and the 30 to 52 inch incremental weight losses, respectively, for representative samplings of NRX-A6 and NRX-A5 fuel elements. The NRX-A6 averages do not include experimental element data. The superior mid-band performance of the NRX-A6 fuel elements is immediately evident, averaging 23.5 grams below the NRX-A5 value. The NRX-A6 and NRX-A5 hot end average incremental weight losses compare remarkably well despite the fact that the NRX-A6 core operated at full power conditions twice as long as the NRX-A5 core.

~~CONFIDENTIAL~~

~~CONFIDENTIAL~~



612540-10

Figure 5-34. (CRD) Radial Distribution of Gross Weight Loss for Matrix-Coating Types (U)

~~CONFIDENTIAL~~

TABLE 5-9

(CRD) NRX-A6 MATRIX-COATING PERFORMANCE (U)

Element Code**	No. in Core	No. Weighed	Avg. Gross Wt. Loss (grams)	Weight Loss Range	Avg. PH Per Element	Avg. YESL (gms)	Avg. CEX (inches)	No. Examined on Viewer
Matrix-NbC								
Bore Coat-Mo Coat								
WWW	284	274	13.2	7.2-41.1	1.9	0.74	1.17	267
WYW	52	52	15.6	10.5-29.0	6.2	0.73	0.27	48
WYY	173	173	13.3	7.4-22.5	7.0	0.91	0.11	162
YWW	400	398	11.5	6.5-28.7	1.6	0.61	1.65	380
YYW	154	153	13.5	7.5-23.5	7.2	0.89	0.19	143
YYY	423	418	13.2	7.0-24.5	8.5	1.42	0.19	400
2.5 NbC**	24	24	17.3	10.8-33.1	2.4	0.68	0.50	22
5.0 NbC**	6	6	17.2	9.5-24.1	0.7	0.65	0.13	6
Nb Resinate**	17	17	16.7	13.4-27.6	1.0	1.29	0.73	15
WSW**	10	10	11.4	6.4-13.9	2.2	0.35	0.03	9
WTW**	16	16	15.5	10.7-20.5	3.6	0.91	0.30	16
YLN**	4	4	16.7	14.3-19.3	2.7	0.97	0.00	3
YSW**	6	6	12.1	10.9-14.7	2.8	0.80	0.25	6
YTW**	15	15	13.9	11.1-17.6	1.1	0.93	0.37	15

*Element Code:

1st Letter - Matrix

2nd Letter - NbC Bore Coat

3rd Letter - Molybdenum Overcoat

W - Westinghouse WNCO

Y - Oak Ridge Y-12

S - WNCO Standard

L - Low Temperature

T - Thick Hot End

**Experimental Elements

Astronuclear
Laboratory

CONFIDENTIAL

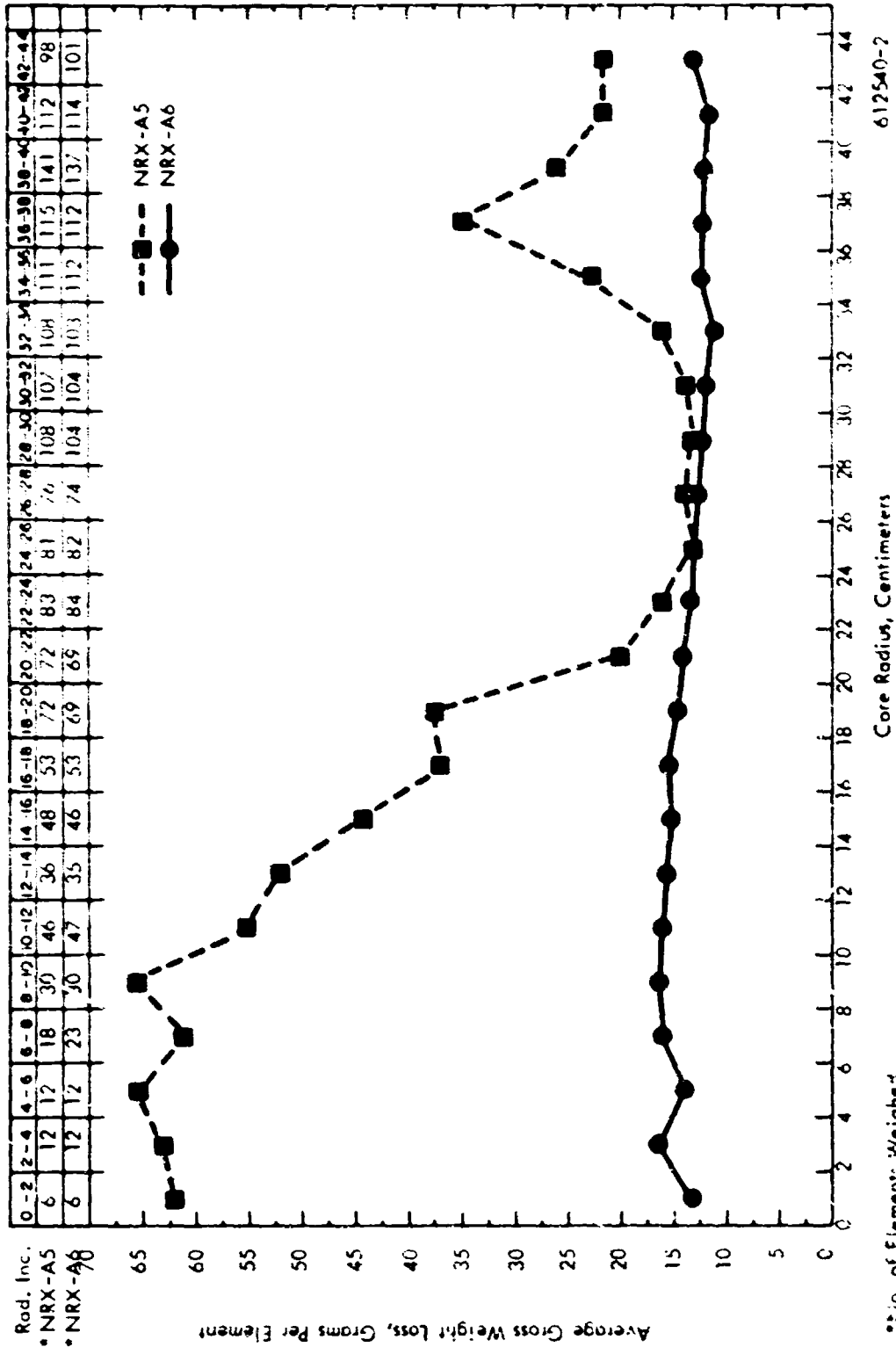
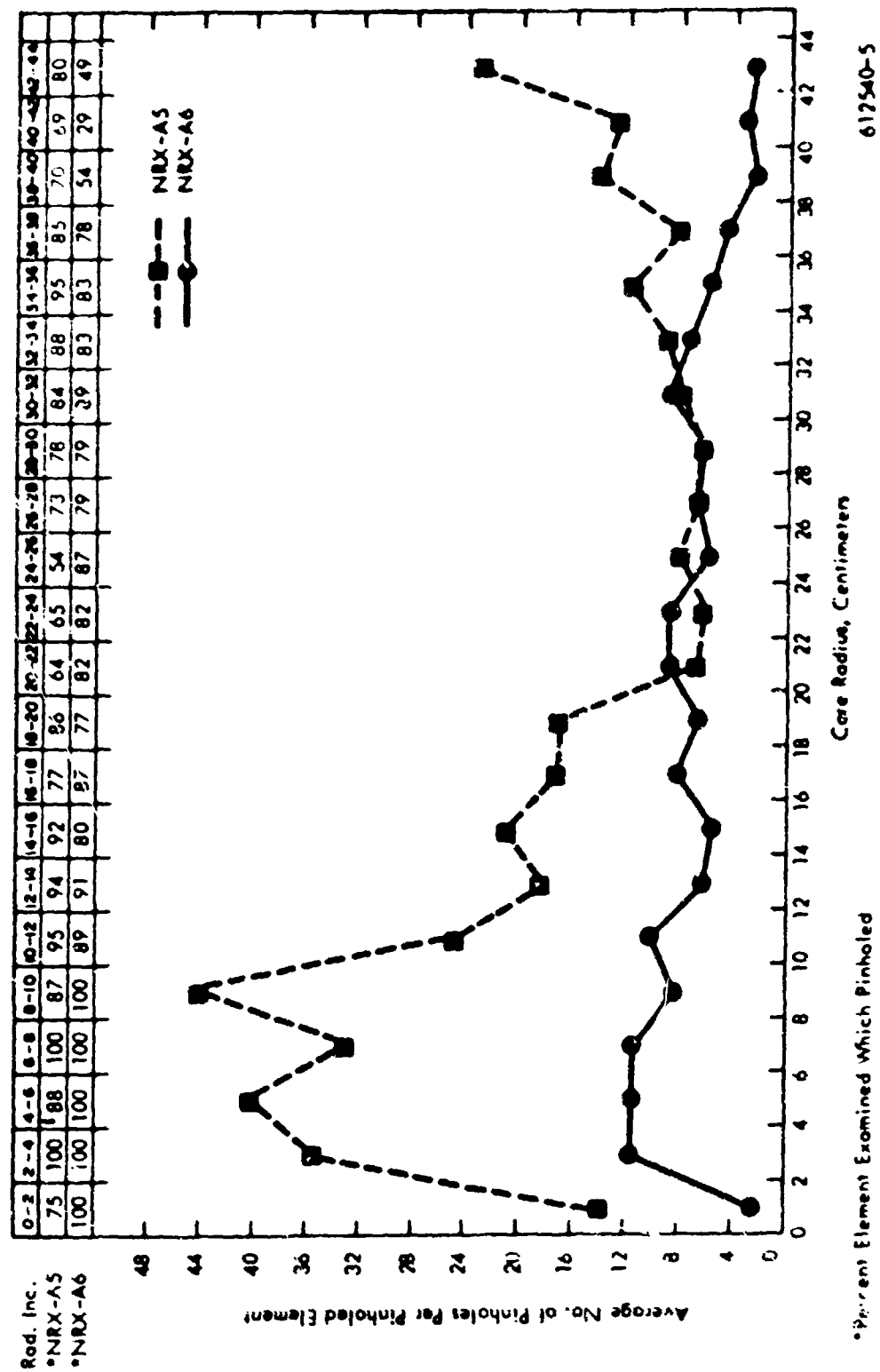


Figure 5-35. (CRU) Radial Distribution of Gross Weight Loss in NRX-A6 and NRX-A5 (U)

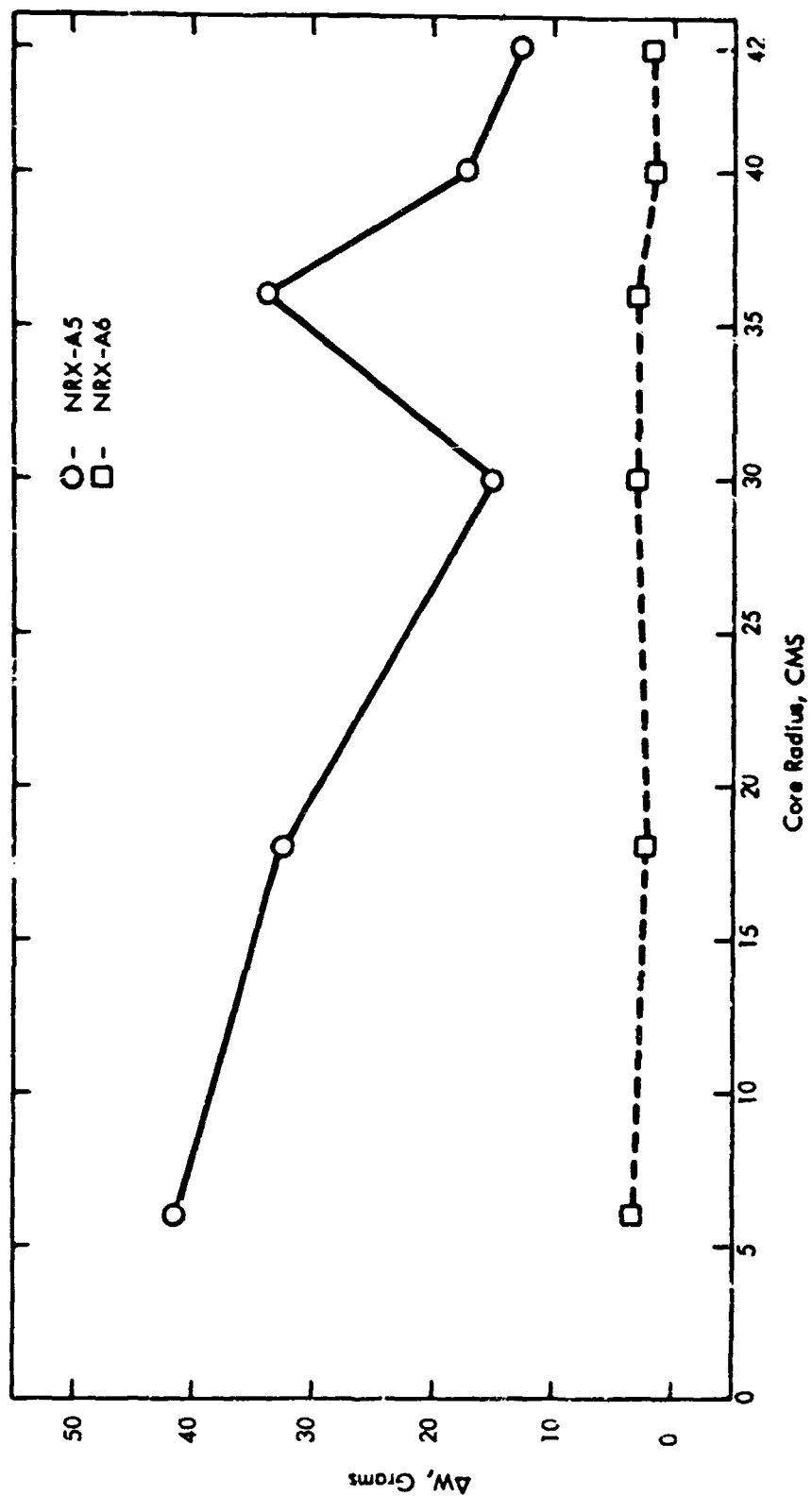
~~CONFIDENTIAL~~



~~CONFIDENTIAL~~

Figure 5-36. (CRU) Comparison of Radial Distribution of Pinhole Frequency and Density in NRX-A6 and NRX-A5 (U)

CONFIDENTIAL



CONFIDENTIAL

Figure 5-37. (CRD) Radial Variations of Incremental Weight Loss in the Axial Region 0-30 Inches for NRX-A5 and NRX-A6 Fuel Elements (CRD)

CONFIDENTIAL

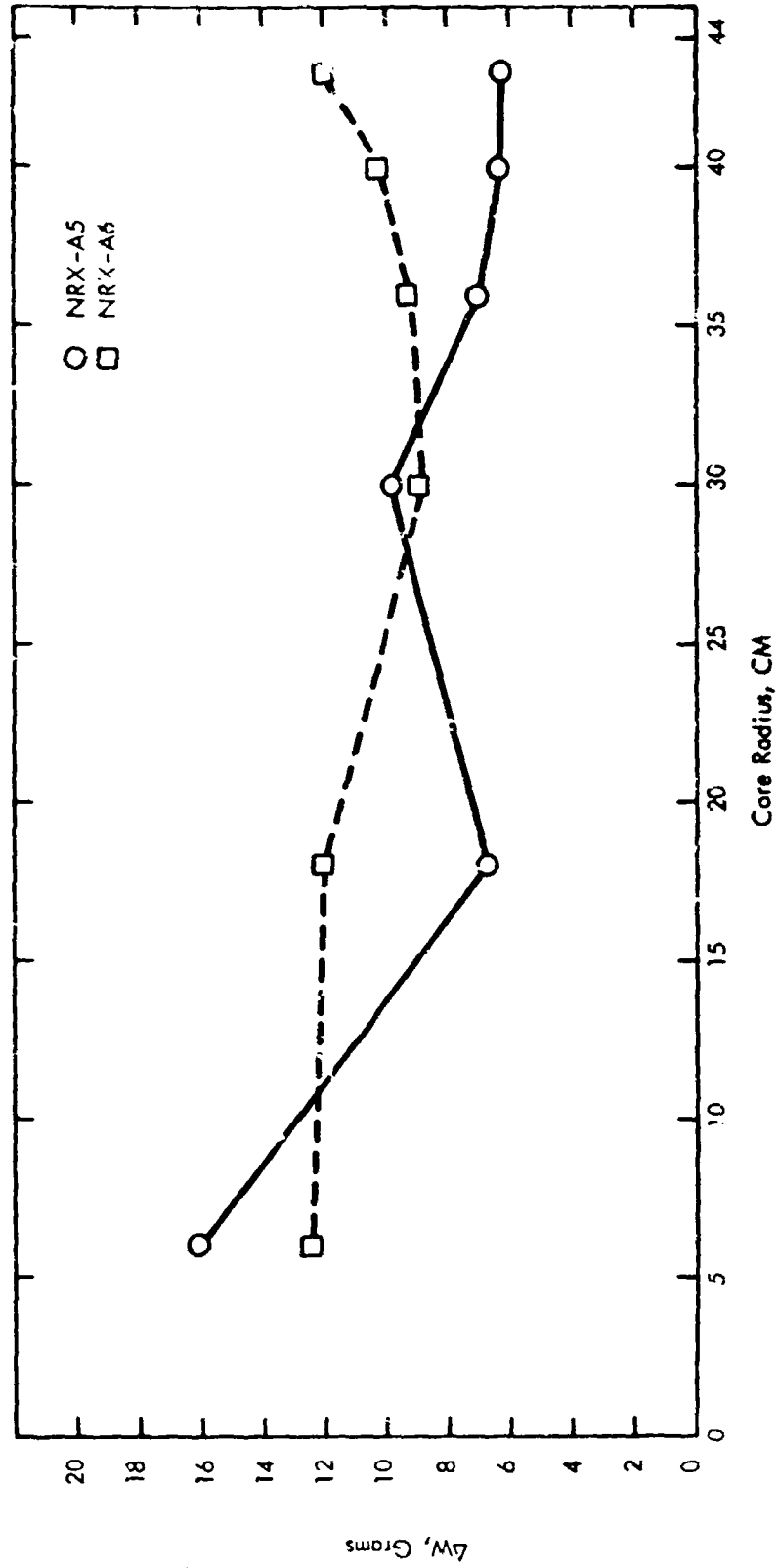


Figure 5-38. (CRD) Radial Variations of Incremental Weight Loss in the Axial Region
30 - 52 Inches for NRX-A5 and NRX-A6 Fuel Elements (CRD)

~~CONFIDENTIAL~~

(CRD) Peripheral Element Performance (U)

(CRD) Notch-type corrosion patterns similar to those observed on NRX-A5 fuel elements (see Reference 41) were again observed on some NRX-A6 peripheral elements (see Figure 5-39). The number of NRX-A6 peripheral elements having notch corrosion, listed in Table 5-10, was much lower than observed in the NRX-A5 experience. The data in this table represents the typical axial range for this phenomenon as lying between 25 inches and the non-fuel tip (51 inches). The individual notches appeared approximately 1 to 1-1/2 inches apart in this range. By combining the data in Table 5-10 with a summary of NRX-A6 peripheral fuel element performance (Table 5-11), it can be demonstrated that higher weight losses and severe notch corrosion or stress (mechanical and/or thermal) were produced in peripheral locations adjacent to thin filler strips. This post-test analysis on the peripheral fuel elements showed that this notching was due to thermal stress at the peripheral corner of the fuel elements. This high thermal stress occurred during startup and was due to the combined effects of the heat flow from the core to the hot buffer filler strips; and partial unfueled elements, and the cooling effect of a high leakage flow between the filler strips at locations where shifting of the element filler strips creates large flow gaps.

(CRD) Deposition and Bonding Effects (U)

(CRD) Surface corrosion effects were mild compared to those in NRX-A4 and NRX-A5. This has been attributed to a more tight, uniform element bundling, improved radial power flattening and superior bore corrosion performance. Inter-element bonding on non-OD-coated fuel elements was associated with the soot and pyrocarbon depositions in the 21 to 27 inch axial region. The difficulties associated with the removal of bonded elements from the core resulted in mechanically-induced breakage of approximately 200 fuel elements. A radial distribution of NRX-A6 fuel element pull-out (Figure 5-40) indicates a greater frequency of occurrence and more severe pullout for this phenomenon in the F and G cluster rows.

(CRD) Experimental Element Performance (U)

(CRD) A matrix-coating performance summary of the experimental elements is presented in Table 5-9. Preliminary comparisons between matrix-additives (25 v/o NbC, 5.0 v/o and Nb Resinate) and bore-coating experiments (S - Standard, L - Low Temperature, and T - Thick Hot End Coatings) can be made. There were 30 NbC matrix-additive and 17 NbC matrix impregnated experimental fuel elements on NRX-A6. With respect to pinholing, surface corrosion and aft-end integrity, the performance of these elements was similar to that of other NRX-A6 elements.

(CRD) In order to eliminate the radial and surface effects on element weight loss, an attempt has been made to estimate a weight loss performance index (f_w)

~~CONFIDENTIAL~~

~~CONFIDENTIAL~~


 Astronuclear
Laboratory



Figure 5-39. (CRD) NRX-A6 Fuel Element "Notch" Corrosion (U)

~~CONFIDENTIAL~~

CONFIDENTIAL

TABLE 5-10
(CRD) NRX-A6 FUEL ELEMENT NOTCH CORROSION SUMMARY (U)

Fuel Element S/N	Core Location	Bore Batch	X Batch	Radius	Fuel Element Flat	Axial Range*	W (grams)	VESL (grams)
11-39360	2J3H	L-255	AA075	43.28	B C D E	25-51 24-51 26-51 49-51	35.3	6.0
11-63004	3J7K	C-357	AA087	43.11	C D	33-51 33-51	10.8	1.0
11-63018	2J9H	F-329	AA068	43.28	D E	32-36 33-38	14.9	1.6
11-63029	2J4H	C-357	AA087	43.49	C D E	26-51 26-51 27-29 50-51	14.2	0.8
11-63124	3J4H	F-332	AA076	43.49	C D E	27-47 27-47 29-3k 37-39	14.5	2.0
11-63133	5J5J	F-332	AA076	43.28	C D	31-37 31-37	10.9	0.8
11-63152	2J5J	F-341	AA091	43.28	C D E	28-52 28-52 31-37	19.8	4.8
11-63154	4J5J	F-341	AA091	43.28	C D	30-51 30-50	20.0	5.2

CONFIDENTIAL

* Notch corrosion appeared approximately 1 to 1-1/2 inches apart in each axial range.

TABLE 5-10 (Continued)

(CRD) NRX-A6 FUEL ELEMENT NOTCH CORROSION SUMMARY (U)

Fuel Element S/N	Core Location	Bore Batch	X Batch	Radius	Fuel Element Flat	Axial Range*	ΔW (grams)	VESL (grams)
11-39361	4J3H	L-255	AA075	43.28	B C D E	27-36 27-39 29-39 34-35	18.7	3.8
11-39335	5J3H	F-329	AA068	43.28	B C D E	30-51 30-51 30-51 40-51	42.6	7.6
11-39327	3J3H	F-329	AA068	43.28	B C D	35-37 30-37 30-33	14.6	1.5
11-39338	6J4H	C-343	AA055	43.49	C D E	30-42 30-50 30-50	16.5	0.8
11-39352	1J3N	M-102	AA056	43.15	C D	25-47 47-51	12.5	0.9
11-39387	1J4H	F-328	AA054	43.49	C D E	30-51 30-47 30-37	23.9	0.7
11-39391	1J5J	F-328	AA054	43.25	C D E	30-51 30-51 30-37	19.2	1.1

* Notch corrosion appeared approximately 1 to 1-1/2 inches apart in each axial range.

CONFIDENTIAL



CONFIDENTIAL

TABLE 5-10 (Continued)
(CRD) NRX-A6 FUEL ELEMENT NOTCH CORROSION SUMMARY (U)

Fuel Element S/N	Core Location	Bore Batch	X Batch	Radius	Fuel Element Flat	Axial Range ^a (U)	AW (grams)	VESL (grams)
11-39399	1J3H	F-329	AA068	43.28	B C D	30-37 30-51 30-32	22.9	0.3
11-39400	6J3H	L-255	AA075	43.28	A F	40-45 40-51	9.6	0.5
11-63022	6J5J	C-357	AA087	43.28	C D	35-50 50-51	9.1	0.5
11-63139	6J9P	C348	AA070	42.76	D E	35-50 35-40	10.6	0.8
11-63148	6J9T	L-275	AA120	42.33	D E F	35-45 35-45 30-35	13.6	0.8
11-63105	3J5J	Status 9, No Visual Data						

CONFIDENTIAL

* Notch corrosion appeared approximately 1 to 1-1/2 inches apart in each axial range.

CONFIDENTIAL



TABLE 5-11
(CRD) PERIPHERAL NRX-A6 FUEL ELEMENT PERFORMANCE SUMMARY (U)

C/P	Status			No. Weighed	Δ WG	Range Δ WG	BS*	Range BS
	0	1	2-5					
J3H	3	3	0	0	24.7	9.6-42.6	33.3	31-35
J3N	6	0	0	0	15.9	12.5-20.8	---	---
J3T	6	0	0	0	15.8	14.0-19.2	---	---
J3U	6	0	0	0	11.9	9.9-14.7	---	---
J4M	6	0	0	0	12.5	10.7-13.9	---	---
J4H (1)	4	2	0	0	16.7	14.2-23.9	34	32-36
J4K	6	0	0	0	10.5	9.3-11.9	---	---
J5H	6	0	0	0	12.9	10.6-19.1	---	---
J5J	4	1	0	1 (2)	15.8	9.1-20.0	29	23-32
J6H	5	0	0	1 (2)	9.3	8.0-10.1	33.5	33-34
J6K	6	0	0	0	9.6	8.3-11.0	---	---
J7H	5	0	0	1	9.3	8.0-10.5	36.5	36-37
J7K	6	0	0	0	9.0	8.3-10.8	---	---
J8K	5	1	0	0 (3)	11.2	9.7-15.1	38	38
J8F	2	1	0	3 (4)	12.9	11.5-13.5	39	35-47
J9H	5	0	0	1	11.4	9.6-14.9	44	44
J9P	6	0	0	0	12.5	10.6-15.8	---	---
J9T	6	0	0	0	11.4	9.0-13.6	---	---
J9U	5	1	0	0	11.2	9.7-15.2	41	41
All	98	9 (5)	0	7 (5)	12.9	8.0-42.6	36 (5)	23-4/ (5)

- (1) Code 12's, Rest Code 11's
 (2) 5J6H Measured Showing ΔWG = 17.5 g
 (3) Two Measured Showing ΔWG = 21.8 g (6J8F) and 28.7 g (2J8F)
 (4) 1J9H Measured Showing ΔWG = 27.2 g
 (5) 22 Breaks in 16 Elements

*BS = Break Station

~~CONFIDENTIAL~~

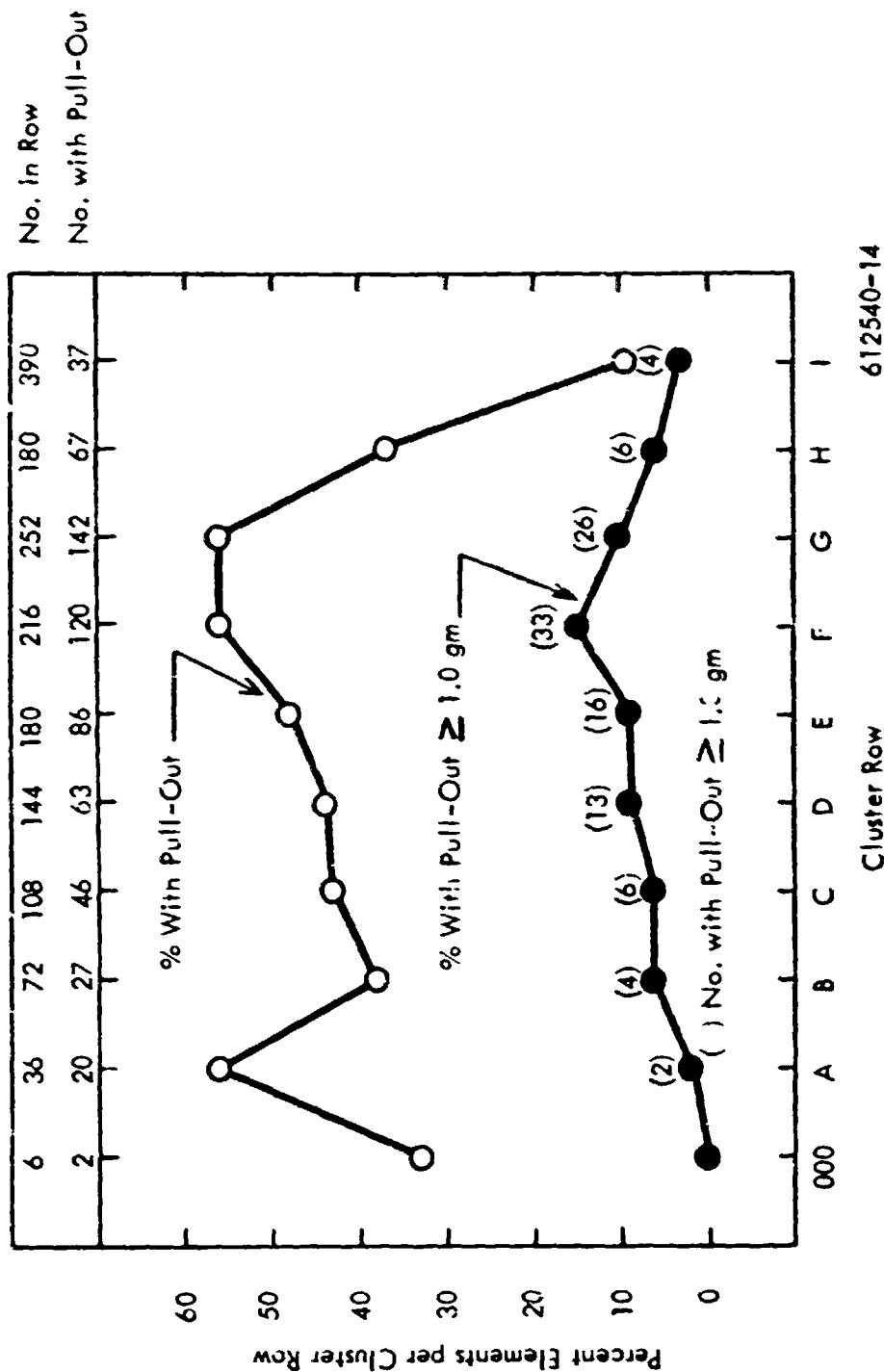


Figure 5-40. (CRD) Radial Distribution of NRX-A6 Fuel Element Pull-Out (U)

~~CONFIDENTIAL~~

CONFIDENTIAL

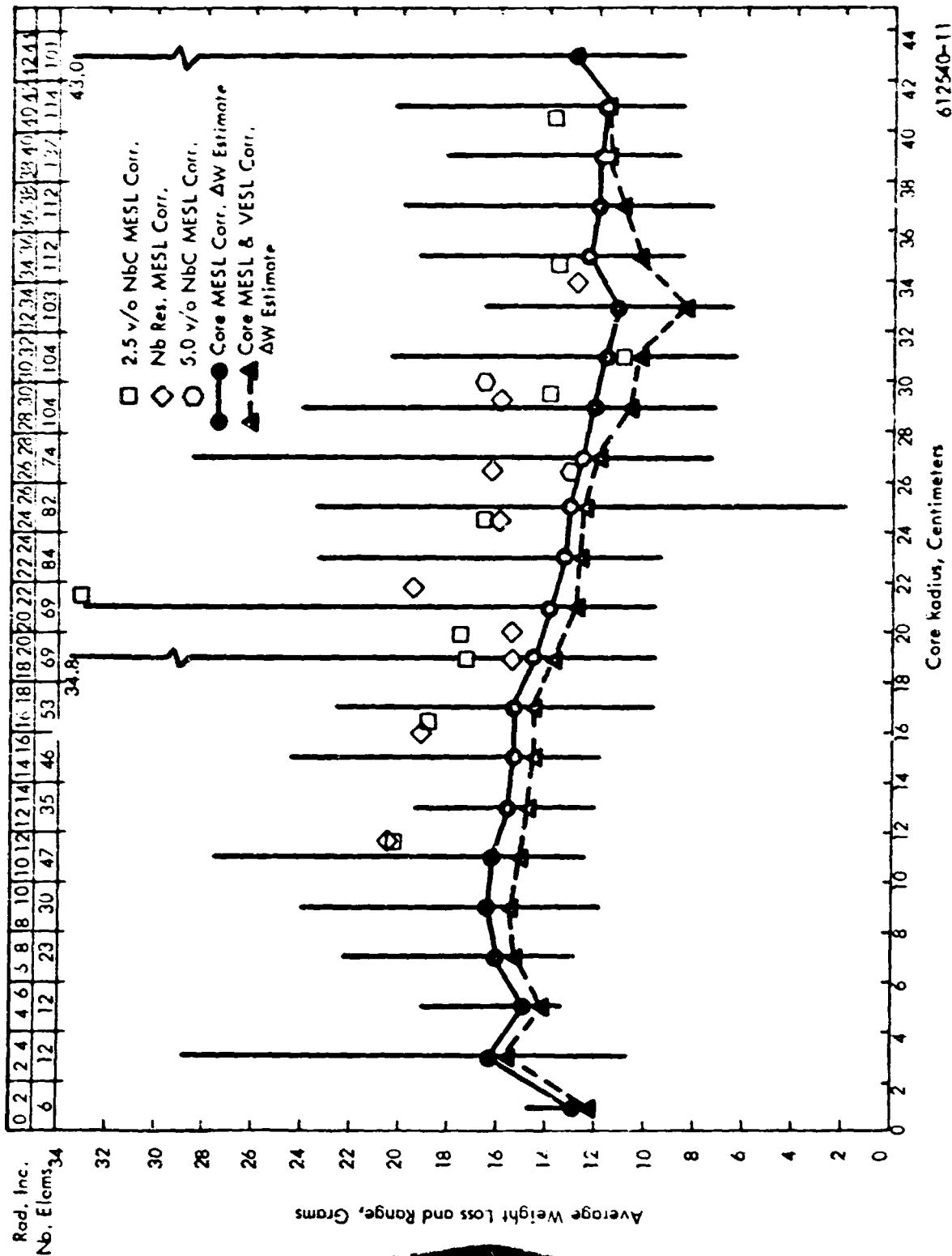


Figure 5-41. (CRD) Radial Distribution of Matrix-Additive ^{235}U

CONFIDENTIAL

~~CONFIDENTIAL~~

for the experimental elements.* The f_w for each experimental element was estimated by dividing its bore weight loss by the core average bore weight loss at that radius. A radial distribution of the NRX-A6 average bore weight loss estimate (gross weight loss minus VESL and MESL estimates) is presented in Figure 5-41. The MESL corrected average weight losses for the matrix-additive elements are included for comparison.

(CRD) Figure 5-42 and Table 5-12 summarize the f_w estimate matrix additive elements. The weight loss data indicate that the experimental element performance was somewhat poorer than that of their radial neighbors or of elements with similar coating histories.

(CRD) Flexure Strength (U)

(CRD) The axial variation in post-reactor flexure strength, averaged for the 79 elements tested, is plotted in Figure 5-43. The average and range of flexure strength for Quality Control testing of NRX-A6 production elements, representing all fuel loadings and various manufacturing histories, has been superimposed on this figure. Also included in Figure 5-43 are the core average, axial variations in flexure strength obtained from the post-operational testing of 56 fuel elements from NRX-A5.**

(CRD) Flexure strength changes from the QC average in NRX-A6 were characterized by an increase in the cold end region, practically no change in the mid-band region and a decrease in the hot end region. With the exception of the cold end increase, these flexure strengths correspond to the axial variations in fuel element incremental weight loss. There is a dramatic difference between the NRX-A6 and NRX-A5 flexure data in the 20 to 25 inch axial region where the higher corrosion damage and correspondingly greater weakening of the NRX-A5 elements occurred.

(CRD) Conclusions on Performance

(CRD) With the exception of some peripheral positions, the time rate of corrosion as seen in Table 5-13 for the NRX-A6 elements was approximately 75 to 80 percent lower than that observed for the elements in the NRX-A4 and NRX-A5 reactors.

*

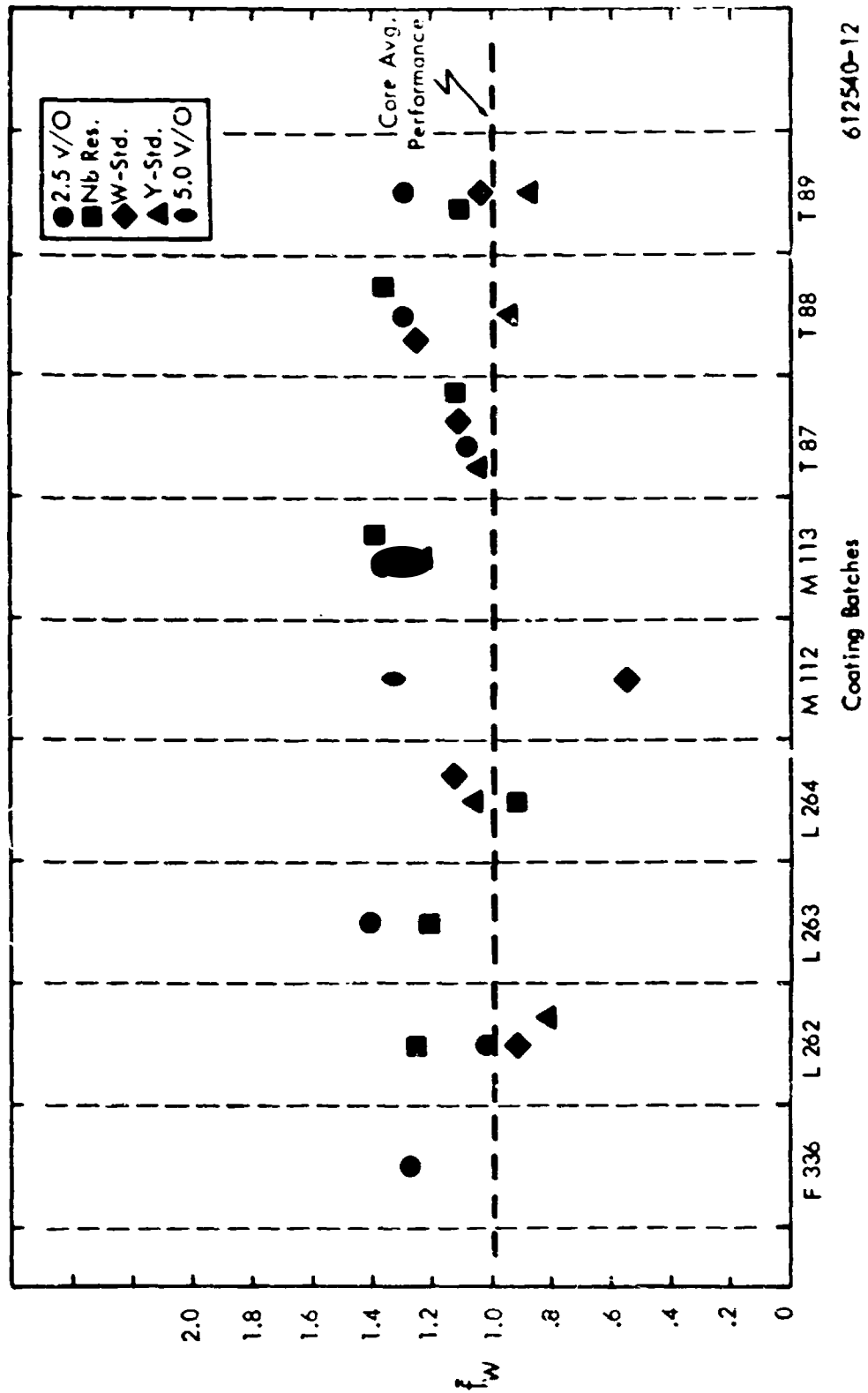
Normally, this is done after core average bore weight loss curves are calculated on a computer by a least-squares method.

**

The Quality Control average flexure strengths for NRX-A5 production elements was nominally about 13 percent lower than that of NRX-A6 elements; 280 psi for NRX-A6 production elements and 244 psi for NRX-A5 production elements.

~~CONFIDENTIAL~~

~~CONFIDENTIAL~~



612540-12

Figure 5-42. (CRD) Weight Loss Index of Performance Estimate for NRX-A6 Experimental Fuel Elements (U)

~~CONFIDENTIAL~~

CONFIDENTIAL

TABLE 5-12

(CRD) OVERALL BORE WEIGHT LOSS PERFORMANCE OF NRX-A6 EXPERIMENTAL
ELEMENTS BASED ON PRELIMINARY ESTIMATES OF PERFORMANCE INDEX (U)

Type	f_w Estimate	f_w Range	% Above Core Average Performance
Core	1.000	-	-
2.5 v/o NbC	1.256	0.919-1.569	25.6
5.0 v/o NbC	1.328	0.756-2.134	32.8
Nb Resinate	1.219	0.844-1.865	21.9

CONFIDENTIAL

~~CONFIDENTIAL~~

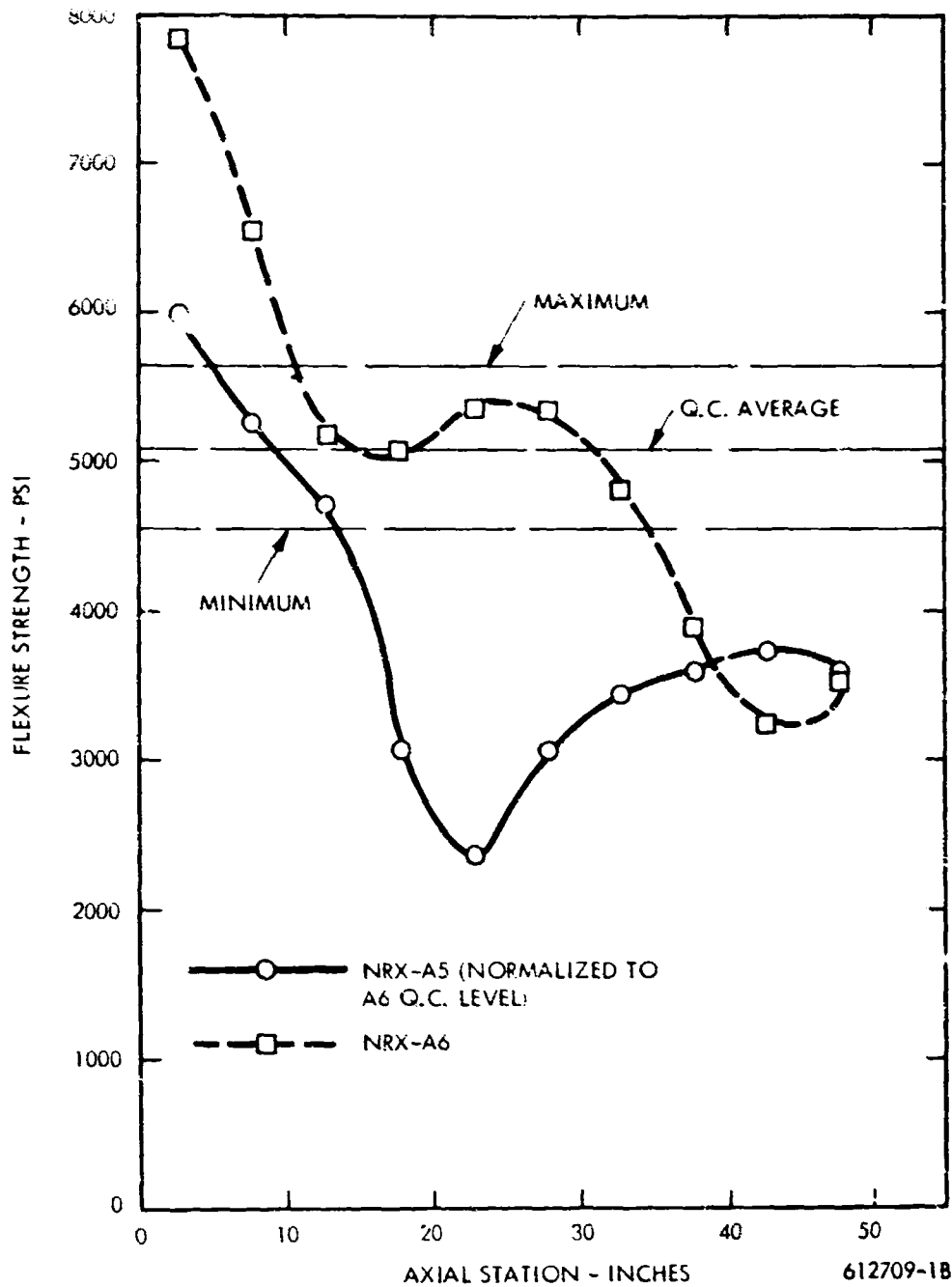


Figure 5-43. (CRD) Core Average Axial Variation in Flexure Strength for 79 NRX-A6 and 63 NRX-A5 Fuel Elements (U)

~~CONFIDENTIAL~~

~~CONFIDENTIAL~~

TABLE 5-13

(CRD) NRX/EST, NRX-A5 and NRX-A6 REACTOR COMPARISONS (U)

	NRX/EST	NRX-A5	NRX-A6
Time at Full Power, minutes	30.3	30.01	60.4
Chamber Temperature (T_C) $\geq 2500^\circ\text{R}$, minutes	51.9	33.0	64.0
No. Cycles, $T_C \geq 2500^\circ\text{R}$	6	2	1
Average ΔW , grams	32.4	27.0	13.10
Avg. No. Pinholes/Pinholed Element	30.7	12.7	6.5
Percent Elements with Channel Exposure	36.5	56.3	28.1
Time Rate of Corrosion (full power), grams/minute	1.07	0.90	0.22

~~CONFIDENTIAL~~

~~CONFIDENTIAL~~



TABLE 5-14

(CRD) COMPARISON OF NRX-A5 and NRX-A6 ELEMENTS BY MANUFACTURER (II)

Condition	NRX-A5 WAFF		NRX-A6 WWW	
	\overline{EW} (gm)	No.	\overline{EW} (gm)	No.
Intact	21.0	253	13.0	241
One Break	40.1	409	14.9	27
More than One Break	34.2	150	15.4	6
Combined	36.6	812	13.2	274

Condition	NRX-A5 Y-12		NRX-A6 YYY	
	\overline{EW} (gm)	No.	\overline{EW} (gm)	No.
Intact	14.4	673	13.1	358
One Break	29.3	56	13.5	43
More than One Break	37.8	8	15.2	7
Combined	15.8	737	13.2	418

~~CONFIDENTIAL~~

~~CONFIDENTIAL~~

(CRD) Pinhole and coolant channel exposure occurrences in NRX-A6 elements were noticeably less frequent than had been observed in NRX-A4 and NRX-A5, as demonstrated in Table 5-13.

(CRD) In general, the corrosion performance and integrity of the aft coated ends of NRX-A6 fuel elements was excellent. The Bearing Area Remaining (BAR) and Coated Area Remaining (CAR) in the 50-52 inch region averaged approximately 95 percent. Corrosion local to the unfueled tip joint region was observed on approximately 30 elements. Preliminary examinations have not yet established whether this corrosion can be attributed to a joint leakage problem or to external surface corrosion effects on these elements.

(CRD) Initial comparisons of the weight losses of experimental elements (NbC additives and impregnated) with radial neighbors showed higher gross weight losses for the experimentals. Studies in progress are expected to show if this difference can be attributed to overall poorer performance or are due to thermal, orificing, or coating batch effects.

(CRD) The higher weight losses observed for certain peripheral positions has been attributed to local thermal and/or mechanical stress problems.

(CRD) CHEMICAL AND RADIOCHEMICAL MEASUREMENT RESULTS (U)

(U) As part of the post-operative evaluation of the NRX-A6 reactor, chemical and radiochemical measurements were performed to determine the following:

(U) 1) Determination of corrosion and migration losses of fission products and fuel or coating materials as measured by "Elephant Gun" samples, fall-out particulate samples, and "FROG" samples.

(U) 2) Determination of radial and axial fission distributions; total number of fissions generated by gross ionization readings, gamma spectrum measurements, and radiochemical fission product analyses performed on a number of fuel elements.

(U) 3) Identification by gross radiation measurements and two-point gamma measurements on individual fuel elements of any regions of asymmetry or of anomalous behavior in the reactor core (e.g., conditions of unusual temperature, incorrect uranium loading, or loss of fuel by hydrogen corrosion).

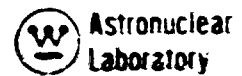
(CRD) 4) Determination of molybdenum, niobium, and uranium concentration as a function of axial position in an element.

(U) 5) Comparison of two-point gamma and axial gamma scan data for detecting high migration losses (overheated elements).

(U) A summary of the results of these measurements are given below; a more detailed discussion is provided in Reference 45.

~~CONFIDENTIAL~~

~~CONFIDENTIAL~~



(CRD) Corrosion and Migration Losses (U)

(U) The NRX-A6 reactor test series included the initial testing of two new devices in an attempt to determine the type and extent of core materials released during the test run and upon cooldown. The first device, which is called the "Elephant Gun", collected gas and plateout samples during the run, and indicated that there was very little corrosion during the first 20 minutes of operation, and the release of migrating fission products to the gas phase was normal and predictable. Samples were not obtained over the complete run period due to a malfunction of the sampling apparatus.

(CRD) The second device, which was called "FROG", was a bank of filters to filter reactor outlet gas. These filters were placed over the reactor nozzle during cooldown operations to reduce contamination and subsequently cleanup of the test cell pad. The maximum activity observed on any of these filters was 8 R/hour, with nominal filters measuring less than 2 R/hour. The particles trapped by the filters varied between 1 and 300 microns in size, with the majority of particles in the range of 15 to 100 microns. A chemical analysis indicated the material was predominantly Nb (58 percent), the remainder being graphite, uranium (5 percent) and molybdenum (.2 percent). Use of the FROG for cooldown was extremely beneficial in reducing contamination to the test cell area, and permitting cleanup operations to begin almost immediately after withdrawal of the test article.

(CRD) Radial and Axial Fission Distribution (Comparison of Two-Point Gamma and Axial Gamma Scan (U)

(CRD) Following the NRX-A6 power test, radial fission distributions were measured by the gross ionization technique, used in all previous reactor tests, and by a two-point gamma system employed for the first time for the NRX-A6. Results of the two-point gamma system were in excellent agreement with those from the gross ionization technique, from the core center to about 41 cm; however, the last few centimeters of the core indicated higher (by about 5 percent) Zr^{95} values for the two-point gamma system than observed by the gross ionization technique. A comparison of gross gamma and two-point gamma radial distribution is shown in Figure 5-44 for a normal sector of the core.

(CRD) A maximum fission density occurred in the region from 18-26 inches from the gas inlet end of the fuel elements. The enhancement in the fission density at the inlet end for centrally located elements relative to peripheral elements was as expected. Gross scalar data and Ba/Ru ratios showed hot end fission product migration trends on elements which the two-point gamma measurements had indicated were overheated.

(CRD) Radial fission distributions measured by the gross ionization technique were in good agreement with those obtained by a two-point gamma method. Hot end

~~CONFIDENTIAL~~

CONFIDENTIAL

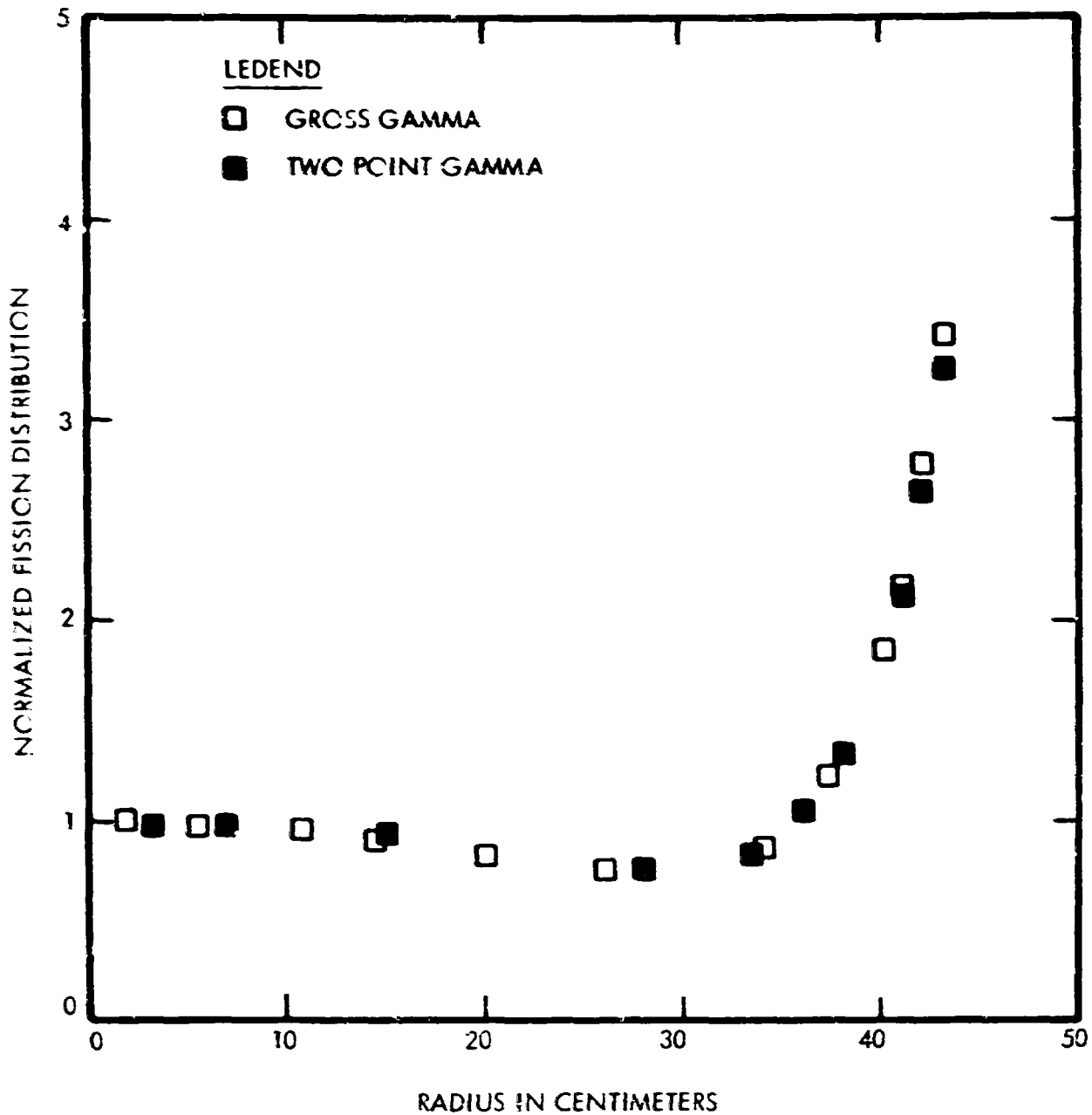


Figure 5-44. (CRD) Comparison of Gross Gamma and Two Point Gamma Radial Fission Distribution (U)

CONFIDENTIAL

~~CONFIDENTIAL~~



(Station 44) two-point data indicated the presence of a few overheated elements in the core. On several the Ba^{140} losses were sufficient to cause variation in gross ion readings. None of the overheated elements were located in any one definite core region but were scattered throughout the core with the majority located in the A, B, and C cluster areas. Discounting such anomalous elements, the deviations for equivalent core locations were as experienced on NRX/EST and NRX-A5, i.e., $\pm 1-2$ percent from G-38 on with a maximum of ± 3 percent at the core edge.

(CRD) Axial Distribution of Uranium, Niobium, and Molybdenum (CRD)

(CRD) Uranium and niobium determinations, performed on 48 one-inch pieces cut from eight elements, indicated no preferential losses of either. No mid-band corrosion areas were found.

(CRD) Molybdenum determinations, on 210 one-inch pieces cut from 35 elements, indicated that the molybdenum remaining on the elements was dependent upon the manufacturing history. Batch variations were somewhat complex and are reported in Reference 39.

(CRD) Energy Generated (U)

(CRD) Gamma spectra were measured along the length of several NRX-A6 elements. Pieces of the elements were then sectioned and analyzed for Mo, Rb and U. Fission product analyses were performed from an additional group of elements to calibrate gross ionization and axial gamma data in terms of absolute fissions. The total fissions generated were then determined.

(CRD) Based upon radiochemical analysis, a total of $1.57 \pm 0.07 \times 10^{23}$ fissions were produced during all runs of the NRX-A6 reactor. In terms of energy release, using the conversion factor, 3.24×10^{10} fissions per second equals 1 Watt; this gave a power integral of 4.85×10^{12} Watt-seconds, which compared to a corrected linear power integral of 4.49×10^{12} Watt-seconds (see Figure 4-3).

(CRD) ENVIRONMENTAL RADIATION (U)

(CRD) During the testing of the NRX-A6 reactor, a dosimetry program was carried out which resulted in the measurement of gamma ray dose rates, fast neutron fluxes ($E > 2.9$ MeV), and thermal neutron fluxes ($E < 0.4$ eV) at 146 locations external to the reactor. Since the NRX-A6 was the first of the NRX reactors to be tested at Test Cell C, the philosophy of the dosimetry program was to obtain an extensive experimental mapping of the radiation environment of this "new" configuration which includes the 360 degree facility shield external to the reactor.

(CRD) Analytical predictions of the gamma ray dose rate based on the point kernel method and fast neutron flux ($E > 2.9$ MeV) based on the FASTER Monte Carlo method at most dosimeter locations are compared with the experimental test data. At most dosimeter locations, predictions and measurements agree to within the uncertainty factors quoted for the predicted data.

~~CONFIDENTIAL~~

~~CONFIDENTIAL~~

(CRD) The passive dosimetry program consisted of the following:

1) Nickel foils and sulfur pellets for fast neutron flux data ($E > 2.9$ MeV), and fission foils including Pu^{239} , Np^{237} and U^{238} foils for neutron energies greater than 10 keV, 0.6 MeV, and 1.5 MeV, respectively.

2) Bare and cadmium covered gold, copper and cobalt foils for thermal neutron flux data ($E < 0.4$ eV).

3) Thermoluminescent dosimeters (TLD's) and cobalt glass plates for gamma ray data.

(CRD) In addition to the passive dosimetry, the NRX-A6 dosimetry program included important calorimetric measurements of heating rates at several locations external to the reactor. A direct readout gamma ray ion chamber located on the test car body roof surface provided excellent correlation of gamma ray dose rate with hydrogen flow in the reactor, and also a correlation of gamma radiation levels obtained during low power and high power tests at this location. This information is shown in Figure 5-45 where the gamma dose rate from the direct readout ion chamber is plotted as a function of Hydrogen Coolant Flow. A significant difference, a factor of approximately 2, in the gamma dose rate is shown between the cold flow test data and the full flow test for this location.

(CRD) A more detailed discussion of environmental radiation may be found in References 12 and 22.

(U) PNEUMATIC ACTUATOR SIDE-BY-SIDE EXPERIMENT

(U) The side-by-side actuator test was performed to obtain data on the effects of a radiation environment on the components and on the operation of a pneumatic control drum actuator similar in design to actuators to be used in the NERVA engine.

(U) One objective of the test was to determine component, subassembly and/or assembly degradation due to the integrated neutron flux and gamma radiation. A second objective was to determine the effectiveness of the coolant gas flow and its ability to remove radiation induced heating.

(U) Description of Test Setup

(U) A block diagram of the test setup is shown in Figure 5-46. The drive supply gas was regulated to a constant pressure of 215 psia and maintained at this constant pressure throughout the test. Coolant was supplied to the actuator through a regulating valve that was controllable from the control room. Both the helium drive and coolant gas passed through an LN_2 heat exchanger. The temperature at the exit of this heat exchanger was on the order of 140°R . The coolant gas pressure and the electrical input and output signals to the actuator originated in the

~~CONFIDENTIAL~~

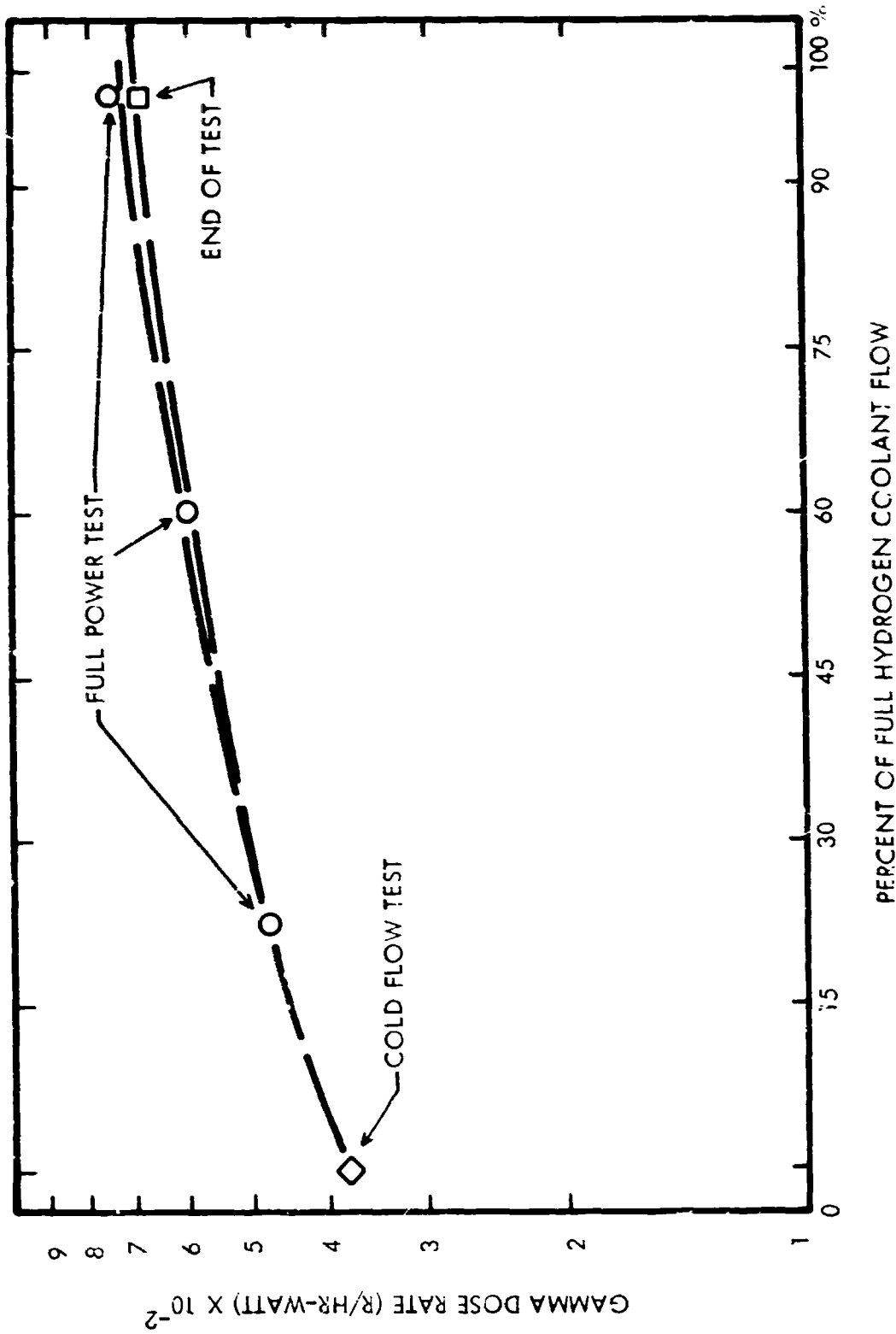


Figure 5-45. (U) Measured Gamma Dose Rate on the Privy Roof as a Function of Hydrogen Coolant Flow for the NRX-A6 Reactor (U)

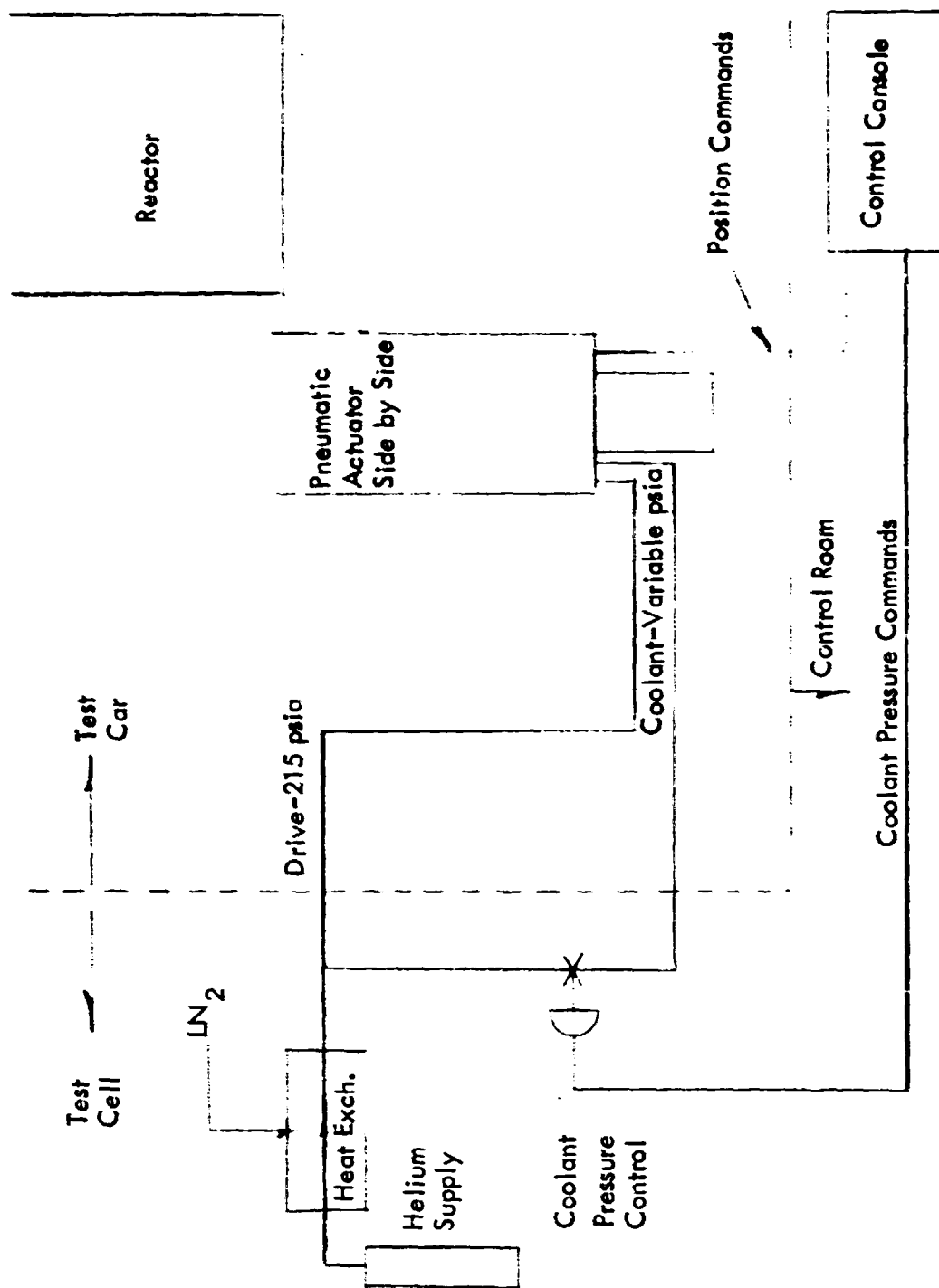


Figure 5-46. (U) Block Diagram of NRX-A6 Side-by-Side Actuator Test Setup

control room and were varied during the test by the side-by-side Test Operator. The actuator experiment was mounted on the test car inside the 360 degree shield next to the reactor at the $\theta = 180$ degree position. The position of the pneumatic actuator side-by-side experiment with respect to the NRX-A6 reactor is shown in Figure 5-47. Figure 5-48 is a drawing of the actuator, pedestal and a simulated drum load enclosed in its housing.

(U) This drawing shows external details of the actuator, pedestal and simulated drum load as well as showing instrumentation impulse lines, instruments and thermocouples. A photograph of the instrumented actuator system is shown in Figure 5-49 prior to the installation of the enclosure. In this photograph, the actuator, pedestal, electrical control wires and many of the instrumentation cables and impulse lines are visible. The Marman clamp, one (1) pressure transducer and several accelerometers are also visible. This photograph is oriented approximately the same as the drawing of Figure 5-48 and can be used for comparative purposes. The completely assembled pneumatic actuator side-by-side test fixture is shown in Figure 5-50. The clamp that mounts the side-by-side experiment to the test car adapter can be seen in this photograph. Also, the electrical leads, thermocouples and plumbing lines are shown. In Figure 5-51 the test fixture is shown mounted on the test car. The dosimeter packets SSA-3 and SSA-5 can be seen in the photograph while dosimeter packets SSA-2 and SSA-4 are hidden since they are mounted diametrically opposite to SSA-3 and SSA-5. SSA-1 cannot be seen in the photograph because it was located on the top of the test experiment near the lifting handle.

(U) The actuator used for this test was an AG-20 type actuator. This actuator was upgraded with XE-1 parts that were considered to be of a sensitive nature and to make the actuator as nearly like an XE-1 as possible without actually testing an XE-1. The XE-1 parts installed were:

- 1) Servo Valve
- 2) Potentiometer
- 3) Piston Rings
- 4) Solenoid Shutoff Valve

(U) The Shutoff Valve was of the new design that was retrofitted into all of the XE-1 actuators. The actuator was also lubricated using molybdenum diselenide as is used in the XE-1 units. One of the major difficulties experienced with the preparation of this test was in adequately instrumenting the actuator so that the test would provide useful information. Installing thermocouples for this purpose proved to be a difficult task. Pressure transducers and impulse lines were installed to measure and provide signals for recording the following pressures:

- 1) Coolant Pressure
- 2) Drive Pressure
- 3) Cylinder No. 1 Pressure
- 4) Cylinder No. 2 Pressure
- 5) Exhaust Pressure

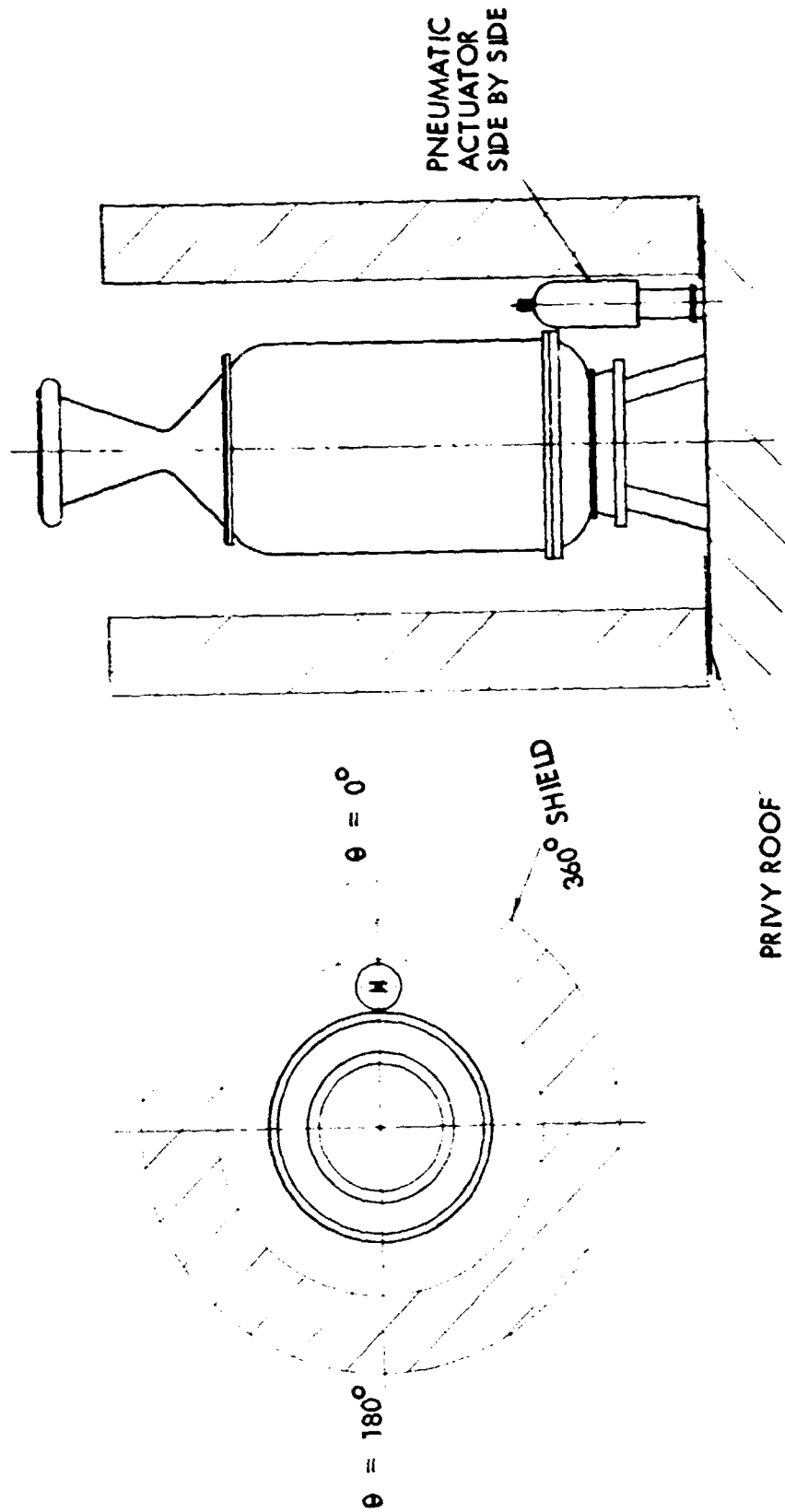


Figure 5-47. (U) NRX-A6 Side-by-Side Actuator Test Position Diagram

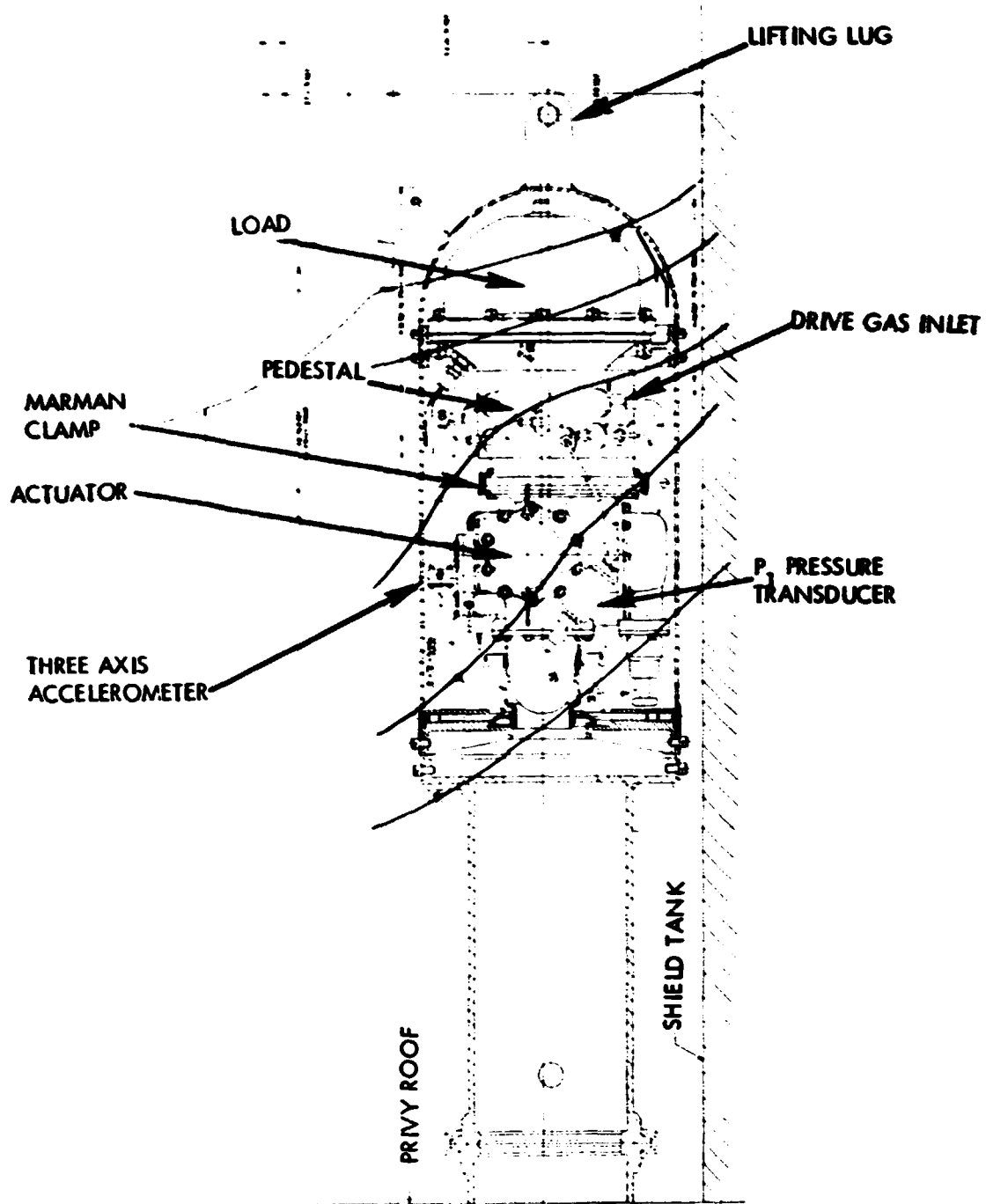


Figure 5-48. (U) Actuator, Pedestal and Simulated Drum Load

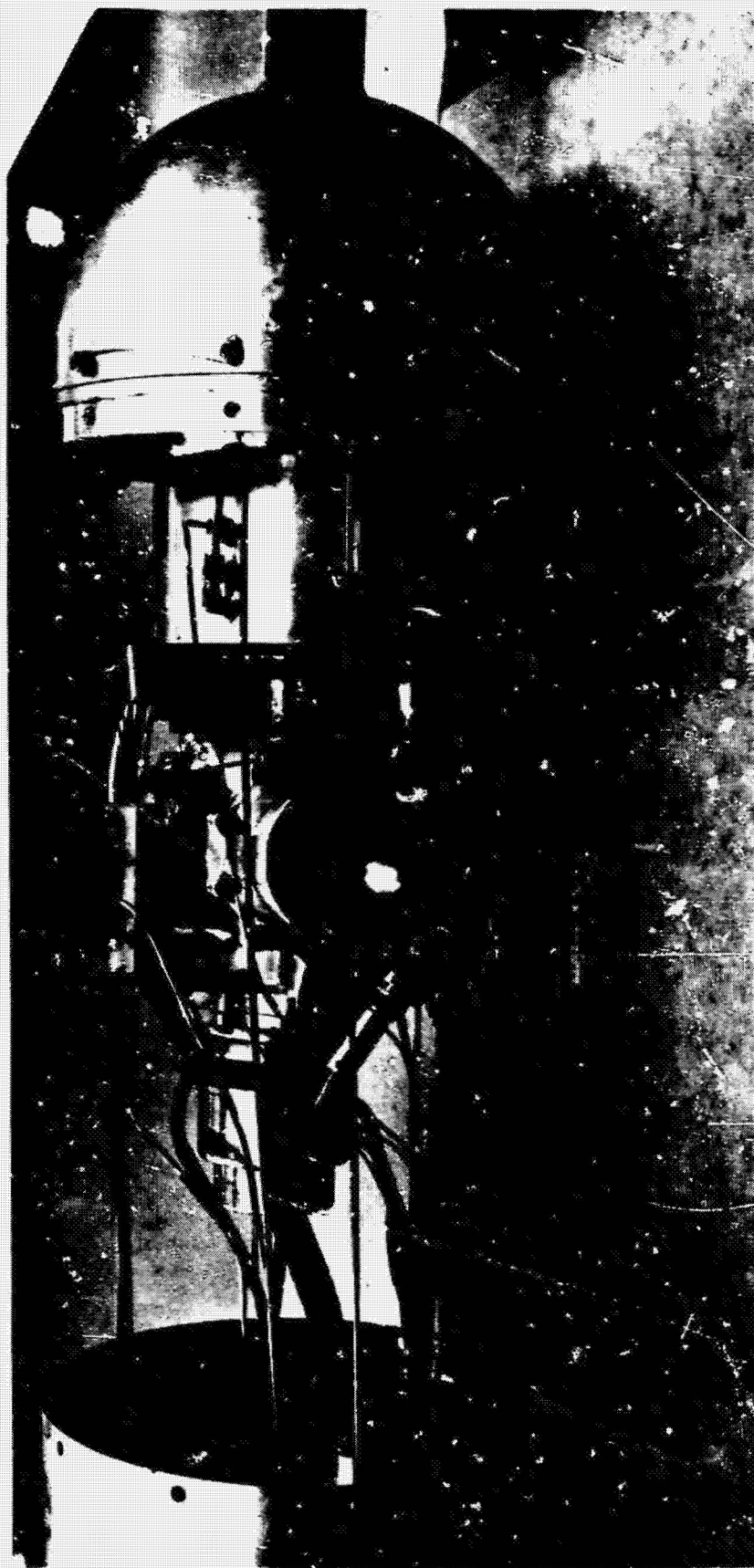


Figure 5-49. (U) NRX-A6 Side-by-Side Actuator Test Assembly

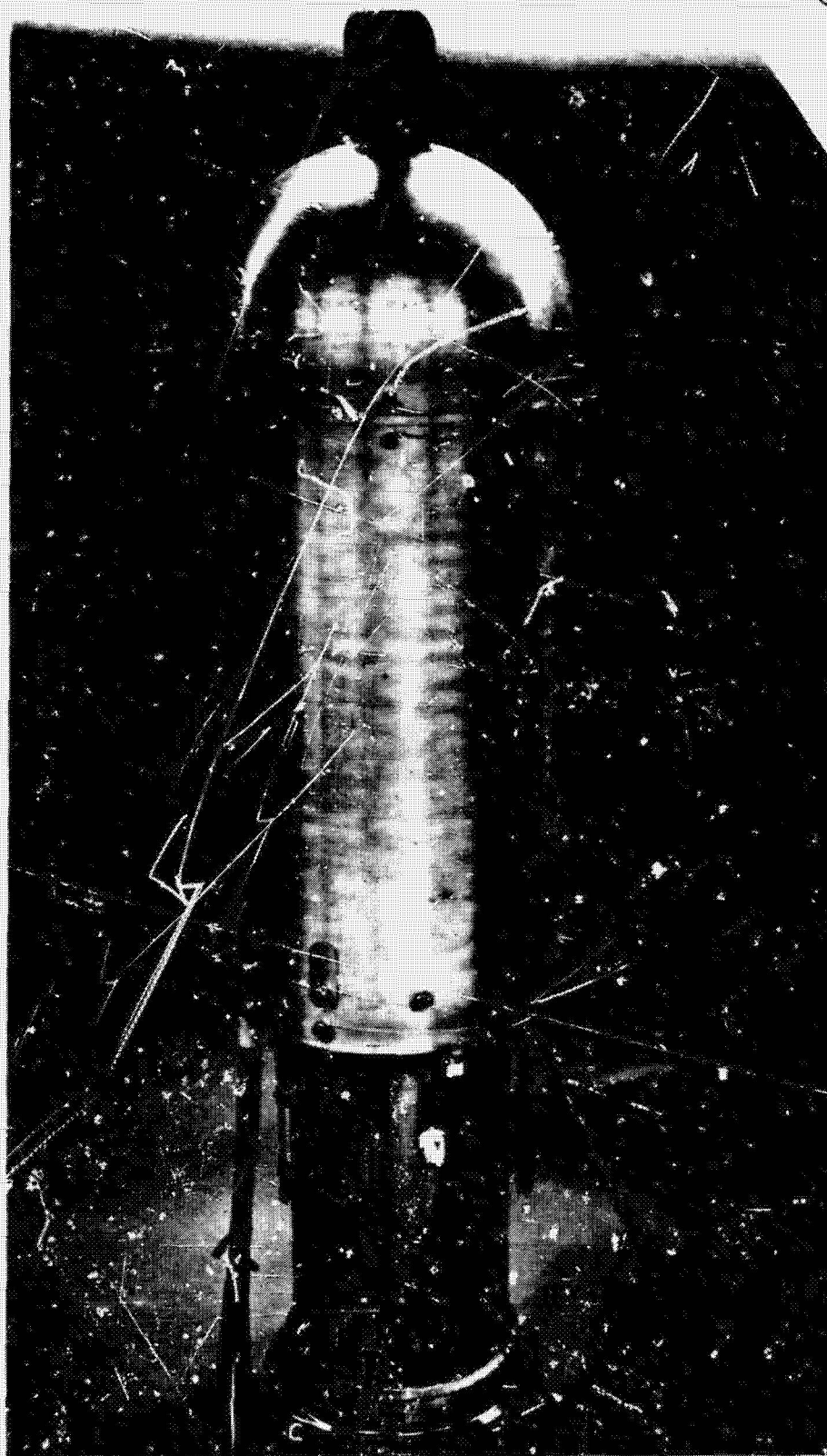


Figure 5-50. (U) Completely Assembled NRX-A6 Side-by-Side Actuator Test Assembly

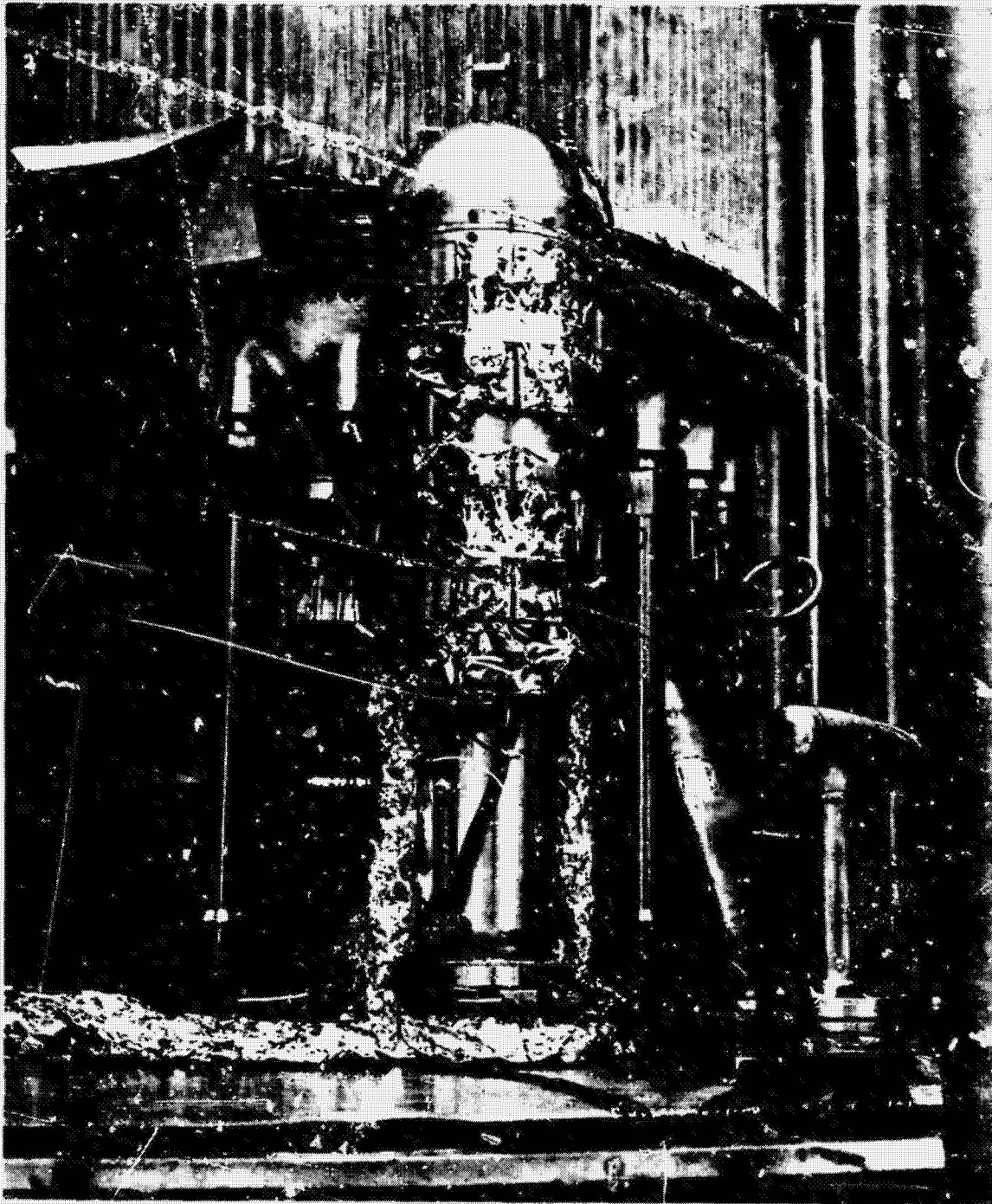


Figure 5-51. (U) NRX-A6 Side-by-Side Actuator Test
Assembly Mounted on Test Car

Thermocouples were installed to give temperatures of critical components as well as give temperature distribution information across the actuator. Thermocouples were installed to measure the following temperatures:

- 1) Coolant Temperature
- 2) Drive Temperature
- 3) Potentiometer Temperature
- 4) Exhaust Temperature
- 5) Torquemotor Temperature
- 6) Cylinder No. 1 and No. 2 Temperature
- 7) Lock Housing Temperature
- 8) Marman Clamp Temperature

(U) In some cases, more than one thermocouple was installed to measure temperatures at different points on a component. For example, four (4) thermocouples were installed at different theta locations to measure the Marman clamp temperature. Also, temperature at various locations within the load were recorded to assure safe operation. In addition to pressure and temperature measurements, three (3) accelerometers were used to record levels of shock and vibration during testing. Dosimeter packets were mounted on the final assembly. These dosimeters, SSA-1 to SSA-5, were used to measure:

- 1) Slow neutron integrated flux ($E < 0.4$ eV)
- 2) Fast neutron integrated flux ($E > 2.9$ MeV)
- 3) Gamma dose

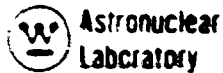
In addition to pressure, temperature, acceleration and radiation, the actuator performance parameters that were measured and recorded were:

- 1) Position command signal
- 2) Actuator position signal
- 3) Torquemotor current

(U) Description of the Test

(U) Prior to operation of the reactor, a closed loop frequency response measurement was performed. A 4 degree peak-to-peak input command was given to the actuator at various frequencies and the feedback position was compared to this input. The frequency response was repeated while the reactor was at full power and again after the reactor was shutdown. In addition to the frequency response, the following test sequence was initiated approximately 15 minutes prior to reactor startup:

- | | |
|----------|---|
| 3.5 min. | Sinusoidal input of 4 degrees p-p at 3 Hz while actuator was positioned at 90 degrees |
| 0.5 min. | Scram, lock and reset |



5.0 min. Sinusoidal input of 40 degrees p-p at 0.5 Hz while actuator was positioned at 90 degrees

0.5 min Scram, lock and reset

9.0 min. Ramp input at 3 degrees/sec; 20 degrees to 160 degrees

0.5 min. Scram, lock and reset

5.0 min. Step between 81 degrees and 99 degrees at 0.1 Hz

0.5 min. Scram, lock and reset

5.0 min. Dwell at static position of 90 degrees

0.5 min. Scram, lock and reset

(U) This test sequence was continued and repeated during reactor testing until approximately 15 minutes after reactor shutdown.

(U) Test Results

(U) The plot in Figure 5-52 shows the three (3) closed loop frequency responses taken before, during and after the test. Very little change in performance occurred between the pre-run test and the full power test. The test performed after the reactor run exhibited an increased bandwidth which is indicative of a reduction in friction of the piston rings.

(U) Although the data was adequate to provide accurate attenuation information, a malfunctioning speed control on the Sanborn recorders made it impossible to separate the adjacent cycles sufficiently to obtain phase shift information. Evaluation of the performance data shows that the actuator can be safely used to drive the control drums on the XE reactors and that the radiation levels experienced were at about the levels predicted for the R and E development reactors.

(U) A summary plot of actuator temperatures and coolant pressure during the reactor full power run are shown in Figure 5-53. In general, the coolant pressure was reduced in controlled increments during reactor full power operation to obtain internal temperature distribution as a function of the cooling pressure. One significant difference between this test and XE and R type tests (where the actuators will be mounted on the pressure vessel or external shield) is the coolant temperature as it enters the actuators. Coolant temperatures on XE and R tests are expected to be very near dome temperature or about 212°F at full power. The actuator side-by-side coolant temperature was on the order of 400 to 450°F. This warmup of coolant in the side-by-side test is due to the relatively long run between the LN₂ heat exchanger and the inlet to the actuator. The closely coupled

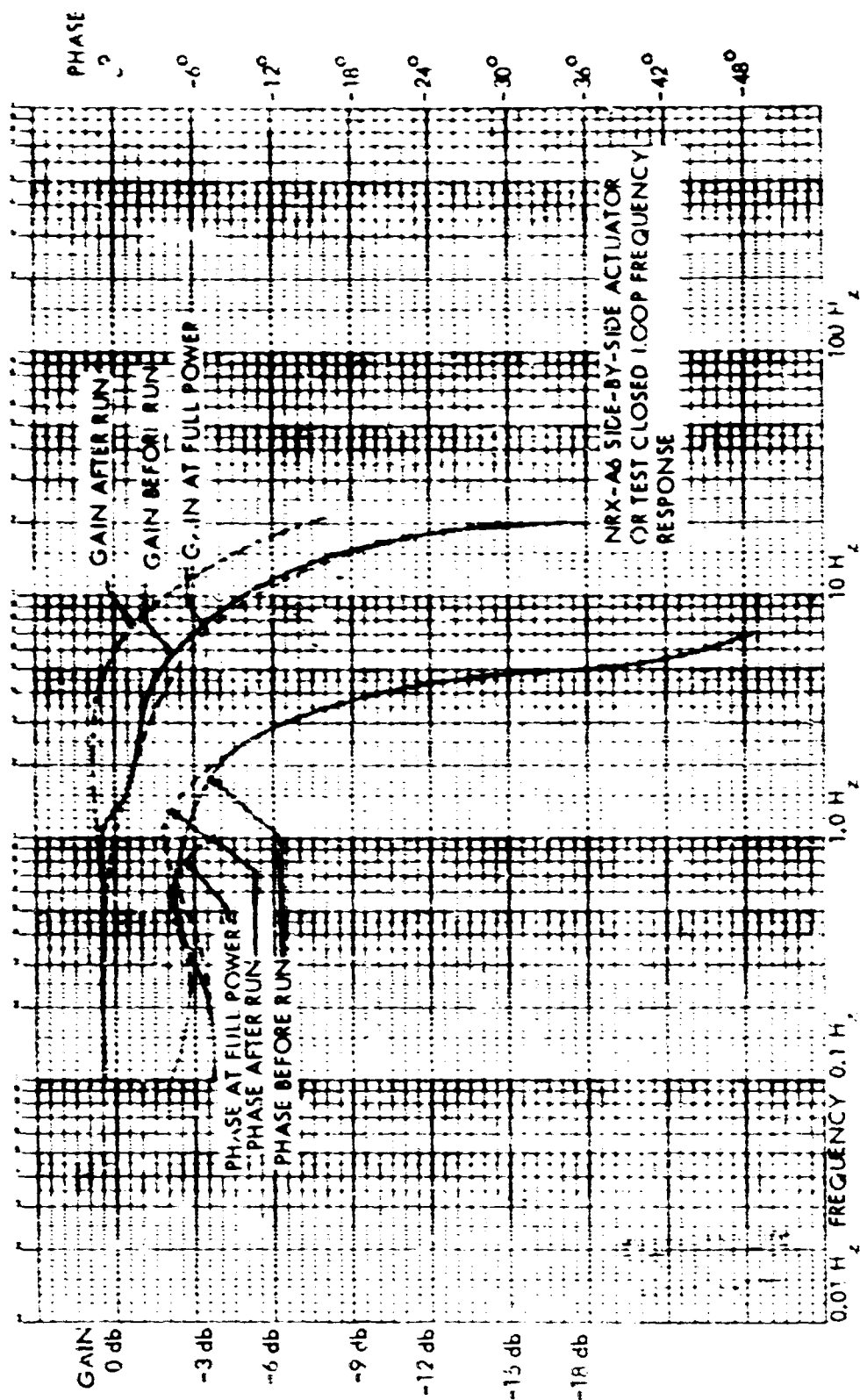


Figure 5-52. (U) Side-By-Side Actuator Test Closed Loop Frequency Response

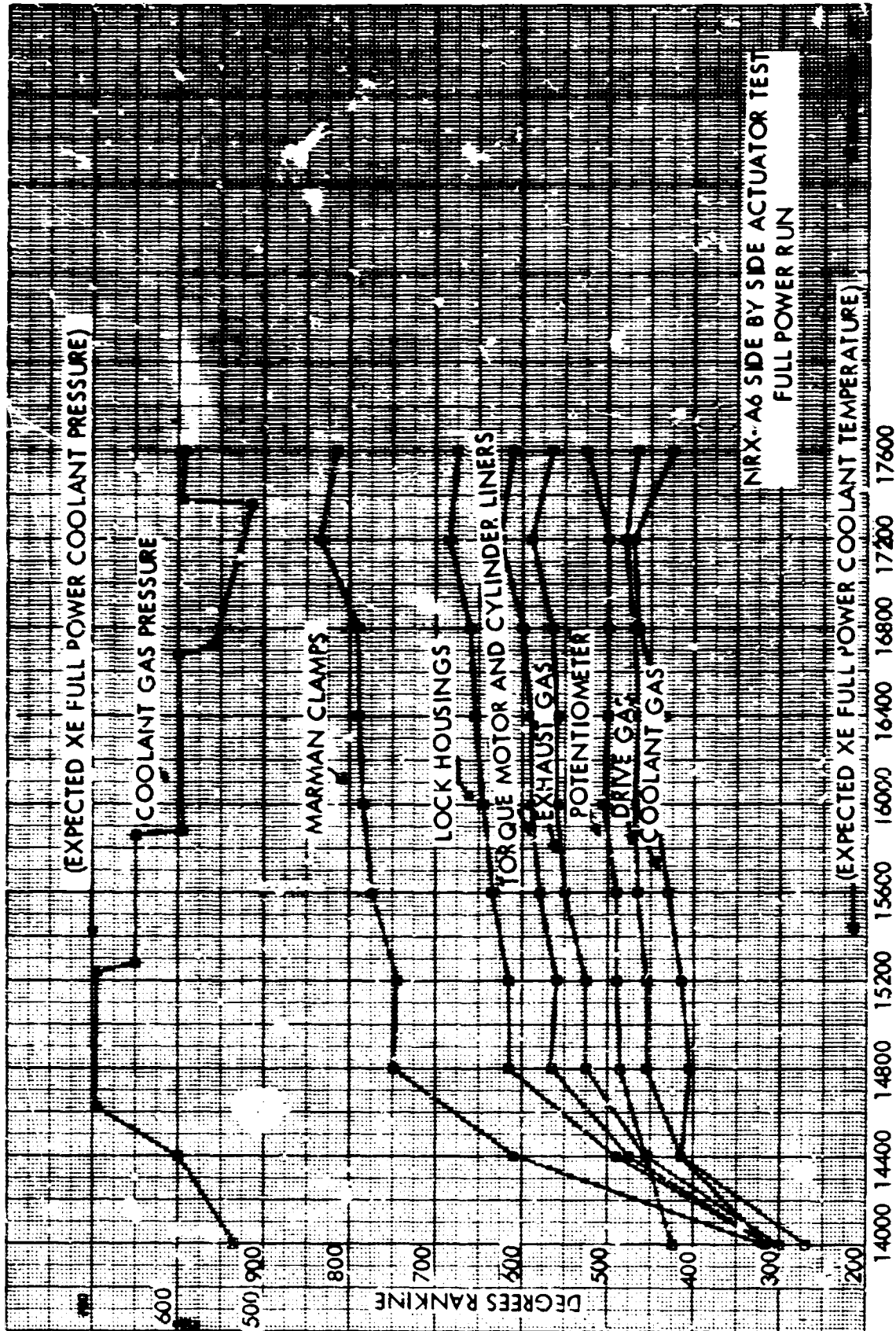


Figure 5-53. (U) NRX-A6 Side-by-Side Actuator Temperatures and Coolant Gas Pressures During Full Power Run

XE and R tests will eliminate this warm-up. Even with the relatively warm coolant gas temperature (450°R) and the experimentally low coolant pressures (550 psi) none of the component temperatures exceeded allowable limits. This gives strong evidence of the adequacy of the actuator coolant flow.

(U) A plot of the gamma dose received by the side-by-side experiment is shown in Figure 5-54. These curves were plotted using data obtained from the dosimeter packets mounted directly on the experiment container. From the figure, it can be seen that the actuator experienced a heating rate on the order of 93 to 116 Watts/lb. This exceeds the expected XE gamma dose by a factor of about 250 and is approximately equal to the gamma dose predicted for the R and E reactors. A plot of the fast neutron flux obtained by using dosimeter data is shown in Figure 5-55. The flux field in the vicinity of the actuator was between 0.1 and 0.2×10^{16} n/cm² which is about 100 greater than predicted field for the XE actuators located above the shield. A similar plot showing slow neutron flux is presented in Figure 5-56. The slow neutron flux levels were between 3 and 5×10^{16} n/cm² at the actuator.

(U) Following the test, the side-by-side pneumatic actuator was completely disassembled and photographed in search of any radiation caused damage. No malfunctions were observed during performance and no unusual wear or damage to internal components was detected upon disassembly. Although many photographs were taken, only a few are presented here. The views selected are of those components felt to be of the most critical nature. Figure 5-57 shows the torquemotor, solder points, lead wire and miscellaneous servo valve components. The photograph in Figure 5-58 shows the lock indication switches, solder connections, wires and the lock and lock shut-off valve in the background. A view of the three deck potentiometer again showing the solder points, wire and insulating sleeves is shown in Figure 5-59. The last photo presented, Figure 5-60, shows the P₁ piston and rack assembly, the P₂ piston and all the piston rings.

(U) Conclusions

(U) The pneumatic control drum actuator will perform as designed while under the influence of a radiation field (and after being subjected to an integrated radiation field) well in excess of the XE predicted field and approximately equivalent to that expected on the R reactor and E engine tests. The coolant flow to the actuator which was designed with the NR heating rates of 350 watts/lb as a parameter are higher than are required for heating rates expected on the XE, R and E programs which are predicted to be on the order of 125 Watts/lb maximum. Coolant flow could probably be reduced and as more experience is obtained this modification will be considered.

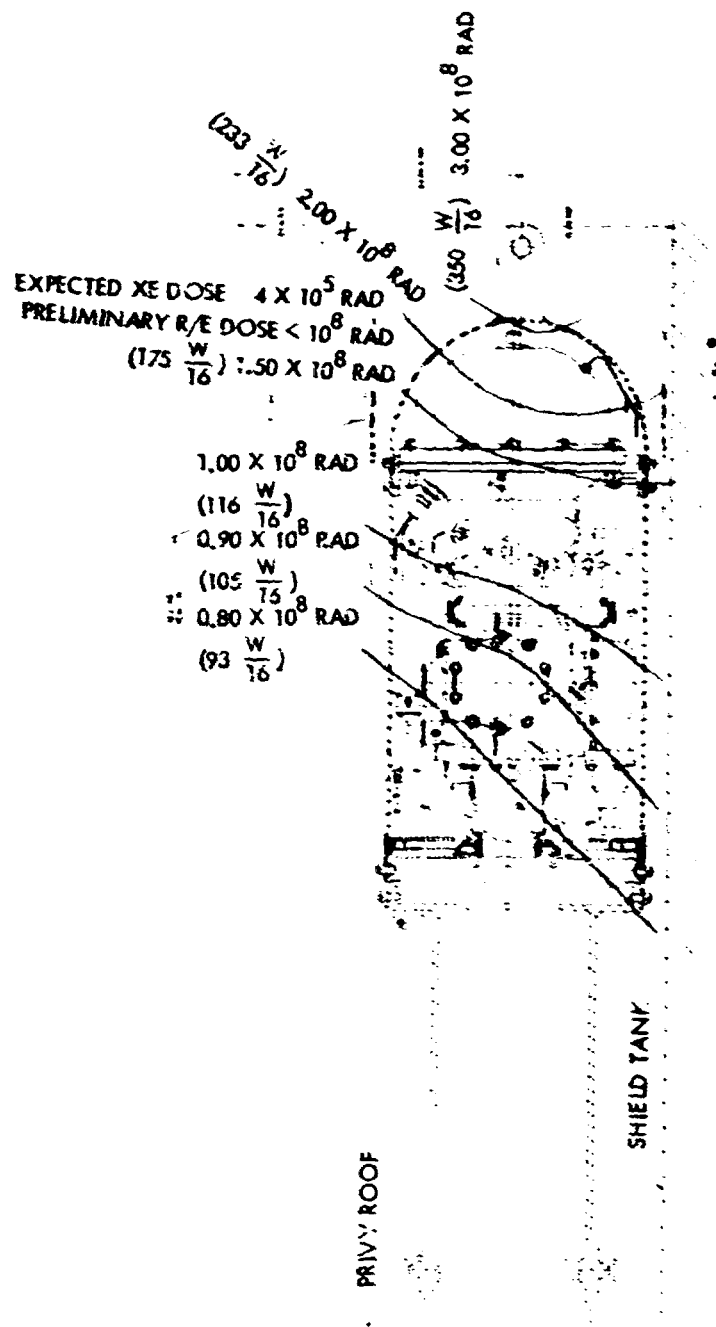


Figure 5-54. (U) NRX-A6 Side-By-Side Actuator Gamma Dose (U)

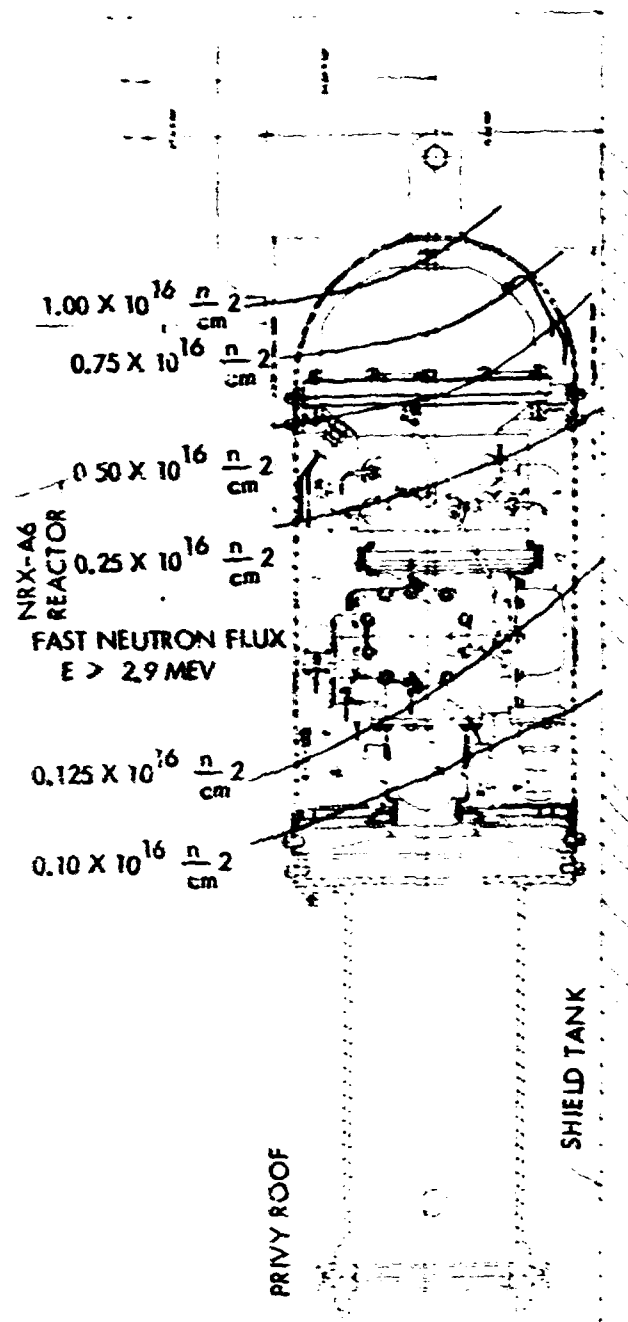


Figure 5-55. (U) NRX-A6 Side-By-Side Actuator
Fast Neutron Flux

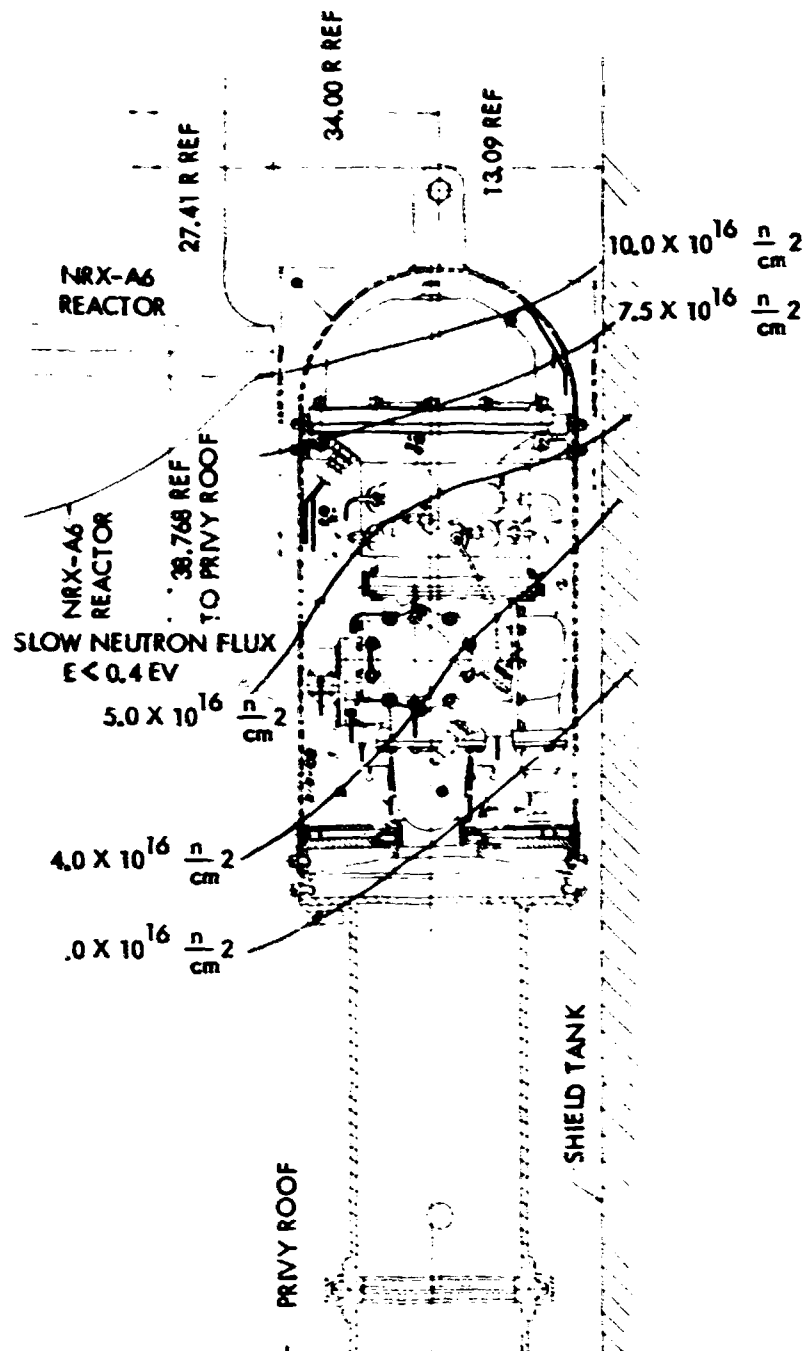


Figure 5-56. (U) NRX-A6 Side-By-Side Slow Neutron Flux

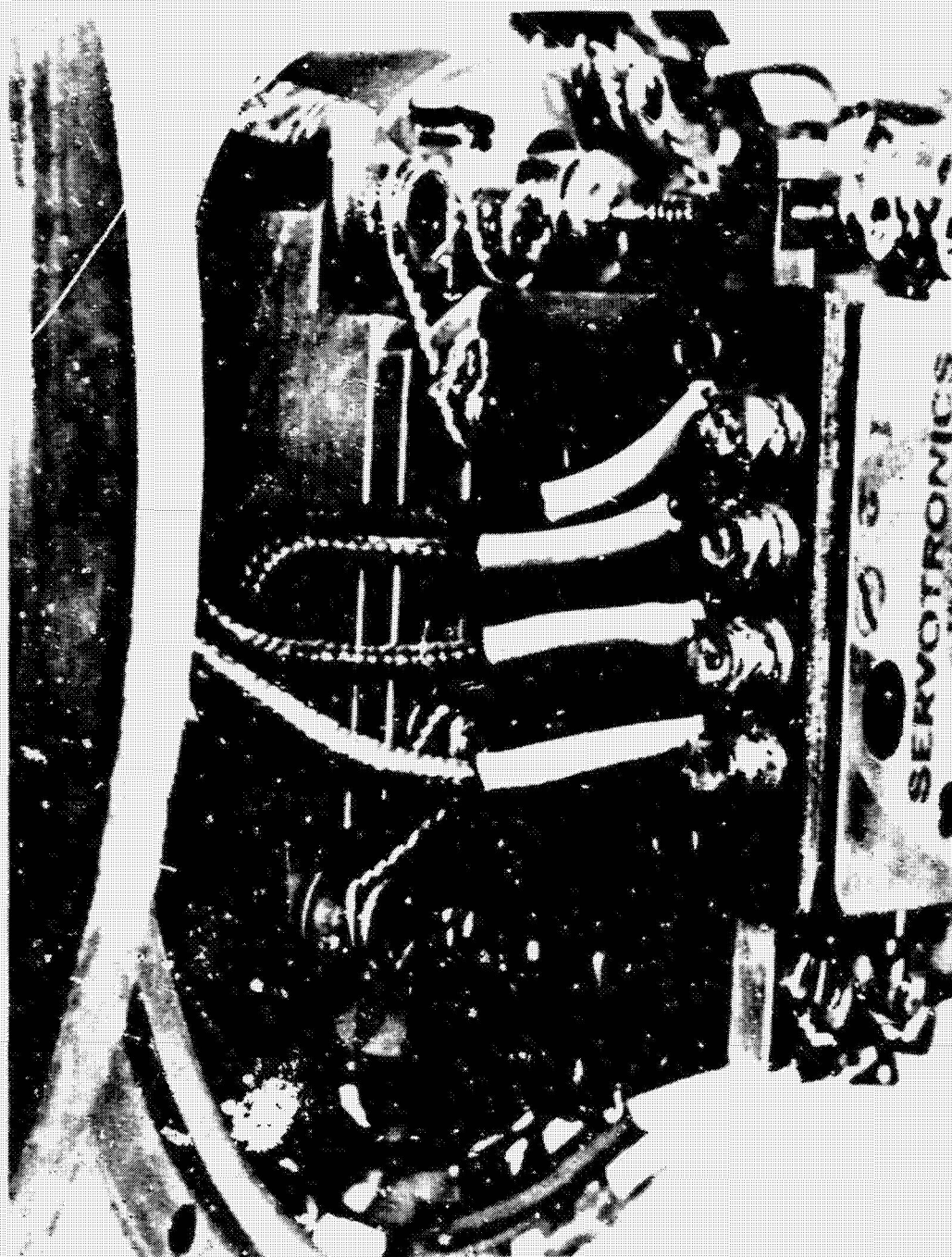


Figure 5-57. (U) NRX-A6 Side-By-Side Actuator Post Test Condition (Torque Motor, Solder Joints, Lead Wires, and Miscellaneous Servo Valve Components).

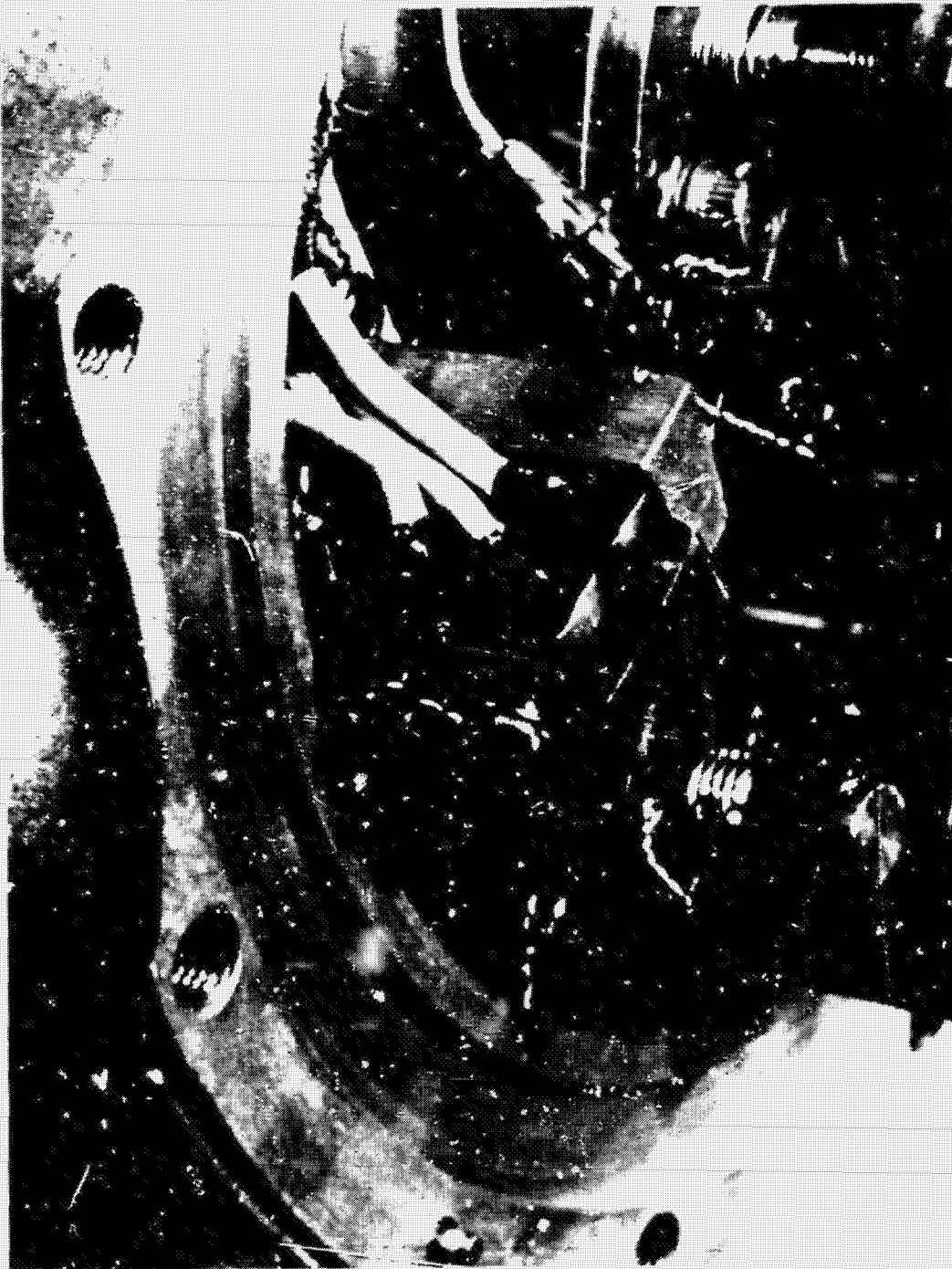


Figure 5-58. (J) NRX-A6 Side-By-Side Actuator Post Test Conditions (locks Indication Switches, Solder Connections, Wires, Lock, and Lock Shut-Off Valve).

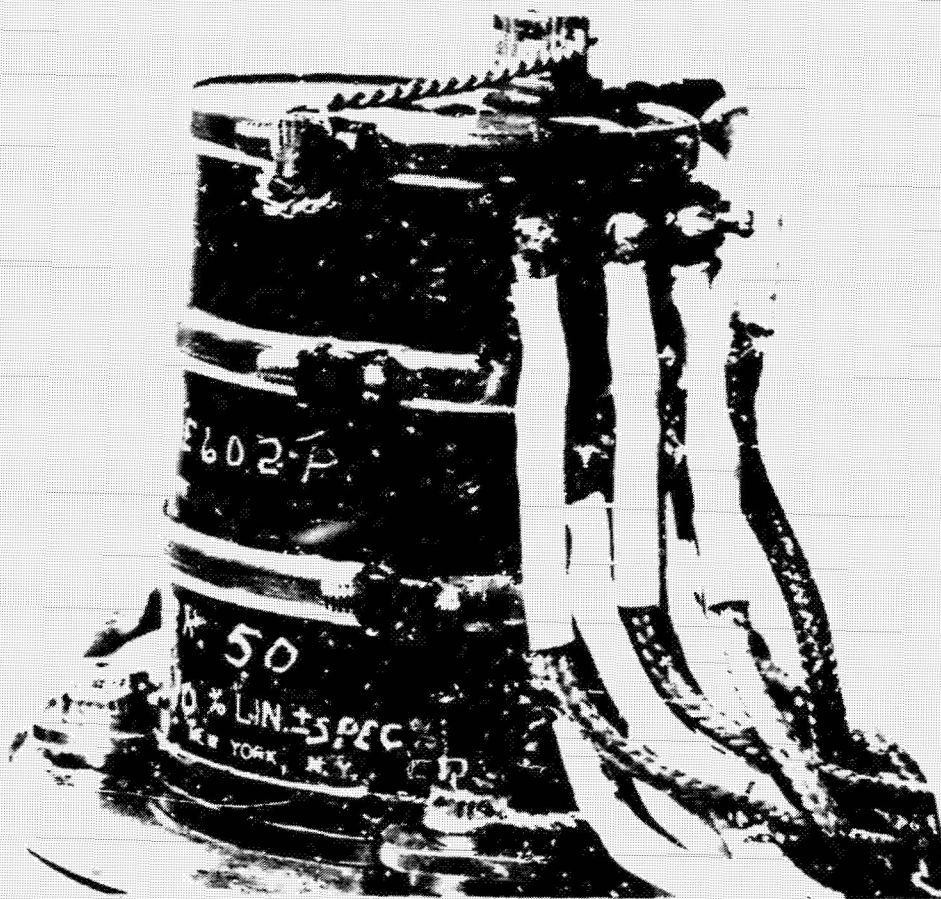


Figure 5-59. (U) NRX-A6 Side-By-Side Actuator Post Test Condition (Three Decs Pot ntiometer, Solder Joints, Wire, and Insulating Sleeves).

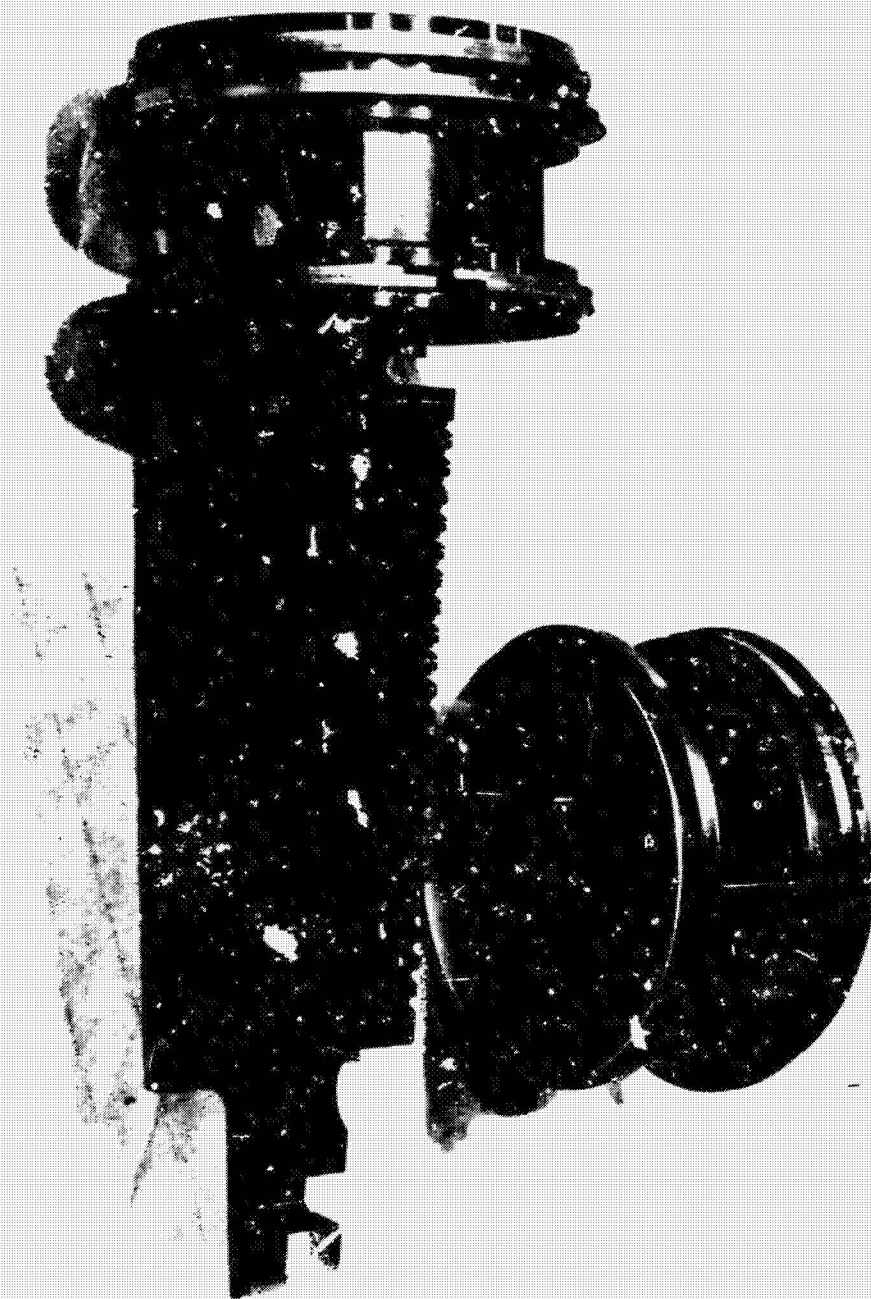


Figure 5-60. (U) NRX-A6 Side-By-Side Actuator Post Test Condition
(P₁ Piston and Rack Assembly, P₂ Piston and All Piston
Rings).

SECTION 6

BIBLIOGRAPHY

1. NERVA Program NRX-A1 Test Final Report, WANL-TNR-176, September, 1964, CRD.
2. NERVA Program NRX-A2 Test Final Report, WANL-TNR-193, March, 1965, CRD.
3. NRX-A3 Final Report, WANL-TNR-210, December, 1965, CRD.
4. NERVA NRX/EST Final Report, AGC-WANL NJD-8, October, 1966, CRD.
5. NRX-A5 Final Report, WANL-TNR-220, July, 1967, CRD.
6. NRX-A5 Nuclear Subsystem Thermal and Nuclear Design Data, WANL-TME-1542, November, 1967, CRD.
7. NRX-A6 Design Review, WANL-TME-1629, June, 1967, CRD.
8. Test Cell "C" Systems Description Document, WANL-TME-1556, March 31, 1967, U.
9. NRX-A5 Control Systems Description, WANL-TME-1592, July, 1967, U.
10. Test Cell C Control Systems Description, NTO-R-0089, August 11, 1966, U.
11. NRX-A6 Test Specification, WANL-TNR-215, September, 1966, U.
12. NRX-A6 Site Test Report, NTO-R-0134, February 9, 1968, U.
13. NRX-A6 Test Series Support Operational Requirements Document, NTO-R-0398, November 10, 1967, U.
14. NRX-A6 Reactor Inerting and Purging, NTO-I-0255, Revision 1, U.
15. NRX-A6 Pre-Test Report, NTO-R-0129, December 5, 1967, U.
16. NRX-A6 Experimental Plan I Test Report, Initial Criticality Flow Tests, Drum Worth Measurements, NTO-R-0130, November 21, 1967, U.
17. NRX-A6 Experimental Plans II and III Test Report, System Interaction Checkout and Full Power Run Aborts, NTO-R-0132, December 8, 1967, U.
18. NRX-A6 Experimental Plan IIIA Test Report, Full Power Duration Test, NTO-R-0133, December 15, 1967, U.
19. NRX-A6 FEP-I Facility Checkout Report, NTO-R-0120, September 14, 1967, U.



Astronuclear
Laboratory

20. NRX-A6 FEP-II Facility Checkout Report, NTO-R-0123, September 21, 1967, U.
21. NRX-A6 FEP-III Facility Checkout Report, NTO-R-0126, October 19, 1967, U.
22. NRX-A6 Reactor Test Analysis Report, WANL-TNR-223, July, 1968, CRD.
23. NRX-A6 Test Prediction Report, WANL-TME-1613, November, 1967, CRD.
24. Report on Emergency Shutdown From 40 lb/sec Hold, LASL Memo J-17-774-67, December 11, 1967, U.
25. WANEF Critical Experiments in Support of NERVA, Quarterly Report, Third Quarter, CY 67, WANL-TME-1739, January, 1968, CRD.
26. NRX-A6 Safety Evaluation Report, WANL-TME-1633 (Including Supplement 1), October, 1967, CRD.
27. NRX-A6 Test Parameter Limits Justification, WANL-TME-1641, July, 1967, U.
28. NRX-A6 Transducer Evaluation Report, WANL-TME-1863, December 1968, CRD.
29. NRX-A6 Post Test Instrumentation Report, AGC-RN-S-0462, June, 1968, U.
30. NRX-A6 Instrumentation Installation Report, WANL-TME-1719, December 3, 1967, CRD.
31. NRX-A6 Transducer Evaluation Report, WANL-TMI-1896, April 25, 1968, CRD.
32. ATO Standard Operating Procedure for End-to-End Instrumentation Check, ATO-SOP-0034, August, 1965, U.
33. CAM A6 Model Equations, WANL-TME-1715, October, 1968, CRD.
34. NRX-A6 Post Test Dynamic Analysis, WANL-TME-1806, September 1968, CRD.
35. NRX-A6 Structural Performance, WANL-TME-1832, August, 1968, CRD.
36. NRX-A6 Post Test Report, Volume I, Disassembly, NTO-R-0141, April, 1968, CRD.
37. NRX-A6 Post Test Report, Volume II, Post-Operative Examinations (to be published).
38. NRX-A6 Post Operative Mechanical Test and Stress Analysis Evaluation, WANL-TME-1796, July, 1968, CRD.

END — DATE FILMED

39. Post Operational Examination of NRX-A6 Fuel Elements: Phase I Report on Weight Loss and Visual Examination Data, WANL-TME-1789, June, 1968, CRD.
40. Post-Operational Examination of NRX-A3 Fuel Elements, WANL-TME-1333, February 11, 1966, CRD.
41. Post-Operational Examination of NRX-A3 Fuel Elements, WANL-TME-1521, May, 1967, CRD.
42. Post-Operational Examination of NRX-A5 Fuel Elements, WANL-TME-1618, July, 1967, CRD.
43. NRX-A5 Reactor Test Analysis Report, WANL-TNR-219, March, 1967, CRD.
44. NRX-A5 Nuclear Subsystem Thermal and Nuclear Design Data Book, WANL-TME-1642, November 15, 1967, CRD.
45. NRX-A6 Chemical and Radiochemical Measurements, NTO-R-0144, April 29, 1968, CRD.

7

22/

75